Universitat de les Illes Balears

Facultat de Ciències
Departament de Biologia

The Two Faces of Janus: Unfolded Protein Response - Autophagy in Cell Death and Survival

PhD Thesis

Amaia Marcilla Etxenike

Mallorca, 2012

Supervisors:
Xavier Busquets and Pablo Escribá

Nosaltres, Xavier Busquets Xaubet, Catedràtic de la Facultat de Ciències de la Universitat de les Illes Balears, i Pablo Escribá Ruiz, Catedràtic de la Facultat de Ciències de laUniversitat de les Illes Balears

CERTIFIQUEM:

Que el present treball titulat "The Two Faces of Janus: Unfolded Protein Response - Autophagy in Cell Death and Survival.", presentat per Amaia Marcilla Etxenike per optar al TÍTOL univesitari oficial de DOCTOR per la Universitat de les Illes Balears dins del programa de doctorat en Biotecnología, Genética y Biología Celular, s'ha realitzat sota la nostra direcció al Departament de Biologia de la Facultat de Ciències de la Universitat de las Illes Balears. Revisat el present treball, autoritzem la seva presentació per que pugui ésser jutjada pel tribunal corresponent.

Palma de Mallorca, 28 de Septiembre de 2012

Director	Director	Autor
Prof Xavier Busquets	**Prof. Pablo Escribá**	**Amaia Marcilla Etxenike**

“I am among those who think that science has great beauty. A scientist in his laboratory is not only a technician: he is also a child placed before natural phenomena which impress him like a fairy tale.” **Marie Curie**

"Our doubts are traitors, and make us lose the good we oft might win, by fearing to attempt" **William Shakespeare**

The Two Faces of Janus

Janus is the Roman god of gates and doors (ianua), and beginnings and endings. He is usually represented with a double-faced head, each looking in opposite directions. He was worshipped at the beginning of harvest time, planting, marriage, birth, and other types of beginnings, especially at the start of important events in a person's life. Janus also represents the transition between primitive life and civilization, countryside and city, peace and war, and the growing-up of young people.

One tradition states that he came from Thessaly and was welcomed by Camese in Latium, where they shared a kingdom. They married and had several children, among which the river god Tiberinus (after whom the river Tiber is named). When his wife died, Janus became the sole ruler of Latium. He sheltered Saturn when he was fleeing from Jupiter. Janus, as the first king of Latium, brought to this people peace and welfare, a time known as the Golden Age. He introduced money, field cultivation, and laws. After his death, he was deified and became the protector of Rome. When Romulus and his associates stole the Sabine Virgins, the Sabines attacked the city. The daughter of one of the guards on Capitolian Hill betrayed her fellow countrymen and guided the enemy into the city. They attempted to climb the hill but Janus made a hot spring erupt from the ground, and the would-be attackers fled the city. Ever since, the gates of his temple were kept open in times of war so the god would be ready to intervene when necessary. In times of peace, the gates were closed. The month of January (the eleventh Roman month) is named after Janus.

Janus was represented with two faces, originally one face was bearded while the other was not (probably a symbol of the sun and the moon). Later both faces were bearded. In his right hand, he was portrayed holding a key. The double-faced head appeared on many Roman coins (http://www.pantheon.org/articles/j/janus.html). The two faces of Janus in this thesis represent the Unfolded Protein Response and the Autophagy which can be both the beginning of the cellular recovery or its end.

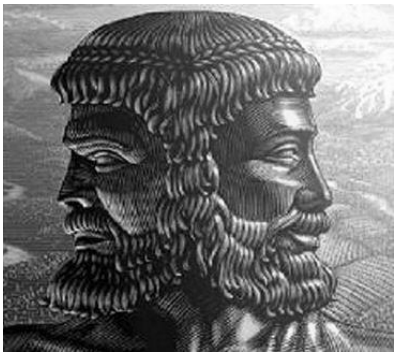

A Miki, mis aitas e Iñi

con todo mi cariño.

Acknowledgements

Durante estos últimos cuatro (+ 2) años me he dedicado a intentar sacar adelante el PhD y aquí estoy por fin. Ha llegado el momento de agradeceros a todos los que habéis estado alegrándome el camino.

En primer lugar, quisiera agradecer a mis directores de tesis por el apoyo que me han brindado. Al Profesor Pablo Escribá por confiar en mí, darme la oportunidad de realizar la tesis y por estar ahí en los momentos cruciales. Al Profesor Xavier Busquets por ser mi guía y principal apoyo a lo largo de esta tesis, gracias por tus ánimos.

También quisiera agradecérselo al Departamento de Biología y a la Universidad de las Islas Baleares donde he realizado la tesis y al Ministerio de Educación (Gobierno de España) por concederme la beca de Formación de Profesorado Universitario (FPU) que ha financiado esta tesis doctoral.

Me gustaría agradecer a mis compañeros de laboratorio que me han acompañado a lo largo de este periplo: Maria Antonia, Laura, Joana, Mónica, David, Maitane, Gwendy, María, Dani, Francis, Vicky, Silvia, Rafa, Maria Antonia F, Joel, Manuel, Raheem, Victor C, Andrea, Margalida y Victor V. ¡Gracias a todos por vuestra ayuda! Habéis hecho del laboratorio algo más que un lugar de trabajo.

Gracias a Ana por echarme una mano el verano pasado. Fue una gozada trabajar contigo, eres la mejor estudiante del mundo.

Quería agradecer especialmente a Laura y Maria Antonia por ser mis amigas desde el principio, gracias por estar siempre ahí chicas. También quería agradecer a Andrea todo su cariño y apoyo ¡eres un solico! Gracias a Joana y Mónica por convertiros en mis amigas en esta última etapa, ha sido un descubrimiento y un placer conoceros. ¡Ha sido un regalo compartir mi vida con todas vosotras chicas!

Me gustaría agradecer también al Profesor José Manuel García-Verdugo y a Mario Soriano-Navarro por su colaboración con la microscopía electrónica.

Gracias a mi cuadri, a todas las furris, por mantenerse cerca de mi a pesar de la distancia y darme tantos ánimos y confianza para terminar. Os echo muchísimo de menos chicas!!

Gracias a Miriam por darme ese soplo positivo que tanto necesitaba al final. Gracias por decirme que escribir la tesis en tres meses (e incluso dos como tú) era posible, eso me dio la energía y la alegría para conseguirlo.

I would like to thank very specially Valerie Moliere for her help with the editing of this thesis. Thanks a lot Val, you have really helped me!

Y para el final me dejo lo más importante. Gracias a mis aitas y a Iñi por estar siempre conmigo. Gracias por ser siempre mi apoyo y mi desahogo. Sin vosotros esto no hubiera sido posible, os quiero!!

Miki, esta tesis va por ti. Eres lo mejor de mi vida. No tengo palabras para decirte cuanto te quiero y lo agradecida que te estoy por ayudarme siempre, ser tan paciente, cariñoso y sonriente. Gracias por quererme tanto, amor.

Contents

Abbreviations

2OHOA	2-Hydroxyoleic acid / Minerval®
5XFAD mice	Mice that co-express and co-inherit Familial AD (FAD) mutant forms of human APP and PS1 transgens under transcriptional control
Aβ	Amyloid β-peptide
AD	Alzheimer's disease
ADAM 9	A disintegrin and metalloproteinase 9
ADAM 10	A disintegrin and metalloproteinase 10
ADAM 17	A disintegrin and metalloproteinase 17
AKT	Protein kinase B
Aph-1	Anterior pharynx-defective 1
APP	Amyloid precursor protein
ASK1	Apoptosis signal regulating kinase 1
ATF6	Activating transcription factor 6
ATF4	Activating transcription factor 4
ATG3	Autophagy-related gene 3 protein
ATG4	Autophagy-related gene 4 protein
ATG5	Autophagy-related gene 5 protein
ATG7	Autophagy-related gene 7 protein
ATG12	Autophagy-related gene 12 protein
ATG14/Barkor	Autophagy-related gene 14 protein
ATG16L1	Autophagy-related protein 16-1
ARA	Arachidonic acid
BACE1	β-site APP cleaving enzyme-1
Bcl-2	B-cell lymphoma 2
Beclin 1	Autophag- related gene 6 protein
BiP	Glucose-regulated protein, 78 KDa (GRP78)

BSA	Bovine serum albumin
C83	Fragment of APP cleaved by the α-secretase at a position 83 amino acids from carboxy (C) terminus
C99	99-amino-acid C-terminal stub from APP cleaved by the β-secretase
CDK	Cyclin-dependent kinases
CHOP	C/EBP homologous protein transcription factor
CMA	Chaperone-mediated autophagy
CSF	Cerebrospinal fluid
DAG	Diacylglycerol
DHA	Docosahexaenoic acid
DHFR	Dihydrofolate reductase
E2F-1	E2F transcription factor 1
ECCAC	European Collection of Cell Cultures
EGFR	Epidermal growth factor receptor
EPA	Eicosapentaenoic acid
ER	Endoplasmatic reticulum
ER stress	Endoplasmatic reticulum stress
ERAD	Endoplasmatic reticulum assisted degradation
FAD	Familial Alzheimer's disease
FBS	Fetal bovine serum
gPE	Glycerophosphoethanolamine
GRP94	Glucose-regulated protein, 94 KDa
GSK-3β	Glycogen synthase kinase 3β
hBDNF	Human brain-derived neurotrophic factor
HPTLC	High performance TLC
IRE1	Inositol requiring enzyme 1
JNK	Jun N-terminal kinase
LC3A / LC3B	Microtubule-associated proteins 1A/1B light chain 3 (MAP1-LC3/Atg8)
LC3-I	LC3 cytosolic isoform I
LC3-II	LC3 isoform II (conjugated to PE)
LOH	Loss of heterozygosity
LP204A1	2-hydroxyarachidonic acid (2OH-ARA)
LP205A1	2-hydroxyeicosapentaenoic acid (2OH-EPA)
LP226A1	2-hydroxydocosahexanoic acid (2OH-DHA)
MAPKs	Mitogen-activated protein kinases
MTOC	Microtubule organizing center
mTOR	Mammalian target of rapamycin

MTs	Microtubules
MTT	Methylthiazolyl diphenyl tetrazolium bromide method
Nct	Nicastrin
NFTs	Neurofibrillary tangles
NSAID	Non-steroidal anti-inflammatory drugs
p150/Vps15	Phosphoinositide 3-kinase adaptor protein
PDI	Protein disulphide isomerase
PE	Phosphatidiletanolamine
P-eIF2α	Phosphorilated eukaryotic initiation factor 2 α
Pen-2	Presenilin enhancer 2
PERK	PKR-like ER kinase
P-GSK-3β	Phospho glycogen synthase kinase 3β (P-Ser9)
PI3K	Phosphatidylinositol 3-kinase
PI3P	Phosphatidylinositol 3-phosphatase
PKC	Protein kinase C
PP1	Protein phosphatase 1
pRb	Retinoblastoma protein
PS1	Presenilin-1
PS2	Presenilin-2
PTEN	Phosphatase and tensin homology protein
PUFAs	Polyunsaturated fatty acids
RA	Retinoic acid
RAM	Radial Arm Maze
RM	Reference memory
sAPPα	(N)-terminal ectodomain from α-secretase cleavage of APP
sAPPβ	(N)-terminal ectodomain from β-secretase cleavage of APP
S1P	Site 1 protease
S2P	Site 2 protease
SPs	Senile plaques
SM	Sphingomyelin
SMS	Sphingomyelin synthase
Tg	Transgenic
TGN	Trans-Golgi network
TLC	Thin Layer Chromatography
TRAF2	TNF-receptor associated factor 2
TZM	Temozolomide
UPR	Unfolded protein response

Vps34	Class III phosphatidylinositol 3-kinase
WM	Working memory
XBP1	X-box-binding protein 1
XBP1s	X-box-binding protein 1 spliced
XBP1u	X-box-binding protein 1 unspliced

Abstract

Resumen

La mayoría de los fármacos utilizados actualmente en terapias para el tratamiento de patologías humanas interactúan con proteínas, modificando su actividad y la de proteínas reguladas por ellas. Esta interacción fármaco-proteína induce cambios en la fisiología celular que revierten el proceso patológico. Sin embargo, los eventos de señalización celular también pueden verse afectados por modificaciones en la composición lipídica de la membrana plasmática y en su estructura. La participación de los lípidos de membrana en las actividades celulares indica que podrían constituir dianas específicas para fármacos. En la terapia lipídica de membrana, los efectos farmacológicos estarían asociados con la modulación de la composición y las propiedades fisicoquímicas de membrana. En este contexto, el ácido 2-hidroxioleico (2OHOA) es un potente fármaco antitumoral que fue diseñado para regular la composición y la estructura de la membrana lipídica así como la función de importantes proteínas de membrana. Por otro lado, el ácido 2-hidroxiaraquidónico (2OHARA; LP204A1), el ácido 2-hidroxieicosapentaenóico (2OHEPA; LP205A1), y el ácido 2-hidroxidocosahexanóico (2OHDHA; LP226A1) son derivados lipídicos hidroxilados que fueron diseñados en nuestro grupo de investigación para el tratamiento del Alzheimer. El objetivo principal de este trabajo se ha basado en el estudio del funcionamiento de estos derivados de ácidos grasos que han sido hidroxilados, en la modulación de las vías de señalización de la UPR (respuesta a las proteínas mal plegadas) y de la autofagia en células de glioma y células neuronales en el estudio del glioma y del alzheimer respectivamente.

Aunque algunos de los mecanismos de acción inducidos por el 2OHOA ya han sido dilucidados, la forma en la que esta molécula ejerce su acción anticancerígena sin matar células no cancerosas todavía se necesita un análisis más exhaustivo. Para abordar este punto hemos estudiado la UPR y la muerte celular inducida por autofagia. Los resultados de este

estudio indican que el tratamiento con 2OHOA activa la vía de UPR que induce muerte celular en tres líneas celulares de glioma estudiadas (1321N1, SF767 y U118), mientras que en la línea celular no cancerosa MRC-5 el 2OHOA activa la vía de supervivencia de la UPR.

Los niveles celulares de los marcadores de UPR y autofagia se determinaron por RT-PCR cuantitativa y western blot en células de glioma 1321N1, SF 767 y U118 y células no tumorales MRC5 incubadas en presencia o ausencia de 2OHOA o palmitato, inductor de estrés de retículo endoplásmico (RE). La respuesta celular a estos agentes se evaluó mediante microscopía de fluorescencia, microscopía electrónica y citometría de flujo. Los tratamientos con 2OHOA indujeron un aumento significativo en la expresión de importantes marcadores de estrés de RE / UPR en las células de glioma humano. A su vez, el tratamiento con 2OHOA indujo parada en la fase G_2/M del ciclo celular en las tres líneas celulares de glioma estudiadas. Por último, 2OHOA indujo autofagia en las líneas celulares de glioma 1321N1, SF 767 y U118, con la aparición de vesículas autofágicas y la inducción de LC3BII. Es importante destacar que el 2OHOA no indujo tales cambios en la línea celular no tumoral MRC-5. Los resultados demuestran que 2OHOA induce estrés de RE / UPR y autofagia en las líneas celulares de glioma humano (1321N1, SF 767 y U118), pero no en células normales normales (MRC-5), lo que pone de relieve las bases moleculares que subyacen tras la eficacia y la falta de toxicidad de este compuesto.

En el contexto de la terapia lipídica de membrana nuevas moléculas han sido diseñadas en nuestro grupo para el tratamiento del Alzheimer: 2OHARA (LP204A1), 2OHEPA (LP205A1), y 2OHDHA (LP226A1). En nuestro grupo de investigación se han obtenido resultados prometedores que demuestran que el tratamiento crónico con LP226A1 en el modelo de ratones de Alzheimer 5XFAD recupera el deterioro de la memoria con el consiguiente aumento de neurogénesis en el hipocampo. Aunque los resultados preliminares en ratones 5XFAD han puesto de manifiesto una recuperación del déficit de memoria, hasta el momento no se había hecho ningún estudio sobre los efectos de estos compuestos para revelar su mecanismo de acción molecular en células neuronales humanas.

En esta tesis se ha estudiado la expresión de proteínas relacionadas con la aparición de Alzheimer en células de neuroblastoma humano diferenciadas a neuronas como las células SH-SY5Y. Estas células se trataron con los tres hidroxiderivados, LP226A1 (2OHDHA), LP204A1 (2OHARA) y LP205A1 (2OHEPA) y se estudiaron los efectos sobre las proteínas implicadas en la aparición y evolución del Alzheimer como son α-, β- y γ-secretasa, tau hiperfosforilada y P-GSK3β. Los resultados indican que, la expresión protéica de PS-1 (γ-secretasa) y BACE1 (β-secretasa) está disminuída tras el tratamiento de las células SH-SY5Y diferenciadas y sin diferenciar con LP226A1, LP205A1 y LP204A1. Por el contrario, la expresión proteíca de ADAM10 (α-secretasa) no está modulada por estos fármacos. Además, el tratamiento con LP226A1 o LP205A1, tras la incubación con Aβ42, rescata a las células SH-SY5Y diferenciadas a neuronas de la muerte celular. Por otra parte,

la incubación de estas células con el péptido Aβ42 induce hiperfosforilación de tau, que se revierte después del tratamiento con LP226A1, LP205A1 y LP204A1. También hemos observado, que el tratamiento de las células SH-SY5Y con estas moléculas inhibe la proteína GSK-3β, impidiendo así la hiperfosforilación de tau. Aunque los mecanismos de acción de estos fármacos hidroxiderivados no están aún completamente dilucidados, nuestros resultados presentan claros indicios de que los componentes clave del Alzheimer como las secretasas, P-tau y P-GSK-3β son regulados, lo que ofrece un potencial para el tratamiento del Alzheimer.

En este contexto, hemos profundizado en los mecanismos moleculares implicados en la recuperación neuronal, prestando especial atención a las vías de la UPR y la autofagia, ya que podrían estar involucradas en la eliminación de NFTs y péptido β amiloide de las placas seniles, puesto que una de las características del Alzheimer la acumulación de proteínas mal plegadas en el cerebro así como la activación de la UPR. Pudimos observar como el tratamiento con los ácidos grasos hidroxilados LP226A1, LP205A1 y LP204A1 provocaron una activación de la vía de supervivencia UPR en células SH-SY5Y diferenciadas, a dosis terapéuticas. Además, el tratamiento de las células SH-SY5Y con los ácidos grasos hidroxilados también activa la respuesta autofágica.

La autofagia, puede funcionar tanto a favor de la muerte celular como de la supervivencia de forma similar al estrés de RE, por lo que puede conferir neuroprotección eliminando las proteínas mal plegadas. En este contexto, hemos observado que las células neuronales SH-SY5Y tratadas con LP226A1, LP204A1 y LP205A1 presentaban cambios en los niveles de varias proteínas implicadas en el proceso de autofagia. Entre ellas, la proteína Beclin-1, varias proteínas ATGs así como la proteína LC3BII que también aumenta su expresión significativamente después del tratamiento de las células SH-SY5Y diferenciadas con los ácidos grasos hidroxiderivados. La autofagia inducida por el tratamiento con los hidroxiderivados podría conferir neuroprotección a las células SH-SY5Y neuronales mediante la eliminación de las proteínas plegadas incorrectamente.

Abstract

Most drugs currently used for human therapy interact with proteins by altering their activity and that of downstream proteins, and producing changes in the cell physiology that reverse the pathological process. However, it is known that changes in membrane lipid composition alter membrane structure, protein-membrane interactions and cell signaling. The participation of membrane lipids in cellular activities indicates that they might constitute targets for drugs whose pharmacological effects would be associated with the modulation of the composition and physicochemical properties of membranes. 2-Hydroxyoleic acid (2OHOA) is a potent antitumor drug designed to regulate membrane lipid composition and

structure and the function of important membrane proteins. In addition, 2-hydroxyarachidonic acid (2OHARA; LP204A1), 2-hydroxyeicosapentaenoic acid (2OHEPA; LP205A1), and 2-hydroxydocosahexanoic acid (2OHDHA; LP226A1) are new hydroxy derivated lipids designed in our group for the treatment of Alzheimer´s Disease (AD). The main goal of this work was to study how these synthetic hydroxy derivates modulate unfolded protein response and the autophagy pathways in glioma cells and neuron-like cells for AD.

Although some of the action mechanisms induced by 2OHOA have been elucidated, the way this molecule exerts its anticancer action without killing non-cancer cells is not fully understood, neither how a common pathway through 2OHOA exerts its activity against human glioma cells. To address this point, we have studied unfolded protein response which has both a pro-death and a pro-survival arm, and autophagy cell death induced by UPR. The results of this study indicate that a 2OHOA treatment activates the pro-death arm of the unfolded protein response in the three glioma cell lines we studied (1321N1, SF767 and U118) while it activates the pro-survival arm in MRC-5 non-cancer cells.

The cellular levels of endoplasmic reticulum (ER) stress, unfolded protein response (UPR) and autophagy markers were determined by quantitative RT-PCR and immunoblotting on 1321N1, SF-767 and U118 human glioma cells and non-tumor MRC-5 cells incubated in the presence or absence of 2OHOA or the ER stress/autophagy inducer, palmitate. The cellular response to these agents was evaluated by fluorescence microscopy, electron microscopy, and flow cytometry. We observed that 2OHOA treatments induced augments in the expression of important ER stress/UPR markers in human glioma cells. Concomitantly, 2OHOA led to the arrest of the three glioma cell lines studied in the G_2/M phase of the cell cycle. Finally, 2OHOA induced autophagy in 1321N1, SF-767 and U118 cells, with the appearance of autophagic vesicles and the up-regulation of LC3BII and ATG proteins. Importantly, 2OHOA failed to induce such changes in non-tumor MRC-5 cells. The present results demonstrate that 2OHOA induces ER stress/UPR and autophagy in human glioma (1321N1, SF-767 and U118 cell lines) but not in normal (MRC-5) cells, by unraveling the molecular bases which underlying this compound's efficacy and lack of toxicity

In the context of the membrane lipid therapy, we designed in our research group new molecules for the treatment of AD: 2OHARA (LP204A1), 2OHEPA (LP205A1), and 2OHDHA (LP226A1). We have obtained promising results which demonstrate that chronic treatment with LP226A1 recovers memory impairment in the 5XFAD mice model of AD with a concomitant increase of the hippocampal neurogenesis. Preliminary results in Alzheimer transgenic mice have revealed restoration of memory deficits. But so far, no studies on human neuronal cells have been undertaken, nor on the effects of these compounds and their action mechanisms.

In this thesis, we studied the expression of several Alzheimer´s disease-related proteins on SH-SY5Y human neuroblastoma cells differentiated into neuron-like cells and treated with the three hydroxy derivates, LP226A1 (2OHDHA), LP204A1 (2OHARA), and LP205A1 (2OHEPA). The proteins studied here are α-, β- and γ-secretases, hyperphosphorilated tau, GSK3β, and P-GSK3β. Our main findings indicate that PS-1 (γ-secretase) and BACE1 (β-secretase) protein expression is down-regulated by LP226A1, LP205A1, and LP204A1 treatments in differentiated and non-differentiated SH-SY5Y cells. On the contrary, ADAM10 (α-secretase) protein expression is not modulated by the drugs. Treatment with LP226A1 or LP205A1, after Aβ42 incubation, rescues differentiated SH-SY5Y cells from cell death. Moreover, Aβ42 incubation induces tau hyperphosphorilation in differentiated SH-SY5Y cells, which is reverted after treatment with LP226A1, LP205A1 and LP204A1. Furthermore, GSK-3β is inhibited, impairing tau hyperphosphorilation after treatment of differentiated SH-SY5Y cells with LP226A1, LP205A1 and LP204A1 (+ Aβ42).

Moreover, we have deepened our understanding into the molecular mechanisms involved in neuronal recovery by paying special attention to UPR and autophagy pathways, which could be involved in the removal of NFTs and amyloid β-peptide in senile plaques. AD is characterized by an accumulation of unfolded or misfolded proteins in the brain. Several reports indicate UPR activation in AD brain, suggesting a possible link between AD and UPR. Our results demonstrate UPR activation in the differentiated SH-SY5Y cells treated with LP226A1, LP205A1, and LP204A1. The hydroxyl derivates treatments only induce the prosurvival arms of the UPR (at therapeutic doses). In addition, the treatment of SH-SY5Y cells with the molecules also activates autophagy response. Only the protective arm of the unfolded protein response is activated at therapeutic doses of hydroxy derivates.

Autophagy, similar to ER stress has both pro-death and pro-survival functions. And it may confer neuroprotection by enhancing a clearance of soluble and aggregated misfolded proteins. In this context, several molecules implicated in the autophagy process are up-regulated in SH-SY5Y neuron-like cells treated with LP226A1, LP204A1, and LP205A1. Beclin-1, ATGs and LC3BII proteins are up-regulated. We believe that autophagy induced by hydroxy derivate treatments could confer neuroprotection to SH-SY5Y neuron-like cells.

1. General Introduction

1.1 The Unfolded Protein Response and ER Stress

1.1.1 The Endoplasmatic Reticulum

The endoplasmatic reticulum (ER) (Figure 1.1) is an organelle that has essential roles in the multiple cellular processes required for cell survival and normal cellular functions (Kim *et al.*, 2008). These processes include synthesis and sorting of secretory and membrane proteins, biosynthesis of phospholipids, cholesterol, steroids, degradation of glycogen, detoxification reactions, and maintenance of calcium homeostasis (Cribb *et al.*, 2005; Fagone and Jackowski, 2009; Braakman and Bulleid, 2011). The lumen of the ER constitutes a unique cellular environment. For instance, the highest concentration of calcium within the cell is found in the ER, owing to active transport by Ca^{2+}-ATPases. Moreover, because of its role in protein folding and transport, the ER is also rich in calcium-dependent molecular chaperones such as glucose-regulated protein, 78 KDa (GRP78, also known as BiP), GRP94, Calnexin, and Calreticulin which help stabilize protein-folding intermediates. The ER lumen also has an oxidative environment, which is crucial for the formation of disulphide bonds mediated by protein disulphide isomerase (PDI) and for proper folding of proteins (Ma and Hendershot, 2004; Rizzuto *et al.*, 2004; Schroder and Kaufman, 2005). Moreover, the ER has essential roles in lipid-membrane biosynthesis and in controlling production of cholesterol and other membrane lipid components. In addition to its biosynthetic capacity, the ER is a signaling organelle due to its ability to release sequestered calcium in response to second messengers (Schroder and Kaufman, 2005).

Molecular chaperone. A molecular chaperone is a protein that aids the folding of other proteins. Some molecular chaperones reside in the lumen of the ER (Kim *et al.*, 2008).

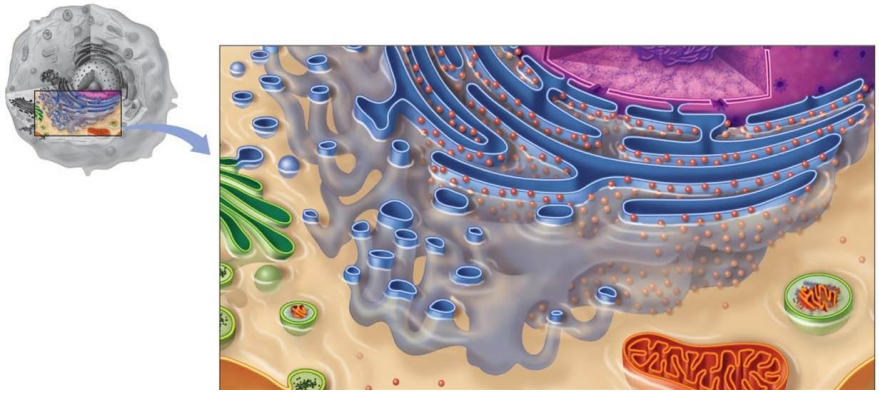

Figure 1.1. Schematic illustration of the endoplasmatic reticulum (ER) in the cell.
Image taken from (http://toulousestreet.wordpress.com/2012/02/).

1.1.2 The Unfolded Protein Response

Multiple disturbances can cause an accumulation of unfolded proteins in the ER, triggering an evolutionarily conserved response named the unfolded protein response (UPR) (Malhotra and Kaufman, 2007; Ron and Walter, 2007). Disturbances in cellular redox regulation caused by hypoxia interfere with disulfide bonding in the ER lumen, leading to protein unfolding or misfolding (Frand *et al.*, 2000). Glucose deprivation also leads to ER stress. Aberrations of calcium regulation in the ER also contribute to protein unfolding problems because of the calcium-dependent nature of some chaperones (Ma and Hendershot, 2004). Viral infection may also trigger the UPR. Recently, a high fat diet has also been linked to ER stress, for example in in liver (Ozcan *et al.*, 2004). In addition, tumor cells are bathed in a hostile microenvironment, and confronted with chronic metabolic stress conditions that favor UPR activation of the and autophagy (Kondo *et al.*, 2005; Moenner *et al.*, 2007). Moreover, certain promising anticancer regimens have been shown to activate concomitantly ER stress and autophagy in cancer cells (Verfaillie *et al.*, 2010). Protein-inclusion-body diseases that are typical of most chronic neurodegenerative diseases, as well as disorders such as inclusion-body myositis, indirectly cause an accumulation of unfolded proteins in the ER. This might occur by exhausting proteasome capacity, and causing an accumulation of unfolded proteins (Yoshida *et al.*, 2001; Lindholm *et al.*, 2006).

ER Stress. An organelle-initiated stress condition typically associated with an accumulation of misfolded and unfolded proteins in the lumen of the ER. ER stress is caused by a diversity of stimuli (Kim *et al.*, 2008). To restore homeostasis in response to ER stress, cells activate an intracellular signaling pathway called the unfolded protein response (UPR).

Unfolded protein response (UPR). A conserved physiological response involving ER-initiated signal-transduction events, induced by an accumulation of unfolded or misfolded proteins in the lumen of the ER. In mammals, the UPR induces signals initiated by ER membrane associated proteins: IRE1, PERK and ATF6 (Kim *et al.*, 2008).

The consequences of triggering the UPR because of ER stress in mammalian cells can be grouped into three types of effectors functions: adaptation, alarm, and cell death (Xu *et al.*, 2005). The initial intent of the UPR is to reestablish homeostasis and normal ER function and adaptative mechanisms which normally involve the activation of genes responsible for protein folding and ER-assisted degradation (ERAD). This helps clear the ER of unfolded proteins, and export them to the cytosol for degradation. The UPR-induced alarm refers to signal transduction events that are commonly associated with cellular stress, including the activation of mitogen-activated protein kinases (MAPKs) and Jun N-terminal kinase (JNK) (Kim *et al.*, 2008). Finally when the adaptative mechanisms activated by the UPR fail to compensate the loss of homeostasis in the cell (for example, when the primary stimulus causing ER stress is excessive), cell death is induced, typically by apoptosis. Cell death mechanisms induced by ER stress are diverse, involving caspase-dependent apoptosis and caspase-independent necrosis (Egger *et al.*, 2003). Moreover, it is becoming increasingly apparent that ER stress induces autophagy (Bernales *et al.*, 2006; Ogata *et al.*, 2006), a catabolic cellular process that promotes cell survival in many contexts but which has been associated with an induction of non-apoptotic cell death in others (Klionsky *et al.*, 2008).

When unfolded proteins accumulate in the ER, resident chaperones become occupied with protein folding releasing transmembrane ER-signalling proteins which are responsible for the UPR. The unfolded protein response in mammalian cells is controlled by three transmembrane ER stress sensors, namely IRE1 (inositol requiring enzyme 1), PERK (PKR-like ER kinase), and ATF6 (activating transcription factor 6). They are kept in an inactive state by binding to the ER chaperone BiP, preventing their oligomerization-induced activation (Verfaillie *et al.*, 2010). When misfolding proteins accumulate, BiP releases these transmembrane signaling proteins, allowing their oligomerization, and initiating the UPR. Together, IRE1, PERK and ATF6 proteins induce signal transduction events that improve the accumulation of misfolded proteins in the ER. Through these signal transduction events, they increase the expression of the ER chaperones, inhibit protein entry into the ER, arrest mRNA translation, and accelerate a retrograde export of proteins from the ER to the cytosol for ubiquitylation and proteasome-mediated degradation (Rao and Bredesen, 2004; Schroder and Kaufman, 2005). In addition, because ER stress can induce autophagy (Bernales *et al.*, 2006; Ogata *et al.*, 2006) this could be another mechanism for removing unfolded proteins. This mechanism may be particularly important when severe protein misfolding results in insoluble protein aggregates that cannot be eliminated by the proteasome.

In figure 1.2, we give an overview of UPR signaling in the cell controlled by three transmembrane ER stress sensors, namely IRE1α, PERK and ATF6. These sensors are kept in an inactive state by binding to the ER chaperon BiP until unfolded proteins accumulate in the ER.

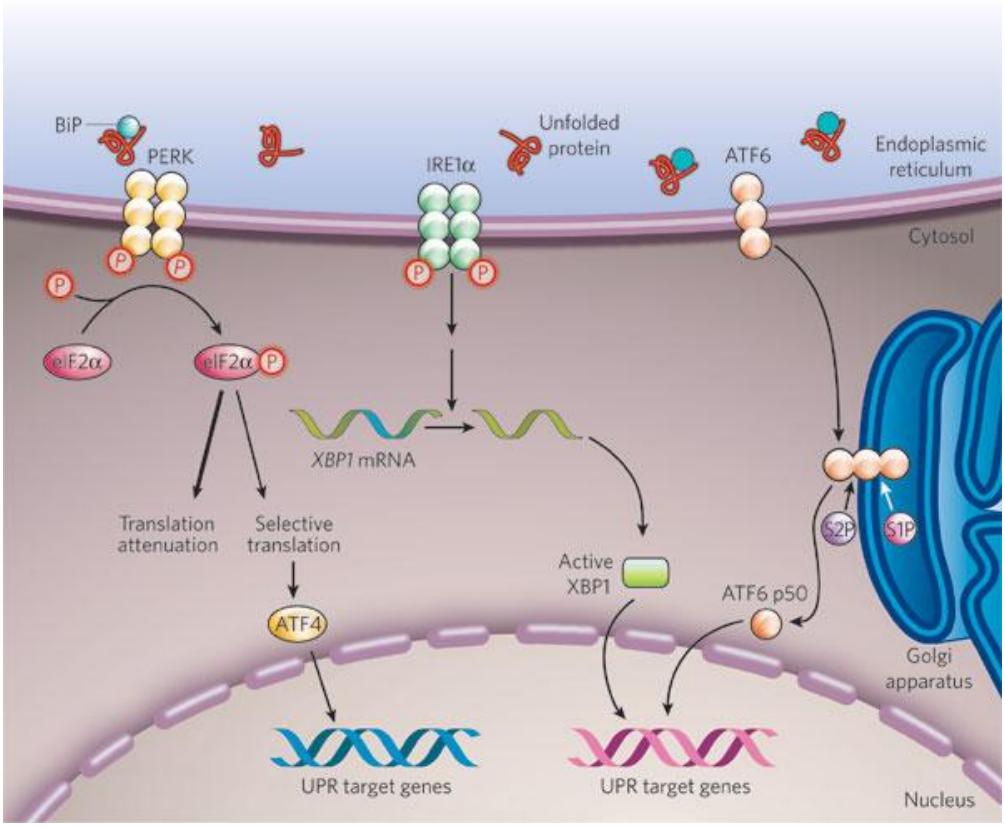

Figure 1.2. Overview of UPR signaling in the cell. Image taken from (Zhang and Kaufman, 2008). In non-stressed cells (not shown), the ER chaperone BiP binds to the luminal domains of the ER-stress sensors IRE1α, PERK and ATF6, maintaining these proteins in an inactive state. During ER stress (shown), BiP preferentially binds to unfolded or misfolded proteins, thus driving the equilibrium of BiP binding away from IRE1α, PERK and ATF6. These three proteins are the initiators of the three main signaling cascades of the UPR. The release of BiP results in the activation of PERK, through PERK homodimerization and trans-autophosphorylation. Activated PERK then phosphorylates the translation-initiation factor eIF2α, reducing the overall frequency of messenger RNA translation initiation. However, selected mRNAs, such as ATF4 mRNA, are preferentially translated in the presence of phosphorylated eIF2α. ATF4 activates the transcription of UPR target genes encoding factors involved in amino-acid biosynthesis, the antioxidative-stress response and apoptosis. The release of BiP also allows IRE1α to dimerize, activating its protein-kinase activity (through autophosphorylation) and its endoribonuclease activity. IRE1α then removes a 26-base intron from XBP1 mRNA. The spliced XBP1 mRNA encodes a potent transcription factor that translocates to the nucleus, activating the expression of UPR target genes. The release of BiP from ATF6 allows ATF6 to translocate to the Golgi apparatus, where it is cleaved by the proteases S1P and S2P, yielding an active cytosolic ATF6 fragment (ATF6 p50). This fragment migrates to the nucleus, activating the transcription of UPR target genes. S1P, site-1 protease; S2P, site-2 protease; XBP1, X-box-binding protein 1. (Zhang and Kaufman, 2008)

The activation of IRE1, PERK and ATF6 initiates a network of intracellular signaling pathways during the UPR. The transcription factor C/EBP homologous protein (CHOP) operates as a downstream component of ER stress pathways at the convergence of IRE1, PERK and ATF6 pathways. Here, we give a detailed explanation of the molecular

transduction events induced by the three transmembrane sensors IRE1, PERK and ATF6 and its main downstream component CHOP.

IRE1. IRE1α is a 100 KDa ER transmembrane protein that has both a kinase and an endoribonuclease domain (Kim *et al.*, 2008). Following a dissociation from BiP, IRE1α undergoes an oligomerization and an activation via autophosphorilaton (Tirasophon *et al.*, 2000). Active IRE1α processes a 26 nucleotide intron from X-box-binding protein 1 (XBP1) mRNA, thus activating the 41 KDa XBP1 transcription factor (Figure 1.2). Active XBP1s (XBP1 spliced) up-regulates genes involved in UPR and ERAD (Lee *et al.*, 2003; Malhotra and Kaufman, 2007). In addition to XBP1s, IRE1α is required for cleavage and post-transcriptional degradation of many mRNA that encode secreted proteins, thereby reducing the protein load on the ER (Hollien and Weissman, 2006).

Although IRE1α displays an intrinsic kinase activity, there are no other known substrates apart from IRE1α itself. However, prolonged activation of IRE1α is capable of transmiting a MAP kinase activation cascade. It has been shown that IRE1α can serve as a molecular platform for the recruitment of the adaptor protein TRAF2 (TNF-receptor associated factor 2), an E2 ubiquitin ligase which leads to the activation of ASK1 (apoptosis signal regulating kinase 1) a MAM3K of the JNK/p38 MAPK pathway (Urano *et al.*, 2000; Nishitoh *et al.*, 2002). Depending on the cellular context, the activation of JNK can either allow cells to adapt to ER stress by initiating autophagy or, as discussed later, promote apoptosis/autophagy in response to persistent or irrecoverable ER stress.

PERK. Like IRE1α, PERK is a protein kinase that undergoes an oligomerization and an activation via autophosphorylation following a dissociation from BiP (Bertolotti *et al.*, 2000). Activated PERK phosphorilates eIF2α (the eukaryotic initiation factor 2 α). This results in its inactivation by shutting off mRNA translation and reducing the protein load to the ER. However certain mRNAs, including ATF4 mRNA, gain a selective advantage of translation under conditions in which eIF2α is phosphorylated (on serine 51) (Lu *et al.*, 2004a) (Figure 1.2). ATF4 protein is a member of the bZIP family of transcription factors, and regulates the promoters of several genes related with the UPR such as the ER chaperones BiP and GRP94. Many of the ATF4 targets increase the levels of chaperones, restore cellular redox homeostasis, and help the ER to either fold proteins or degrade them (Kim *et al.*, 2008).

Furthermore, ATF4 induces a second transcription factor, CHOP (C/EBP-homologous protein) (Harding *et al.*, 2000; Ma *et al.*, 2002). CHOP has been implicated in ER stress-induced apoptosis, and is also involved in regaining homeostasis.The latter function is mediated by an activation of PP1 (protein phosphatase 1) which dephosphorylates P-eIF2α (Connor *et al.*, 2001).

The role of the PERK pathway in cell death regulation is unclear. Compounds that sustain phosphorilation of eIF2α (see chapter 3) provide cytoprotection during circumstances

that induce ER stress (Boyce *et al.*, 2005). However, prolonged suppression of protein synthesis is typically incompatible with cell survival and might be expected to induce autophagy. Autophagy is generally a survival mechanism but it has been associated with an induction of non-apoptotic cell death in several contexts (Levine and Kroemer, 2008).

ATF6. Once ATF6 is freed from BiP, it translocates from the ER to the Golgi where it is cleaved into two fragments by the Golgi enzymes S1P (site 1 protease) and S2P (site 2 protease) (Ye *et al.*, 2000; Shen *et al.*, 2002). These transcription factors are released into the cytosol, and migrate into the nucleus to regulate gene expression (Ye *et al.*, 2000). ATF6 stimulates ER stress genes as a homodimer or upon dimerization with XBP1s. ATF6 also collaborates with IRE1α to induce XBP1s expression (ATF6 induces the transcription of XBP1 mRNA which is spliced by the endoribonuclease activity of IRE1α). Interestingly, Yoshida et al. found that XBPu (XBP unspliced) interacts directly with the active form of ATF6 by targeting it for proteasomal degradation. This may provide a negative feedback loop to decrease XBP1 expression (Yoshida *et al.*, 2009). Known or suspected target genes of ATF6 include BiP and PDI, resulting in increased ER chaperone activity (Yamamoto *et al.*, 2007).

CHOP. The transcription factor C/EBP homologous protein (CHOP, also known as DDIT3/GADD153) operates as a downstream component of ER stress pathways at the convergence of IRE1, PERK and ATF6 pathways. CHOP is normally expressed at low levels in unchallenged conditions (Johnson *et al.*, 2011). Its gene promoter contains binding sites for all of major inducers of the UPR, including ATF4, ATF6 and XBP. Various studies have reported that these transcription factors have causative roles in inducing CHOP gene transcription (Harding *et al.*, 2000; Scheuner *et al.*, 2001; Harding *et al.*, 2003). Overexpression of the 29 KDa CHOP protein induces apoptosis through a mechanism that can be inhibited by BCL-2 (B-cell lymphoma 2) (McCullough *et al.*, 2001).

From ER Stress to Cell Death. When the initial cellular responses fail to restore the ER homeostasis, sustained ER stress causes the UPR to switch from an adaptative to a cell death pathway. However, the molecular elements of this switch are still elusive. With the exception of few components of the UPR for which a dominant prosurvival role (BiP) (Morris *et al.*, 1997) or proapoptotic role (CHOP) (Zinszner *et al.*, 1998; Maytin *et al.*, 2001) has been assigned by genetic studies, each UPR sensor holds a dualistic role in propagating adaptative as well as toxic signals (Verfaillie *et al.*, 2010).

For instance, genetic deletion of PERK or interference with eIF2α phosphorylation impairs cell survival (Harding *et al.*, 2000; Scheuner *et al.*, 2001), while artificially increasing PERK activity increases cell survival (Lu *et al.*, 2004b). However it has also been shown that sustained PERK induction is lethal, whereas the equivalent duration of IRE1 signaling is not. This suggests that the transition from protective to proapoptotic UPR

function involves a switch in IRE1 signaling along with enduring PERK activity (Lin *et al.*, 2009).

The main effector of PERK-mediated apoptosis is CHOP which can also be induced by ATF4, ATF6 and XBP1 (as seen before). However, the PERK-eIF2α branch appeared to be essential for CHOP up-regulation, reviewed in (Verfaillie *et al.*, 2010). CHOP activity is also regulated translationally by the limited CHOP mRNA lifetime (Rutkowski *et al.*, 2006) and posttranslationally by p38MAPK phosphorylation, which enhances its propapoptotic activity (Maytin *et al.*, 2001).

While the stability of prosurvival and prodeath mRNAs and proteins have been studied under conditions of mild or severe ER stress, ATF4-dependent prosurvival gene is likely to be more sustained when PERK is activated transiently and to a limited extent. In contrast, as a consequence of the intrinsic instability of the proapoptotic mRNAs and proteins, the apoptotic program mediated by the ATF4 target CHOP, would only be activated when the protective mechanisms failed and required a more sustained PERK activation (Rutkowski *et al.*, 2006).

Similar to PERK, IRE1 signaling has also been implicated in promoting or impairing cell survival. For example, when unfolded proteins accumulate, artificially extending IRE1´s RNase function led to enhanced survival (Han *et al.*, 2008b; Lin *et al.*, 2009), and the knock down of XBP1 impaired cell survival (Lee *et al.*, 2003). This points to a general protective role for the IRE1-XBP1 signaling during ER stress. However, in another report, IRE1 overexpression in HEK293T cells led to its activation in the absence of ER stress and cell death (Wang *et al.*, 1998).

Thus, the emerging consensus is that the amplitude and the temporal activation of specific arms of the UPR are crucial elements in determining cellular fate following ER stress.

1.1.3 ER Stress, Disease and Drug Discovery

ER stress has been associated with a wide range of diseases, including cancer, neurodegeneration, stroke, bipolar disorder, cardiac disease, diabetes, muscle degeneration and others (Oyadomari and Mori, 2004). Attempts to exploit the knowledge about the mechanisms linking ER stress to diseases for drug discovery have only started, but several targets for potential drug discovery are emerging.

ER Stress and Cancer. Exaggerated growth and competition for nutritional resources in the tumor determines the hostile environment of the cancer mass, which results in increased levels of hypoxia and decreased levels of glucose. During high rates of proliferation, many processes are affected and could suffer from higher levels of misfolded

proteins, DNA damage, and an insufficient supply of nutrients in the ER to meet the demand of rapidly dividing cells (Luo *et al.*, 2009). For these reasons, an adaptative defense strategy is employed by the cell to counteract the continued exposure to stress. Chronically elevated levels of ER stress assist in protecting a cancer cell from the unfavorable environment in which they exist by causing a higher chaperone availability (Schonthal, 2009). However, additional ER stress, beyond a certain critical point, results in the activation of a series of events that culminate in cell death induction due to a lack of compensating resources (Johnson *et al.*, 2011). While the basally-elevated levels of ER stress in tumor cells may actually be protective against chemotherapies, evidence also shows that further stimulation of ER stress in these cells is accompanied by an enhancement of cell death, a situation that can be exploited for anti-neoplasic treatments (Johnson *et al.*, 2011).

ER stress and apoptosis/autophagy can be used as glioma targets to develop novel chemotherapeutic agents (Johnson *et al.*, 2011). ER stress-inducing agents have the potential to become powerful anticancer agents for gliomas and other cancer cells (Johnson *et al.*, 2011). Numerous reports suggest that ER stress mediated apoptosis is able to cause selective glioma cell death. Recent Phase I clinical trial results indicate that combining of ER stress-inducing compound Bortezomib (Kardosh *et al.*, 2008) and Temozolomide, the chemotherapeutic current standard to treat malignant glioma, reduced tumor growth in patients diagnosed with glioma (Kubicek *et al.*, 2009). These data indicate that ER stress induction in glioma cells could be a valuable option to develop novel effective anti-neoplasic agents; however more studies are necessary to completely unravel the potential of such an approach reviewed by (Johnson *et al.*, 2011).

ER Stress and Alzheimer´s Disease. The accumulation of misfolded proteins is a characteristic feature of many neurodegenerative diseases (Gorman, 2008; Soto and Estrada, 2008; Winklhofer *et al.*, 2008). Neurodegenerative diseases are often described as protein conformational disorders (Soto, 2003).

Alzheimer's disease (AD) is an age-related neurodegenerative disorder, accompanied by neuronal loss and the formation of senile plaques in the brain. AD is characterized by an accumulation of unfolded or misfolded proteins in the brain. Several reports indicate an activation of UPR in AD brains (Hoozemans *et al.*, 2005; Unterberger *et al.*, 2006; Hoozemans *et al.*, 2009), suggesting a possible link between AD and ER stress. One of the proposed mechanisms of AD progression is the accumulation of amyloid β-peptide in cerebral neuritic plaques. Amyloid β activates UPR signaling, such as PERK or XBP-1 splicing, which in turn is suggested to prevent amyloid β neurotoxicity (Lee do *et al.*, 2010; Casas-Tinto *et al.*, 2011). Amyloid β-peptide is generated by a cleavage of amyloid precursor protein (APP). Presenilin-1 (PS1) and β-site APP cleaving enzyme-1 (BACE1) are important components of γ-secretase- and β-secretase-mediated cleavage of APP, respectively (see more details below). Interestingly, a familial AD-linked PS1 mutation has been shown to be

associated with ER stress (Katayama *et al.*, 1999). And eIF2α phosphorylation was proven to increase BACE1 levels (O'Connor *et al.*, 2008). PDI has been suggested to attenuate protein misfolding in neurodegenerative disease (Hosoi and Ozawa, 2012).

In recent years, research into the basic mechanisms of UPR and ER stress–related diseases has progressed rapidly. Indeed, there have been reports of several compounds that can target ER stress–regulated proteins such as eIF2α (Boyce *et al.*, 2005), IRE1 (Wiseman *et al.*, 2010; Volkmann *et al.*, 2011), and GRP78 (Kudo *et al.*, 2008).

1.2 Autophagy

Different situations that induce ER stress also lead to autophagy induction. As discussed above, ER stress response is activated to protect cells from different alterations affecting this organelle. However, when the intensity or duration of ER damage cannot be restored by this response, ER stress can also lead to cell death (Schroder and Kaufman, 2005). Likewise, autophagy can help cells cope with ER stress or participate in the mechanism of ER stress-induced cell death (Ding *et al.*, 2007b; Matus *et al.*, 2008; Soto and Estrada, 2008; Winslow and Rubinsztein, 2008).

1.2.1 What is Autophagy?

Autophagy is a cellular catabolic degradation response to starvation or stress whereby cellular proteins, organelles and cytoplasm are engulfed, digested and recycled to sustain cellular metabolism (Levine and Klionsky, 2004; Mizushima, 2007). Constitutive, basal autophagy also has an important homeostatic function, by maintaining protein and organelle quality control. Although most evidence support a role for autophagy in sustaining cell survival, paradoxically, cell death resulting from progressive cellular consumption has been attributed to unrestrained autophagy (Baehrecke, 2005; Debnath *et al.*, 2005; Reef *et al.*, 2006).

The mechanisms that regulate the mutually-opposed survival and death roles for autophagy are still unknown. The most plausible explanation is that catabolism through autophagy is predominantly survival-supporting, but that an imbalance in cell metabolism, where autophagic cellular consumption exceeds the cellular capacity for synthesis, promotes cell death (Mathew *et al.*, 2007).

1.2.2 Autophagy Machinery

There are three forms of autophagy: macroautophagy, chaperone-mediated autophagy (CMA) and microautophagy. Here we will focus on macroautophagy, which we will call autophagy (Ravikumar *et al.*, 2010), as it is the type of autophagy that we observe.

During autophagy, phagophores (also called pre-autophagosomal structures or isolation membrane), elongate and fuse while engulfing a portion of cytoplasm within double-membrane vesicles, called autophagosomes. The autophagosomes first fuse with endosomes to form hybrid organelles called amphisomes that later fuse with acidic lysosomes where the entrapped cytosolic contents are degraded (Ravikumar *et al.*, 2010) (Figure 1.3).

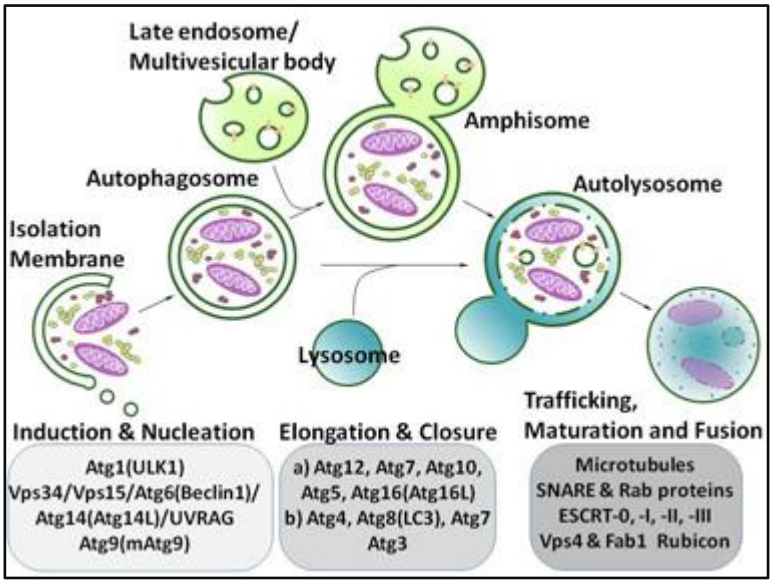

Figure 1.3 Autophagy process. Image taken from: (http://www.mssm.edu/research/labs/yue-laboratory) Autophagy has been divided in several steps: 1) Induction and nucleation with the formation of an isolation membrane (also called phagophore); 2) Elongation of this isolation membrane that leads to the formation of the autophagosome; 3) The autophagy process ends with the fusion of the autophagosome and the lysosome, the digestion of the autophagosome content and the release of the digested components back to the cytosol. In the figure are also represented the proteins that participate in each part of the process.

The molecular mechanisms responsible for the regulation of autophagy have not yet been completely elucidated, although genetic and biochemical analyses performed in the last few years have identified several autophagy genes (Atg) that participate in the regulation of

this cellular process. These genes can be grouped according to their functions at key stages of the autophagy pathway: initiation, elongation, maturation and fusion with the lysosomes.

Initiation of Autophagosome Formation. The membrane source from which autophagosomes arise is still a matter of debate. It has been hypothesized that autophagosomes can either be generated de novo from intracellular precursor molecules or, that they could arise from from other intracellular membrane structures like the ER (Axe *et al.*, 2008). The latter hypothesis has recently been supported by more evidence suggesting that ER could contribute to an autophagosome formation (Hayashi-Nishino *et al.*, 2009; Yla-Anttila *et al.*, 2009). The formation of new autophagosomes requires the activity of the class III phosphatidylinositol 3-kinase (PI3K) Vps34.Vps34 is part of the autophagy-regulated macromolecular complex (Beclin-Vps34 complex) consisting of Beclin 1/Atg6, Atg14/barkor and p150/Vps15 (Kihara *et al.*, 2001; Itakura *et al.*, 2008; Sun *et al.*, 2008) (Figure 1.4). The activity of Vps34 is enhanced by Beclin 1 (Furuya *et al.*, 2005). Several Beclin 1 binding proteins that induce autophagy have been identified: ambra-1 (Fimia *et al.*, 2007), UVRAG (Liang *et al.*, 2006) and bif-1 (Takahashi *et al.*, 2007) (Figure 1.4). On the other hand, the binding of antiapoptotic proteins Bcl-2 or Bcl-X_L to Beclin 1 inhibits autophagy (Pattingre *et al.*, 2005) (Figure 1.4). A second macromolecular complex implicated in the initiation step of autophagosome phormation is the FIP200-ULK1/Atg1 complex (Chan *et al.*, 2007).

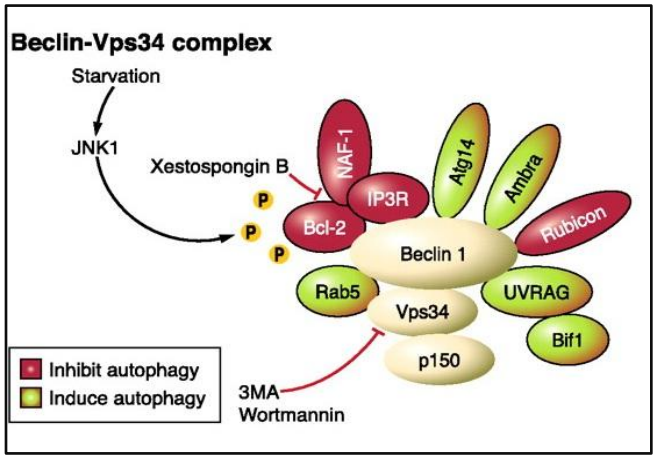

Figure 1.4 Beclin-Vps34 macromolecular complex for nucleation. Image taken from (Ravikumar *et al.*, 2010) Beclin-Vps34 macromolecular complex regulate the initiation of pre-autophagosomal structures (PAS) or phagophores formation. Several Beclin 1 binding proteins that regulate mammalian autophagy have been identified (red, inhibit autophagy; green, induce autophagy). Phosphorylation of Bcl-2 results in its dissociation from Beclin 1 to induce autophagy. NAF-1 interacts with Bcl-2 at the ER and stabilizes the Bcl-2-Beclin 1 interaction.

Elongation. Two ubiquitin-like reactions are involved in the elongation of pre-autophagosomal structures. In the first of these reactions, the ubiquitin-like protein Atg12 is covalently tagged to Atg5 (Mizushima *et al.*, 1998b). Atg12 is first activated by Atg7 (E1 ubiquitin activating enzyme-like) and then transferred to Atg10 (E2 ubiquitin activating enzyme-like). Atg12 is finally covalently linked to Atg5 (Mizushima *et al.*, 1998b). The Atg12-Atg5 complex then forms a conjugate with ATG16L1 (Prentice *et al.*, 2004). This complex is essential for the elongation of the pre-autophagosomal membrane, but dissociates from fully-formed autophagosomes (Figure 1.5).

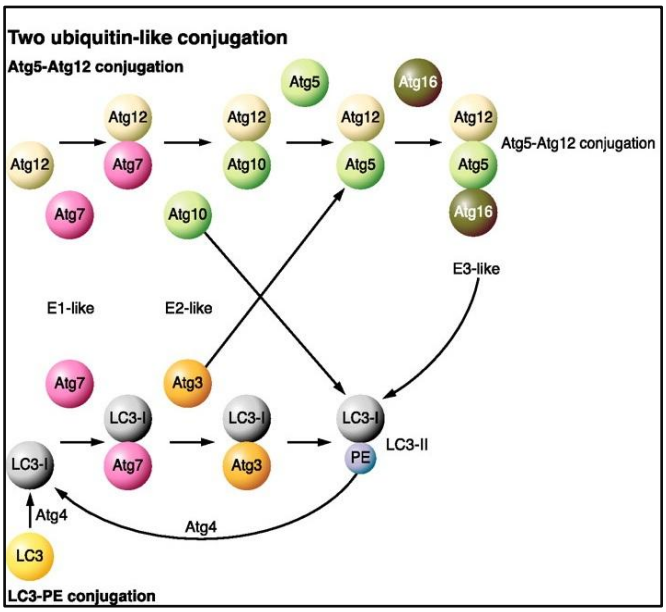

Figure 1.5 Two Ubiquitin-like conjugation complexes involved in the pre-autophagosoms elongation. Image taken from (Ravikumar *et al.*, 2010)**.** Two ubiquitin-like conjugation systems [Atg5-Atg12 conjugation and LC3-phosphatidyl ethanolamine (PE) conjugation] are involved in the elongation of PAS. The Atg5-Atg12 congugation involves Atg7 (E1-like) and Atg10 (E2-like), while Atg7 and Atg3 act as the E1-like and E2-like, respectively, in LC3-PE conjugation. The Atg12-Atg5 is noncovalently conjugated to Atg16L1 (Atg12-Atg5.Atg16L1). The Atg12-Atg5.Atg16L1 complex exhibits an E3-like activity towards LC3-PE conjugation. Cross-talk between the two ubiquitin-like systems has been implicated.

The second ubiquitin-like reaction involves the protein microtubule-associated protein 1 light chain 3 (MAP1-LC3/LC3/Atg8). LC3 is synthesized as a precursor form and is cleaved by the protease Atg4B (Hemelaar *et al.*, 2003), resulting in the cytosolic isoform LC3-I. LC3-I is conjugated to phosphatidiletanolamine (PE) in a reaction involving Atg7 (E1-like) and Atg3 (E2-like) to form LC3-II (Kihara *et al.*, 2001) (Figure 1.5). LC3-II is

specifically targeted to the elongating autophagosome membrane and, unlike the Atg12-Atg5.Atg16L1 complex, remains on completed autophagosomes until fusion with the lysosomes. After which, LC3-II on the cytoplasmic face of autolysosomes can be dilapidated by Atg4 and recycled (Tanida *et al.*, 2004). The relatively specific association of LC3-II with autophagosomes makes it an excellent marker for studying autophagy (Klionsky *et al.*, 2008).

Cross-talk between the two ubiquitin-like systems has been reported. The Atg12-Atg5.Atg16L1 complex can function in an E3 ubiquitin ligase-like manner to facilitate LC3-I conjugation to PE (Hanada *et al.*, 2007). The Atg16L1 complex is believed to bring LC3 to the site of lipidation for the final conjugation with PE, but the mechanism by which LC3 is targeted to specific membranes remains to be identified (Fujita *et al.*, 2008). Atg10 can interact with LC3 and facilitate LC3 conjugation to PE (Nemoto *et al.*, 2003). Similarly, Atg3 coimmunoprecipitates with Atg12, and overexpression of Atg3 increases Atg5-Atg12 conjugation (Tanida *et al.*, 2002b) (Figure 1.5).

Maturation and Fusion. Autophagosomes move bidirectionally along microtubules with a bias towards the microtubule organizing center (MTOC), where the lysosomes are enriched (Ravikumar *et al.*, 2010). Autophagosomes first fuse with endosomes and then with lysosomes where the fate of autophagosomes ends (Ravikumar *et al.*, 2010). In addition to the fusion machinery, proper lysosomal function is also essential for a fusion to be successful, and lysosomal acidification is required for normal fusion (Ravikumar *et al.*, 2010).

1.2.3 UPR and Autophagy

As described above, the accumulation of unfolded proteins triggers the UPR, thus promoting the inhibition of a general protein synthesis as well as an increased translation of several transcription factors that enhance the expression of ER stress genes. Evidence for a link between UPR and autophagy was obtained by Kouroku et al (Kouroku *et al.*, 2007) regarding the signaling pathways by which eIF2α phosphorilation can modulate autophagy through PERK- eIF2α dependent Atg12 up-regulation in response to polyQ protein accumulation (Kouroku *et al.*, 2007). This suggests that controlling the expression of autophagy-related genes by eIF2α down-stream targets could be one of the mechanisms connecting both events.

Activation of the IRE1 arm of the ER stress response has also been shown to regulate autophagy (Ogata *et al.*, 2006). The proautophagic actions of IRE1 seem to rely on the ability of this protein to interact with the cytosolic adaptor TRAF-2 and activate JNK (Ogata *et al.*, 2006). In addition, JNK has been shown to control Beclin 1 expression to regulate ceramide-induced autophagy (Li *et al.*, 2009). It is therefore conceivable that an activation of

the IRE1/TRAF2/JNK arm of ER stress may regulate autophagy through a modulation of Beclin 1 function and expression.

1.2.4 Autophagy, Disease and Drug Discovery

Autophagy and Cancer. From the above discussion, it is clear that ER stress and autophagy can activate both prosurvival mechanisms as well as pro-death programs, especially under persistent ER stress conditions. Thus, the activation of UPR and autophagy may either impede or facilitate drug-mediated cell killing, and will depend on the type of cancer and the cytotoxic agents used.

While growing number of reports have started to identify molecular elements of cross-talk between ER stress and autophagy, our knowledge of the functional outcome of the activation of these pathways in cancer cells responding to chemocerapeutics is still very limited.

A wide array of conventional and experimental chemotherapeutics agents have been shown to stimulate ER stress and autophagy in cancer cells. For example, tunicamycin, thapsigargin and brefeldin A activate autophagy in colon and prostate cancer cells thus mitigating ER stress and protecting against cell death (Ding *et al.*, 2007a). By contrast, cannabinoid treatment activates ER stress and autophagy leading to apoptotic cell death of glioma and pancreatic cancer cells but not of nontransformed embryonic fibroblasts or primary astrocytes (Salazar *et al.*, 2009). Likewise, other agents such as Nelfinavir (Gills *et al.*, 2008) or Melanoma differentiation associated gene-7/interleukin 24 (mda-7/IL-24) (Yacoub *et al.*, 2008) activate an ER stress response that promotes autophagy and apoptosis of cancer cells.

Understanding the precise molecular mechanism that regulate the extent of autophagy activation in response to different signals is therefore crucial in designing new antitumoral therapies based on the modulation of the ER stress-autophagy response.

Autophagy and Alzheimer´s Disease (AD). The accumulation of extracellular plaques including aggregated amyloid-β (Aβ) peptide and intracellular tangles, is associated with the pathogenesis of AD. Since Aβ is generated in the endo-lysosomal pathway, the produced Aβ is normally found in autophagosomes and lysosomes. However, in a disease state, impeded turnover of increased autophagic vacuoles due to reduced fusion or altered endocytic pathway could cause autophagic stress as shown by the accumulation of autophagic components (Nixon, 2007). Although the alteration mechanism in autophagy is complex in AD, an induction and an activation of autophagy using autophagy-related proteins such as beclin could promote a degradation of Aβ and reduce AD pathology. This would raise the possibility of using inducers of autophagy as a therapeutic target of AD

(Pickford *et al.*, 2008). However, other therapeutic modulation targeting late step in the autophagy pathway should also be considered since an impaired clearance of autophagic vacuoles has been observed in AD animal models and AD patients (Boland *et al.*, 2008; Lee *et al.*, 2011).

1.3 Cancer

The term cancer includes a range of different pathologies that present a deregulation in cell division, a loss of differentiation, an increased of cell survival and an increased of cell migration capacity as a common features (Corner and Bailey, 2001).

Tumorigenesis in humans is a multistep process which reflects genetic alterations that drive a progressive transformation of normal human cells into highly-malignant derivates (Hanahan and Weinberg, 2000).

The process by which normal cells become progressively transformed to malignant derivates can be the result of endogenous processes such as errors in the replication of deoxyribonucleic acid (DNA), the intrinsic chemical instability of certain DNA bases, the loss of heterozygosity (LOH) or from an attack by free radicals generated during metabolism. DNA damage can also result from interactions with exogenous agents such as ionizing radiation, UV radiation, and chemical carcinogens (Bertram, 2000). Cells have developed ways to repair such damages but, for various reasons, errors can occur, and permanent changes in the genome induce mutations (Bertram, 2000).

The transition from normal to tumor cell involves processes in which genes involved in homeostatic mechanisms that control cell proliferation and death participate. If these changes and mutations induce an activation of genes that stimulate the proliferation or protect the cell from death, we refer to them as proto-oncogenes. If mutations inactivate genes that normally inhibit proliferation, we refer to them as tumor suppressor genes (Bishop, 1996).

The hallmarks of cancer comprise six biological capabilities acquired during the multistep development of human tumors. They include sustaining proliferative signaling, evading growth suppressors, resisting cell death, enabling replicative immortality, inducing angiogenesis, and activating invasion and metastasis (Hanahan and Weinberg, 2011).

1.3.1 Glioma

Malignant gliomas are the most common primary brain tumors. Gliomas, which include astrocytomas, oligodendrocytomas, ependymomas, and glioblastomas although

relatively rare (1.3% incidence, 2.2% total cancer deaths), typically represent 30% of all adult brain tumors, and 80% of all adult primary brain malignant tumors (http://www.cancer.org accessed July 26, 2012). They are characterized by a local proliferation and infiltration throughout the brain parenchyma, and a robust angiogenesis. Current conventional treatments include surgery, radiation therapy and chemotherapy. Several chemotherapeutic agents, such as temozolomide (TZM), cisplatin, carmustine and lomustine have been used to slow the progression of these incurable cancers (Johnson *et al.*, 2011). However, glioma cells often acquire resistance to these agents (Hegi *et al.*, 2005). The median survival time for patients diagnosed with glioblastoma is about 12 months (Furnari *et al.*, 2007). For this reason, research efforts to search for molecular pathways to develop novel antiglioma agents and therapies are warranted.

There are several types of brain tumors, as mentioned before, and they are classified by the World Health Organization based on their cellular origin and histologic appearance.

Astrocytomas: Most tumors that develop in the brain itself start in glial cells called astrocytes. These tumors are called astrocytomas. About 2 out of 10 brain tumors are astrocytomas. Most astrocytomas can spread widely throughout the brain and mix with the normal brain tissue, which can make them very hard to remove with surgery. It is very rare for them to spread outside of the brain or spinal cord. Astrocytomas are often classified as low grade, intermediate grade, or high-grade, based on how the cells look under the microscope. The highest-grade astrocytoma, known as **glioblastoma** (or glioblastoma multiforme), is the the fastest growing one. These tumors make up about two-thirds of astrocytomas and are the most common malignant brain tumors in adults (http://www.cancer.org accessed July 26, 2012).

Oligodendrogliomas: These tumors start in brain cells called oligodendrocytes. Like astrocytomas, most of them can grow into (infiltrate) nearby brain tissue and cannot be completely removed with surgery. Oligodendrogliomas rarely spread outside the brain or spinal cord. Very aggressive forms of these tumors are known as anaplastic oligodendrogliomas. Only about 2% of brain tumors are oligodendrogliomas (http://www.cancer.org accessed July 26, 2012).

Ependymomas: These tumors arise from ependymal cells which line the ventricles. They can range from fairly low-grade (less aggressive) tumors to higher-grade ones, and are called anaplastic ependymomas. Ependymomas do not spread outside the brain or spinal cord. Ependymomas may block the exit of cerebrospinal fluid (CSF) from the ventricles, causing the ventricles to large – a condition called hydrocephalus. Unlike astrocytomas and oligodendrogliomas, ependymomas usually do not grow into (infiltrate) normal brain tissue. As a result, some (but not all) ependymomas can be completely removed and cured with surgery. But because they can spread along ependymal surfaces and CSF pathways, treating them can sometimes be difficult (http://www.cancer.org accessed July 26, 2012).

The most frequent genetic alteration found in glioma is the loss of heterozygosity of chromosome 10q, which contains functional copies of tumor suppressor genes (Fujisawa *et al.*, 2000). A key signaling pathway in the development of primary glioblastomas is the EGFR/PTEN/Akt/mTOR pathway. In fact, EGFR amplification has been identified as a genetic hallmark of glioblastomas (Kleihues and Sobin, 2000). PTEN (phosphatase and tensin homology, whose gene is located at 10q23.3), inhibits the PI3P signal, thereby inhibiting cell proliferation (Teng *et al.*, 1997). In addition, the signaling pathway Ras/MAPK is also activated in many gliomas (Tatevossian *et al.*, 2010) and phosphorylates nuclear transcription factors that induce the expression of genes promoting cell cycle progression, such as cyclin D1 (Furnari *et al.*, 2007).

The cell cycle involves a series of events which result in DNA duplication and cell division. It is divided into two stages: mitosis (M), the process of nuclear division; and interphase, the interlude between two M phases. Interphase includes the first gap phase (G_1), the DNA replication phase (S) and the second gap phase (G_2). Cells in G_1 can, before commitment to DNA replication, enter a resting (or quiescent) state called G_0, which accounts for most of the non-growing, nonproliferating and differentiated (mature) cells in the human body. The progression from one stage to the next is carefully controlled by the sequential formation, activation and subsequent degradation or modification of a series of cyclins and their partners, the cyclin-dependent kinases (CDKs), a family of serine/threonine protein kinases that are activated at specific points of the cell cycle. Transition from one stage to the next is regulated at a number of checkpoints which prevent premature entry into the next phase of the cycle (Vermeulen *et al.*, 2003; Macdonald *et al.*, 2004).

The retinoblastoma protein (pRb) and p53 regulate the cell cycle primarily by governing the G_1 to S phase transition, and are major targets of inactivating mutations in glioblastomas. The absence of these cell cycle guardians renders tumors particularly susceptible to inappropriate cell division driven by constitutively active mitogenic signaling effectors, such as PI3K and MAPK. In its hypophosphorylated state, pRb blocks proliferation by binding and inhibiting the proliferation-inducing transcription factors E2F. This prevents the expression of genes that are essential for a progression from G_1 into S phase (Sherr and McCormick, 2002). Upon mitogenic stimulation, the activation of the MAPK cascade leads to the association of the CDK4/cyclin D1 complex that phosphorylates pRB, thereby releasing active E2F. In turn, $p16^{INK4}$ binds to CDK4, inhibits the CDK4/cyclin D1 complex and, therefore, the G1 to S transition (Sherr and Roberts, 1999). In glioblastomas, disruption of the $p16^{INK4}$ gene occurs through homozygous deletion (Kleihues and Sobin, 2000). The p53 tumor suppressor is a transcription factor that prevents the propagation of cells with unstable genomes, predominantly by halting the cell cycle in the G1 phase or instigating a program of apoptosis or proliferative arrest (Vousden and Lu, 2002). Loss of p53, through either point mutations that prevent DNA binding or loss of chromosome 17p, is a frequent

and early event in the pathological progression of secondary glioblastomas (Ichimura *et al.*, 2004; Furnari *et al.*, 2007).

1.3.2 Treatment of Glioma and ER Stress

Gliomas have been shown to be sensitive to agents that interfere with ER stress. Agents affecting ER Ca^{2+} homeostasis, such as flavonoids, curcumin, and non-steroidal anti-inflammatory drugs (NSAID), such as celecoxib, cause protein unfolding and highly activate ER stress and cell death in glioma cells (Thastrup *et al.*, 1990; Bilmen *et al.*, 2001; Johnson *et al.*, 2002; Pyrko *et al.*, 2007a; Das *et al.*, 2010). Agents directly interfering with protein folding or maturation, such as tunicamycin or brefeldin A, cause an induction of ER stress and cell death. Agents able to affect misfolded protein removal, which are inhibitors of proteasome activity, such as specific agents like bortezomib (Kardosh *et al.*, 2008) and human immunodeficiency virus protease inhibitors (HIV-PIs) (Pyrko *et al.*, 2007b; Kardosh *et al.*, 2008), are associated with high levels of ER stress-induction in glioma cells, and cause gliotoxicity. Ideal candidate molecules for chemotherapeutic potential would increase ER stress in cancer cells enough to activate the pro-death arms of ER stress, yet only induce the prosurvival arms in normal cells, resulting in tumor specific effects. Such a strategy could result from a decreased ability of tumor cells to cope with additional ER stress compared to normal cells. This provides two options for targeting ER stress as an antineoplastic therapy: (1) the ER stress cascade itself could be targeted to induce cell death directly, or (2) ER stress could be exacerbated to make cells susceptible to other chemotherapies (Schonthal, 2009).

1.3.3 Membrane Lipid Therapy: Anti-tumoral Effect of 2OHOA

Previous works showed that the membrane lipid structure influences cell signaling (Escribá *et al.*, 1995; Escribá *et al.*, 1997; Vögler *et al.*, 2004). Thus, for example, the presence of the nonlamellar-prone lipid glycerophosphoethanolamine (gPE) favors the binding of heterotrimeric Gi proteins and $G_{\beta\gamma}$ dimmers to model membranes, whereas $G_{\alpha i}$ subunit prefers lamellar structures. Consequently, the association of both G protein-coupled receptors and G proteins to the plasma membrane makes them susceptible to their lipid environment so that lipid-protein interactions are crucial to their function. Furthermore, the types and relative abundance of lipids in the membrane not only control numerous functions but also regulate the localization and activity of membrane proteins (Vögler *et al.*, 2004). Thus, molecules that interact with membrane lipids and modify the composition and structure of cell membranes can change the localization and/or activity of membrane

proteins. The result of these effects is the modulation of certain signaling pathways that reverse the pathological state.

Due to this participation in cellular activities, membrane lipids might constitute targets for drugs whose pharmacological effects would be associated with a modulation of the composition, structure and physicochemical properties of membranes, as stated in the Membrane Lipid Therapy (Escribá, 2006). Indeed, G proteins, PKC, and heat shock proteins are among the proteins regulated by membrane-lipid therapy, and the therapeutic agents used (for example, 2OHOA) can inhibit cell proliferation or induce apoptosis and cell differentiation (Escribá *et al.*, 2008).

In this context, it was demonstrated that the antitumor effect of antracyclines and the ensuing modifications in cell signaling, involved interactions with the plasma membrane without unspecific interactions with other cell targets (Triton and Yee, 1982; Escribá *et al.*, 1995). Based on these results, 2-hydroxy-9-cis-octadecenoic acid (2OHOA), patented and registered as Minerval®, was rationally designed by our group. A first approach showed that 2OHOA binds to membranes and modifies the biophysical properties of the lipid bilayer in model membranes (Barceló *et al.*, 2004; Martinez *et al.*, 2005).

The mechanism of action of 2OHOA is associated with important changes in membrane lipid composition, primarily a recovery of sphingomyelin (SM) levels, which are markedly low in glioma (and other types of cancer) cells before treatment (Barceló-Coblijn *et al.*, 2011). The rapid sphingomyelin synthase (SMS) activation by 2OHOA suggests that this could be one of the first critical events in its effects against tumors (Barceló-Coblijn *et al.*, 2011). This modification in the membrane lipid composition results in changes in the localization and activity of peripheral signaling proteins (Martínez *et al.*, 2005b). Further studies demonstrated that 2OHOA induces cell cycle arrest in human lung adenocarcinoma cells by causing, both in vitro and in vivo PKC translocation to the plasma membrane and by downregulating the expression of certain cyclins, CDKs, E2F- 1 and dihydrofolate reductase (DHFR), a protein directly involved in DNA synthesis (Martínez *et al.*, 2005a; Martínez *et al.*, 2005b; Lladó *et al.*, 2009). Interestingly, DHFR downregulation is also involved in the effect of 2OHOA on human leukemia cells, where it induces ligand-independent Fas receptor (FasR) capping and apoptosis (Lladó *et al.*, 2010). In addition, cell cycle arrest was followed by cancer cell differentiation in human glioma cells, as a result of the translocation of Ras to the cytosol and the subsequent inhibition of the ERK (MAPK) pathway. These effects in turn contribute to the inactivation of the cyclin/CDK/RB/E2F-1/DHFR and PI3K/Akt pathways. Moreover, an increased expression of the cyclin/CDK inhibitors p21Cip1 and p27Kip1 caused further reductions in the phosphorylation of Rb and triggered autophagic cell death (Terés *et al.*, 2012).

Despite the efficiency of 2OHOA against cancer, it is a safe non-toxic compound with IC_{50} values of 30 to 150-fold greater in non-tumor IMR90 fibroblasts cells than in tumor

cells (Lladó *et al.*, 2010). This lack of toxicity was confirmed by GLP (Good Laboratory Practice) studies, showing that the minimum lethal dose is greater than 3,000 mg/kg and that no undesired side effects were observed at therapeutic doses (Martínez *et al.*, 2005a; Terés *et al.*, 2012).

In this context, although the first steps in the anticancer mechanism of action of 2OHOA are known, the last cellular and molecular events that cause cancer cell death still remain unclear. In the present study, we provide evidence of the molecular mechanisms underlying the death of various human glioma cell lines, which explains not only the efficacy of this compound against cancer cells but also its safety based on a lack of action against normal cells.

As we discussed above, ideal candidate molecules for chemotherapeutic potential would increase ER stress in cancer cells enough to activate the pro-death arms of ER stress, yet only induce the prosurvival arms in normal cells, resulting in tumor specific effects. With this idea in mind we tried to figure out whether the unfolded protein response (UPR) induced by ER stress was involved in the action mechanism of 2OHOA against cancer (glioma). Despite the effectiveness of 2OHOA against cancer, it is a safe non-toxic compound. For this reason, the UPR could be the specific action mechanism by which 2OHOA exerts its activity against glioma cells, as tumor cells have a decreased ability to cope with additional ER stress compared to normal cells.

In a previous study, we showed that cancer cells have very low membrane sphingomyelin and high phosphatidylethanolamine levels (Barceló-Coblijn *et al.*, 2011). In glioma and other types of cancer cells, but not normal cells, 2OHOA induces changes in these lipids to reach values found in healthy tissues. The present study sheds light on the signaling events that follow an activation of this molecular switch. In this thesis, we demonstrate a selective induction of several key effectors of ER stress/UPR by 2OHOA in three human glioma cell lines while only inducing the prosurvival arms of the UPR in normal cells. Moreover, we provide cellular and molecular evidence that 2OHOA induces autophagy in these glioma cells but not in non-cancer cells. This may constitute a novel therapeutic strategy to combat glioma when cells are reluctant to enter apoptosis.

In conclusion, the design of new lipid molecules like 2OHOA that can modulate ER stress/UPR constitutes a promising and novel approach to treat gliomas and other neoplasias.

1.4 Alzheimer´s Disease

Alzheimer´s disease (AD) is a highly debilitating neurodegenerative disorder that affects millions of people, with an enormous impact on our society. AD is the primary cause of dementia among the elderly, and one of the major health problems worldwide. In 2006,

there were 26.6 million sufferers in the world. This disease is predicted to affect 1 in 85 people globally by 2050 (Brookmeyer *et al.*, 2007). Since its first description by Alois Alzheimer in 1907 (Alzheimer, 1907; Berchtold and Cotman, 1998), noticeable but insufficient scientific understanding of this complex pathology has been achieved.

There are two main forms of the disease: **Familial Alzheimer's disease** (FAD), also called Early onset Familial Alzheimer's disease (EOFAD), is an uncommon form of Alzheimer's disease that usually strikes earlier in life (usually between 50 and 65 years of age, but as early as 15). This form of AD is inherited in an autosomal dominant fashion, identified by genetics and other characteristics such as the onset age. It accounts for approximately half of the early-onset Alzheimer's disease cases. Familial AD requires the patient to have at least one first degree relative with a history of AD. Non-familial cases of AD are referred to as "**sporadic**" **AD**, where genetic risk factors are minor or unclear.

While early-onset familial AD is estimated to account for only 5% of total Alzheimer's disease (Harvey *et al.*, 2003), it has presented a useful model in studying various aspects of the disorder. Currently, the early-onset familial AD gene mutations are guiding the vast majority of animal model-based therapeutic discovery and developments for AD.

1.4.1 Alzheimer´s Disease Pathogenicity

Alzheimer´s disease pathology is characterized by the formation of two types of protein aggregates in the brain: amyloide plaques or senile plaques (SPs), which form an extracellular lesion composed by Aβ peptide; and intracellular neurofibrillary tangles (NFTs), which are composed of hyperphosphorilated filaments of the microtubule-associated protein tau. Genetic evidence implicates deregulated Aβ homeostasis as an early event in Alzheimer´s disease pathology (Masters *et al.*, 1985).

1.4.1.1 Amyloid Cascade Hypothesis

The Amyloid Cascade Hypothesis which affirms that the deposition of amyloid β peptide in the brain is a central event in Alzheimer´s disease pathology, has dominated research for the past twenty years (Karran *et al.*, 2011).

Two key observations resulted in the original formulation of the Amyloid Cascade Hypothesis. First, the detection of Aβ as a main constituent of SPs (Glenner and Wong, 1984) and, second, mutations of the amyloid precursor protein (APP) (Goate *et al.*, 1991), Presenilin-1 (PS-1) and Presenilin-2 (PS-2) genes (Levy-Lahad *et al.*, 1995; Sherrington *et al.*, 1995), which were found in families with early onset of AD.

Amyloid Precursor Protein (APP) Processing: APP is produced in large quantities in neurons and is metabolized very rapidly (Lee *et al.*, 2008). Multiple alternate pathways

exist for APP proteolysis. Some of which lead to the generation of the Aβ peptide (Figures 1.6 and 1.7) while some do not (Figure 1.7). After sorting in the endoplasmic reticulum and Golgi, APP is delivered to the axon, where it is transported by fast axonal transport to synaptic terminals (Koo et al. 1990). (Koo *et al.*, 1990).

Crucial steps in APP processing occur at the cell surface and in the trans-Golgy network (TGN). From the TGN, APP can be transported to the cell surface or directly to an endosomal compartment. Clathrin-associated vesicles mediate both these steps. On the cell surface, APP can be proteolyzed directly by α-secretase, and then γ-secretase (a process that does not generate Aβ, see Figure 1.7), or reinternalized in clathrin-coated pits into another endosomal compartment containing the proteases BACE1 (β secretase) and γ-secretase. The latter results in the production of Aβ (Figures 1.6 and 1.7), which is then dumped into the extracellular space following vesicle recycling or degraded in lysosomes. Although most APP must pass through the cell surface as part of its processing, this step is very rapid, as little APP is on the surface at any point in time. Why some surface APP is internalized into endosomes and why some proteolyzed directly by α-secretase is unclear, although the segregation of APP and BACE1 into lipid rafts may be a crucial element (Ehehalt et al. 2003) (Ehehalt *et al.*, 2003). Finally, to complete the APP cycling loop, retrograde communication occurs between endosomal compartments and the TGN, mediated by a complex of molecules called retromers.

The enzymes that cleave APP have been extensively characterized. BACE1, a transmembrane protease, is directly involved in the cleavage of APP at the +1 and +11 sites of Aβ. Neurons from BACE1−/− mice do not produce Aβ, confirming that BACE1 is the neuronal β-secretase (Cai et al. 2001) (Cai *et al.*, 2001). Following BACE1 cleavage and the release of the sAPPβ ectodomain, the APP C-terminal fragment is cleaved by the γ-secretase complex at one of several sites varying from +40 to +44 to generate Aβ peptides (1–40 and 1–42 being most common), and the APP intracellular domain (Figure 1.6).

γ-secretase is a multiprotein complex composed of presenilin 1 (PS1) or presenilin 2 (PS2); nicastrin (Nct), a type I transmembrane glycoprotein; and Aph-1 (anterior pharynx-defective 1) and Pen-2 (presenilin enhancer 2), two multipass transmembrane proteins (Figure 1.6) (Bergmans and De Strooper, 2010). This complex is essential for the sequential intramembranous proteolysis of a variety of transmembrane proteins. PS1 and PS2 contain two aspartyl residues that play crucial roles in intramembranous cleavage (De Strooper *et al.*, 1999; Wolfe *et al.*, 1999). The functions of the various γ- secretase proteins and their interactions in the complex are not yet fully defined. It has been suggested that the ectodomain of nicastrin recognizes and binds to the aminoterminal stubs of previously cleaved transmembrane proteins. Aph-1 aids the formation of a precomplex, which interacts with PS1 or PS2 while Pen-2 enters the complex to initiate the cleavage of PS1 or PS2 to

form an N-terminal 28-kDa fragment and a C-terminal 18-kDa fragment, both of which are critical to the γ-secretase complex (Takasugi *et al.*, 2003).

Several aspects of the standard model need to be mention. α-cleavage of APP (+17) is attributed to the ADAM (a disintegrin and metalloproteinase) family of proteases (Asai *et al.*, 2003; Jorissen *et al.*, 2010) and occurs, to a large extent, on the cell surface. However, there is some α-secretase activity in the trans-Golgi. This is of some significance because the activation of the protein kinase C (Mills and Reiner, 1999) causes a significant increase in α-cleavage of APP by increasing the transport of APP to the cell surface (Hung *et al.*, 1993), by blocking the access of cell surface APP to endosomes, and by stimulating α-cleavage in the TGN (Skovronsky *et al.*, 2000). Because α-cleavage occurs within the Aβ sequence, it prevents Aβ generation. Indeed, an increased expression of ADAM 10 or SIRT1, a regulator of ADAM 10 gene expression, significantly attenuated Aβ deposition and cognitive deficits in a mouse model of AD (Postina *et al.*, 2004; Donmez *et al.*, 2010).

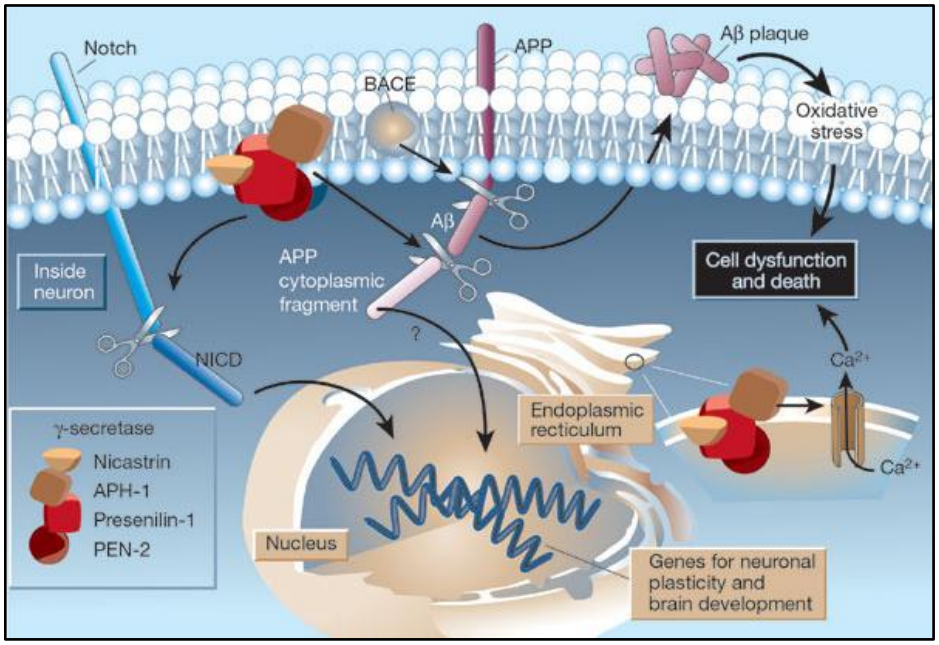

Figure 1.6 The γ-secretase complex, and its roles in brain development and Alzheimer's disease. Presenilin-1, nicastrin, APH-1 and PEN-2 form a functional γ-secretase complex, located in the plasma membrane and endoplasmic reticulum (ER) of neurons. The complex cleaves Notch (left) to generate a fragment (NICD) that moves to the nucleus and regulates the expression of genes involved in brain development and adult neuronal plasticity. The complex also helps in generating the amyloid β-peptide (Aβ; centre). This involves an initial cleavage of the amyloid precursor protein (APP) by an enzyme called BACE (or β-secretase). The γ-secretase then liberates Aβ, as well as an APP cytoplasmic fragment, which may move to the nucleus and regulate gene expression. Mutations in presenilin-1 that cause early-onset Alzheimer's disease enhance γ-secretase activity and Aβ production, and also perturb the ER calcium balance. Consequent neuronal degeneration may result from membrane-associated oxidative stress, induced by aggregating forms of Aβ (which create Aβ plaques), and by the perturbed calcium balance. Figure taken from (Mattson, 2003).

The cleavage and processing of APP can be divided into a non-amyloidogenic pathway and into an amyloidogenic pathway. In the prevalent non-amyloidogenic pathway, APP is cleaved by the α-secretase at a position 83 amino acids from the carboxy (C) terminus, producing a large amino (N)-terminal ectodomain (sAPPα) which is secreted into the extracellular medium (Kojro and Fahrenholz, 2005). Importantly, cleavage by the α-secretase occurs within the Aβ region, thereby precluding Aβ formation. The amyloidogenic pathway is an alternative cleavage pathway for APP which leads to Aβ generation. The initial proteolysis is mediated by the β-secretase at a position located 99 amino acids from the C terminus. This cut results in the release of sAPPβ into the extracellular space, and leaves the 99-amino-acid C-terminal stub (known as C99) within the membrane, with the newly-generated N terminus corresponding to the first amino acid of Aβ. Subsequent cleavage of this fragment (between residues 38 and 43) by the γ-secretase liberates an intact Aβ peptide. Most of the full-length Aβ peptide produced is 40 residues in length (Aβ40), whereas a small proportion (approximately 10%) is the 42 residue variant (Aβ42). The Aβ42 variant is more hydrophobic and more prone to fibril formation than Aβ40 (Jarrett *et al.*, 1993). This longer form is also the predominant isoform found in cerebral plaques (Younkin, 1998). The details of amyloidogenic and non-amyloidogenic processing of APP are illustrated in Figure 1.7.

As we mention above, mutations in the three genes -APP, PS1 and PS2- are known to cause autosomal dominant AD, which generally manifests itself with an early-onset pathogenesis (St George-Hyslop and Petit, 2005).

The Aβ peptide was first identified as a component of extracellular amyloid plaques in the mid-1980s. Not long after, reports describing the existence of intracellular Aβ were published (Grundke-Iqbal *et al.*, 1989). These findings also suggested that the occurrence of intracellular Aβ might not have bene an age-dependent event. Curiously, however, the authors also reported that the Aβ-immunoreactive material was frequently present in NFT-containing neurons (Grundke-Iqbal *et al.*, 1989), perhaps an indicator that these two pathologies could be linked (Blurton-Jones and Laferla, 2006).

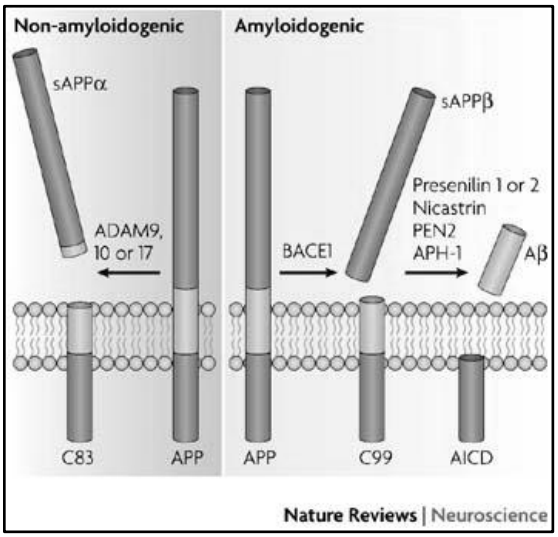

Figure 1.7 The amyloid-β(Aβ) peptide is derived via proteolysis from a larger precursor molecule called the amyloid precursor protein (APP), a type 1 transmembrane protein consisting of 695–770 amino acids. APP can undergo proteolytic processing by one of two pathways. Figure taken from (LaFerla *et al.*, 2007). Most is processed through the non-amyloidogenic pathway, which precludes Aβ formation. The first enzymatic cleavage is mediated by α-secretase, of which three putative candidates belonging to the family of a disintegrin and metalloprotease (ADAM) have been identified: ADAM9, ADAM10 and ADAM17. Cleavage by α-secretase occurs within the Aβ domain, thereby preventing the generation and release of the Aβ peptide. Two fragments are released, the larger ectodomain (sAPPα) and the smaller carboxy-terminal fragment (C83). Furthermore, C83 can also undergo an additional cleavage mediated by γ-secretase to generate P3 (not shown). APP molecules that are not cleaved by the non-amyloidogenic pathway become a substrate for β-secretase (β-site APP-cleaving enzyme 1; BACE1), releasing an ectodomain (sAPPβ), and retaining the last 99 amino acids of APP (known as C99) within the membrane. The first amino acid of C99 is the first amino acid of Aβ. C99 is subsequently cleaved 38–43 amino acids from the amino terminus to release Aβ, by the γ-secretase complex, which is made up of presenilin 1 or 2, nicastrin, anterior pharynx defective and presenilin enhancer 2. This cleavage predominantly produces Aβ1–40, and the more amyloidogenic Aβ1–42 at a ratio of 10:1. AICD, APP intracellular domain; APH-1, anterior pharynx defective; PEN2, presenilin enhancer2.

1.4.1.2 Tau-mediated Neurodegeneration

Tau is a cytoplasmic protein that binds to tubulin during its polymerization, stabilizing microtubules (MTs). Aside from its well-established role in promoting the stabilization of MTs, tau may have additional functions because of its interactions with other structures and enzymes (for example, with the plasma membrane (Brandt *et al.*, 1995; Maas *et al.*, 2000), the actin cytoesqueleton (Fulga *et al.*, 2007) and with src tyrosine kinases (Lee, 2005).

AD is characterized by an extensive deposition of Aβ peptide and the formation of neurofibrillary tangles (NFTs) consisting in hyperphosphorylated Tau as intraneuronal inclusions (Selkoe, 1986). Aβ hypothesis states that Aβ deposition directly affects neurons inducing NFTs and neuronal death leading to dementia (Takashima, 2012). However, the

number of NFTs, unlike the extent of Aβ deposition, correlates strongly with the degree of dementia (Gomez-Isla *et al.*, 1997). In diseased brains, synaptic and neuronal loss are prominent in regions with detectable NFTs, implicating NFT formation in AD associated memory impairment and dementia (Masliah *et al.*, 1992). Before NFT formation, tau is hyperpphosphorylated by glycogen synthase kinase 3β (GSK-3β) activation and forms granular tau oligomers. This hyperphosphorylated tau is associated with synapse loss (Kimura *et al.*, 2007), while granular tau oligomers are involved in neuronal death (Kimura *et al.*, 2010).

It has been suggested that NFTs in themselves are not toxic. Instead, the processes of NFT formation, neuronal death and neuronal dysfunction may underlie the pathogenic mechanism (Ramsden *et al.*, 2005; Spires *et al.*, 2006).

The formation of tau fibrils follows three sequential steps (Kimura *et al.*, 2007; Maeda *et al.*, 2007; Takashima, 2008). First, hyperphosphorylated monomeric tau binds together to form soluble oligomers. Second, the soluble tau oligomers take on a β-sheet structure, forming insoluble tau aggregates. These aggregates become granular-shaped oligomers consisting of approximately 40 tau molecules. Third and finally, the increased concentration of granular tau causes these oligomers to fuse, forming tau fibrils.

As a major tau kinase, GSK-3β induces tau hyperphosphorylation, as one of the earliest events of NFT formation (Ishiguro *et al.*, 1988; Ishiguro *et al.*, 1993). However, additional kinases may be involved in this process (Morishima-Kawashima *et al.*, 1995).

Aβ activates GSK-3β, inducing tau hyperphosphorylation in hippocampal neurons. It is this GSK-3β activation that leads to reduce hippocampal long term potentiation and eventual memory impairment in APP Tg mice (Takashima, 2012). Evidence shows that activation of GSK-3β is a key factor in AD-associated memory impairment. This promotes the idea that inhibitors of GSK-3β, may be potential therapeutic agents for this disease (Takashima, 2012).

1.4.2 Preliminary Results: Alzheimer´s Disease Treatment

In the context of the membrane lipid therapy (see section 1.3.3) new molecules were designed in our group for the treatment of AD. We developed a series of synthetic carbon alpha hydroxylated derivatives [2-hydroxyarachidonic acid (LP204A1), 2-hydroxyeicosapentaenoic acid (LP205A1), and 2-hydroxydocosahexanoic acid (LP226A1)] from its lipid precursors [arachidonic acid (ARA), eicosapentaenoic acid (EPA), docosahexaenoic acid (DHA)].

We chose these molecules because 24 h-treatments of human neuroblastoma SH-SY5Y cells with ARA (20:4), EPA (20:5) and DHA (22:6) increased sAPPα secretion and

membrane fluidity, whereas treatments with stearic acid (SA, 18:0), oleic acid (OA, 18:1), linoleic acid (LA, 18:2) and α-linolenic acid (ALA, 18:3) did not (Yang *et al.*, 2011). These results suggested that not all unsaturated fatty acids but only those with 4 or more double bonds, such as ARA, EPA and DHA, were able to increase membrane fluidity and lead to increase in sAPPα secretion (Yang *et al.*, 2011).

Docosahexanoic acid (DHA) is an omega n-3 polyunsaturated fatty acid found in fish and some marine algae. Sixty percent of the fatty acids that make up neuronal cell membranes of the retina consist of DHA, which is found particularly concentrated in synaptic membranes (Bazan and Scott, 1990). DHA is essential for prenatal brain development, and for healthy postnatal brain function.

Alzheimer disease patients have significantly lower DHA levels compared to control subjects, and serum cholesteryl ester-DHA levels are progressively reduced depending on the severity of clinical dementia (Tully *et al.*, 2003). A previous omega-3 fatty acid treatment (a mixture of DHA and EPA) clinical trial in Sweden demonstrated a significant ($P < .05$) reduction in MMSE (mini mental state examination) decline rate in the omega-3 fatty acid-treated group compared with the placebo group in a subgroup of patients with a very mild cognitive dysfunction. This was observed at 6 and 12 months (Freund-Levi *et al.*, 2006).

It has already been proven that DHA rich diets reduce PS-1 levels (Green *et al.*, 2007). Drugs which modulate γ-secretase activity as (R) – flurbiprofen effectively reduce amyloid plaque formation (Imbimbo *et al.*, 2007) and rescue memory deficits (Kukar *et al.*, 2007) in APP-transgenic mice. Moreover, our research group has obtained similar results related to memory improvement in 5XFAD mice treated with LP226A1 (Fiol M.A., manuscript in preparation). 5XFAD mice co-express and co-inherit Familial AD (FAD) mutant forms of human APP (the Swedish mutation: K670N, M671L; the Florida mutation: I716V; the London mutation: V717I) and PS1 (M146L; L286V) transgens under transcriptional control of the neuron-specific mouse Thy-1 promoter (Oakley *et al.*, 2006). We found a significant impairment in memory in the 5XFAD mouse model in both working memory (WM) and reference memory (RM) function (Olton and Samuelson, 1976; Olton and Papas, 1979; Wirsching *et al.*, 1984) by the Radial Arm Maze (RAM) test together with a decrease in hippocampal neurogenesis at 7 months of age, when there is a massive accumulation of Aβ (Fiol M.A., manuscript in preparation). Chronic treatment with LP226A1 resulted in the recovery of spatial memory impairment, with a major improvement in working memory. This improvement in spatial memory was concomitant with a recovery in the hippocampal neurogenesis rate (Fiol M.A., manuscript in preparation).

In this thesis, we have studied the expression of several Alzheimer´s disease-related proteins on SH-SY5Y human neuroblastoma cells differentiated into neuron-like cells and treated with the three hydroxy derivates, LP226A1 (2OH-DHA), LP204A1 (2OH-ARA), and LP205A1 (2OH-EPA). The proteins we have studied are α-, β- and γ-secretases,

hyperphosphorilated tau, GSK3β, and P-GSK3β. We have noticed a down-regulation of β- and γ-secretases, a hyperphosphorilated tau, and an inhibition of GSK3β after treatment. These results suggest that these hydroxy derivates may slow down AD progression by reducing the accumulation of amyloid β-peptide and NFTs.

Moreover, we have deepened our understanding of the molecular mechanisms involved in neuronal recovery by paying special attention to the UPR and autophagy pathways as they could be involved in the removal of NFTs and amyloid β-peptide in senile plaques. AD is characterized by an accumulation of unfolded or misfolded proteins in the brain, and several reports indicate the activation of UPR in AD brains (Hoozemans *et al.*, 2005; Unterberger *et al.*, 2006; Hoozemans *et al.*, 2009), suggesting a possible link between AD and UPR.

Our results demonstrate UPR activation in the SH-SY5Y cells treated with LP226A1, LP205A1 and LP204A1. The hydroxy derivate treatments only induce the prosurvival arms of the UPR (at therapeutic doses). In addition, the treatment of SH-SY5Y cells with the molecules also activated autophagy response.

For this reason, UPR and autophagy could be an action mechanism by which LP226A1, LP205A1 and LP204A1 exert their activites.

2. Aim of the Study

The main goal of the present study was to investigate unfolded protein response and autophagy pathways induced by treatments with different hydroxy fatty acid derivatives in the context of central nervous system (CNS, brain) conditions, such as glioma and Alzheimer´s Disease. My approach was as follows:

- To study the effect on cell viability and cell cycle progression of several human glioma cells in comparison with non-cancer cells, all treated with 2OHOA;
- To analyze the unfolded protein response induced by 2OHOA treatment of human glioma cells in comparison with non-cancer cells;
- To study autophagy cell death process induced by 2OHOA treatment of human glioma cells in comparison with non-cancer cells;
- To investigate α, β and γ secretase regulation in SH-SY5Y neuron-like cells treated with LP226A1, LP204A1 and LP205A1;
- To investigate P-Tau and GSK-3β regulation in SH-SY5Y neuron-like cells treated with LP226A1, LP204A1 and LP205A1;
- To determine whether unfolded protein response and autophagy are implicated in the neuro protective effects linked to LP226A1, LP204A1 and LP205A1 treatments of SH-SY5Y neuron-like cells.

3. ER Stress and Autophagy in the Selective Effect of 2OHOA against Human Glioma

3.1 Introduction

2-Hydroxyoleic acid (the α-hydroxy derivative of oleic acid, 2OHOA, Minerval), binds to the plasma membrane, and alters the organization of its lipids (Barceló *et al.*, 2004), by increasing the propensity to form non-lamellar (hexagonal H_{II}) lipid phases (Barceló *et al.*, 2004; Martinez *et al.*, 2005; Cordomi *et al.*, 2010). Interestingly, this modification inhibits the growth of lung cancer (A549) cells and induces apoptosis in human leukemia (Jurkat) cells (Martínez *et al.*, 2005a; Martinez *et al.*, 2005; Lladó *et al.*, 2010). The changes that 2OHOA produces to the membrane structure influences the location and activity of amphitropic membrane proteins involved in proliferation/differentiation signaling (Barceló *et al.*, 2004; Martinez *et al.*, 2005; Cordomi *et al.*, 2010). This eventually leads to a down-regulation of E2F-1 and dihydrofolate reductase (DHFR), both pivotal proteins in cancer cell proliferation (Martínez *et al.*, 2005a; Lladó *et al.*, 2009). Although the first steps in the anticancer mechanism of action of 2OHOA are known, in this context, we are still unclear which last cellular and molecular events cause the cancer cell to die. In this study, we provide evidence of the molecular mechanisms underlying the death of various human glioma cell lines, and we explain not only the efficacy of this compound against cancer cells but also its safety due to its limited action against normal cells.

In a cell, the endoplasmic reticulum (ER) fulfills three main functions: 1) protein folding, glycosylation and sorting; 2) synthesis of cholesterol and other lipids; and 3) maintenance of Ca^{2+} homeostasis (Jakobsen *et al.*, 2008). Disrupting any of these processes causes ER stress, and activates the unfolded protein response (UPR) (Jakobsen *et al.*, 2008).

These disruptions, can be achieved with a number of cytotoxic agents, such as brefeldin A (Klausner *et al.*, 1992), tunicamycin (Han *et al.*, 2008a) or the fatty acid palmitate (Karaskov *et al.*, 2006). The molecular elements associated with UPR up-regulate genes that support the recovery from ER stress or that initiate apoptosis in cases of severe cell damage (Jakobsen *et al.*, 2008).

Three main pathways mediate UPR signaling: the inositol-requiring enzyme 1 (IRE1) pathway; the eukaryotic translation initiation factor 2a kinase 3 (PERK) pathway; and the activating transcription factor 6 (ATF6) pathway (Jakobsen *et al.*, 2008). Key proteins in these pathways include IRE1α (involved in the regulation of apoptosis and the differentiation/proliferation MAPK-dependent pathways) and its ribonuclease product XBP1 (a transcription factor that induces the expression of genes involved in restoring protein folding or degrading unfolded proteins) (Kim *et al.*, 2008). Together with XBP1, ATF4 and ATF6 regulate the expression of the C/EBP homologous protein (CHOP), one of the main effectors of ER stress/UPR-induced apoptosis (Oyadomari and Mori, 2004). Another important element is PERK, whose intrinsic kinase activity is induced by oligomerization, resulting in the phosphorylation of the eukaryotic translation initiation factor 2α (eIF2α) and the suppression of global mRNA translation. Under these conditions, only selected mRNAs are translated, including ATF4 (Lu *et al.*, 2004a), which induces the expression of genes involved in the restoration of ER homeostasis and in autophagy (Lu *et al.*, 2004a; Fujita *et al.*, 2007; Kouroku *et al.*, 2007). Accordingly, compounds that promote the sustained phosphorylation of eIF2α, such as salubrinal (Boyce *et al.*, 2005), may exert cytoprotective effects. However, a prolonged suppression of protein synthesis is incompatible with cell survival, resulting in autophagy (Kim *et al.*, 2008), Thus, eIF2α phosphorylation and ATF4 both stimulate the expression of genes associated with autophagy (Lu *et al.*, 2004a; Kouroku *et al.*, 2007).

Autophagy is a cellular process that mediates the recycling of cytoplasmic macromolecules and structures through the formation of membrane double-bounded vacuoles. Called autophagosomes, these vacuoles engulf and degrade large portions of cells (Mizushima *et al.*, 2008; Martinet *et al.*, 2009). Autophagy has also been associated with the induction of non-apoptotic cell death (Kim *et al.*, 2008). The accumulation of misfolded protein aggregates in the ER that cannot be degraded by the proteosome results in the up-regulation of the UPR and the expression of autophagy-related genes (Ogata *et al.*, 2006; Kouroku *et al.*, 2007). Although both the UPR and autophagy can function independently, recent studies have shown that these processes may be linked and share a common function. They either exert cytoprotective (under basal or metabolic stress conditions) or cytocidal effects (after acute cellular damage) (Kondo *et al.*, 2005; Moenner *et al.*, 2007).

ER stress is the starting point from which autophagy or apoptosis can be induced. Activation of ER stress and autophagy represents though a promising therapeutic strategy to

treat cancer (Verfaillie *et al.*, 2010). This is why we decided to investigate the roles of ER stress and autophagy in the anticancer effects of 2OHOA against human glioma, the most common type of primary tumor in the CNS and one with the highest mortality rates of all cancers (Yang *et al.*, 2010).

We found that treating 1321N1, SF-767 and U118 cells with 2OHOA provoked such effects including: induction of ER stress-related genes, cell cycle arrest through the accumulation of cells in the G_2/M phase, and autophagic cell death. By contrast, 2OHOA treatment of non-cancer MRC-5 human fibroblast cells failed to induce these key mediators of ER stress, cell growth arrest, and autophagy. These findings partly explain the specificity of 2OHOA against glioma cells, and the lack of undesired toxic effects when animals are treated with this compound (Martínez *et al.*, 2005a). In addition, this novel therapeutic approach may constitute an innovative treatment for gliomas with very high mortality rates, based on the specific induction of ER stress and autophagy.

3.2 Results

3.2.1 2OHOA Impairs Cell Proliferation and Viability in 1321N1, SF-767 and U118 Human Glioma Cells

In order to evaluate cell proliferation in the different cell lines after 2OHOA or palmitate treatments, we carried out an MTT assay based on the mitochondrial function (succinate dehydrogenase activity). We observed that 2OHOA (50-1000 µM, 24-72 h) had modest effects on the cell proliferation of non-cancer human fibroblast MRC-5 cells (Fig. 3.1 A), while palmitate, a potent inducer of ER stress used as a positive control (Karaskov *et al.*, 2006), significantly impaired MRC-5 cell proliferation (Fig 3.1 B). By contrast, 2OHOA and palmitate both inhibited the proliferation of 1321N1 human astrocytoma cells (Fig. 3.1 C and D), SF-767 (Fig. 1 E and F) and U118 (Fig. 3.1 G and H) human glioma cells, but only 2OHOA was specific against these glioma cell lines.

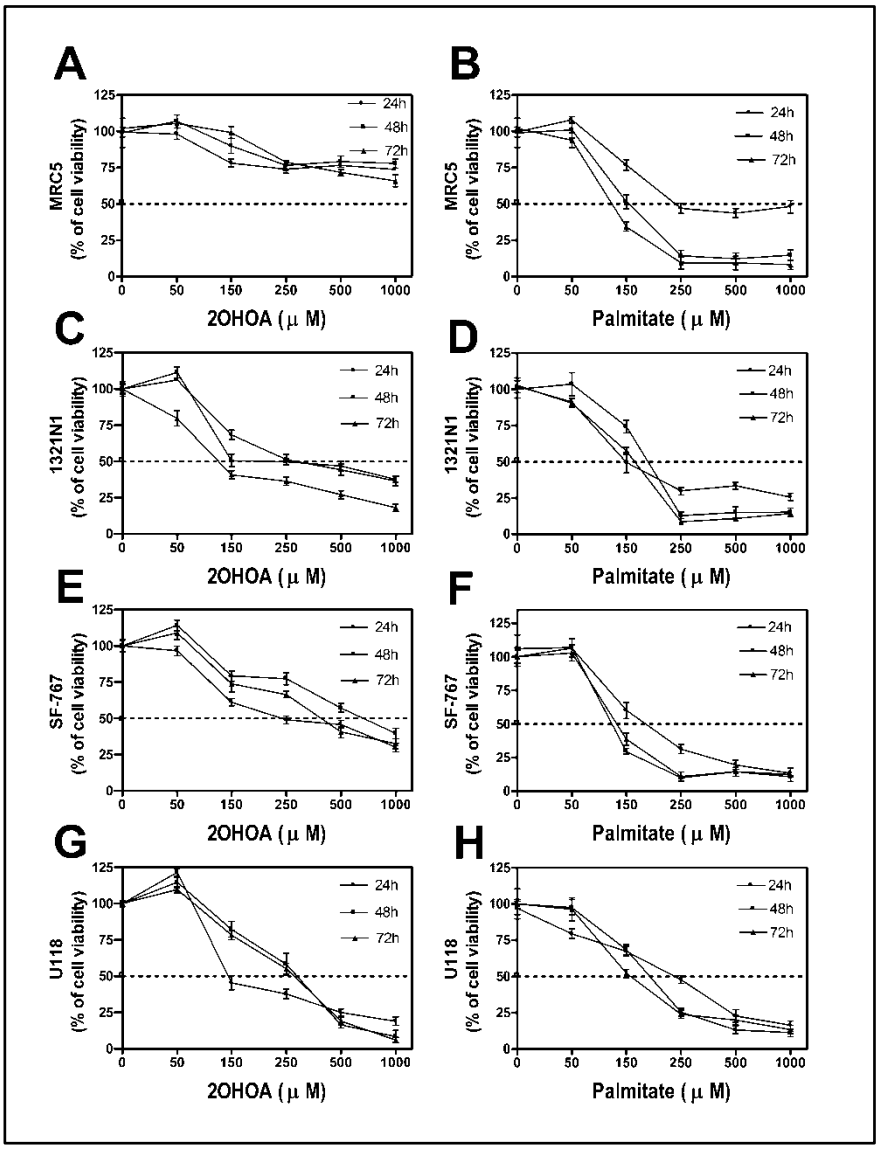

Figure 3.1 Effects of 2OHOA and palmitate on the proliferation of MRC-5 (A, B), 1321N1 (C, D), SF-767 (E, F), and U118 (G, H) cells. Human glioma (1321N1, SF-767 and U118) cells and fibroblasts (MRC-5) were exposed to increasing doses (50-1000 μM) of 2OHOA or palmitate for different periods of time (24 h, 48 h or 72 h). Cell viability was determined using the MTT method. **A**. Treatments with 2OHOA did not inhibit MRC-5 cell growth below 50% at the highest incubation concentrations and times, so that IC50 value could not be determined. **B**. By contrast, the IC50 values for palmitate in MRC-5 cells were: 24h, 200 μM; 48h, 150 μM and 72h, 120 μM (n=6). **C**. The IC50 values for 2OHOA in 1321N1 cells were: 24h, 250 μM; 48h, 150 μM and 72h, 100 μM (n=6). **D**. The IC50 values for palmitate in 1321N1 cells were: 24h, 160 μM; 48h, 200 μM and 72h, 160 μM (n=6). **E**. The IC50 values for 2OHOA in SF-767 cells were: 24h, 600 μM; 48h, 350 μM and 72h, 200 μM (n=6). **F**. The IC50 values for palmitate in SF-767 cells were: 24h, 160 μM; 48h, 120 μM and 72h, 110 μM (n=6). **G**. The IC50 values for 2OHOA in U118 cellswere: 24h, 150 μM; 48h, 265 μM and 72h, 260 μM (n=6). **H**. The IC50 values for palmitate in U118 cells were: 24h, 250 μM; 48h, 175 μM and 72h, 150 μM (n=6).

To further analyze cell viability we used the Trypan Blue Exclusion method. We observed that 2OHOA (50-1000 µM, 24-72 h) had modest effects on the cell viability and proliferation of non-cancer human fibroblast MRC-5 cells, except when using the highest dose of 1000 µM (Fig. 3.2 A - C). By contrast, 2OHOA (50-1000 µM, 24 - 72 h) inhibited the proliferation and increased cell death in a time and dose-dependent manner in 1321N1 (Fig. 3.2 D - E), SF-767 (Fig. 3.2 G - I) and U118 (Fig. 3.2 J - L) human glioma cells.

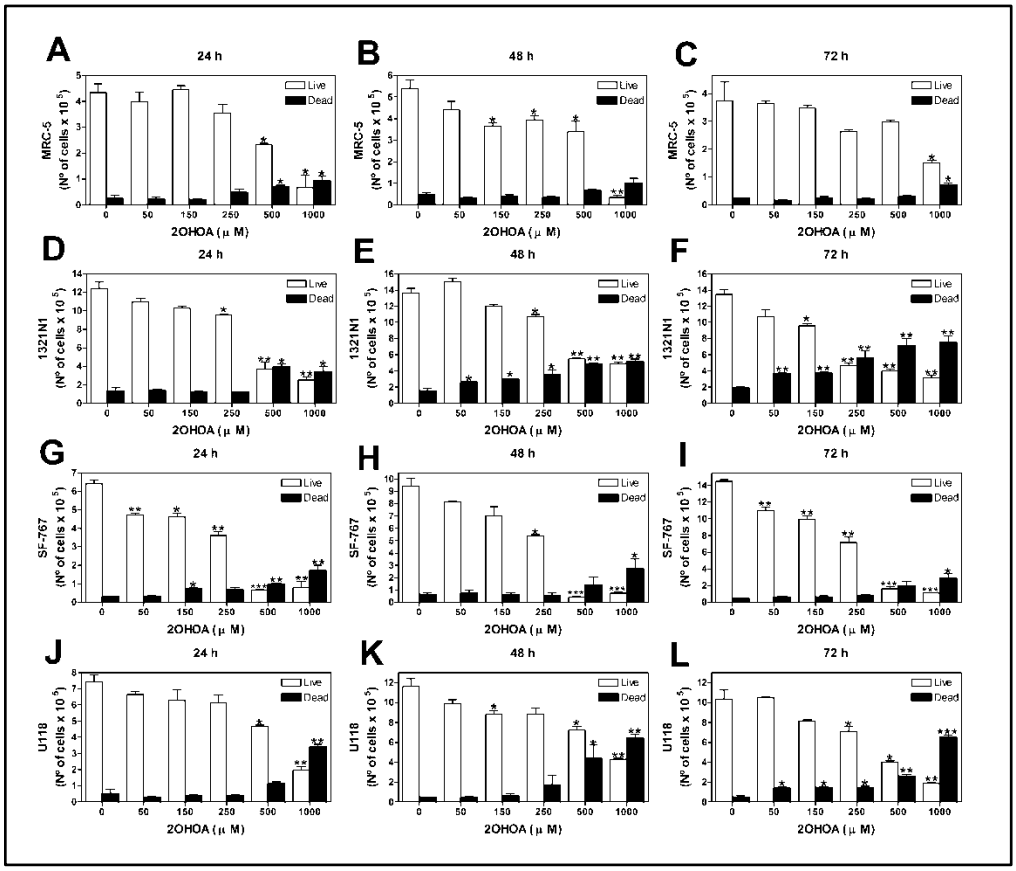

Figure 3.2 2OHOA effects on cell viability in 1321N1, SF-767 and U118 human glioma cells and MRC-5 human fibroblasts (Trypan blue exclusion method) Glioma, and MRC-5 non-tumor cell viability. 1321N1, SF-767 and U118 human glioma cells and MRC-5 human fibroblasts were exposed to increasing doses (50-1000 µM) of 2OHOA for different periods of time (24h, 48h or 72h). Total number of live and dead MRC-5 cells treated with 2OHOA 24h (A), 48h (B) and 72h (C). Total number of live and dead 1321N1 cells treated with 2OHOA 24h (D), 48h (E) and 72h (F). Total number of live and dead SF-767 cells treated with 2OHOA 24h (G), 48h (H) and 72h (I). Total number of live and dead U118 cells treated with 2OHOA 24h (J), 48h (K) and 72h (L). The number of cells presented in the graphs is the total number of cells per well (9.6 cm^2). Cells were plated at 50% confluence at the following densities: 2 x 10^4 cells/cm^2 (1.86 x 10^5 cells/well) for MRC-5 cells; 6 x 10^4 cells/cm^2 (6 x 10^5 cells/well) for 1321N1cells and 3 x 10^4 cells/cm^2 (3 x 10^5 cells/well) for SF-767 and U118 cells. After 72 h confluence was reached. (*p<0.05, **p<0.01, ***p<0.001; n=3)

3.2.2 2OHOA Activates ER stress/UPR Signaling Pathways in 1321N1, SF-767 and U118 but not in MRC-5 Cells

To determine whether inhibition of 1321N1, SF-767 and U118 cell growth by 2OHOA was mediated by ER stress/UPR signaling, we examined the expression of key molecules in the three main signal transduction cascades activated by ER stress/UPR. Treatment of 1321N1, SF-767 and U118 cells with either 2OHOA or palmitate (150 µM; 12 h) significantly increased the P-eIF2α protein levels, while a similar increase in P-eIF2α protein was only produced by palmitate in MRC-5 cells (Fig. 3.3 A, B, C and D). Thus, the effects of 2OHOA on P-eIF2α accumulation appeared to be specific to glioma cells. Phosphorylated eIF2α attenuates general protein translation and selectively activated transcription and translation of the ATF4 transcription factor (Lu *et al.*, 2004a). Both 2OHOA and palmitate (150 µM; 24 h) induced a significant increase in ATF4 gene expression in 1321N1 cells, but not in MRC-5cells, further demonstrating the specificity of 2OHOA against glioma cells (Fig. 3.4 A and B).

Activation of IRE1α resulted in an increase in the expression of the XBP1 transcription factor (Yoshida *et al.*, 2001; Calfon *et al.*, 2002). 2OHOA and palmitate (150 µM; 24 h and 48 h) markedly up-regulated IRE1α protein levels in 1321N1, SF-767 and U118 cells (Fig. 3.3 B, C and D), and up-regulated mRNA levels in 1321N1 astrocytoma cells (Fig 3.4 D). By contrast, the same treatments produced only a mild increase in IRE1α protein and mRNA expression in MRC-5 cells (Fig. 3.3 B; Fig. 3.4 C). The mRNA transcripts of the spliced activated form of the X-box binding protein 1 gene (sXBP1), a downstream target of ATF6 and IRE1α augmented in both cell lines (1321N1 and MRC-5) after 2OHOA treatment (150 µM; 24 h) (Fig. 3.4 E and F). These observations indicate that 2OHOA activates the UPR signaling in both cell lines, although more weakly in the non-cancerous MRC-5 cells.

We then studied the so-called ATF6 branch of the UPR signaling pathway, which was activated by palmitate (150 µM; 24 h) in both 1321N1 and MRC-5 cells, provoking a significant up-regulation of ATF6 mRNA expression (Fig 3.4 G and H). By contrast, 2OHOA treatment (150 µM; 24 h) only increased significantly ATF6 mRNA expression in human glioma (1321N1) cells (Fig 3.4 H). However, this increase was not sufficient to be considered biologically relevant.

In situations of chronic ER stress, the P-eIF2α, IRE1α and ATF6 signaling pathways induce a transcription and translation of the proapoptotic factor CHOP. In response to treatment with 2OHOA or palmitate (150 µM), CHOP expression increased in 1321N1, SF-767, and U118 cells, at the protein level (48 h, Fig. 3.3 J - L). It also increased at mRNA levels in 1321N1 astrocytoma cells (Fig 3.4 J). While palmitate administration also increased CHOP mRNA and protein expression in MRC-5 cells, 2OHOA did not have such effect (Fig.

3.3 I and Fig. 3.4 I). Together these findings demonstrate the differential effect of 2OHOA in these glioma cells compared to MRC-5 normal human fibroblasts (selectivity not evident with palmitate, which induces ER stress in both normal and glioma cells).

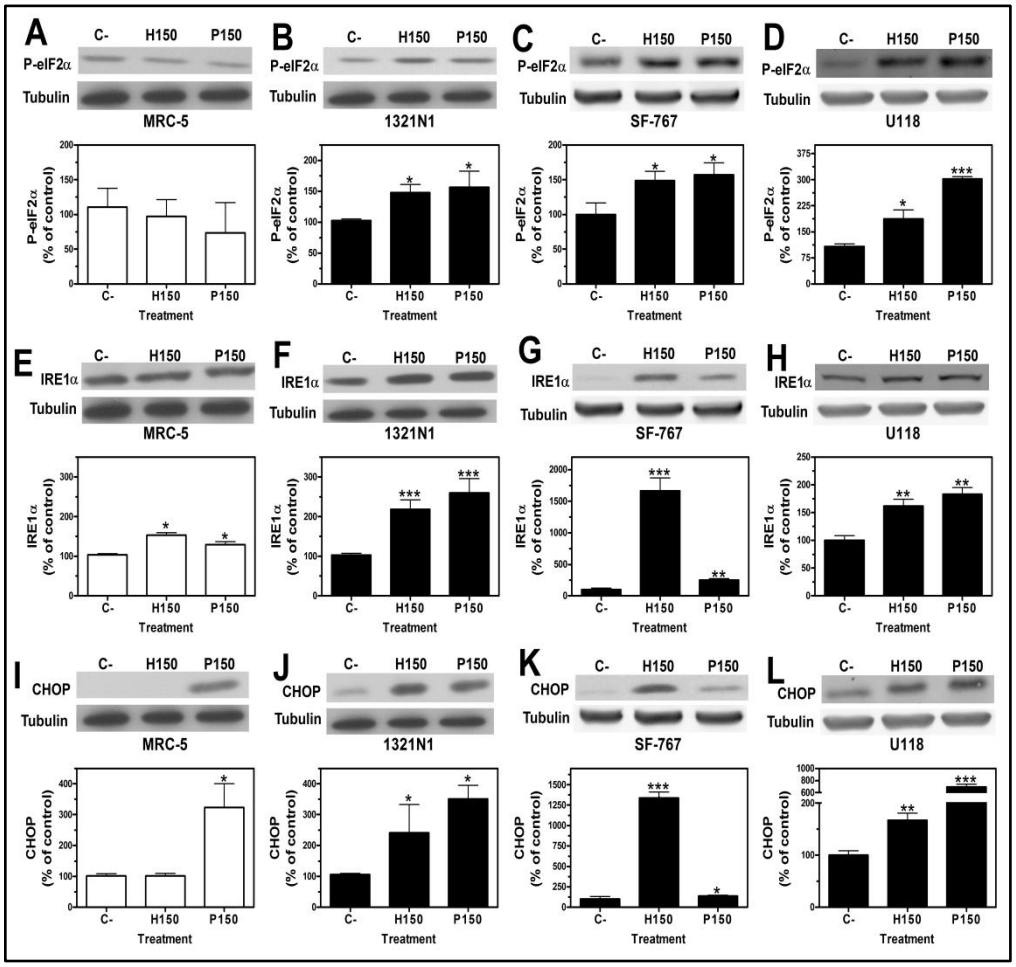

Figure 3.3 2OHOA activation of ER stress/UPR signaling pathways in 1321N1, SF-767 and U118 but not in MRC-5 cells. P-eIF2α, IRE1α and CHOP protein levels in 1321N1, SF-767 and U118 human glioma cells and in non-cancer MRC-5 human fibroblast cells determined by immunoblotting. Upper panels: a representative immunoblot showing P-eIF2α, IRE1 α or CHOP and Tubulin levels in each cell line after exposure to 2OHOA (H) or palmitate (P: 150 μM). Lower panels: Bar diagram showing the mean ± SEM P-eIF2α, IRE1 α or CHOP expression in each cell line after exposure to 2OHOA (H) or palmitate (P) (150 μM) compared to untreated controls (C). **A**. P-eIF2α expression in MRC-5 cell line **B**. P-eIF2α expression in 1321N1 cell line **C**. P-eIF2α expression in SF-767 cell line **D**. P-eIF2α expression in U118 cell line after exposure to 2OHOA (H) or palmitate (P) (150 μM; 12h). **E**. IRE1α expression in MRC-5 cell line **F**. IRE1α expression in 1321N1 cell line **G**. IRE1α expression in SF-767 cell line **H**. IRE1α expression in U118 cell line after exposure to 2OHOA (H) or palmitate (P) (150 μM; 48h). **I**. CHOP expression in MRC-5 cell line **J**. CHOP expression in 1321N1 cell line **K**. CHOP expression in SF-767 cell line **L**. CHOP expression in U118 cell line after exposure to 2OHOA (H) or palmitate (P) (150 μM; 48h) (*p<0.05, **p<0.01, ***p<0.001; n=6).

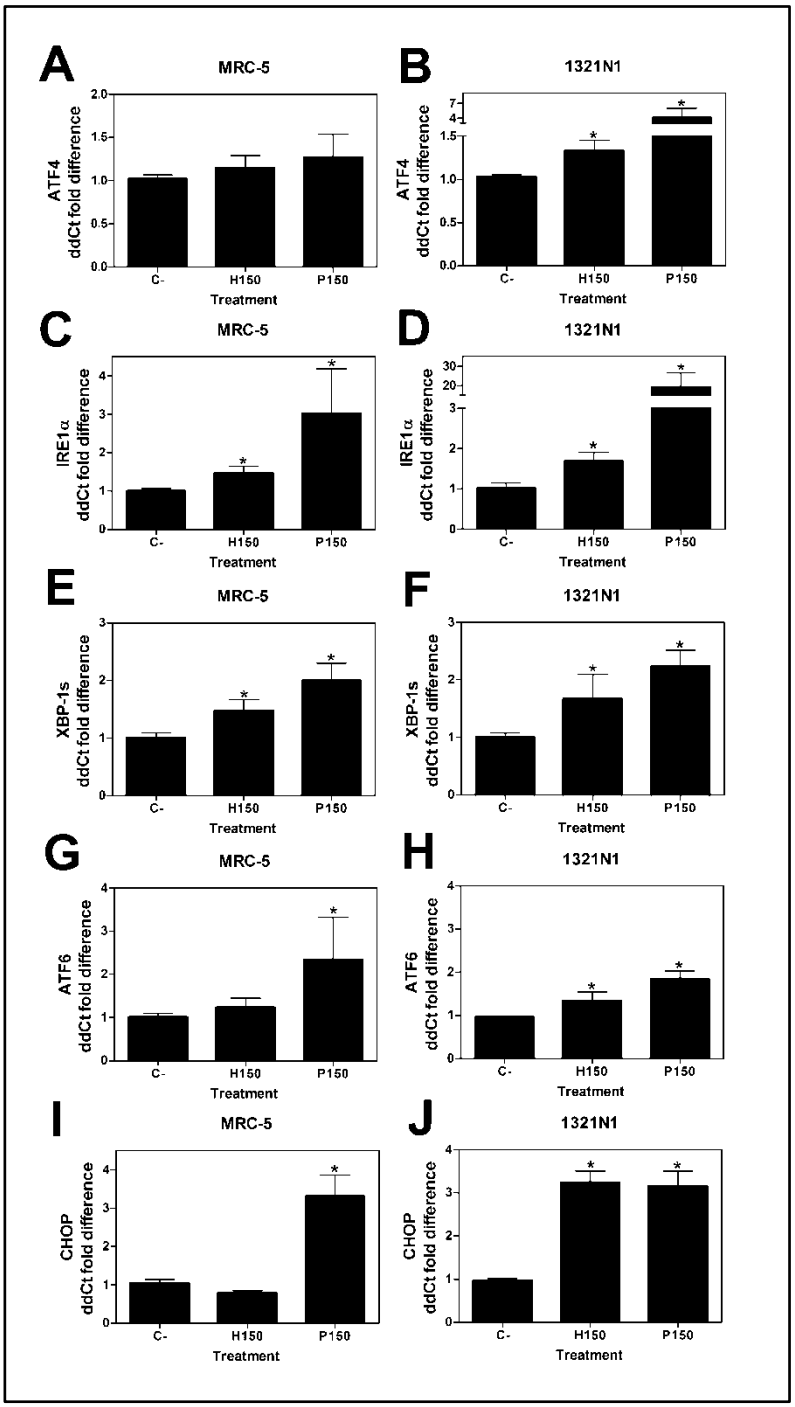

Figure 3.4 Relative mRNA levels of ER stress/UPR transcripts q RT-PCR analysis of the mRNA expression of ATF4 **(A)**, **(B)**; IRE1α **(C)**, **(D)**; spliced form of XBP1 **(E)**, **(F)**; ATF6 **(G)**, **(H)** and CHOP **(I)**, **(J)** genes in MRC-5 non-cancer human fibroblasts cells and 1321N1 human astrocytoma cells after treatment with 2OHOA (H) or palmitate (P) (150 μM; 24h). Results are expressed as ddCt values using the following formula: ddCt = E X (Ctc-Ctx)/E Bact(Ctc-Ctx). (*P<0.05; n=6) in a bar diagram showing the mean ± SEM (standard error of the mean).

3.2.3 2OHOA Induces Cell Cycle Arrest in 1321N1, SF-767 and U118 but not of MRC-5 Cells

The proportion of cells in the different phases of the cell cycle was evaluated by measuring the intracellular DNA content after exposure to 2OHOA and palmitate (150 μM; 72 h). Cell cycle progression and growth of human MRC-5 fibroblast cells were not affected by 2OHOA exposure (percentage of cells in the G_2/M phase: Control, 29.82 ± 3.67%; 2OHOA, 27.09 ± 0.20%; *p<0.05. Fig. 3.5 A - C). By contrast, when compared to untreated controls, 2OHOA treatment inhibited 1321N1 cell proliferation, and increased the proportion of cells in the G_2/M phase (Control, 19.13 ± 2.84%; 2OHOA, 32.71* ± 1.97%; *p<0.05. Fig. 3.5 D-F).

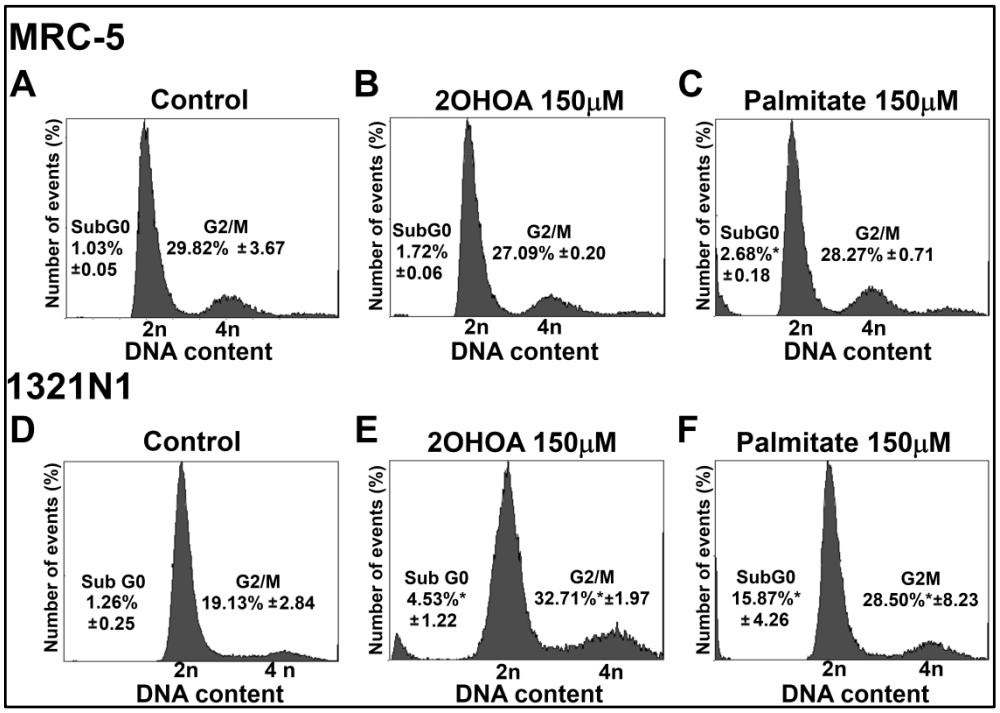

Figure 3.5 2OHOA induction of G_2/M cell cycle arrest of 1321N1 cells but not of MRC-5 cells Cell cycle assessment and G_2/M phase arrest. Analysis of the DNA content (flow cytometry) of MRC-5 and 1321N1 cells exposed to 2OHOA or palmitate (150 μM for 72 h). **A**. Analysis of the DNA content in untreated MRC-5 cells. **B**. Analysis of the DNA content in MRC-5 cells exposed to 2OHOA (150 μM for 72 h) or **(C)** palmitate (150 μM for 72 h), showing the proportion of cells in Sub G0 and G2/M phases. **D**. Analysis of the DNA content of untreated 1321N1 cells. **E**. Analysis of the DNA content of 1321N1 cells exposed to 2OHOA (150 μM for 72 h) or **(F)** palmitate (150 μM for 72 h), showing the proportion of cells in Sub G0 and G2/M phases. Statistical analysis of the DNA content of 1321N1 cells exposed to 2OHOA or palmitate (150 μM) revealed a significant increase (*p<0.05; n=6) in the G_2/M phase peak when compared with untreated cells (C-). No significant differences in Sub G0 values were detected in MRC-5 cells exposed to 2OHOA (150 μM)) when compared with untreated cells (C-).

Indeed, 2OHOA treatment in 1321N1, SF-767 and U118 induced significant decreases in the expression of both cyclin B1 (Fig. 3.6 B - D) and Cdk1/Cdc2 (Fig. 3.6 F - H). This is indicative of cell cycle arrest in the G_2/M phase; it did not occur however in MRC-5 cells (Fig. 3.6 A and E).

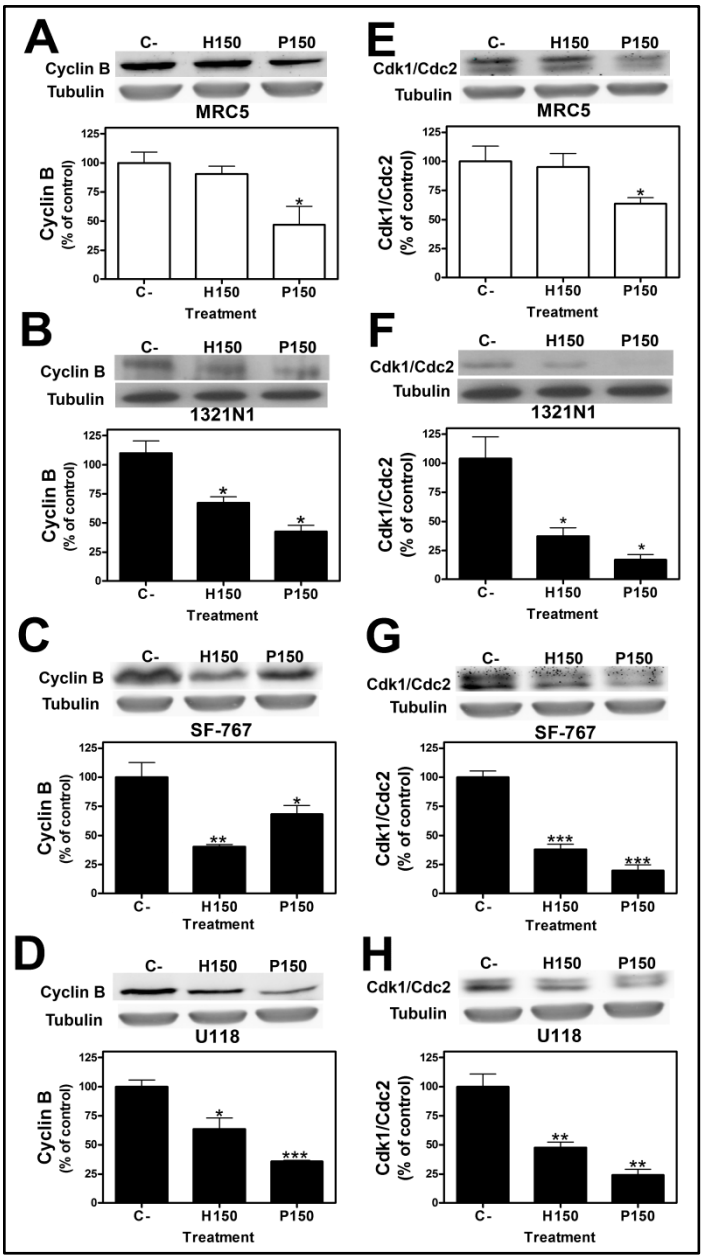

Figure 3.6 2OHOA inhibition of Cyclin B and Cdk1/Cdc2 proteins in 1321N1, SF-767 and U118 human glioma cells but not in non cancer MRC-5 cells Cyclin B and Cdk1/Cdc2 proteins in 1321N1, SF-767 and U118 human glioma cells and MRC-5 non cancer cells. **A, B, C** and **D** present in the upper panels: a representative immunoblot showing cyclin B expression after exposure to 2OHOA (H) or palmitate (P: 150 μM; 24 h). Lower panels: Bar diagram showing the mean ± SEM values of cyclin B expression in **(A)** MRC-5, **(B)** 1321N1, **(C)** SF-767 and **(D)** U118 cells, upon exposure to 2OHOA (H) or palmitate (P: 150 μM; 24h) when compared with untreated controls (C). **E, F, G** and **H** show a representative immunoblot of Cdk1/Cdc2 expression after exposure to 2OHOA (H) or palmitate (P: 150 μM; 48 h, upper panels). The lower panels show the bar diagram indicating the mean ± SEM values of Cdk1/Cdc2 expression in **(E)** MRC-5, **(F)** 1321N1, **(G)** SF-767 and **(H)** U118 cells after exposure to 2OHOA (H) or palmitate (P: 150 μM; 48h) when compared with untreated controls (C). (*p<0.05, **p<0.01, ***p<0.001; n=6).

3.2.4 2OHOA Induces Autophagy in 1321N1, SF-767 and U118 but not in MRC-5 Cells

Some features of apoptosis, not observed in MRC-5 cells (Fig.3.7 A-B), appear to be induced in human astrocytoma (1321N1) cells upon exposure to 2OHOA, such as the flow cytometry sub-G0 peak, poly ADP ribose polymerase (PARP) (Fig. 3.7 C) or caspase 8 partial proteolysis (Fig. 3.7 D). The latter was also observed in U118 cells after treatment with 2OHOA (Fig. 3.7 H). However, this induction of apoptotic features did not fully explain cell death induced by 2OHOA in 1321N1, SF-767 and U118 glioma cells. We did not observe PARP degradation induction in SF-767 and U118 cells treated with 2OHOA (Fig. 3.7 E and G), nor Caspase 8 proteolysis in SF-767 cells (Fig. 3.7 E). As 2OHOA induces tumor regression and cancer cell death (Lladó *et al.*, 2009), we also assessed the role of autophagy in the induction of cell death by 2OHOA. Acidic vesicles (lysosomes and autophagosomes characteristic of autophagy) were not observed in non-tumor MRC-5 cells treated with vehicle or 2OHOA (150 µM; 48 h, Figs. 3.8 A and B), whereas exposure to palmitate (150 µM; 48 h) induced the formation of acidic autophagic vesicles in these cells (Fig. 3.8 C) The relative integrated fluorescence density of the lysosomes in MRC-5 cells (5 x 104 cells per experiment) was as follows: untreated control 11.54 ± 3.36%; 2OHOA (150 µM) 16.88 ± 2.45%; Palmitate (150 µM) 100* ± 3.65%; *$p<0.05$ (Fig. 3.8 D).

Both 2OHOA and palmitate (150 µM; 48 h) induced a marked increase in the generation of lysosome/autophagosome vesicles in human astrocytoma (1321N1) cells (Fig. 3.8 F, G) compared to untreated cells (Fig. 3.8 E), in which the relative integrated fluorescence density of the lysosomes was as follows: untreated control 3.1 ± 0.37%; 2OHOA (150 µM) 81** ± 6.18%; Palmitate (150 µM) 100** ± 6.12%; **$p<0.01$ (Fig. 3.8H). Thus, 2OHOA specifically promoted the generation of autophagosomes in cancer cells, whereas palmitate induced unspecific production of acidic vesicles in both normal and cancer cells.

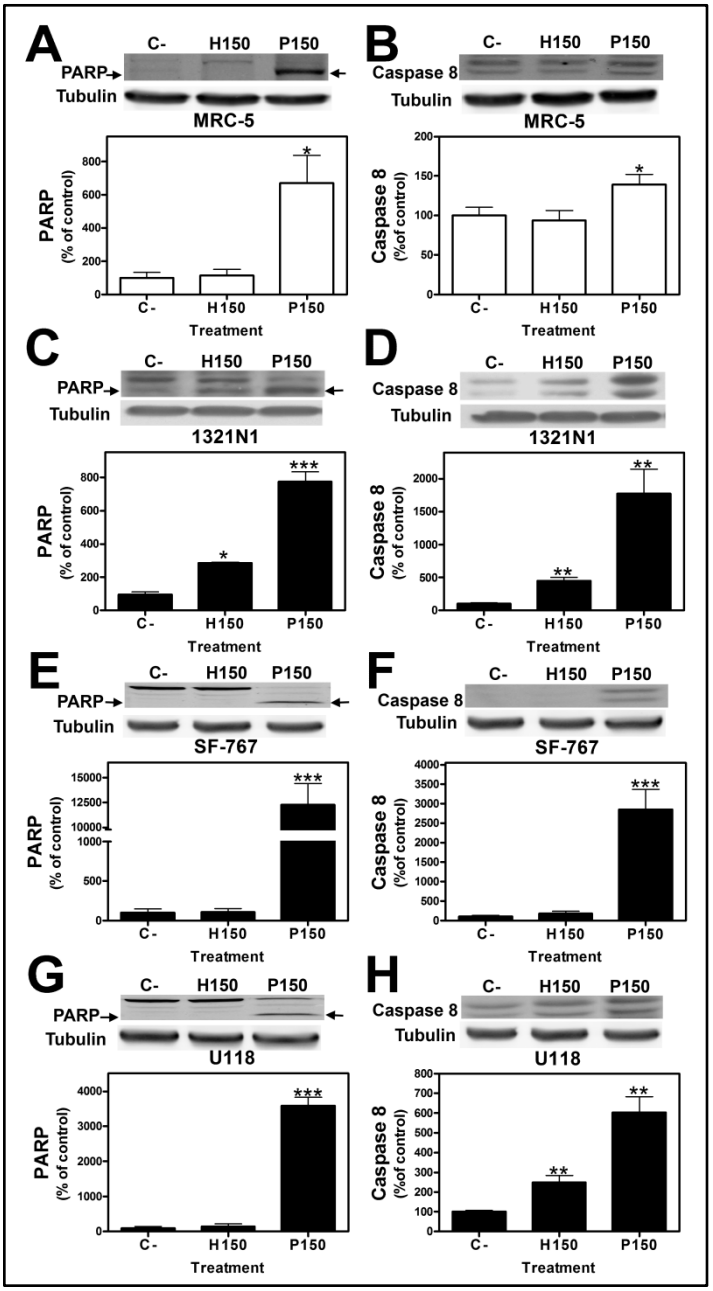

Figure 3.7 Expression of PARP and Caspase 8 in 1321N1, SF-767, U118 human glioma cells and non cancer MRC-5 cells after treatment with 2OHOA. PARP and Caspase 8 proteins in 1321N1, SF-767, U118 human glioma cells and MRC-5 non-cancer cells. Upper panels: a representative immunoblot showing PARP (**A, C, E** and **G**) or Caspase 8 (**B, D, F** and **H**) expression in every cell line after exposure to 2OHOA (H) or palmitate (P: 150 µM; 72 h). Lower panels: Bar diagram showing the mean ± SEM values of PARP expression in MRC-5 **(A)**, 1321N1 **(C)**, SF-767 **(E)** and U118 **(G)** cells or Caspase 8 in MRC-5 **(B)**, 1321N1 **(D)**, SF-767 **(F)** and U118 **(H)** cells after exposure to 2OHOA (H) or palmitate (P: 150 µM; 72h) when compared with untreated controls (C, *p<0.05, **p<0.01, ***p<0.001; n=6).

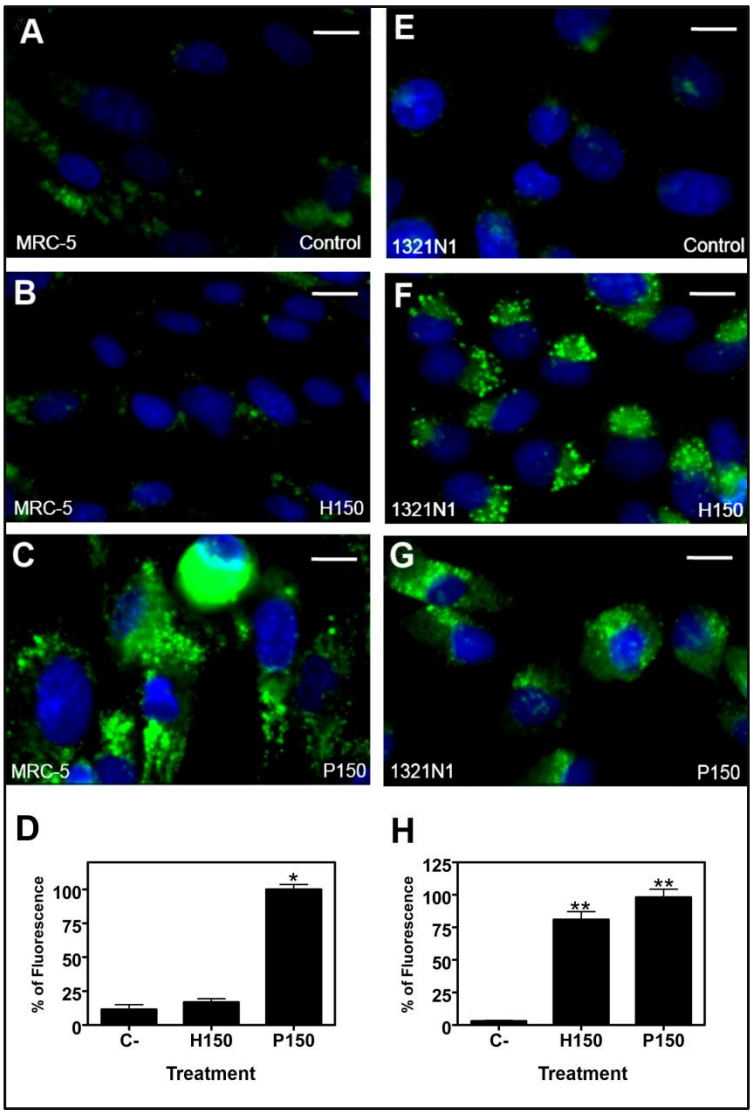

Figure 3.8 2OHOA induction of acidic vesicles in 1321N1 but not in MRC-5 cells. Analysis of acidic vesicles in cells stained with Hoechst and LysoSensor Green to visualize nuclei and lysosomes, respectively. The images were captured by live cell imaging and all represent merged images of Hoechst (blue) and LysoSensor Green (green). The acidic vesicles in photomicrographs were analyzed with Image J 1.38x software. Neither the vehicle (FBS, **A**) nor 2OHOA (150µM; 48h, **B**) resulted in the formation of acidic vesicular organelles (lysosomes and autophagosomes) in non-cancer MRC-5 human fibroblast cells, as detected by the LysoSensor fluorescence probe, whereas palmitate (150µM, 48h: **C**) induced acidic vesicle formation. Graphs show the integrated fluorescence density of the lysosomes (5 x 104 cells per experiment) in MRC-5 cells **(D)**: Control, 11.54 ± 3.36%; 2OHOA (150µM), 16.88 ± 2.45%; Palmitate (150µM), 100* ± 3.65%; *p<0.05. No vesicular organelles accumulated in 1321N1 human astrocytoma cells treated with the vehicle alone (control, **E**), while exposure to 2OHOA **(F)** or palmitate **(G)** (150µM; 48h) resulted in the appearance of acidic vesicular organelles. Integrated fluorescence density of lysosomes in 1321N1 cells (5 x 104 cells per experiment) **(H)**: Control, 3.1 ± 0.37%; 2OHOA (150µM) 81** ± 6.18%; P (150µM) 100** ± 6.12%; **p<0.01 (n=6 experiments). Scale bar = 10 µm (8A, 8B, 8E, 8F, 8I, 8J); 15 µm (8C, 8G and 8K).

To further confirm that autophagy was induced, we assessed the expression of the autophagy markers ATG7, ATG5, LC3B I and LC3B II. Treatment with 2OHOA or palmitate (150 µM; 72 h) significantly augmented both LC3B-I and LC3B-II in 1321N1, SF-767 and U118 cells compared to MRC-5 cells (Fig. 3.9 A-D). ATG7 was also up-regulated in 1321N1 cells compared to MRC-5 cells (Fig.3.9 E and F). ATG5 was up-regulated in SF-767 cells (Fig.3.9 G). However, U118 cell line did not show up-regulation of ATG7 (Fig 3.9 H) or ATG5 (data not shown) 12 hours after treatment, suggesting an earlier induction of these molecules.

Finally, astrocytoma cell degradation upon 2OHOA treatment was further investigated by electron microscopy. This revealed fragments of 1321N1 cells and dense vesicles associated with double-layered autophagosomes (Fig. 3.10). The cytoplasm of control (untreated) 1321N1 cells was densely packed with abundant polyribosomes, mitochondria, dictyosomes, and intermediate filament bundles (Fig. 3.10 A and 3.10 E). After 48 hours in the presence of the lowest concentration of 2OHOA used in this study (150 µM), the nucleus of 1321N1 cells was no different to that of control cells. Notably, 2OHOA induced the appearance of lipid droplets and dense bodies, the latter scattered throughout the cytoplasm with morphological characteristics of autophagosomes (Fig 3.10 B to D and 3.10 F to H). The abundance of these dense bodies was concentration-dependent (Fig 3.10 B to D), and their heterogeneity increased in function of the concentration of 2OHOA. At both low and high 2OHOA concentrations, distended ER membranes and a loss of ER were observed in the cytoplasm consistent with the ER stress and the autophagic process (Fig.3.10 F to 3.10 H). Figure 3.10 I shows in detail early extensions of double endoplasmic reticulum (ER) membranes beginning to surround a mitochondrion, which is characteristic of the autophagic process. These results further support the specificity of the effects of 2OHOA against glioma cells, implicating autophagy as the final cellular effect induced by this compound in these cancer cells.

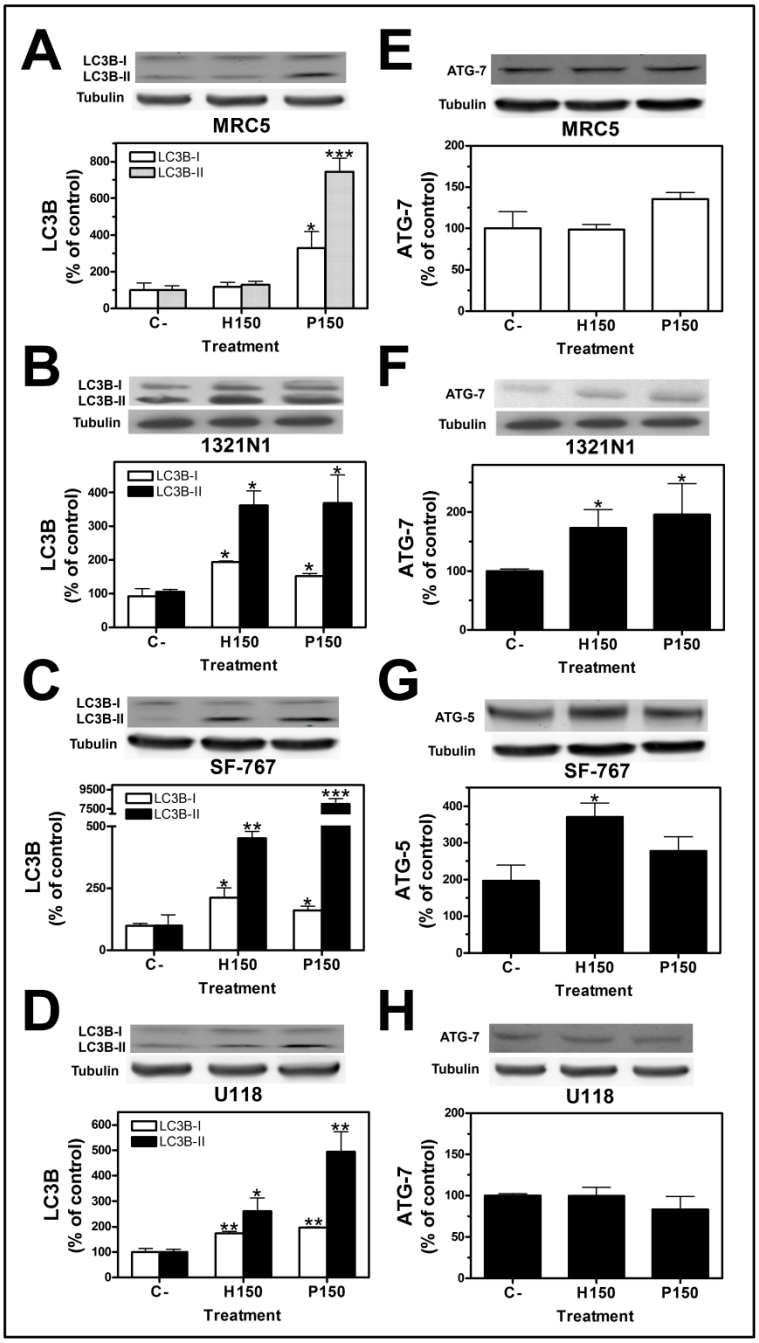

Figure 3.9 Expression of ATG 7, ATG5 and LC3BI, LC3BII in 1321N1, SF-767, U118 and MRC-5 cells after treatment with 2OHOA. The effects of 2OHOA and palmitate on the levels of ATG 7, ATG5, LC3BI and LC3BII were determined by immunoblots. Exposure of 1321N1 **(B)**, SF-767 **(C)** and U118 **(D)** cells to 2OHOA or palmitate (150 μM, 72h) induced a significant increase in LC3BI and LC3BII protein expression while in MRC-5 **(A)** only palmitate induced significant increases of these proteins. Exposure of 1321N1 cells to 2OHOA or palmitate (150 μM, 72h) induced a significant increase in ATG7 **(F)** protein expression while in MRC-5 **(E)**, and U118 **(H)** did not induce significant changes. Finally exposure of SF-767 cells to 2OHOA or palmitate (150 μM, 72h) induced a significant increase in ATG5 **(G)** protein expression (*p<0.05, **p<0.01, ***p<0.001; n=6).

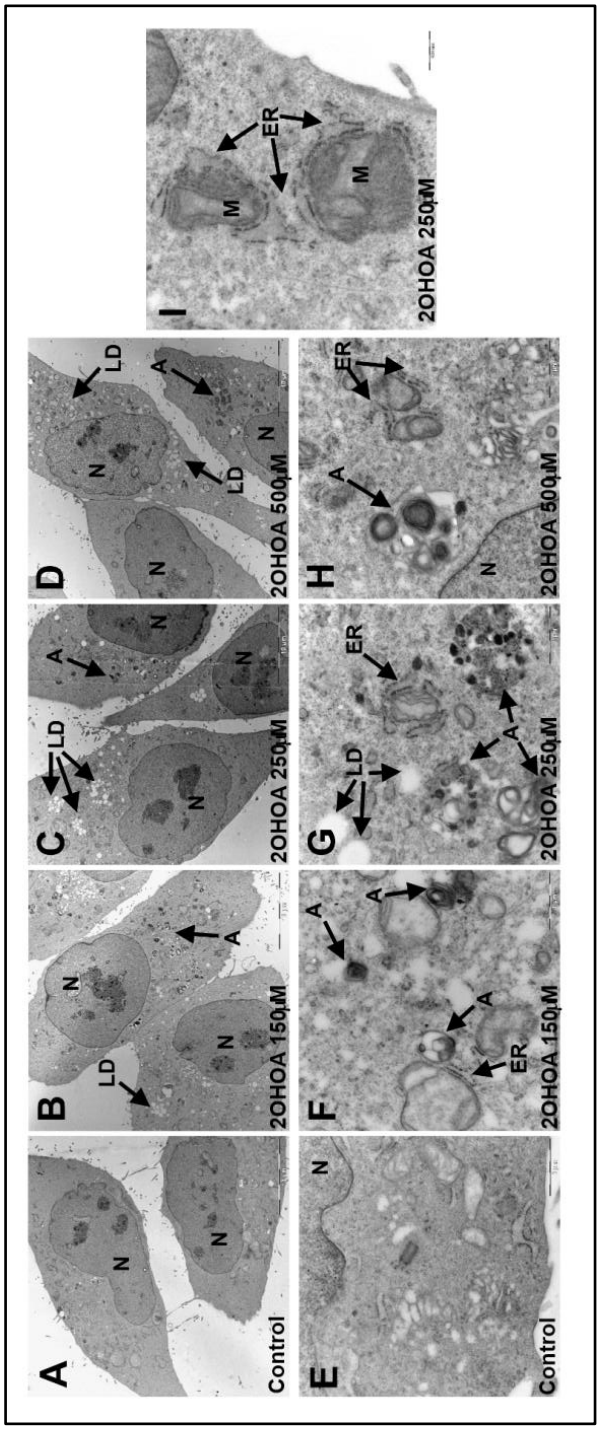

Figure 3.10 Electron microscopy of 1321N1 cells treated with 2OHOA: induction of Autophagosomes. Electron microscopy of 1321N1 cells maintained for 48 h in the absence (control: 3.10**A** and 3.10**E**) or presence of 2OHOA (150 µM: 10**B** and 3.10**F**; 250 µM: 3.10**C**, 10**G** and 3.10**I**; 500 µM: 3.10**D** and 3.10**H**). N: Nuclei; **A**: Autophagosomes; LP: Lipid Droplets; ER: Rough Endoplasmatic Reticulum; M: Mitochondria. Scale bar = 10 µm (3.10**A**-3.10**D**); 1 µm (3.10**E**-3.10**H**) and 500 nm (3.10**I**).

3.2.5 Changes in Phospholipids Composition of 1321N1 and MRC-5 Cells Treated with 2OHOA

Lipid composition is altered in several human pathologies, including cancer. For this reason, we investigated the impact of 2OHOA treatment on 1321N1 and MRC-5 cell glycerophospholipid composition. After extraction, lipids were separated by high performance thin layer chromatography (HPTLC). Treatment of MRC-5 cells with 2OHOA (24 h, 150 μM) did not change the phospholipid (PL) composition (Figure 3.11A). In contrast, treatment of 1321N1 cells with 2OHOA (24 h, 150 μM) induced a very significant increase in sphingomyelin (SM) levels that was accompanied by a significant decrease in phosphatidylcholine (PC) levels (Figure 3.11B).

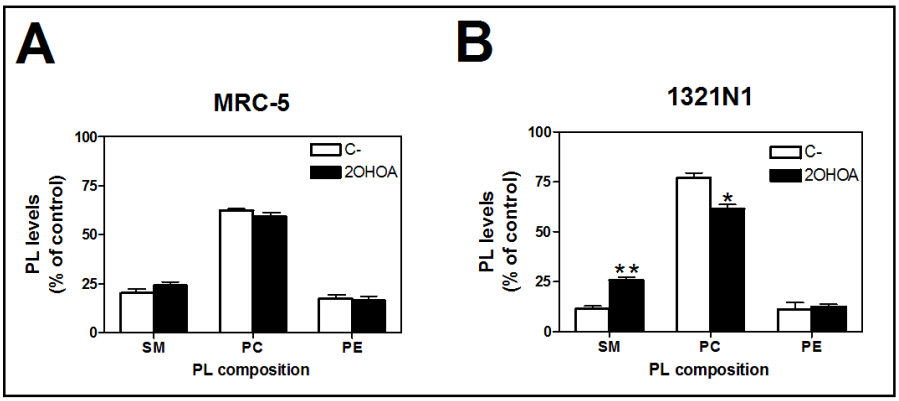

Figure 3.11 Phospholipid composition in MRC-5 and 1321N1 cells after treatment with 2OHOA. (A) Total SM, PC and PE content in MRC-5 cells treated with 2OHOA (24 h,150 μM). **(B)** Total SM, PC and PE content in 1321N1 cells treated with 2OHOA (24 h, 150 μM). PL levels were determined by HPTLC analysis of the total lipids extracted from control and treated cells. The results are expressed as percentage of untreated cells. Values represent the mean ±SEM, n = 3. The asterisks indicate a significant effect of the treatment as compared with the control (*p<0.05).

To corroborate whether the observed changes in lipid composition were associated with the effects of 2OHOA against cancer, our research group further analyzed the effects of 2OHOA on the phospholipid composition of human leukemia (Jurkat) cells, nonsmall lung cancer (A549) cells, additional human glioma cell lines (1321N1 and SF767) cells, and in non-tumor (MRC-5) cells (Barceló-Coblijn *et al.*, 2011). Exposure to 2OHOA (200 μM, 24 h) significantly increased the SM content of cancer cells (2.4-fold in Jurkat, 2.7-fold in A549, 2.2-fold in 1321N1, and 36.0% in SF767 cells) but not that of MRC-5 cells. These data not only revealed the ability of 2OHOA to regulate the phospholipid composition of

tumor cells, but also indicated that this effect was specific to cancer cells. Interestingly, all cancer cells studied here had approximately half the SM content of the non-tumor MRC-5 cells, suggesting a relevant role for this lipid in tumorigenesis.

3.3 Discussion

2OHOA is a potent anticancer drug that inhibits cancer cell growth and induces tumor regression in animal models of cancer, with no undesired side effects, as shown by the regulatory toxicity studies carried out by Harlan Laboratories following strict Good Laboratory Practices (GLP) guidelines. In this context, 2OHOA has recently been granted the status of orphan drug for the treatment of glioma by the European Medicines Agency (EMA). While previous studies have demonstrated that 2OHOA provoked cell cycle arrest (Martínez *et al.*, 2005a; Martínez *et al.*, 2005b) in cancer cells, the precise molecular and cellular mechanisms underlying the selective induction of glioma cell death is not yet fully understood.

We decided to investigate the mechanism of 2OHOA-induced cell death in 1321N1 glioma cells for a number of reasons. First, previous studies in our laboratory have demonstrated a 2OHOA-induced glioma regression in both animal xenograft models of human glioma and in nude mice (see below). Second, unlike most chemotherapeutic agents, this drug is highly selective, and does not induce the death of healthy cells, even at very high doses/concentrations. Finally, while apoptosis has been implicated in the general mechanism of action of 2OHOA against various types of cancer cells (Lladó *et al.*, 2010), SF-767 glioma cells do not initiate the apoptosis program, although other lines of glioma cells seem to undergo ER stress and apoptosis (Shingu *et al.*, 2010; Johnson *et al.*, 2011). Thus, we still do not know how cell death occurs in such cases.

2OHOA selectively inhibits glioma cells growth with an IC50 of ~100 µM in 1321N1, SF-767 and U118 cells as opposed to that of >1000 µM in MRC-5 non cancer cells. This justifies the lack of toxic effects at therapeutic doses (Marcilla-Etxenike, 2012). In addition, 2OHOA induces cell cycle arrest in 1321N1, SF-767 and U118 cells, resulting in a significant accumulation of 1321N1 cells in the G_2/M phase. Indeed, cyclin B and cdk1/cdc2 are down-regulated when glioma cells are exposed to 2OHOA. Previous studies have shown glioma cells to undergo autophagy when exposed to compounds that induce cell cycle arrest in the G_2/M phase (Hansen *et al.*, 2007; Shingu *et al.*, 2010). While autophagy provides a means of recycling cytosolic molecules/structures involved in cell survival, it can also represent a non-apoptotic cell death program. Autophagy involves the fragmentation of cells after the engulfment of proteins, organelles and cytosol in vesicles called autophagosomes, which eventually fuse with lysosomes to form autolysosomes (Chen *et al.*, 2010). In a variety of cells and tumors, including human glioma, autophagy signaling, UPR and abnormal cell

growth are intimately related (Fujita *et al.*, 2007; Kouroku *et al.*, 2007; Kim *et al.*, 2008). The high rate of cancer cell proliferation is associated with an increased protein and lipid synthesis, and active metabolism, which in turn induces a certain level of ER stress (Schonthal, 2009; Verfaillie *et al.*, 2010). Furthermore, as tumors progress, cancer cells experience increasing nutrient starvation and hypoxic conditions, resulting in the accumulation of unfolded or misfolded proteins. This in turn leads to an activation of UPR signaling (Kim *et al.*, 2008; Schonthal, 2009; Verfaillie *et al.*, 2010).

Autophagy is triggered in certain stress situations, with the aim of promoting cell survival by inducing cellular adaptations to associated conditions (Chen *et al.*, 2010; Dalby *et al.*, 2010; Wang *et al.*, 2010). However, increasing evidence suggests that autophagy also serves as a trigger for cell death (Chen *et al.*, 2010; Dalby *et al.*, 2010; Wang *et al.*, 2010).

As was shown above, some features of apoptosis were induced in 1321N1 and U118 cells but not in SF-767 by exposure to 2OHOA (sub-G0 peak, poly ADP ribose polymerase [PARP] or caspase 8 partial proteolysis) (Fig.3.7). However, this induction of apoptotic features did not fully explain the cell death induced by 2OHOA. Therefore we examined the role of autophagy induced by the ER stress/UPR signaling pathway in relation to the growth inhibition effects of 2OHOA in 1321N1, SF-767 and U118 human glioma cells, and non-cancer MRC-5 cells. Treatments with 2OHOA or palmitate activated ER stress in 1321N1, SF-767, and U118 cells within 12 h. This is proven by the increase in phosphorylated eIF2α protein, a marker of ER stress. Phosphorylation of eIF2α induces cellular adaptation to various stress conditions by inhibiting protein synthesis and, subsequently, by activating the expression of the ATF4 transcription factor (Lu *et al.*, 2004a). We found that both 2OHOA and palmitate significantly increase ATF4 expression in 1321N1 cells, while neither eIF2α phosphorylation nor ATF4 gene expression were evident in non-cancer MRC-5 cells exposed to 2OHOA. Along with previous findings, this further demonstrates the specificity of 2OHOA to these glioma cells, and explains the observed lack of side-effects in animal models of cancer and GLP studies in mice, rats and dogs.

Since compounds that induce sustained eIF2α phosphorylation provide cytoprotection in situations of ER stress (Boyce *et al.*, 2005), the maintenance of eIF2α in an inactive state is somehow beneficial. However, a prolonged suppression of protein synthesis is incompatible with cell survival, and leads to autophagy (Fujita *et al.*, 2007; Kouroku *et al.*, 2007; Kim *et al.*, 2008). Exposure of MRC-5 fibroblasts to 2OHOA does not induce eIF2α and ATF4 expression, nor inhibit cell growth. This is further evidence of its specificity in these glioma cells, and demonstrates the role of eIF2α and ATF4 in 2OHOA-induced cell death of 1321N1, SF-767, and U118 cells.

The second ER stress pathway studied, the IRE1α signaling pathway, was also activated by 2OHOA in 1321N1, SF-767, and U118 cells. 2OHOA induced a significant increase in IRE1α in 1321N1, SF-767, and U118 cells when compared to the modest increase

in MRC-5 cells. Interestingly, the spliced activated form of XBP1s, a downstream target of ATF6 and IRE1α, was up-regulated by 2OHOA in both 1321N1 and MRC-5 cells. Strong expression of the spliced form of XBP1 is associated with cell survival, whereas expression of the unspliced variant of XBP1 is associated with apoptosis (Davies *et al.*, 2008). Our results suggest that the up-regulation of XBP1 is not essential for cell death, as observed in MRC-5 cells. This indicates that the activation of other factors besides XBP1 is necessary to induce autophagy.

Under persistent ER stress, the PERK, IRE1α, and ATF6 signaling pathways induce the expression of the pro-apoptotic factor CHOP. In line with its activation of ER stress/UPR, 2OHOA induces CHOP expression in 1321N1, SF-767, and U118 human glioma cells but not in MRC-5 cells, whereas palmitate up-regulated CHOP in glioma and non-cancer cells. As CHOP is one of the most important downstream effector proteins of ER stress, its specific activation by 2OHOA in 1321N1, SF-767, and U118 cells is consistent with the severe induction of ER stress. CHOP activation often leads to the induction of cell death and although CHOP is one of the main effectors of apoptosis (Oyadomari and Mori, 2004), 2OHOA did not trigger apoptosis in SF-767 cells despite inducing marked CHOP expression. Nevertheless, autophagy activation in various glioma cell lines that are usually resistant to apoptosis has recently been associated with CHOP overexpression (Jia *et al.*, 2010).

Increasing our understanding of the molecular basis of cell death induced by activating ER stress/UPR signaling is of considerable interest, since many proteins in these pathways constitute important potential drug targets (Johnson *et al.*, 2011). In the study of (Barceló-Coblijn *et al.*, 2011), we showed that cancer cells have very low membrane sphingomyelin and high phosphatidylethanolamine levels. In glioma and other types of cancer cells but not in normal cells, 2OHOA induces changes in these lipids to reach values found in healthy tissues. The present study sheds light on the signaling events that follow the activation of this molecular switch. Here, we demonstrate the selective induction of several key effectors of ER stress/UPR cell death (P-eIF2α, IRE1α, ATF4 and CHOP) by 2OHOA in three human glioma cells. Moreover, we provide cellular and molecular evidence that 2OHOA induces autophagy in these cells. This may constitute a novel therapeutic strategy to combat glioma when cells are reluctant to enter apoptosis. As a matter of fact, we have demonstrated that 2OHOA has a greater efficacy than temozolomide, the reference drug for the treatment of glioma, in subcutaneous and orthotopic xenograft models of human glioma in nude mice (Terés *et al.*, 2012). In conclusion, the design of new lipid molecules such as 2OHOA that can modulate ER stress/UPR, constitutes a promising and novel approach to treat gliomas and other neoplasias.

4. Alzheimer's Disease: Effects of LP226A1, LP204A1 and LP205A1 on SH-SY5Y Neuroblastoma Cell Line

4.1. Introduction

Alzheimer's disease (AD), the most common neurodegenerative disorder, is in part characterized by the formation of two types of protein aggregates in the brain: amyloid plaques, which form an extracellular lesion composed of the Aβ peptide; and intracellular neurofibrillary tangles (NFTs), which are composed of hyperphosphorilated filaments of the microtubule-associated protein tau. Genetic evidence implicates deregulated Aβ homeostasis as an early event in Alzheimer´s disease pathology (Masters *et al.*, 1985). For this reason, most Alzheimer´s disease therapeutics have targeted the Aβ peptide, although tau-targeted therapies are also being pursued (Barten and Albright, 2008; Gura, 2008).

Many hypotheses have been proposed to explain the origin of the pathology. The "amyloid cascade hypothesis" (Figure 4.1), suggests that the deposition of Aβ is the initial pathological event in AD leading first to the formation of senile plaques (SPs), then to neurofibrillary tangles (NFTs), neuronal cell death, and finally todementia. While there is considerable evidence supporting this hypothesis, some observations seem inconsistent: (a) SPs and NFTs may develop independently, and (b) SPs and NFTs may be products rather than causes of neurodegeneration in AD (Reitz, 2012).

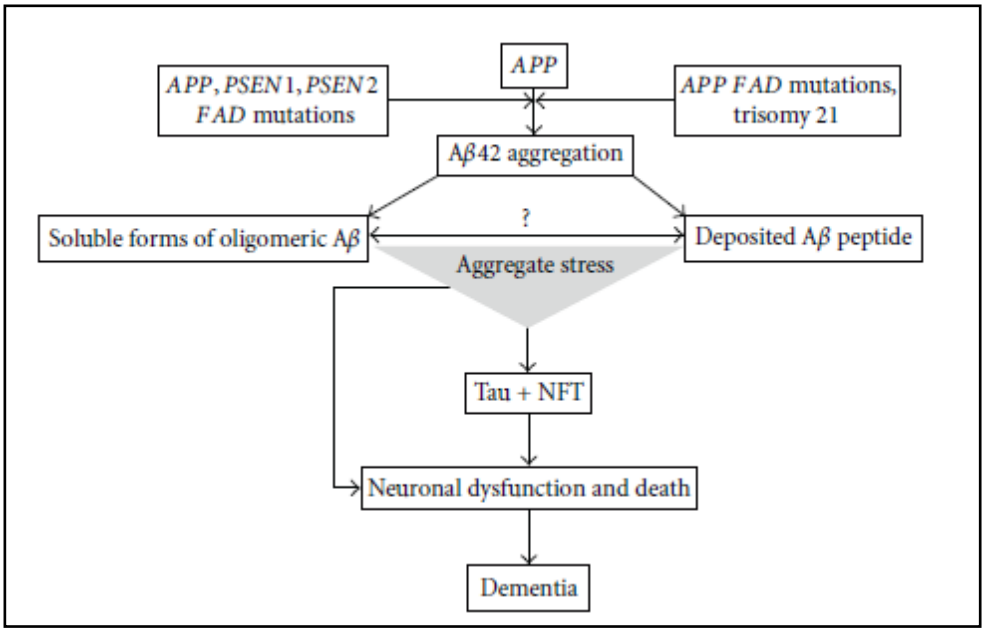

Figure 4.1 Amyloid cascade hypothesis (ACH). Figure taken from Reitz, *et al*, 2012. Two key observations resulted in the original formulation of the ACH. First, the detection of Aβ as the main constituent of the SPs (Glenner and Wong, 1984) and second mutations of the Amyloid Precursor Protein (APP) (Goate *et al.*, 1991), PSEN1and PSEN2 genes (Levy-Lahad *et al.*, 1995; Sherrington *et al.*, 1995), which were found in families with early onset AD (FAD) As a consequence of these observations, the presence of Aβ within SPs was interpreted as an effect of these mutations that subsequently led to cell death and dementia. It was assumed that this amyloid deposition could explain the pathogenesis of all types of AD.

Once synthesized and post-translationally modified, Amyloid Precursor Protein (APP), can be processed in its mature form by at least two proteolytic pathways: the so-called "non-amyloidogenic" and the "amyloidogenic" pathways (Figure 4.2). While, in the first pathway, the enzymes implicated (α- and γ- secretases) cleave APP within the Aβ sequence, thus impeding the formation of the Aβ peptide, in the second pathway (in which β- and γ- secretases are implicated) we found toxic Aβ formation, mainly 40 and 42 (Claeysen *et al.*, 2012). APP can be proteolyzed directly by α-secretase and then γ-secretase, a process that does not generate Aβ, or reinternalized into another endosomal compartment containing the proteases β secretase and γ-secretase that results in the production of Aβ. The interplay between APP localization and α-, β- and γ- secretases determines the degree of Aβ production. The intracellular localization and trafficking of APP are complicated with APP found at the Golgi, trans-Golgi network (TGN), endosomes and plasma membrane. Moreover the secretases involved can also be found in various sub-cellular compartments (Claeysen *et al.*, 2012).

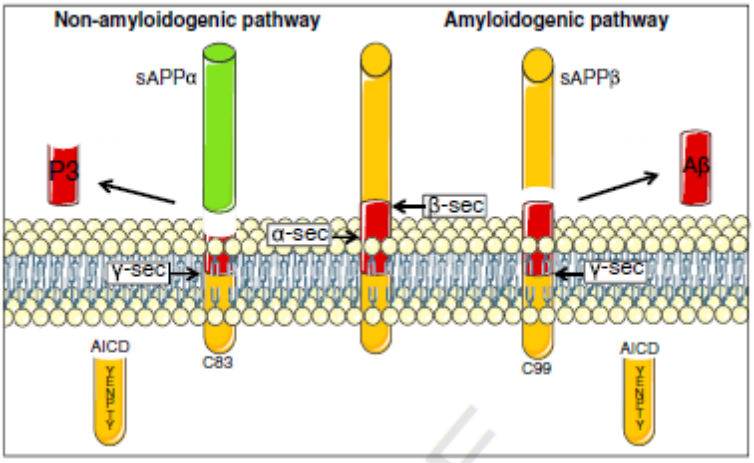

Figure 4.2 Schematic representation of APP processing. Figure taken from Claeysen, *et al*, 2012. In the non-amyloidogenic pathway, α-secretase cleaves APP within the Aβ ectodomain (sAPPα) and the membrane anchored C-terminal fragment (C83). The subsequent action of γ-secretase releases two peptides: the APP intracellular domain (AICD) and P3. In the amyloidogenic pathway, β-secretase cleaves APP releasing the soluble sAPPβ and the C terminal fragment C99, which is cleaved by γ-secretase to produce AICD and Aβ.

α-Secretases (ADAM). Several transmembrane proteases belonging to the metalloproteases have been proposed to act as α-secretases. The most accredited enzymes for this role are the members of the A Desintegrin and Metalloprotease (ADAM) family: ADAM9, 10 and 17 (Fahrenholz *et al.*, 2000; Asai *et al.*, 2003; Kuhn *et al.*, 2010). It has been demonstrated that while ADAM17 and 9 are involved in a regulated cleavage, ADAM10 is the major ADAM family member responsible in constitutive activity in neurons (Kuhn *et al.*, 2010). ADAM10 is in fact highly expressed in the brain while ADAM9 (Weskamp *et al.*, 1996) and ADAM17 (Black *et al.*, 1997) are found at low concentrations. It is currently known that ADAM10 is synthesized in the Endoplasmatic Reticulum (ER) as a proenzyme. It is mostly present in the Golgi at steady state (Lammich *et al.*, 1999), but is found in its mature form at the cell surface. Studies have shown that α-secretase activity in neurons is present mostly at the cell surface (Parvathy *et al.*, 1999). The relevance of ADAM10 in APP processing and AD is well documented in several publications. It is understood that overexpression of ADAM10 is able to increase α-cleavage, while the opposite effect, a reduction of the non-amyloidogenic pathway activity, is seen with an inhibition of ADAM10 (Lammich *et al.*, 1999; Lopez-Perez *et al.*, 2001). The ADAM10 intracellular trafficking, a key point in regulating the non-amyloidogenic pathway, can be regulated by muscarinic receptors (Cisse *et al.*, 2011). Furthermore, it has also been suggested that cholesterol plays a modulator role in α-secretase activity (Kojro *et al.*, 2001; Allinson *et al.*, 2003). Cholesterol-lowering drugs up-regulate α-secretase activity (Kojro *et al.*, 2010).

β-Secretases (BACE1). Interestingly, while α-secretase cleavage of APP is highly active in non neuronal cells, the amyloidogenic pathway is predominant in neurons, probably due to high levels of β-secretase in these cells (Haass *et al.*, 1992; Seubert *et al.*, 1993). β-Secretase has been identified as the enzyme BACE1 (Sinha *et al.*, 1999; Vassar *et al.*, 1999; Yan *et al.*, 1999), although a minor activity has been also attributed to BACE2 (Farzan *et al.*, 2000). It has been observed that BACE1 inhibition lowers the levels of Aβ in the brain (Sankaranarayanan *et al.*, 2008). BACE activity is influenced by pH, the most favorable environment being an acidic pH (about 5), such as in endosomes (Knops *et al.*, 1995). BACE1 acts in fact primarily on endosomes, but its action has also been revealed in lysosomes, and at the cell membrane lipid rafts. SorLA, for instance, a member of the low lipoprotein receptor superfamily, binds APP. It functions as an adaptor protein by linking it to retromers (a family of proteins that mediate the recovery of transmembrane proteins from the endosomes to the trans-Golgi network) (Claeysen *et al.*, 2012). Furthermore, studies have recently demonstrated that Aβ can mediate its own production through a feedback mechanism on APP and BACE by acting as a transcription factor (Bailey *et al.*, 2011).

γ-Secretases (PS-1). Following the first APP cleavage by α- or β-secretases, the γ-secretase complex cleaves the C-terminal fragments (C83 and C99), an activity present at both cell surface and in endosomes (Fukumori *et al.*, 2006). This process is known as "Regulated Intramembrane Proteolysis" (RIP) (Lichtenthaler, 2011). The γ-secretase complex is composed of Nicastrin (Nct), Anterior Pharynx defective one (APH1), Presenilin Enhancer 2 (PEN2), Presenilin 1 (PS-1), and/or 2 (PS-2) (Shirotani *et al.*, 2004; Wolfe, 2009; Bergmans and De Strooper, 2010). In this complex, the active site is represented by presenilins. The cleavage of C83 and C99 brings to the formation of p3 and Aβ (mainly 40 and 42) together with an APP intracellular domain (AICD). Mutations at presenilin level are present in the majority of familial AD cases (Bertram *et al.*, 2010). Indeed, inhibition of the two presenilins completely abolishes the formation of Aβ (Herreman *et al.*, 2000; Seiffert *et al.*, 2000). The primary warning to targeting γ-secretase for Alzheimer´s disease therapeutics is that APP is not the only substrate of γ-secretase. The most important alternative cleavage substrate is the Notch receptor (De Strooper *et al.*, 1998; De Strooper and Konig, 1999). The unfortunate consequence is that potent γ-secretase inhibitors have serious gastrointestinal and immunological side effects (Wong *et al.*, 2004). As a result of this draw-back, the field has shifted towards developing γ-secretase modulators. These compounds either selectively inhibit γ-secretase cleavage of APP, leaving Notch cleavage unaffected, or alter γ-secretase cleavage of APP to favor Aβ 40 production rather than Aβ42 (Aguzzi and O'Connor, 2010). Aβ42 seems to be more closely associated with the development of amyloid pathology than its counterpart, Aβ40 (Aguzzi and O'Connor, 2010). Drugs that modulate γ-secretase activity in this manner include non-steroidal anti-inflamatory drugs (NSAIDs) such as ibuprofen (Weggen *et al.*, 2001). One such γ-secretase-modulating compound, the NSAID (R)-Flurbiprofen, effectively reduced amyloid plaque formation (Imbimbo *et al.*, 2007) and

rescued memory deficits (Kukar *et al.*, 2007) in APP transgenic mice. However, it failed to significantly enhance cognitive performance of patients with AD in Phase III clinica trials (Myriad-Genetics, 2008).

Hyperphosphorilated Tau. AD is characterized by an extensive deposition of Aβ outside of neurons, and the formation of neurofibrillary tangles (NFTs) consisting of hyperphosphorilated tau, as intraneuronal inclusions (Selkoe, 1986). Tau is a cytoplasmic protein that binds to tubulin during its polymerization by stabilizing microtubules. In AD, tau is abnormally phosphorilated resulting in aggregate generation of (NFTs) that are toxic to neurons (Reitz, 2012). Before NFT formation, tau is hyperphosphorilated by glycogen syntase kinase 3β (GSK3β) activation and forms granular tau oligomers. This hyperphosphorylated tau is associated with synapse loss (Kimura *et al.*, 2007). A recent study found that reducing tau alleviated Aβ-induced memory impairment in APP transgenic mice (Roberson *et al.*, 2007), suggesting that tau contributes to memory impairment in APP Tg mice. It has also been reported that Aβ activates GSK3β, inducing tau hyperphosphorilation in hippocampal neurons, and that it is this GSK3β activation that leads to an eventual memory impairment in APP Tg mice (Takashima *et al.*, 1993).

As we mentioned in the general introduction in the context of the membrane lipid therapy new molecules were designed in our group for the treatment of AD. We have developed a series of synthetic carbon alpha hydroxylated derivatives [2-hydroxyarachidonic acid (LP204A1), 2-hydroxyeicosapentaenoic acid (LP205A1) and 2-hydroxydocosahexanoic acid (LP226A1)] from its lipid precursors [arachidonic acid (ARA), eicosapentaenoic acid (EPA), docosahexaenoic acid (DHA)]. We chose these molecules because treatments of human neuroblastoma SH-SY5Y cells with ARA (20:4), EPA (20:5) and DHA (22:6) for 24 hours increased sAPPα secretion and membrane fluidity (Yang *et al.*, 2011). Moreover, Alzheimer´s disease patients have significantly lower DHA levels compared to control subjects (Tully *et al.*, 2003). Thus, we hypothesized that a treatment with a derivate of DHA could compensate this deficiency, recovering the fluidity and normal functioning of the membranes of healthy neurons. It has already been proven that DHA rich diets reduce PS-1 levels (Green *et al.*, 2007), and that drugs which modulate γ-secretase activity reduce amyloid plaque formation (Imbimbo *et al.*, 2007) and rescue memory deficits (Kukar *et al.*, 2007) in APP-transgenic mice. Moreover, we have obtained in our research group similar results related to memory improvement in 5XFAD transgenic mice treated with LP226A1, LP205A1 or LP204A1 (Fiol M.A., manuscript in preparation).

In this chapter, we studied the effects of LP226A1 (2OH-DHA), LP204A1 (2OH-ARA) and LP205A1 (2OH-EPA) hydroxy derivates, in the regulation of the expression of α-, β- and γ-secretases, hyperphosphorilated tau and GSK3β Alzheimer´s disease related proteins on SH-SY5Y neuroblastoma cells (a cellular model of Alzheimer´s disease).

4.2. Results

4.2.1 Cell Viability Study of SH-SY5Y Neuroblastoma Cells Treated with LP226A1, DHA, LP205A1, EPA, LP204A1 or ARA.

Previous studies have shown that Docosahexanoic acid (DHA) induces neuronal survival in Alzheimer´s Disease models (Zhao *et al.*, 2011). Here, we evaluated the effects of DHA, Eicosapentanoic acid (EPA) and Arachidonic acid (ARA) in comparison with their 2-hydroxy derivates LP226A1, LP205A1 and LP204A1 on SH-SY5Y human neuroblastoma cells viability. Cell viability was determined by an MTT assay. In this context, LP226A1 (0 – 600 µM; 24 h, 48 h and 72 h) reduced the cell viability of SH-SY5Y cells below 50 % at a concentration of 125 µM (Figure 4.3A). In contrast, DHA (0 – 600 µM; 24 h, 48 h and 72 h) reduced the cell viability of SH-SY5Y cells below 50 % at a concentration of 250 µM (Figure 4.3B). In addition, LP205A1 and EPA (0 – 600 µM; 24 h, 48 h and 72 h) both reduced cell viability of SH-SY5Y cells below 50 % at a concentration of 250 µM (Figure 4.3C and D). Finally, LP204A1 (0 – 600 µM; 24 h, 48 h and 72 h) reduced cell viability of SH-SY5Y cells below 50 % at a concentration of 250 µM (Figure 4.3E), while ARA reduced cell viability of SH-SY5Y cells below 50 % at concentrations of 70 , 80 and 90 µM at 24 h, 48 h and 72 h of treatment, respectively (Figure 4.3F). These results demonstrated a similar toxicity of the polyunsaturated fatty acids (DHA, EPA and ARA) and their 2-hydroxy analogs (LP226A1, LP205A1 and LP204A1) on the treatment of SH-SY5Y cells.

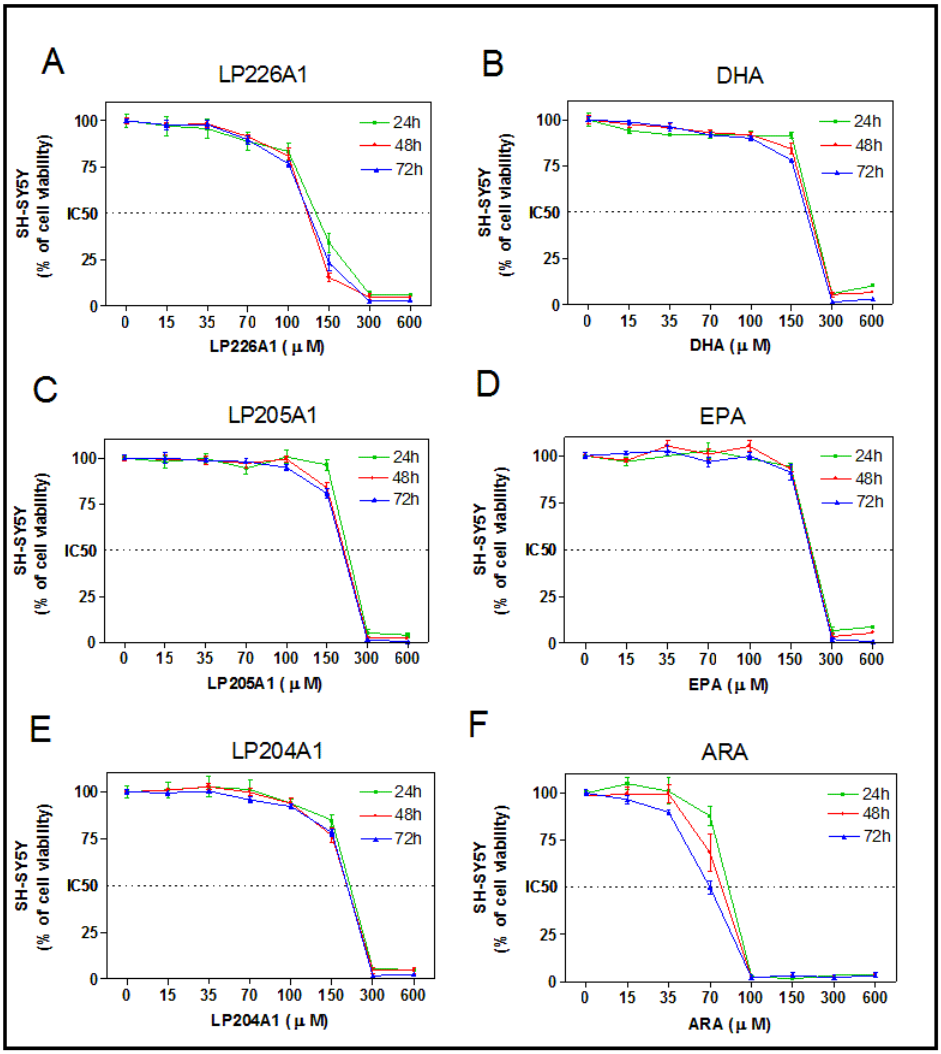

Figure 4.3 Cell Viability of SH-SY5Y human neuroblastoma cells assessed by MTT assay. SH-SY5Y neuroblastoma cells were exposed to increasing doses (15-600 µM) of LP226A1 (A), DHA (B), LP205A1 (C), EPA (D), LP04A1 (E), and ARA (F) for different periods of time (24 h, 48 h or 72 h). Values are expressed as percentage of non treated control, n = 5.

4.2.2 Down-regulation of γ-secretase (PS-1) in SH-SY5Y Neuroblastoma Cells Treated with LP226A1, LP205A1 or LP204A1.

It has already been shown in APP-transgenic mice that DHA rich diets reduce PS-1 levels (Green *et al.*, 2007), and that drugs, which modulate γ-secretase activity as (R) – flurbiprofen, effectively reduce amyloid plaque formation (Imbimbo *et al.*, 2007) and rescue memory deficits (Kukar *et al.*, 2007). In this context, we have obtained in our research group similar results related to memory improvement in 5XFAD transgenic mice treated with LP226A1, LP205A1 and LP204A1 (Fiol M.A., manuscript in preparation). We have therefore analyzed PS-1 protein levels in SH-SY5Y neuroblastoma cells treated with LP226A1, LP205A1 and LP204A1, to see if PS-1 was down-regulated after treatment. Here, we observed a significant down-regulation of PS-1 protein levels in a dose-dependent manner (from 10 to 90 μM) in SH-SY5Y cells treated with LP226A1 at 24 h, 48 h and 72 h (Figure 4.4 A-C). Ttreatments of SH-SY5Y cells with LP204A1 or LP205A1 (from 20 to 45 μM) also induced a very significant PS-1 down-regulation at 24 h, 48 h and 72 h (Figure 4.4 D-F). These results show for the first time that LP226A1, LP205A1 and LP204A1 down-regulate γ-secretase (PS-1) in SH-SY5Y neuroblastoma cell line, suggesting they could be suitable drugs for the treatment of Alzheimer.

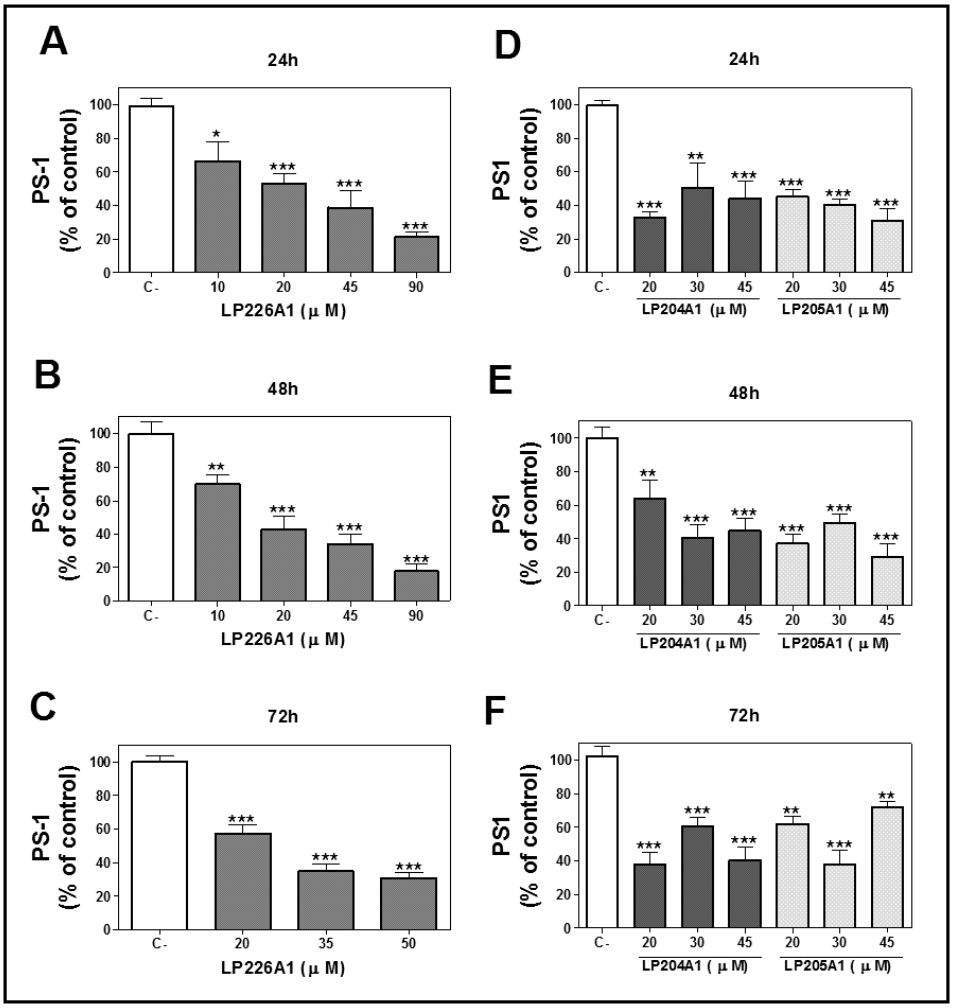

Figure 4.4. PS-1 down-regulation in SH-SY5Y cells treated with LP226A1, LP204A1, and LP205A1. PS-1 protein levels in SH-SY5Y neuroblastoma determined by immunoblotting. Each bar diagram is showing the mean ± SEM of PS-1 expression after exposure to LP226A1 (10-90 μM) at 24 h (A), 48 h (B) and 72 h (C) compared to untreated controls (C-). And PS-1 expression after exposure to LP204A1 or LP205A1 (20, 30 or 45 μM) at 24 h (D), 48 h (E) and 72 h (F) compared to untreated controls (C-). Values are expressed as percentage of control, n = 4. The asterisks indicate a significant effect of the treatment as compared with the non treated control (*p<0.05, **p<0.01, ***p<0.001).

4.2.3 Down-regulation of β-secretase (BACE1) in SH-SY5Y Neuroblastoma Cells Treated with LP226A1, LP205A1 or LP204A1.

Previous studies have shown that a DHA-derived Neuroprotectin D down-regulates BACE1 expression (Zhao *et al.*, 2011). For this reason, we studied BACE1 (β-secretase)

protein levels in SH-SY5Y neuroblastoma cells treated with LP226A1, LP205A1 or LP204A1. We wanted to see if these hydroxy derivates down-regulated BACE1 (β-secretase). In this context, treatments with LP226A1 for 24 h (Figure 4. 5 A) and 72 h (Figure 4. 5 B), as well as with LP204A1 and LP205A1 for 24 h (Figure 4. 5 C) and 72 h (Figure 4. 5 D) markedly reduced BACE1 protein levels in a concentration-dependent manner. These results further suggest a suitability of these drugs for the treatment of Alzheimer throughout the β amyloid cascade inhibition.

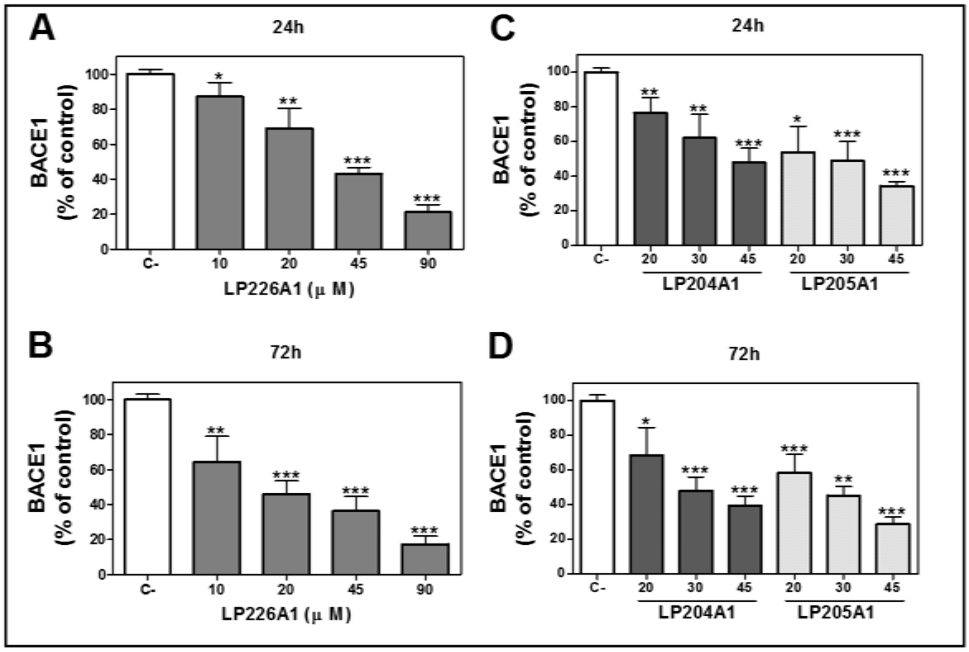

Figure 4.5. BACE1 down-regulation in SH-SY5Y cells treated with LP226A1, LP204A1, and LP205A1. BACE1 protein levels in SH-SY5Y neuroblastoma determined by immunoblotting. Each bar diagram is showing the mean ± SEM of BACE1 expression after exposure to LP226A1 (10-90 μM) at 24 h (A), 72 h (B) compared to untreated controls (C-). BACE1 expression after exposure to LP204A1 or LP205A1 (20, 30 or 45 μM) at 24 h (C) and 72 h (D) compared to untreated controls (C-). Values are expressed as percentage of control, n = 4. The asterisks indicate a significant effect of the treatment as compared with the non treated control (*p<0.05, **p<0.01, ***p<0.001).

4.2.4 SH-SY5Y Neuroblastoma Cell Differentiation into Neuron-like Cells

In the above described experiments we have used exponentially growing SH-SY5Y neuroblastoma cells which are often used as an *in vitro* model for Alzheimer Disease (Lopes *et al.*, 2010). This cell line is a human neuroblastoma derived from SK-N-SH cells. These cells present an immature phenotype in culture (Biedler *et al.*, 1978). They are typically locked in an early neuronal differentiation stage, characterized biochemically by the low presence of neuronal markers (Biedler *et al.*, 1978; Gilany *et al.*, 2008). To further investigate the effects of our compounds, we differentiated SH-SY5Y cells into a mature neuron-like phenotype, with neuritis outgrowth and branches. For this purpose, we exposed SH-SY5Y cells to retinoic acid (RA) and human brain derived neurotrophic factor (hBDNF) sequentially, in serum-free medium. This process gave rise to homogeneous populations of cells with neuronal morphology (Encinas *et al.*, 2000; Jamsa *et al.*, 2004).

The first step was pre-differentiating the cells with RA for 5 days by avoiding light. The cells were then incubated with hBDNF in the absence of serum. To validate the differentiation process, we first studied the morphology of cells upon differentiation, and observed an increased number of neuritis and branches on differentiated cells, compared to exponential growing cells that maintained a typical epithelial morphology (Figure 4.6A). Changes in nestin, a specific non-differentiated neuronal cell marker, were evaluated by Western Blot immunoassay. A significant decrease of nestin was detected after differentiation (Figure 4.6B). We also observed a complete decrease in cellular proliferation. We therefore examined how the differentiation process affected the cell cycle progression, and we noticed a cell cycle arrest in the differentiated cells where the distribution of cells in G_1 phase shifted from 45.17 ± 0.4 % to 58.35 ± 0.6 % (Figure 4.6C). In order to corroborate these data, changes in cyclin-dependent kinase 4 (Cdk4) (Figure 4.6D) and cyclin-dependent kinase 6 (Cdk6) (Figure 4.6E), were also evaluated by Western Blot immunoassay. A significant decrease of these proteins, whose activity is restricted to the G_1-S phase, was detected after differentiation. G_1-S phase is controlled by the regulatory subunits D-type cyclins. As a result, we also studied changes on Cyclin D 3 (Figure 4.6G), and observed a significant decrease after differentiation. Finally, we discovered a down-regulation of dihydrofolate reductase (DHFR), an enzyme responsible for DNA synthesis (Figure 4.6F).

Since the SH-SY5Y cell differentiation process was accomplished successfully, we pursued our experiments on SH-SY5Y differentiated cells.

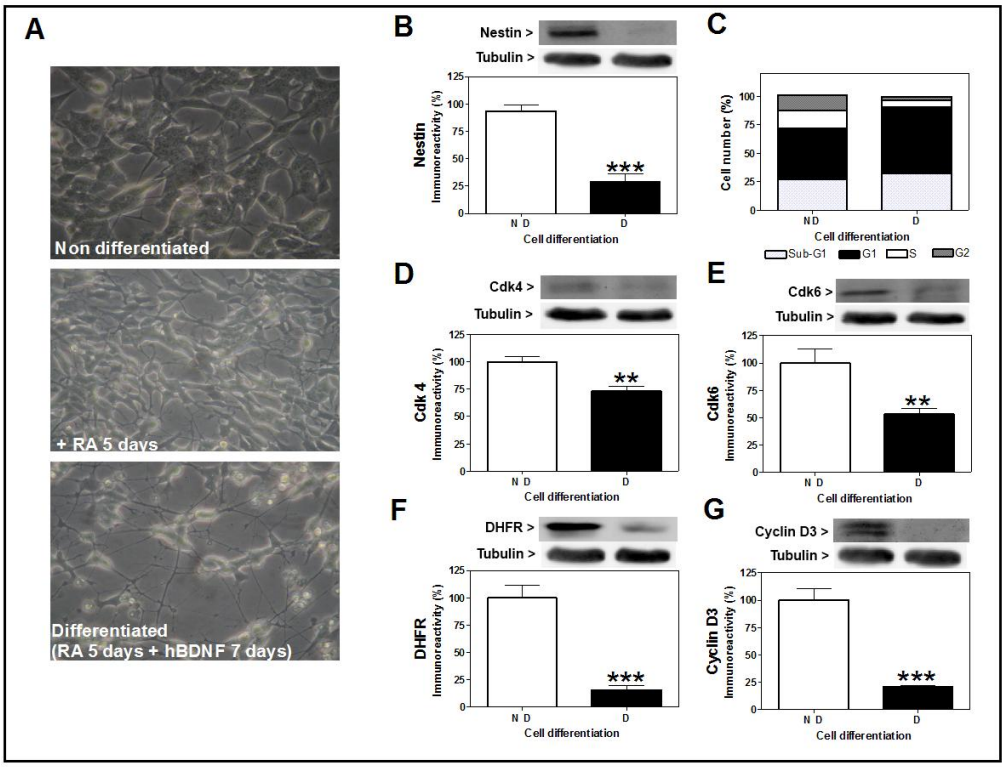

Figure 4.6. SH-SY5Y neuroblastoma cell differentiation into neuron-like cells. (A) Representative phase-contrast micrographs (20 x magnification) of SH-SY5Y cells non-differentiated; after 5 days incubation with RA and completely differentiated with RA + hBDNF. (B) Nestin protein levels determined by immunoblotting in non differentiated (ND) and differentiated (D) SH-SY5Y cells. Each bar diagram shows the mean ± SEM of Nestin. (C) Bar diagram shows the percentage of SH-SY5Y cells in Sub-G_1, G_1, S and G_2/M phases with respect to the total cell number. (D) Cdk4, (E) Cdk6, (F) DHFR, (G) Cyclin D3 protein levels determined by immunoblotting in non differentiated (ND) and differentiated (D) SH-SY5Y cells. Each bar diagram shows the mean ± SEM of protein. Values of immunoblots are expressed as percentage of non differentiated cells, n = 4. The asterisks indicate a significant effect of the treatment as compared with the non treated control (**p<0.01, ***p<0.001).

4.2.5 Cell Viability Study of Differentiated SH-SY5Y Cells Treated with LP226A1, LP205A1, LP204A1, DHA or EPA.

Using the MTT assay, we evaluated the effect of DHA and EPA in comparison with their 2 hydroxy derivates LP226A1, LP205A1, and LP204A1 on differentiated SH-SY5Y human neuron-like cells viability. In this context, treatments with LP226A1 and LP205A1 showed an IC_{50} of 18 µM (Figure 4.7A). However, LP204A1 was shown to be much more cytotoxic with an IC_{50} of 7.5 µM (Figure 4.7A). This could be due to the fact that LP226A1 (2OH-DHA) and LP205A1 (2OH-EPA) are polyunsaturated omega-3 fatty acids (ω-3) while LP204A1 (2OH-ARA) is a polyunsaturated omega-6 fatty acid (ω-6). On the other hand, treatment with DHA and EPA proved to be slightly less cytotoxic in comparison with

treatment with LP226A1 and LP205A1, respectively. DHA and EPA showed an IC_{50} of 28 µM and 23 µM respectively.

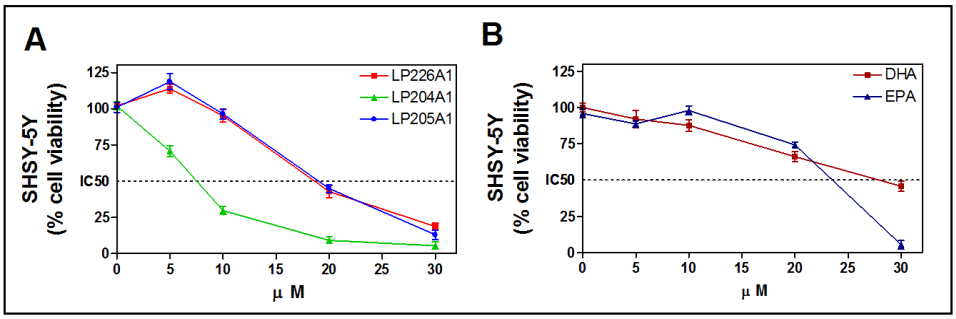

Figure 4.7 Cell Viability of differentiated SH-SY5Y human neuron-like cells assessed by MTT assay. differentiated SH-SY5Y cells were exposed to increasing doses (5-30 µM) of (A) LP226A1, LP205A1 or LP04A1 and (B) DHA or EPA for 24 h. Values are expressed as percentage of non treated control, n = 5.

To study the morphological effect of these drugs on the differentiated SH-SY5Y cells, we analyzed the cell shape and the number of branches by phase contrast micrographs before and after treatment (Figure 4.8). We did not observe important changes in the number of cells nor the general shape after treatment with LP226A1 or LP205A1 at 5 and 10 µM (Figure 4.8). However, we did observe a slight reduction in the number of branches at 10 µM. Treatments with LP204A1 resulted in cell damage, especially at 10 µM (Figure 4.8). The number of cells and neuritis were both seriously affected by the treatment with LP204A1.

In this context, we paid special attention to LP226A1 and LP205A1 treatments at doses of 5 and 10 µM (therapeutic doses) in the subsequent experiments. Nevertheless, we also extended our studies to LP204A1 treatments and higher doses (20 and 30 µM, toxic doses) of all molecules to obtain a complete picture of the influence of these drugs.

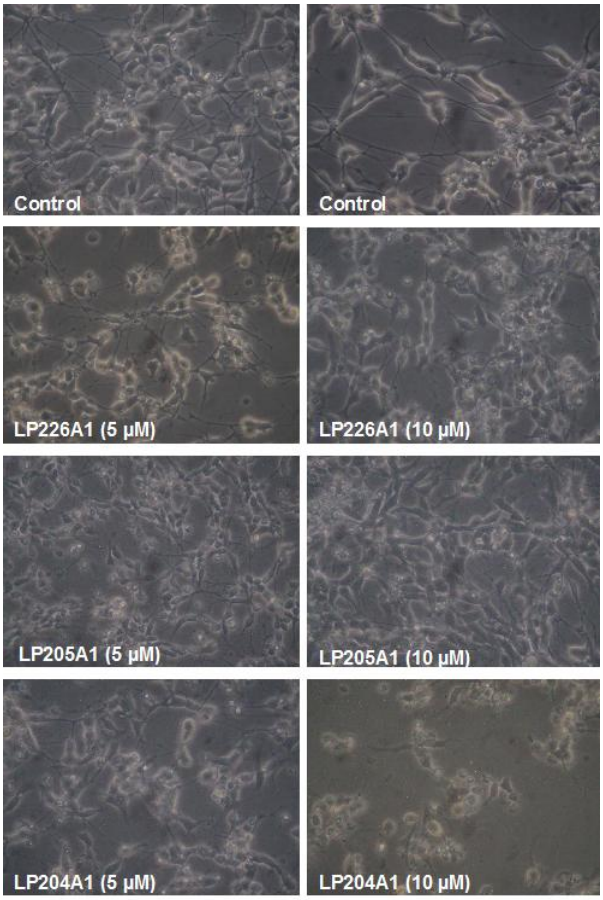

Figure 4.8. Representative phase-contrast micrographs (20 x magnification) of differentiated SH-SY5Y cells treated with LP226A1, LP205A1 or LP204A1 (5 and 10 µM, 24h).

4.2.6 Down-regulation of γ-Secretase (PS-1) in Differentiated SH-SY5Y Neuron-like cells treated with LP226A1, LP205A1 or LP204A1.

Previous experiments showed down-regulation of PS-1 after treatment with LP226A1, LP205A1, or LP204A1 in non-differentiated SH-SY5Y cells. To determine whether the observed changes were exclusive on neuroblastoma cells, or, in contrast, if the drugs were also down-regulating PS-1 in the neuron-like SH-SY5Y cells, we performed Western Blot immunoassays at different times and doses in previously differentiated SH-SY5Y cells. As early as 7 h after treatments with LP226A1, LP204A1 or LP205A1, our results showed a significant decrease of PS-1 protein levels in a dose-dependent manner

(Figure 4.9A). PS-1 down-regulation was even stronger after a 24 h-treatment (Figure 4.9B). No important differences on PS-1 down-regulation were observed among the three different compounds after 7 h. However, after a 24 h-treatment, LP204A1 down-regulated PS-1 protein expression more strongly than with LP226A1 or LP205A1. These results confirm our previous observations from section 4.2.2 about PS-1 protein down-regulation in non-differentiated SH-SY5Y cells after treatments with LP226A1, LP204A1 and LP205A1.

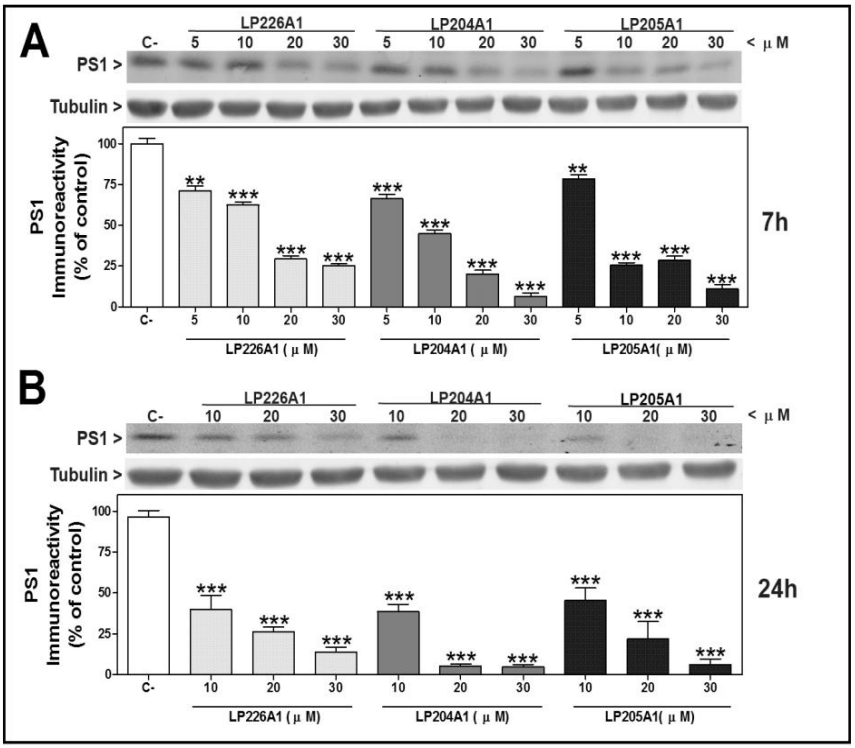

Figure 4.9 PS-1 down-regulation in differentiated SH-SY5Y cells treated with LP226A1, LP204A1, and LP205A1. PS-1 protein levels in SH-SY5Y neuron-like cells determined by immunoblotting. Each bar diagram is showing the mean ± SEM of PS-1 expression after exposure to LP226A, LP204A1 or LP205A1 (5 -30 µM) at 7 h (A) compared to untreated controls (C-). (B) PS-1 expression after exposure to LP226A, LP204A1 or LP205A1 (10 -30 µM) at 24 h compared to untreated controls (C-). Values are expressed as percentage of control, n = 3. The asterisks indicate a significant effect of the treatment as compared with the non treated control (**p<0.01, ***p<0.001).

4.2.7 Down-regulation of β-secretase (BACE1) in Differentiated SH-SY5Y Cells Treated with LP226A1, LP205A1 or LP204A1.

BACE1 was down-regulated in differentiated SH-SY5Y cells after 24 h-treatments with LP226A1, LP205A1 and LP204A1 (Figure 4.10). The three different lipids, LP226A1, LP204A1 and LP205A1, equally down-regulated BACE1 protein expression. No significant differences on BACE1 protein expression were detected after a 7 h-treatment (data not shown). In order to obtain these data, we performed Western Blot immunoassays at different time points and doses in previously differentiated SH-SY5Y cells.

Interestingly, β-secretase (BACE1) activity was down-regulated in 5XFAD (APP/PS1) transgenic mice (Oakley *et al.*, 2006) when treated with LP226A1 (Torres M; personal communication). These results support BACE1 protein down-regulation observed in differentiated SH-SY5Y cells after treatment with LP226A1.

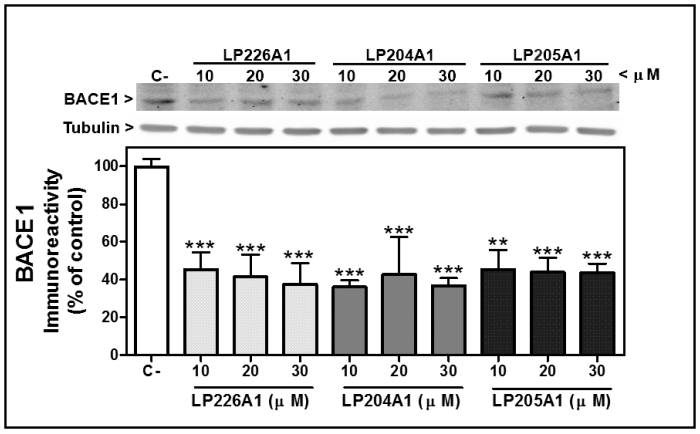

Figure 4.10 BACE1 down-regulation in differentiated SH-SY5Y cells treated with LP226A1, LP204A1 and LP205A1. BACE1 protein levels in SH-SY5Y neuron-like cells determined by immunoblotting. The bar diagram shows the mean ± SEM of BACE1 expression after exposure to LP226A, LP204A1 or LP205A1 (10 -30 μM) at 24 h compared to untreated controls (C-). Values are expressed as percentage of control, n = 3. The asterisks indicate a significant effect of the treatment as compared with the non treated control (**p<0.01, ***p<0.001).

4.2.8 α-Secretase (ADAM10) in Differentiated SH-SY5Y Cells Treated with LP226A1, LP205A1 or LP204A1.

Previous studies have shown that levels of mature ADAM-10 were unaltered by the dietary supplementation with DHA in 3x Tg-AD mice (Green *et al.*, 2007). However, it has also been proposed that DHA-derived neuroprotectin D1 (NPD1) induced a significant increase of ADAM10 in human neuronal-glial (HNG) primary cells (Zhao *et al.*, 2011). For this reason, we studied mature ADAM10 expression in our differentiated SH-SY5Y neuron-like cells after treatments with LP226A1, LP204A1 and LP205A1. In this context, after a 7 h-treatment and at lower doses, ADAM-10 was not significantly up-regulated with LP226A1 (Figure 4.11A). Treatments with LP204A1 or LP205A1 scarcely affected ADAM10 protein expression, except with the highest dose of LP205A1 which up-regulated ADAM10 significantly after a 7 h-treatment (Figure 4.11A). 24 h-treatments with LP226A1, LP204A1 and LP205A1 did not affect ADAM10 protein expression (Figure 4.11 B).

After performing these experiments, we can postulate that ADAM10 is not importantly regulated by any of the molecules (LP226A1, LP204A1 and LP205A1) employed to treat SH-SY5Y neuron-like cells. As LP226A1 is a hydroxyl-derivate of DHA, this would be in agreement with Green *et al*., 2007 who demonstrated that ADAM10 was unaltered by the dietary supplementation with DHA in 3x Tg-AD mice.

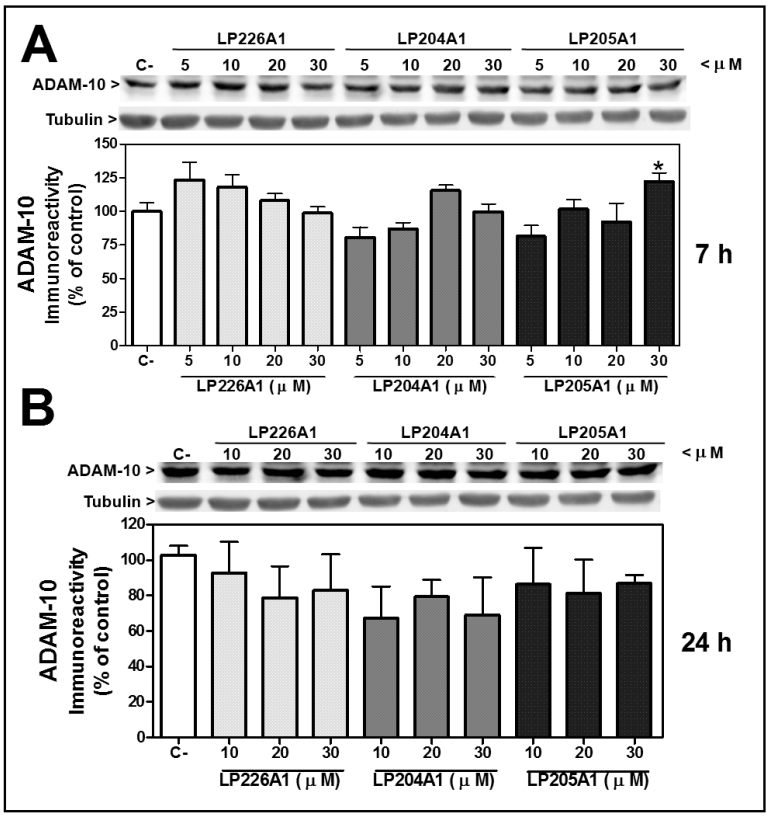

Figure 4.11 ADAM10 regulation in SH-SY5Y differentiated cells treated with LP226A1, LP204A1 and LP205A1. ADAM 10 protein levels in SH-SY5Y neuron-like cells determined by immunoblotting. Each bar diagram is showing the mean ± SEM of ADAM10 expression after exposure to LP226A, LP204A1 or LP205A1 (5 - 30 μM) at 7 h (A) compared to untreated controls (C-). (B) ADAM10 expression after exposure to LP226A, LP204A1 or LP205A1 (10 -30 μM) at 24 h compared to untreated controls (C-). Values are expressed as percentage of control, n = 3. The asterisks indicate a significant effect of the treatment as compared with the non treated control (*$p<0.05$).

4.2.9 Cell Viability Study of Differentiated SH-SY5Y Cells Incubated with Aβ42 Peptide and Treated with LP226A1, LP205A1, DHA or EPA

Cultured differentiated SH-SY5Y cells were incubated with 1.2 to 20 μM of Aβ42 peptide. The cell viability was monitored after 24 h by carrying out an MTT reduction assay. Figure 4.12A shows the results of the MTT assay, indicating that Aβ42 peptide was increasingly more toxic from 5 μM up to 20 μM, and that the IC_{50} for these cells was established at 12.5 μM. Hence, for the following experiments, we took doses of 5 μM (78%

viability) and 10µM (60% viability) to damage the cells but leaving a margin for cell recovery after treatments with the molecules (LP226A1, LP204A1, and LP205A1).

Differentiated SH-SY5Y cells incubated with a final concentration of 5 µM Aβ42 peptide were treated with LP226A1, LP204A1 or LP205A1 (5 to 30 µM). The cell viability was also monitored after 24 h by carrying out an MTT assay (Figure 4.12B). The results of the MTT assay indicated that Aβ42 peptide incubation reduced cell viability to 75 %. However, after treatment with 5 µM LP226A1 or LP205A1 it recovered up to 100 % viability. The cell viability recovery was maintained with LP205A1 10 µM treatment, and improved up to 120 % with LP226A1 10 µM treatment. LP205A1 (20 µM) treatment did not attenuate cell death anymore, while LP226A1 (20 µM) treatment still maintained 100 % cell viability. On the other hand, treatment with LP204A1 did not enhance cell viability at any dose. 30 µM was a toxic dose in all cases.

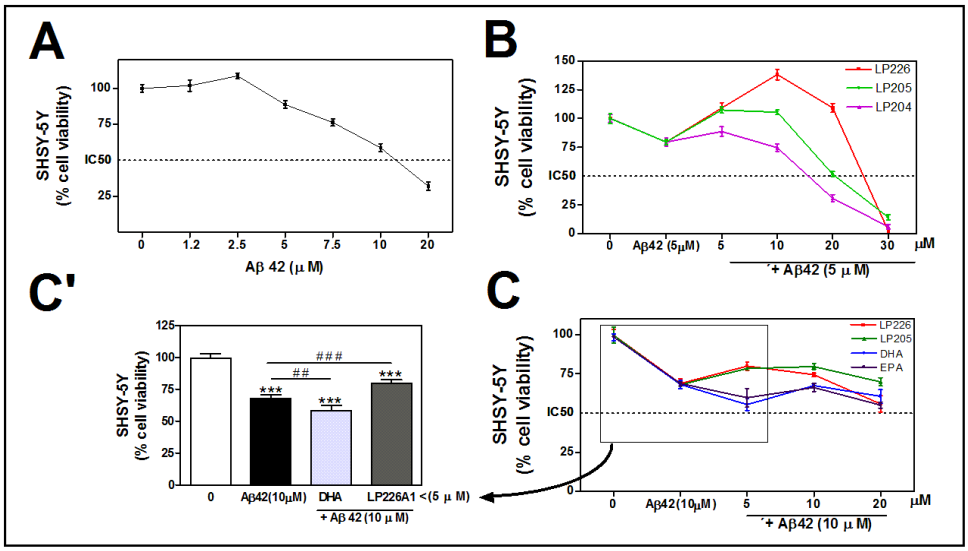

Figure 4.12 Cell Viability of SH-SY5Y human neuron-like cells assessed by MTT assay. SH-SY5Y differentiated cells were exposed to increasing doses of (A) Aβ42 peptide (1.2-20 µM); (B) Aβ42 peptide (5 µM) with or without LP226A1, LP205A1 or LP04A1 (5 to 30 µM); (C) Aβ42 peptide (10 µM) with or without LP226A1, LP205A1, DHA or EPA (5 to 20 µM) and (C') Aβ42 peptide (10 µM) with or without LP226A1 or DHA (5 µM) for 24 h. Values are expressed as percentage of non-treated control, n = 5. (**p<0.01, ***p<0.001).

Finally, differentiated SH-SY5Y cells, which were incubated with 10 µM of Aβ42 peptide, were treated with LP226A1, LP205A1, DHA or EPA (5 to 20 µM). The cell viability was again monitored after 24 h by carrying out an MTT assay (Figure 4.12C). The

results indicated that Aβ42 peptide incubation reduced cell viability to 65 %, and after treatments with 5 µM LP226A1 or LP205A1, partially recovered to 78 % viability. However, the treatment with DHA or EPA (5 µM) did not show such enhanced cell viability (Figure 4.12C and 4.12C´). Doses of 10 and 20 µM of all compounds did not induce any improvement with respect to 5 µM dose.

4.2.10 Down-regulation of γ-Secretase (PS-1) in Differentiated SH-SY5Y Cells Incubated with Aβ 42 Peptide and Treated with LP226A1, LP204A1, LP205A1, DHA or EPA

Differentiated SH-SY5Y cells incubated with a 5 µM of Aβ42 peptide, were treated concomitantly with LP226A1, LP204A1 or LP205A1 (5 to 30 µM) (Figure 4.13A), or with DHA or EPA (Figure 4.13B). PS-1 expression was monitored after 24 h by carrying out a Western Blot immunoassay. The results in Figure 4.13A indicate a significant down-regulation of PS-1 in SH-SY5Y cells after incubation with Aβ42 peptide and treatments with LP226A1, LP205A1 and LP204A1 in a dose-dependent manner. We did not find any difference in the expression of PS-1 between non-treated (control) cells and cells incubated with Aβ42 peptide.

Results in Figure 4.13B showed a down-regulation of PS-1 in SH-SY5Y cells after incubation with Aβ42 peptide and a treatment with DHA. By contrast, a treatment with EPA (+Aβ42 peptide) significantly up-regulated PS-1 at all doses.

Down-regulation of PS-1 after treatment with DHA was slightly smaller than the down-regulation induced by LP226A1 treatment. In addition, EPA and LP205A1 (its hydroxy derivate) regulated PS-1 expression in an opposite manner. While EPA up-regulated PS-1, LP205A1 down-regulated the protein. Therefore LP226A1 and LP205A1 hydroxy derivates were more effective in down-regulating PS-1 than their natural counterparts (DHA and EPA).

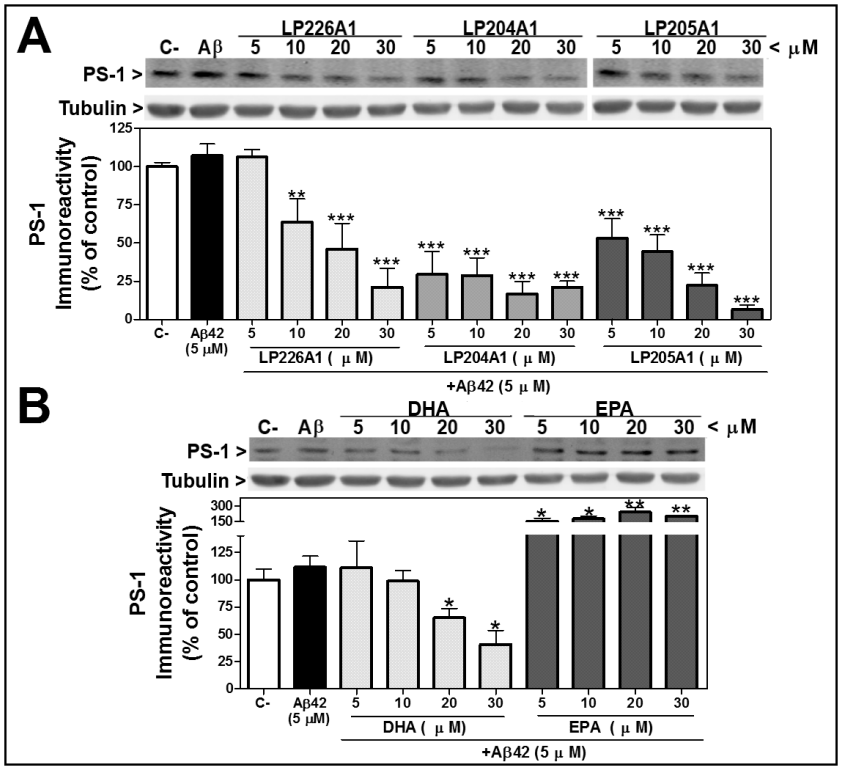

Figure 4.13 PS-1 down-regulation in differentiated SH-SY5Y cells incubated with Aβ 42 and treated with LP226A1, LP204A1, LP205A1, DHA and EPA. PS-1 protein levels in SH-SY5Y neuron-like cells determined by immunoblotting. Each bar diagram is showing the mean ± SEM of PS-1 expression after exposure to Aβ42 peptide with or without LP226A, LP204A1 or LP205A1 (5 -30 μM) at 24 h (A) compared to untreated controls (C-). (B) PS-1 expression after exposure to Aβ42 peptide with or without DHA or EPA (10 -30 μM) at 24 h compared to untreated controls (C-). Values are expressed as percentage of control, n = 3. The asterisks indicate a significant effect of the treatment as compared with the non treated control (*p<0.05, **p<0.01, ***p<0.001).

4.2.11 Down-regulation of β-Secretase (BACE1) in Differentiated SH-SY5Y Cells Incubated with Aβ 42 Peptide and Treated with LP226A1, LP204A1, LP205A1, DHA or EPA

SH-SY5Y neuron-like cells incubated with a final concentration of 5 μM Aβ42 peptide, were treated concomitantly with LP226A1, LP204A1 or LP205A1 (5 to 30 μM) (Figure 4.14A) or with DHA or EPA (Figure 4.14B). BACE1 expression was monitored after 24 h by carrying out a Western Blot immunoassay. The results in Figure 4.14A indicated a significant down-regulation of BACE1 in SH-SY5Y cells after incubation with Aβ42 peptide and treatment with LP226A1, LP205A1 or LP204A1 in a dose-dependent manner.

Interestingly, we did not find any difference in the expression of BACE1 between non-treated (control) cells and cells incubated with Aβ42 peptide.

In contrast, results in Figure 4.14B showed a down-regulation of BACE1 in SH-SY5Y cells after incubation with Aβ42 peptide and treatment with DHA or EPA (+Aβ42 peptide) in a dose-dependent fashion.

Down-regulation of BACE1 after treatments with DHA or EPA was slightly smaller than the down-regulation induced by LP226A1 or LP205A1 (their hydroxyl derivates) treatments.

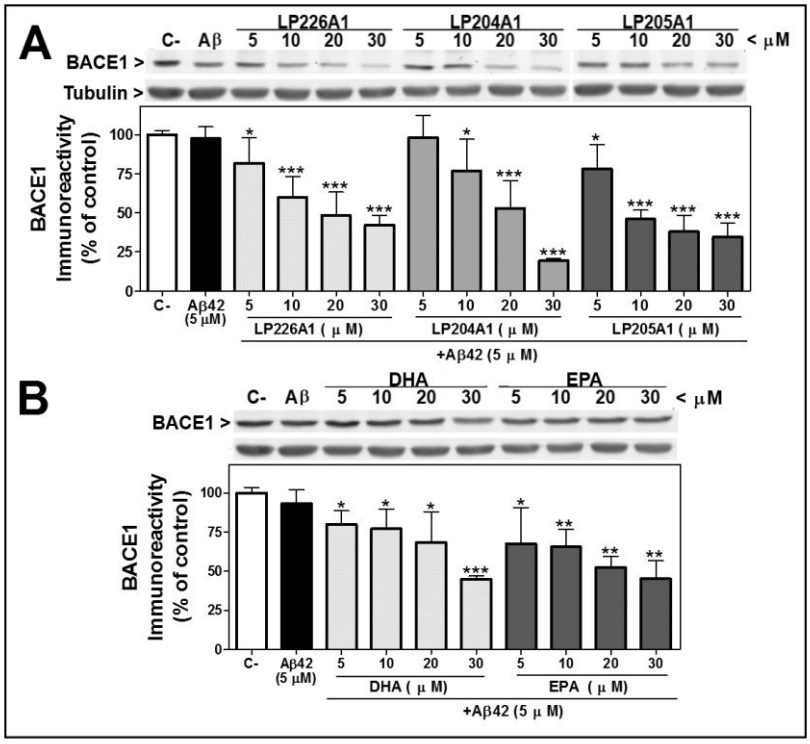

Figure 4.14 BACE1 down-regulation in differentiated SH-SY5Y cells incubated with Aβ 42 and treated with LP226A1, LP204A1, LP205A1, DHA and EPA. BACE1 protein levels in SH-SY5Y neuron-like cells determined by immunoblotting. Each bar diagram is showing the mean ± SEM of BACE1 expression after exposure to Aβ42 peptide with or without LP226A, LP204A1 or LP205A1 (5 -30 μM) at 24 h (A) compared to untreated controls (C-). (B) BACE1 expression after exposure to Aβ42 peptide with or without DHA or EPA (10 -30 μM) at 24 h compared to untreated controls (C-). Values are expressed as percentage of control, n = 3. The asterisks indicate a significant effect of the treatment as compared with the non treated control (*p<0.05, **p<0.01, ***p<0.001).

4.2.12 Regulation of α-Secretase (ADAM10) in Differentiated SH-SY5Y cells Incubated with Aβ 42 Peptide and Treated with LP226A1, LP204A1, LP205A1, DHA or EPA

Differentiated SH-SY5Y cells, incubated with a final concentration of 5 µM Aβ42 peptide, were treated with LP226A1, LP204A1 or LP205A1 (5 to 30 µM) (Figure 4.15A) or with DHA or EPA (Figure 4.15B). ADAM10 expression was monitored after 24 h by carrying out a Western Blot immunoassay. The results in Figure 4.15A only indicate a significant down-regulation of ADAM-10 in SH-SY5Y cells after incubation with Aβ42 peptide and treatments with LP226A1 or LP204A1 at 20 and 30 µM. Interestingly, we did not find any difference in the expression of ADAM10 between non-treated (control) cells and cells incubated with Aβ42 peptide, LP205A1 (+Aβ42 peptide) or cells treated with lower doses of LP226A1 (+Aβ42 peptide) or LP204A1 (+Aβ42 peptide).

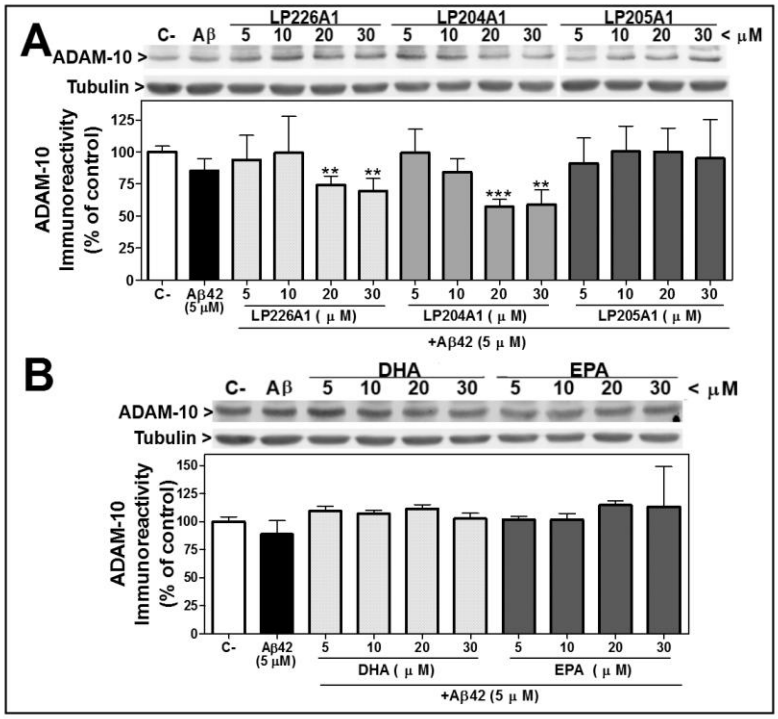

Figure 4.15 ADAM10 regulation in differentiated SH-SY5Y cells incubated with Aβ 42 and treated with LP226A1, LP204A1, LP205A1, DHA and EPA. ADAM10 protein levels in SH-SY5Y neuron-like cells determined by immunoblotting. Each bar diagram is showing the mean ± SEM of ADAM10 expression after exposure to Aβ42 peptide with or without LP226A, LP204A1 or LP205A1 (5 -30 µM) at 24 h (A) compared to untreated controls (C-). (B) ADAM10 expression after exposure to Aβ42 peptide with or without DHA or EPA (10 - 30 µM) at 24 h compared to untreated controls (C-). Values are expressed as percentage of control, n = 3. The asterisks indicate a significant effect of the treatment as compared with the non treated control (**p<0.01, ***p<0.001).

In contrast, results in Figure 4.15B did not show any regulation of ADAM10 in SH-SY5Y cells after incubation with Aβ42 peptide and treatments with DHA or EPA (+Aβ42 peptide).

4.2.13 Down-regulation of P-Tau (AT8) in Differentiated SH-SY5Y Cells Incubated with Aβ 42 Peptide and Treated with LP226A1, LP204A1, LP205A1, DHA or EPA

AD is characterized by the extensive deposition of amyloid β (Aβ) outside of neurons, and the formation of neurofibrillary tangles (NFTs) consisting of hyperphosphorilated tau as intraneuronal inclusions (Selkoe, 1986). Aβ hypothesis states that Aβ deposition directly affects neurons, inducing NFTs and neuronal death leading to dementia (Hardy and Selkoe, 2002). A recent study found that reducing tau alleviated Aβ-induced memory impairment in APP transgenic mice (Roberson *et al.*, 2007). Before NFT formation tau is hyperphosphorilated by glycogen synthase kinase 3β (GSK3β) activation (see below) and forms granular tau oligomers. This hyperphosphorilated tau is associated with synapse loss (Kimura *et al.*, 2007).

It has been previously shown that AT8 monoclonal antibody requires tau protein to be phosphorylated at both serine 202 and threonine 205 (Goedert *et al.*, 1995). The epitope of AT8 can be produced by phosphorilating tau with GSK3 (Mandelkow *et al.*, 1993).

Considering that Aβ deposition can induce NFTs (consisting on hyperphosphorilated tau), differentiated SH-SY5Y cells incubated with 5 μM of Aβ42 peptide were treated concomitantly with LP226A1, LP204A1 or LP205A1 (5 to 30 μM) (Figure 4.16). The hyperphosphorilated tau (AT8) expression was monitored after 24 h by a Western Blot immunoassay. The results in Figure 4.16 indicate a very significant up-regulation of AT8 in SH-SY5Y cells after incubation with Aβ42 peptide. Interestingly, treatments with LP226A1 or LP204A1 after Aβ42 peptide incubation induced a significant down-regulation of AT8 in a dose-dependent manner, recovering AT8 basal levels of non-treated cells. Treatments with LP205A1 after Aβ42 peptide incubation also induced a significant down-regulation of AT8 and recovered the basal levels of non-treated cells.

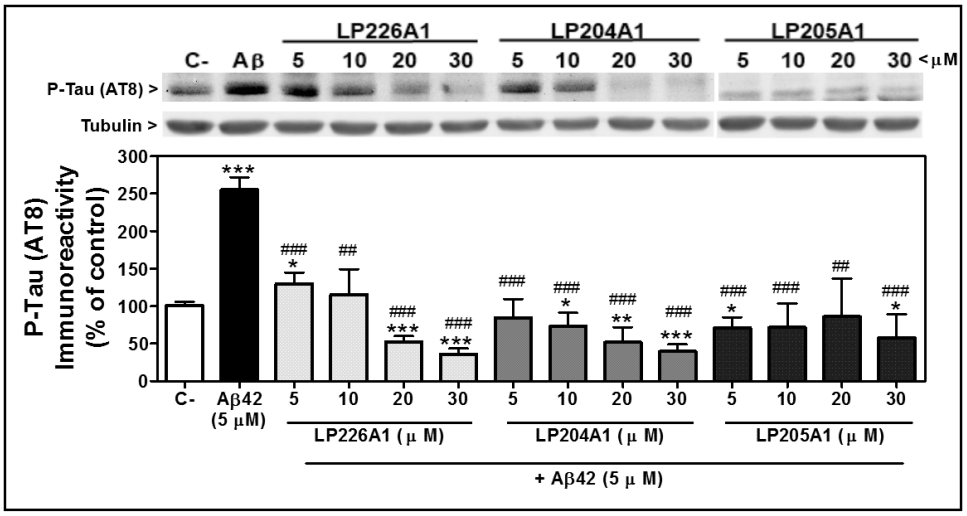

Figure 4.16 P-Tau down-regulation in differentiated SH-SY5Y cells incubated with Aβ 42 and treated with LP226A1, LP204A1, LP205A1, DHA and EPA. P-Tau (AT8) protein levels in SH-SY5Y neuron-like cells determined by immunoblotting. Each bar diagram is showing the mean ± SEM of P-Tau expression after exposure to Aβ42 peptide with or without LP226A, LP204A1 or LP205A1 (5 -30 μM) at 24 h compared to untreated controls (C-). Values are expressed as percentage of control, n = 3. The asterisks indicate a significant effect of the treatment as compared with the non treated control (*p<0.05, **p<0.01, ***p<0.001). In this case, # indicate a significant effect of the treatment as compared with the Aβ42 treated cells (#p<0.05, ##p<0.01, ###p<0.001).

4.2.14 Up-regulation of P-GSK3β (Ser 9) in Differentiated SH-SY5Y cells Incubated with Aβ 42 Peptide and Treated with LP226A1, LP204A1, LP205A1, DHA or EPA

As a major tau kinase, GSK3β induces tau hyperphosphorilation as one of the earliest events in NFT formation (Ishiguro *et al.*, 1988; Ishiguro *et al.*, 1993). The inactivation of GSK3β has been shown to correlate with reduced neuronal degeneration *in vivo* (Noble *et al.*, 2005). Thus, we studied the effect of our compounds in the inhibition of GSK3β by phosphorylation at Ser9.

For this reason, SH-SY5Y neuron-like cells incubated with 5 μM of Aβ42 peptide, were treated with LP226A1, LP204A1 or LP205A1 (5 to 30 μM) (Figure 4.17). GSK3 and P-GSK3β expressions were monitored after 24 h by carrying out a Western Blot immunoassay. The results in Figure 4.17 indicated a very significant up-regulation of P-GSK3β in SH-SY5Y cells after incubation with Aβ42 peptide and treatments with LP226A1, LP204A1 or LP205A1. Moreover, GSK3β was down-regulated by LP226A1, LP204A1 or LP205A1 (+Aβ42 peptide) in a dose-dependent manner. However, GSK3α was only down-regulated by LP204A1 30 μM and LP205 20 and 30 μM. We did not find any difference in the expression of either GSK3α, GSK3β nor P-GSK3β between non-treated (control) cells and cells incubated with Aβ42 peptide.

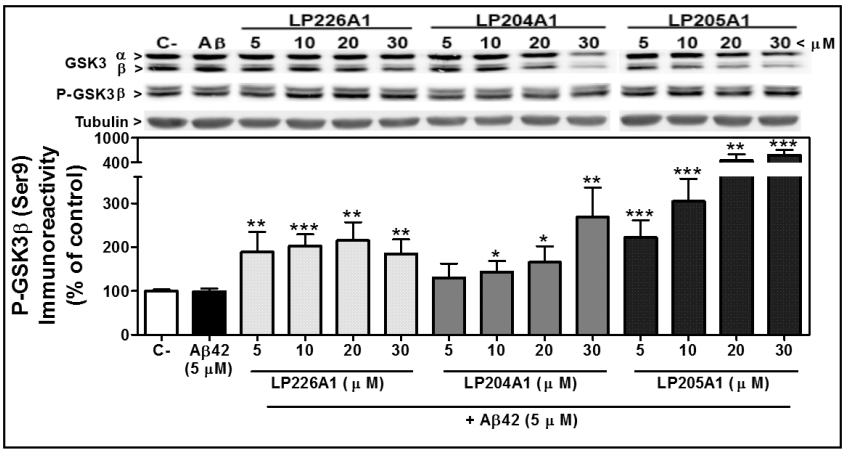

Figure 4.17 P-GSK3β up-regulation in differentiated SH-SY5Y cells incubated with Aβ 42 and treated with LP226A1, LP204A1, LP205A1, DHA and EPA. P-GSK3β and GSK3 protein levels in SH-SY5Y neuron-like cells determined by immunoblotting. Each bar diagram is showing the mean ± SEM of P-GSK3β expression after exposure to Aβ42 peptide with or without LP226A, LP204A1 or LP205A1 (5 -30 μM) at 24 h compared to untreated controls (C-). Values are expressed as percentage of control, n = 3. The asterisks indicate a significant effect of the treatment as compared with the non treated control (*p<0.05, **p<0.01, ***p<0.001). In this case, P-GSK3β values are corrected by total GSK3β values. The upper panel shows a representative immunoblot of P -GSK3β and total GSK3.

4.3. Discussion

The results of the present study have shown that the three hydroxy derivates employed in this work: LP226A1 (OH-DHA), LP205A1 (OH-EPA), and LP204A1 (OH-ARA) impaired SH-SY5Y neuroblastoma cell viability at doses above 150 µM. This is very similar to cell viability impairment caused by the non-modified compounds DHA, ARA and EPA (Figure 4.3). These data show that the drugs being studied here for the treatment of AD (LP226A1, LP204A1, and LP205A1) show no different cytotoxicity than the original PUFAs (DHA, ARA and EPA) known to be safe in the treatment of SH-SY5Y neuroblastoma cells.

A widely-pursued method of combating protein aggregation diseases is to inhibit the production of the monomeric form of the protein with the aim of reducing the amount of protein available to aggregate. In the case of Alzheimer's disease, the amyloidogenic Aβ fragment associated with amyloid plaques is derived from proteolytic processing of a longer non-aggregating precursor protein (APP). Therefore, pharmacological inhibition of the enzymes responsible for Aβ formation (γ-secretase and β-secretase) is a prime strategy for blocking Aβ production. The γ-secretase complex consists of four proteins, the catalytic activity of which is thought to be mediated by presenilin 1 (PS-1) and PS-2 proteins. The γ-secretase complex is responsible for the carboxy-terminal cleavage of APP to produce Aβ40 or Aβ42. The amino-terminal cleavage of APP results from the β-secretase activity. In turn, β-secretase cleavage of APP seems to be due to the activity of BACE1 protein. The primary drawback of targeting γ-secretase for Alzheimer's disease therapeutics is that APP is not the only substrate of γ-secretase. The most notable alternative cleavage substrate is the Notch receptor (De Strooper *et al.*, 1998; De Strooper and Konig, 1999). The notch signaling pathway is important for cell-cell communication, which involves gene regulation mechanisms that control multiple cell differentiation processes during embryonic and adult life. Notch signaling also has a role in the neuronal function and development, stabilization of arterial endothelial fate and angiogenesis, among others. As a result of this drawback, the field has shifted towards the development of γ-secretase modulators. γ-Secretase modulator (GSM) compounds appear to lower the production of Aβ42 without inhibiting proteolysis of other γ -secretase substrates such as Notch. On the other hand, researchers still struggle with the development of effective BACE1 inhibitors. In this chapter, we show that LP226A1, LP204A1, and LP205A1 down-regulate PS-1 (Figure 4.4) and BACE1 (Figure 4.5) proteins in SH-SY5Y neuroblastoma cells. This suggests that they could be suitable drugs for the treatment of Alzheimer´s disease.

Due to the difficulty of finding a suitable and accessible cell model for AD studies human neuroblastoma cells are often used. However, these cells are tumor cells with oncogenic and mitogenic properties (Biedler *et al.*, 1978). For this reason, we decided to differentiate SH-SY5Y cells into neuron-like phenotype to carry out our studies (Figure 4.6).

In this context, we evaluated the effect of DHA and EPA in comparison with their 2 hydroxy derivates LP226A1, LP205A1 and LP204A1 on differentiated SH-SY5Y human neuron-like cells viability (Figure 4.7). LP226A1 and LP205A1 showed an IC_{50} of 18 µM (Figure 4.7A) while LP204A1 showed an IC_{50} of 7.5 µM (Figure 4.7A) in differentiated SH-SY5Y cells. In contrast, treatment with DHA and EPA proved to be slightly less cytotoxic compared with LP226A1 and LP205A1 treatments, respectively. These cell viability studies allowed us to divide the doses of treatment with LP226A1 and LP205A1 into two groups: therapeutic doses (5-10 µM) and toxic doses (20-30 µM). Treatments with LP204A1 could also be divided into two groups but a bit differently: therapeutic doses (5 µM) and toxic doses (10-30 µM).

Furthermore, previous experiments showing down-regulation of PS-1 and BACE1 proteins, after treatments with LP226A1, LP205A1 and LP204A1 in SH-SY5Y non-differentiated cells, were validated in differentiated SH-SY5Y into neuron-like cells. Here we showed PS-1 (Figure 4.9) and BACE1 (Figure 4.10) down-regulation up on LP226A1, LP205A1 and LP204A1 treatments of SH-SY5Y cells differentiated into human neuron-like cells. In addition, BACE1 protein activity was also down-regulated in 5xFAD transgenic mice after treatments with LP226A1. On the contrary, ADAM10 expression was not modulated by the drugs in differentiated SH-SY5Y human neuron-like cells.

Incubation of SH-SY5Y human neuron-like cells with Aβ42 peptide reduced cell viability. Interestingly, treatments with LP226A1 or LP205A1 (5 and 10 µM), after Aβ42 incubation, rescued differentiated SH-SY5Y cells from cell death (Figure 4.12). A similar result was obtained by (Zhao *et al.*, 2011) with DHA-derived neuroprotectin D1 treatments. Moreover, treatments with LP226A1, LP205A1 and LP204A1 (+ Aβ42) showed a down-regulation of PS-1 (Figure 4.13) and BACE1 (Figure 4.14), similar to the down-regulation observed after treatments with the drugs only (without Aβ42). No difference was observed on secretases expression between non-treated controls and Aβ42 treated cells. This could be due to the fact that α-, β- and γ-secretases were implicated in the cleavage of APP for Aβ42 production. However, Aβ42 peptide is not able to modulate secretases expression. On the contrary, hyperphosphorilated tau (AT8) expression was up-regulated after incubation with Aβ42 (Figure 4.16) compared to non-treated cells. This is in consonance with previous data demonstrating that Aβ activates GSK-3β, and induces tau hyperphosphorylation in hipocampal neurons (Takashima, 2012). Our data also showed that LP226A1, LP205A1 and LP204A1 (+ Aβ42) treatments down-regulated hyperphosphorilated tau (AT8) up to similar levels of non-treated cells (Figure 4.16). Therefore, the hydroxy derivates inhibited tau hyperphosphorilation induced by Aβ42. Moreover, we also observed GSK-3β inhibition throughout Serine 9 phosphorilation (P-GSK-3β) after treatments of SH-SY5Y differentiated cells with LP226A1, LP205A1 and LP204A1 (+ Aβ42) (Figure 4.17). Again, evidence shows that inhibitors of GSK-3β may be potential therapeutic agents for this disease (Takashima, 2012).

For the sake of clarity, we present here a concise overview of the main findings reported in this chapter. First of all, PS-1 (γ-secretase) and BACE1 (β-secretase) protein expression were down-regulated by LP226A1, LP205A1 and LP204A1 treatments in differentiated SH-SY5Y and non-differentiated cells. ADAM10 (α-secretase) protein expression was however not modulated by the drugs. Treatments with LP226A1 or LP205A1 (5 and 10 μM), after Aβ42 incubation, rescued SH-SY5Y differentiated cells from cell death. Moreover, Aβ42 incubation induced tau hyperphosphorilation in SH-SY5Y differentiated cells that was reverted after treatments with LP226A1, LP205A1 and LP204A1. Furthermore, GSK-3β was inhibited throughout Serine 9 phosphorilation (P-GSK-3β), impairing tau hyperphosphorilation after treatments of differentiated SH-SY5Y cells with LP226A1, LP205A1 and LP204A1 (+ Aβ42).

Although the working mechanisms of these hydroxy derivate drugs are not yet fully understood, we showed clear indications that they modulate the main molecular players of AD, that is expression of key secretases, P-tau and P-GSK-3β, offering a promising potential to treat AD.

5. ER Stress and Autophagy: Effects of LP226A1, LP204A1 and LP205A1 on SH-SY5Y Neuron-like Cells

5.1. Introduction

5.1.1 ER Stress

Chronic neurodegenerative diseases, such as Alzheimer´s disease, are a group of progressive disorders characterized by the gradual loss of neuronal function in distinct areas of the central nervous system, leading to impaired brain functioning (Soto, 2003; Gorman, 2008; Salminen *et al.*, 2009). Emerging evidence suggests that ER stress may play a pivotal role in the development or pathology of many neurodegenerative diseases (Doyle *et al.*, 2011).

Physiological or pathological processes that disturb protein folding in the ER cause ER stress. The initial response of a cell to ER stress is the activation of a set of pro-survival signaling pathways called the unfolded protein response (UPR). The activation of the UPR causes a shut-down of global protein synthesis, and activates mechanisms that allow cells to deal with unfolded protein accumulation (Doyle *et al.*, 2011). For example, it enhances the protein folding capacity by increasing ER chaperone expression and up-regulates the degradation of misfolded proteins. This coordinated biochemical response to ER stress is a mechanism of cell survival. However, if the stress is prolonged or excessive, programmed cell death pathways (apoptosis) occur.

Molecular chaperones are proteins that bind to non-native proteins by recognition of exposed hydrophobic regions. Through cycles of binding and release, they prevent an aggregation thereby allowing correct folding to occur more efficiently (Leach and Williams, 2000).

In mammals, the three major ER stress sensors are IRE1, PERK and ATF6 (Ron and Walter, 2007). The ER-luminal domain of IRE1, PERK and ATF6 interacts with the ER chaperone glucose-regulated protein 78 (GRP78 or BiP). However, upon accumulation of unfolded proteins, BiP dissociates from these molecules, leading to their activation (Schroder and Kaufman, 2005). Activation of IRE1, PERK and ATF6 initiates a network of intracellular signaling pathways during the UPR.

The IRE1 axis. IRE1 exists in two highly conserved isoforms: IRE1α and IRE1β. IRE1α is expressed ubiquitously whereas IRE1β is only expressed in gut epithelial cells (Boot-Handford and Briggs, 2010). The cytoplasmic domain of IRE1 contains a serine/threonine kinase domain and a C-terminal endoribonuclease domain (Calfon *et al.*, 2002). ER stress leads to the dissociation of BiP from IRE1, resulting in the autophosphorilation of IRE1α and the activation of its RNAse activity. The downstream consequence of IRE1-mediated endoribonuclease activity is non-conventional splicing of XBP1 (Calfon *et al.*, 2002). IRE1-mediated XBP1 mRNA splicing causes a shift in the reading frame. Consequently, spliced XBP1 (XBP1s) mRNA is produced. XBPs possesses a potent transcriptional transactivation domain in its C-terminal region (Calfon *et al.*, 2002), that induces the expression of genes involved in restoring protein folding or degrading unfolded proteins (Kim *et al.*, 2008). In addition, IRE1 can induce the activation of Jun N-terminal kinase (JNK) (Urano *et al.*, 2000). JNK activation results in enhanced autophagy (Ogata *et al.*, 2006). This allows cells to adapt to stress by initiating autophagy.

The PERK axis. PERK is an ER-associated transmembrane serine/threonine protein kinase. Upon accumulation of unfolded proteins in the ER lumen, PERK dimeritation and trans-autophosphorilation lead to the activation of its kinase domain (Harding *et al.*, 1999). PERK-mediated phosphorilation of the α subunit of the eukaryotic translation initiation factor 2 α (eIF2α) at Ser51 leads to translation attenuation (Harding *et al.*, 1999). Although phosphorilation of eIF2α inhibits general translation initiation, it increases translation of activating transcription factor 4 (ATF4) (Lu *et al.*, 2004a). ATF4 induces the expression of genes involved in the restoration of ER homeostasis and in autophagy (Lu *et al.*, 2004a; Fujita *et al.*, 2007; Kouroku *et al.*, 2007).

The ATF6 axis. In mammals there are two alleles of ATF6, ATF6α, and ATF6β. Both are synthesized in all cell types as ER transmembrane proteins. In unstressed cells, ATF6 is localized at the ER membrane and bound to BiP (Haze *et al.*, 1999). In response to ER stress, BiP dissociation permits trafficking of ATF6 to the Golgy complex, where ATF6 is sequentially cleaved by two proteases (Haze *et al.*, 1999). The processed forms of ATF6α

and ATF6β translocate to the nucleus and activate target genes. Studies of $ATF6^{-/-}$ cells have recently shown that ATF6 is responsible for transcriptional induction of several ER proteins which includes chaperones, folding enzymes and ER-associated degradation components (ERAD) (Wu *et al.*, 2007).

The most important feature of UPR is to increase the transactivation function of transcription factors such as ATF4, ATF6 and XBP1. Once activated, these transcription factors coordinate transcriptional induction of ER chaperones and genes involved in ERAD to enhance the protein folding capacity of the cell and to decrease the unfolded protein load to the ER, respectively (Boot-Handford and Briggs, 2010). However if the damage is too severe and ER homeostasis cannot be restored, apoptosis occurs (Kaufman, 2002). It is not clear at which point the switch between pro-survival and pro-apoptotic signaling occurs, nor which mechanisms underline cell death.

CHOP, also known as growth arrest and DNA damage-inducible gene 153 (GADD153), is a member of the C/EBP transcription factor family. This 29 kD transcription factor is expressed at low levels in unstressed cells and is strongly induced in response to ER stress (Zinszner *et al.*, 1998). It can be induced by all three arms of the UPR. The pro-apoptotic effect of CHOP is linked to down-regulation of BCL-2 and enhanced production of reactive oxygen species (ROS) (McCullough *et al.*, 2001).

5.1.2 Autophagy

Autophagy, similar to ER stress has both pro-death and pro-survival functions. Accumulating evidence indicates that autophagy may confer neuroprotection by enhancing clearance of soluble and aggregated misfolded proteins. Conversely, deregulation of autophagy may lead to neurodegeneration (Nedelsky *et al.*, 2008). Synthesis of proteins in the ER is monitored by an elaborate quality control mechanism that allows only correctly folded proteins to be transported to their final destination. Misfolded or unassembled proteins are retained in the ER and subsequently degraded by the ERAD. In the ERAD pathway, ER chaperones recognize the misfolded proteins, and ER reductases remove disulfide bonds to facilitate their transport to the cytosol where they are degraded by the proteosome (Vembar and Brodsky, 2008). To remove the aggregates of misfolded proteins that cannot be degraded by the ERAD, the UPR activates autophagy (Ogata *et al.*, 2006).

Different conditions that induce ER stress lead to the induction of autophagy (Verfaillie *et al.*, 2010). Both the PERK/eIF2α and the IRE1 arms of the UPR have been implicated in the regulation of autophagy (Talloczy *et al.*, 2002; Ding *et al.*, 2007b). The pro-autophagic actions of IRE1 seem to rely on the ability of IRE1 to activate c-Jun N-terminal kinases (JNK). JNK has been shown to regulate autophagy through BCL-2 phosphorylation, which disrupts its interaction with Beclin-1 (Wei *et al.*, 2008). It has also

been shown that PERK-eIF2α-dependent ATG12 up-regulation is also required for autophagy induction in response to polyglutamine protein accumulation (Kouroku *et al.*, 2007). PERK-dependent transcription factors ATF4 and CHOP have been proven to induce transcriptional activation of LC3B and ATG5 during hypoxia (Kouroku *et al.*, 2007). However the detailed molecular mechanism behind the activation of autophagy during ER stress is not yet fully elucidated.

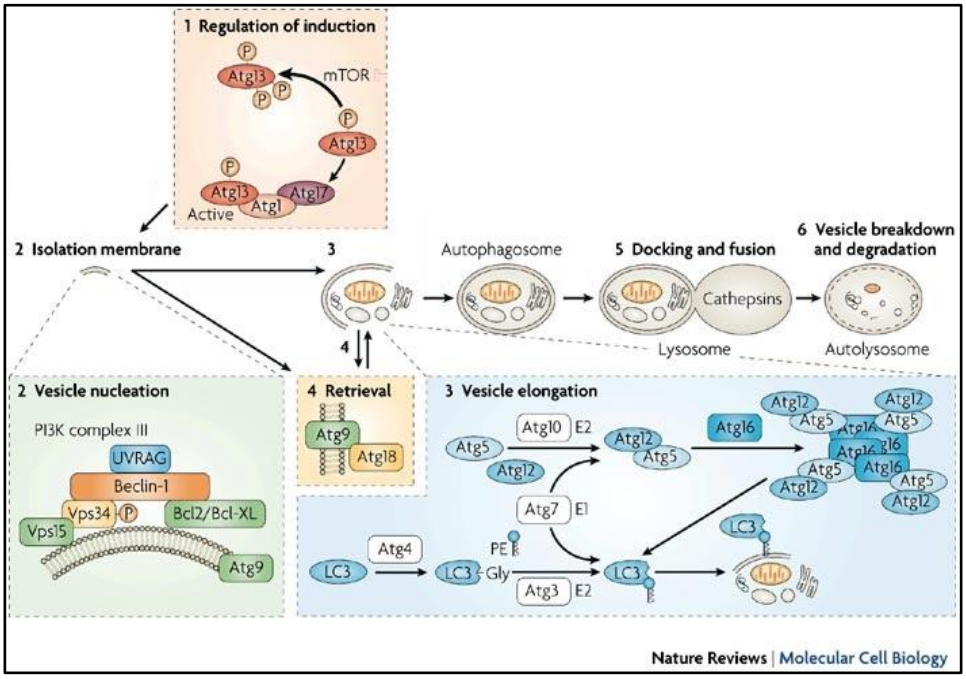

Figure 5.1 Schematic representation of autophagic process. Figure taken from (Maiuri *et al.*, 2007).

Autophagy starts with the engulfment of cytoplasmic material (cytosol and/or organelles) by the isolation membrane, which sequesters material in double-membraned vesicles named autophagosomes. The first regulatory process (see figure 5.1, step 1) involves the de-repression of the mTOR Ser/Thr kinase, which inhibits autophagy by phosphorylating autophagy protein-13 (Atg13). When mTOR is inhibited, re-association of dephosphorylated Atg13 with Atg1 stimulates its catalytic activity, and induces autophagy. Among the initial steps of vesicle nucleation is the activation of mammalian Vps34, a class III phosphatidylinositol 3-kinase (PI3K), to generate phosphatidylinositol-3-phosphate (PtdIns3P) (step 2). Vps34 activation depends on the formation of a multiprotein complex in

which beclin-1 (Becn1; the mammalian orthologue of Atg6), UVRAG (UV irradiation resistance-associated tumor suppressor gene), and a myristylated kinase (Vps15, or p150 in humans) participate (Maiuri *et al.*, 2007).

Two ubiquitin-like conjugation systems are part of the vesicle elongation process (step 3). One pathway involves the covalent conjugation of Atg12 to Atg5 with the help of the E1-like enzyme Atg7 and the E2-like enzyme Atg10. The second pathway involves the conjugation of phosphatidylethanolamine (PE) to LC3/Atg8 (LC3 is one of the mammalian homologues of Atg8) by the sequential action of the protease Atg4, the E1-like enzyme Atg7 and the E2-like enzyme Atg3. Lipid conjugation leads to the conversion of the soluble form of LC3 (named LC3-I) to the autophagic-vesicle-associated form (LC3-II). LC3-II is used as a marker of autophagy because its lipidation and specific recruitment to autophagosomes increases its electrophoretic mobility on gels compared with LC3-I. The mechanism of retrieval in which the Atg9 complex participates has been so far poorly studied (step 4) (Maiuri *et al.*, 2007).

Autophagosomes undergo maturation by fusion with lysosomes to create autolysosomes (steps 5 and 6). In the autolysosomes, the inner membrane as well as the luminal content of the autophagic vacuoles are degraded by lysosomal enzymes that act optimally within this acidic compartment (Maiuri *et al.*, 2007).

5.1.3 ER Stress and Alzheimer´s Disease

As mentioned above, a disruption of ER functioning is associated with the accumulation of misfolded proteins, a characteristic feature of many neurodegenerative diseases (Gorman, 2008; Soto and Estrada, 2008; Winklhofer *et al.*, 2008) which are often described as protein conformational disorders (Soto, 2003). Normally, the accumulation of misfolded proteins triggers an unfolded protein response.

Protein folding *in vivo* is an inefficient process and is aided by molecular chaperones, which increase folding efficiency. In addition, degradation systems such as ERAD, the endo-lysosomal pathway and autophagy rapidly remove misfolded proteins. However, an accumulation of misfolded proteins can still occur due to errors during transcription and translation, mutations, toxic compounds or cellular stress (Vembar and Brodsky, 2008). In the native conformation, hydrophobic patches are usually placed within the interior of soluble proteins to maintain the lowest energy state (Soto and Estrada, 2008). Misfolded proteins have hydrophobic patches exposed which allow them to interact with other proteins and aggregate. In most cases, the native monomeric protein is mainly composed of α-helix, whereas the misfolded polymers are rich in β-sheet conformation (Soto and Estrada, 2008). Neurons rely on the removal of misfolded proteins to maintain homeostasis (Komatsu *et al.*, 2006). The accumulation of misfolded proteins is a characteristic feature of many

neurodegenerative diseases including AD, (Tabira *et al.*, 2002), Parkinson´s disease (PD) (Baba *et al.*, 1998), transmissible spongiform encephalopathy (Ferreiro *et al.*, 2006), and also acute neurodegenerative disorders such as traumatic brain injury (Smith *et al.*, 2003), and cerebral ischemia (Hu *et al.*, 2000).

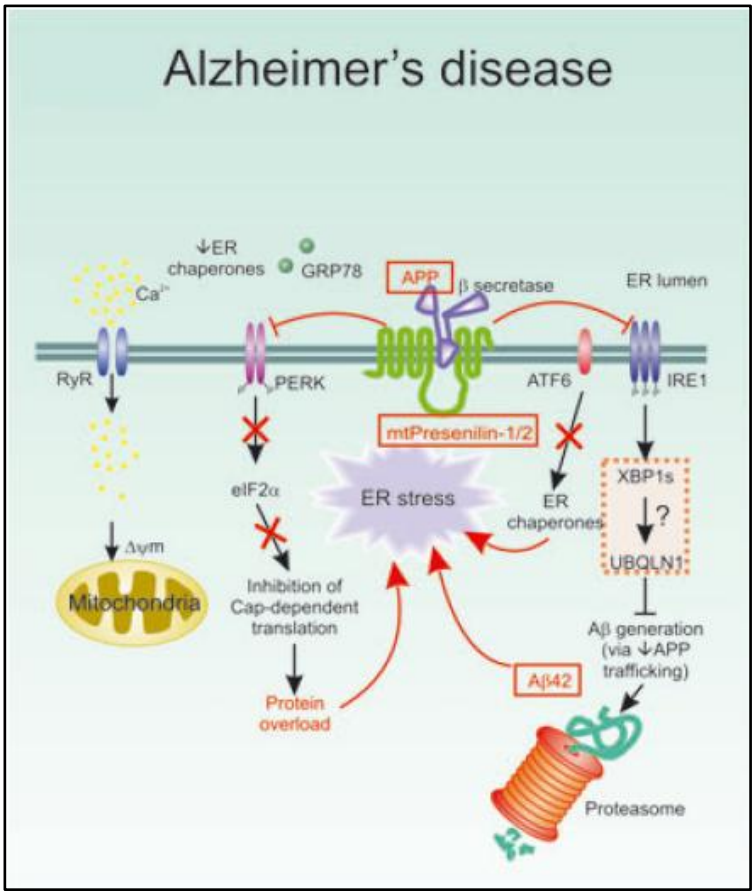

Figure 5.2 Schematic diagram of ER stress in Alzheimer´s disease. Figure taken from (Doyle et al., 2011)

As we mentioned in the previous chapter, AD is characterized by the presence of senile plaques with a core of extracellular β-amyloid protein and intracellular neurofibrillary tangles containing hyperphosphorilated tau (Nordberg, 2004). β-Amyloid is cleaved from its precursor protein APP, through the action of β-secretase (BACE) and γ-secretase (PS-1), can produce β-amyloid protein, most frequently Aβ40 and Aβ42 (Lin *et al.*, 2007). Although the evolution of senile plaques is closely related to neurodegeneration and the evolution of AD,

there is no direct causal relationship between β-amyloid deposition and neurodegeneration (Doyle *et al.*, 2011). Soluble oligomeric forms of β-amyloid have been suggested to be lethal intermediates (Imaizumi *et al.*, 2001; Ishibashi *et al.*, 2006; Rochet, 2007). Neurofibrillary tangles contain twisted pairs of helical filaments formed by the aggregation of hyperphosphorilated tau (Selkoe, 2001). Presenilin (PS), a component of γ-secretase complex, is widely expressed in the ER and Golgy apparatus (Blennow *et al.*, 2006).. Presenilin is an integral membrane protein located primarily in the ER, and its mutations are linked to the majority of early forms of AD (Selkoe, 2001). It has been shown to influence the activity of two of the key ER sensors, IRE1 and PERK. Presenilin mutations reduce phosphorylation of PERK and eIF2α, resulting in failure to attenuate protein synthesis, and causing protein accumulation in the ER (Katayama *et al.*, 2001). Mutant PS-1 is also known to bind and inhibit IRE1, thereby reducing or delaying the transcription of ER chaperones such as BiP. This has been consistently found to be down-regulated in AD (Katayama *et al.*, 2001). Indeed, the increased sensitivity of neurons to ER stress is attributed to the decreased levels of BiP mRNA (Doyle *et al.*, 2011).

ER has multiple vital functions: (i) protein folding, posttranslational modifications, and transport to the Golgi complex, (ii) maintenance of cellular calcium homeostasis, (iii) synthesis of lipids and sterols, and (iv) regulation of cellular survival via a complex transducer and signaling network (Baumann and Walz, 2001; Schroder and Kaufman, 2005; Bernales *et al.*, 2006; Gorlach *et al.*, 2006; Ron and Walter, 2007; Kim *et al.*, 2008).

Ca^{2+} homeostasis is important for the proper function of ER chaperones and protein folding. Alterations in Ca^{2+} homeostasis lead to reduced chaperone activity, protein misfolding and UPR initiation. Aβ peptides have been shown to cause a depletion of ER Ca^{2+} stores. In addition PS-1 mutations increase Aβ42 levels, and have also been proven to impair ER Ca^{2+} homeostasis (Leissring *et al.*, 2001).

Autophagosomes and precursor autophagosomes are abundant in dystrophic neurites from human AD brains, suggesting that the later stages of autophagy may be deregulated (Nixon et al., 2005). Autophagic vacuoles contain the proteases and substrates necessary to cleave APP, suggesting that the abnormal accumulation of autophagic vacuoles in affected neurons of the AD brain may act as a reservoir for the production of toxic aggregates and contribute to Aβ42 deposition (Nixon et al., 2005).

The purpose of this chapter was to study whether the γ and β-secretase down-regulation, observed in the previous chapter, was accompanied by a UPR and autophagy induction after treatments of SH-SY5Y neuron-like cells with the hydroxy derivates.

5.1.4 Results

5.2.1. BiP/GRP78 Chaperone Regulation after LP226A1, LP204A1 and LP205A1 Treatments of Differentiated SH-SY5Y Cells

Molecular chaperones are proteins that bind to non-native protein conformers by recognition of exposed hydrophobic segments.Through cycles of binding and release, they prevent an aggregation thereby allowing productive folding/assembly to occur more efficiently (Leach and Williams, 2000).

Previous studies have shown that the ER chaperone immunoglobulin binding protein (BiP/GRP78) may bind to, and facilitate correct folding of nascent APP (Yang *et al.*, 1998). These data also suggest a transient and direct interaction of GRP78 with APP in the ER that modulates intracellular APP maturation and processing, and may facilitate its correct folding (Yang *et al.*, 1998). Mutant PS-1 is also known to bind and inhibit IRE1, thereby reducing or delaying the transcription of ER chaperones such as GRP78, which has consistently been found to be down-regulated in AD (Katayama *et al.*, 2001). In fact the increased sensitivity of neurons to ER stress is attributed to decreased levels of GRP78 mRNA (Doyle *et al.*, 2011).

For this reason, differentiated SH-SY5Y cells treated with LP226A1, LP204A1 or LP205A1 (5 to 30 µM) (Figure 5.3A) were also incubated concomitantly with a final concentration of 5 µM Aβ42 peptide (Figure 5.3B). BiP/GRP78 expression was monitored after 7 or 24 h by carrying out a Western Blot immunoassay. The results in Figure 5.3A indicated a significant dose-dependent up-regulation of BiP in SH-SY5Y cells treated with LP226A1, LP204A1, and LP205A1 for 7 h. LP205A1 induced stronger up-regulation of BiP than LP204A1. LP226A1 induced the weakest up-regulation of BiP among the three drugs. In addition, the results in Figure 5.3B indicate a very significant dose-dependent up-regulation of BiP in SH-SY5Y cells after incubation with Aβ42 peptide and 24 h-treatments with LP226A1, LP205A1, and LP204A1. Interestingly, incubation of SH-SY5Y with Aβ42 peptide up-regulated very significantly the BiP protein expression (Figure 5.3B), and the up-regulation of BiP after a 24 h-treatment was stronger than after a 7 h-treatment.

These results demonstrated that after a 7 h-treatment in SH-SY5Y cells, the three hydroxy derivates LP226A1, LP204A1, and LP205A1 already up-regulated BiP, a protective chaperone. Moreover, treatments with LP226A1, LP205A1 or LP204A1 (plus incubation with Aβ42 peptide) for 24 h also up-regulated BiP in SH-SY5Y cells above the levels induced by Aβ42 peptide incubation.

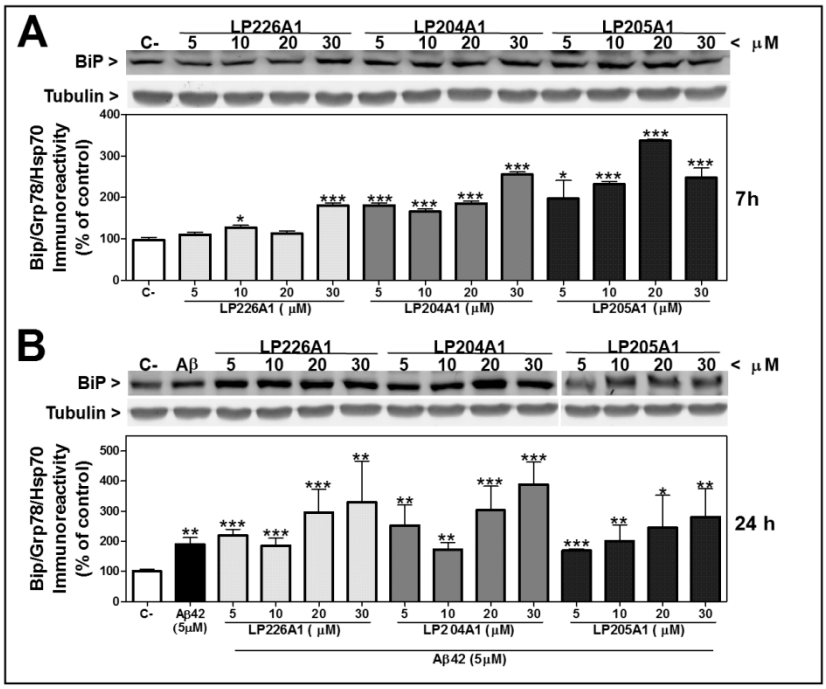

Figure 5.3 BiP/Grp78 up-regulation in differentiated SH-SY5Y cells treated with LP226A1, LP204A1 and LP205A1, and incubated with or without Aβ 42 for 7 h or 24 h. BiP protein levels in SH-SY5Y neuron-like cells were determined by immunoblotting. Each bar diagram is showing the mean ± SEM of BiP expression after treatments with (A) LP226A, LP204A1 or LP205A1 (5-30 µM) for 7 h, compared to untreated controls (C-). (B) BiP expression after exposure to Aβ42 peptide (5 µM), with or without LP226A, LP204A1 or LP205A1 (5-30 µM) treatment for 24 h, compared to untreated controls (C-). Values are expressed as percentage of control, n = 3. The asterisks indicate a significant effect of the treatment as compared with the non-treated control (*p<0.05, **p<0.01, ***p<0.001).

Moreover, differentiated SH-SY5Y cells were treated with DHA or EPA (5 to 30 µM) and incubated with a final concentration of 5 µM Aβ42 peptide. BiP/GRP78 expression was monitored after 24 h by carrying out a Western Blot immunoassay (Figure 5.4). The results in Figure 5.4 showed an up-regulation of BiP in SH-SY5Y cells after incubation with Aβ42 peptide and treatments with DHA or EPA (+Aβ42 peptide) in a dose-dependent manner. Up-regulation of BiP after treatments with DHA or EPA was slightly smaller than the up-regulation induced by LP226A1 or LP205A1 (their hydroxy derivates) treatments.

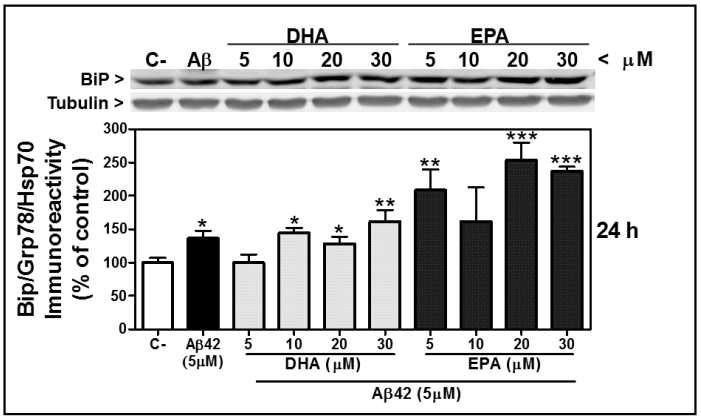

Figure 5.4 BiP/Grp78 up-regulation in differentiated SH-SY5Y cells treated with DHA or EPA and incubated with Aβ 42 for 24 h. BiP protein levels in SH-SY5Y neuron-like cells were determined by immunoblotting. Each bar diagram is showing the mean ± SEM of BiP expression after exposure to Aβ42 peptide (5 µM) with or without treatment with DHA or EPA (5 -30 µM) for 24 h compared with untreated controls (C-). Values are expressed as percentage of control, n = 3. The asterisks indicate a significant effect of the treatment as compared with the non-treated control (*p<0.05, **p<0.01, ***p<0.001).

5.2.2. PDI Chaperone Regulation after LP226A1, LP204A1 and LP205A1 Treatments of Differentiated SH-SY5Y Cells

Protein disulfide isomerase (PDI) is a member of the thioredoxin (TX) superfamily. PDI is believed to accelerate the folding of disulfide-bonded proteins by catalyzing the disulfide interchange reaction, which is the rate-limiting step during protein folding in the luminal space of the ER (Noiva and Lennarz, 1992). Such exchange reactions can occur intramolecularly, leading to a rearrangement of disulfide bonds in a single protein. Oxidized PDI can catalyze the formation of a disulfide bridge (Noiva and Lennarz, 1992). In sporadic AD, nitric oxide (NO)-induced S-nitrosylation of PDI inhibits its enzymatic activity,

resulting in an accumulation of polyubiquitinated proteins (Uehara *et al.*, 2006). Thus, PDI prevents the neurotoxicity associated with ER stress and misfolding (Uehara *et al.*, 2006).

As shown in this chapter, SH-SY5Y neuron-like cells treated with LP226A1, LP204A1, and LP205A1 (5 to 30 µM) (Figure 5.5A) were also incubated concomitantly with 5 µM Aβ42 peptide (Figure 5.5B). PDI expression was monitored after 7 h or 24 h by carrying out a Western Blot immunoassay. The results in Figure 5.5A indicated a significant dose-dependent up-regulation of PDI in SH-SY5Y cells treated with LP226A1 or LP205A1 for 7 h. On the contrary, a 7 h-treatment with LP204A1 did not up-regulated PDI protein expression. In addition, the results in Figure 5.5B indicate a very significant dose-dependent up-regulation of PDI in SH-SY5Y cells after incubation with Aβ42 peptide, and 24 h-treatments with LP226A1, LP205A1, or LP204A1. LP205A1 induced the weakest up-regulation of PDI among the three drugs.

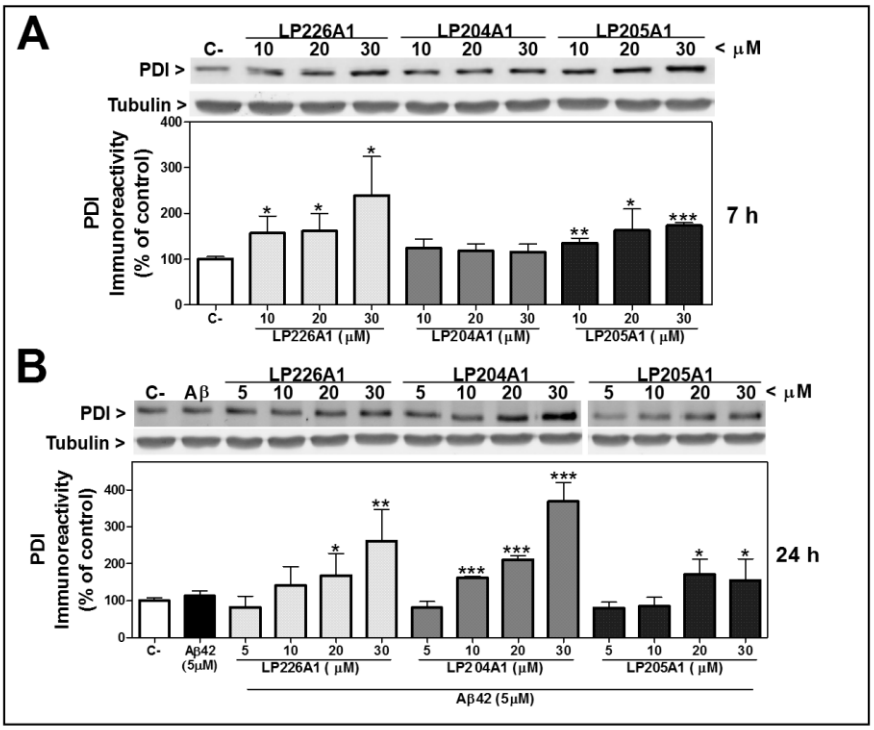

Figure 5.5 PDI up-regulation in differentiated SH-SY5Y cells treated with LP226A1, LP204A1 or LP205A1 and incubated with or without Aβ 42 for 7 h or 24 h. PDI protein levels in SH-SY5Y neuron-like cells were determined by immunoblotting. Each bar diagram is showing the mean ± SEM of PDI expression after treatment with (A) LP226A, LP204A1 or LP205A1 (5 -30 µM) for 7 h compared with untreated controls (C-) or (B) after exposure to Aβ42 peptide (5 µM) with or without LP226A, LP204A1 or LP205A1 (5 -30 µM) treatment for 24 h compared with untreated controls (C-). Values are expressed as percentage of control, n = 3. The asterisks indicate a significant effect of the treatment as compared with the non treated control (*p<0.05, **p<0.01, ***p<0.001).

Differentiated SH-SY5Y cells were treated with DHA or EPA (5 to 30 µM), and incubated concomitantly with a final concentration of 5 µM Aβ42 peptide. PDI expression was monitored after 24 h by carrying out a Western Blot immunoassay (Figure 5.6). The results in Figure 5.6 showed an up-regulation of PDI in SH-SY5Y cells after incubation with Aβ42 peptide and treatments with DHA or EPA (+Aβ42 peptide). Up-regulation of PDI after treatments with DHA or EPA was slightly smaller than the up-regulation induced by LP226A1 or LP205A1 (their hydroxy derivates) treatments.

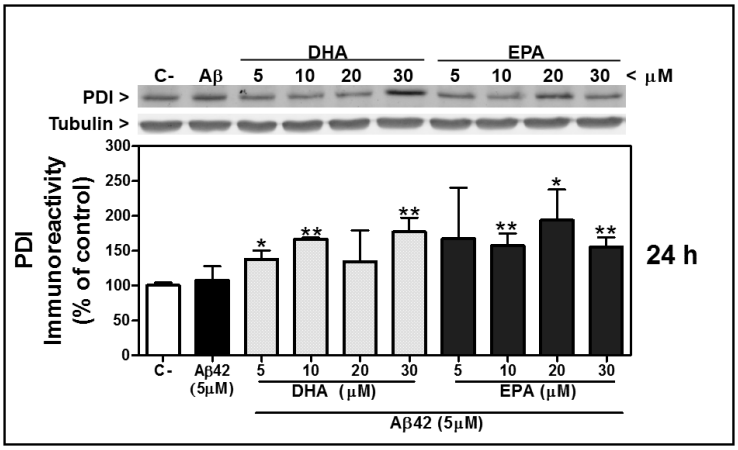

Figure 5.6 PDI up-regulation in differentiated SH-SY5Y cells treated with DHA or EPA, and incubated with Aβ 42 for 24 h. PDI protein levels in SH-SY5Y neuron-like cells were determined by immunoblotting. Each bar diagram is showing the mean ± SEM of PDI expression after exposure to Aβ42 peptide (5 µM) with or without treatment with DHA or EPA (5 -30 µM) for 24 h compared with untreated controls (C-). Values are expressed as percentage of control, n = 3. The asterisks indicate a significant effect of the treatment as compared with the non treated control (*p<0.05, **p<0.01, ***p<0.001).

5.2.3. Calnexin Chaperone Regulation after LP226A1, LP204A1 and LP205A1 Treatments of Differentiated SH-SY5Y Cells

A decade has passed since the discovery of Calnexin (CNX). Intensive studies of this protein functions have clearly established its role as molecular chaperone by assisting glycoprotein folding and participating in ER quality control. But the extent to which the cell relies on the functions of CNX relative to other ER chaperones has been difficult to assess. Certainly the lectin-oligosacharide component of the interaction is dispensable for viability since glycosidase I and glycosidase II deficient mammalian and yeast cells grow normally (Leach and Williams, 2000). Ranging from subtle to essential, mixed results have been

obtained when CNX genes have been disrupted with phenotypes. Much of the complexity can be attributed to the redundant nature of the ER chaperones wherein the synthesis of BiP or PDI is upregulated as a compensatory response to impairments in the Calnexin/Calreticulin system (Leach and Williams, 2000).

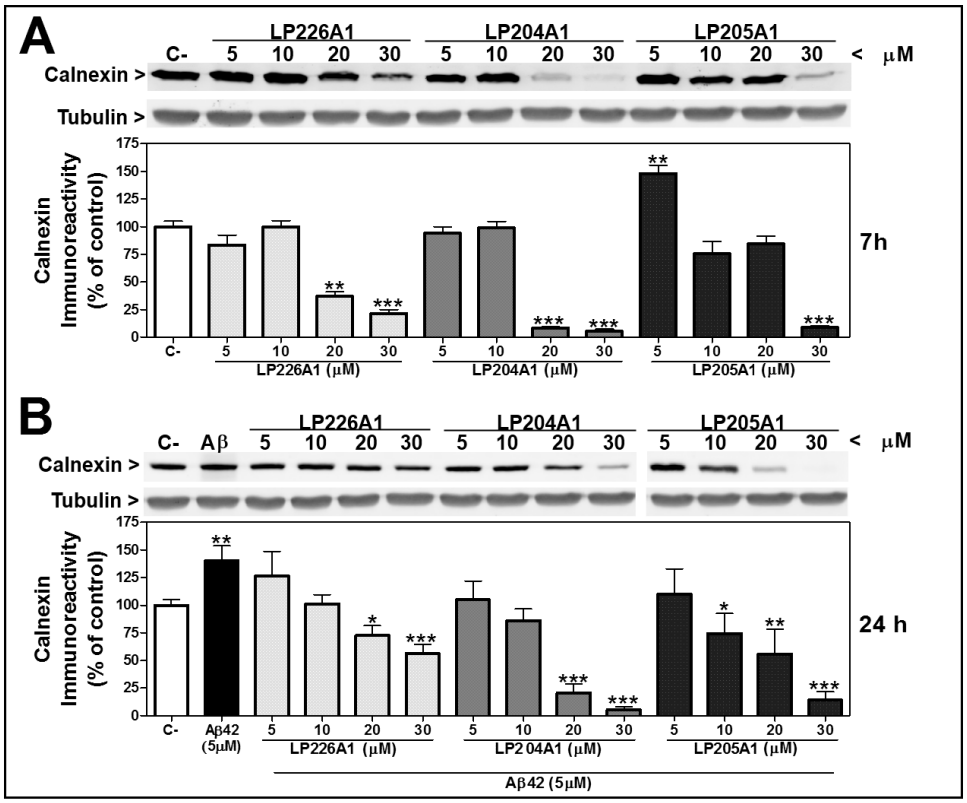

Figure 5.7 CNX down-regulation in differentiated SH-SY5Y cells treated with LP226A1, LP204A1 or LP205A1, incubated with or without Aβ 42 for 7 h or 24 h. CNX protein levels in SH-SY5Y neuron-like cells were determined by immunoblotting. Each bar diagram is showing the mean ± SEM of CNX expression after treatment with (A) LP226A, LP204A1 or LP205A1 (5-30 µM) for 7 h, compared with untreated controls (C-). (B) CNX expression after exposure to Aβ42 peptide (5 µM) with or without LP226A, LP204A1 or LP205A1 (5-30 µM) treatment for 24 h, compared with untreated controls (C-). Values are expressed as percentage of control, n = 3. The asterisks indicate a significant effect of the treatment as compared with the non treated control (*p<0.05, **p<0.01, ***p<0.001).

In this section, differentiated SH-SY5Y cells treated with LP226A1, LP204A1 or LP205A1 (5 to 30 µM) (Figure 5.7A) were incubated with a final concentration of 5 µM Aβ42 peptide (Figure 5.7B). CNX expression was monitored after 7 h or 24 h by carrying out a Western Blot immunoassay. The results in Figure 5.7A indicated a down-regulation of

CNX in SH-SY5Y cells treated with LP226A1, LP204A1 or LP205A1 for 7 h at 20 and 30 µM. By contrast, 7 h-treatments with 5 µM or 10 µM of LP226A1, LP204A1 and LP205A1 did not down-regulated CNX protein expression. The results in Figure 5.7B indicated a dose-dependent down-regulation of CNX in SH-SY5Y cells after incubation with Aβ42 peptide (5 µM), and 24 h-treatments with LP226A1, LP205A1 or LP204A1. CNX down-regulation was significant at doses of 20 and 30 µM. Interestingly, an incubation of SH-SY5Y with Aβ42 peptide up-regulated very significantly the CNX protein expression (Figure 5.7B).

SH-SY5Y neuron-like cells were also treated with DHA or EPA (5 to 30 µM) and incubated concomitantly with 5 µM of Aβ42 peptide. CNX expression was monitored after 24 h by carrying out a Western Blot immunoassay (Figure 5.8). The results in Figure 5.8 showed an up-regulation of CNX in SH-SY5Y cells after incubation with Aβ42 peptide. However, treatment with DHA or EPA (+Aβ42 peptide) did not change the CNX expression in SH-SY5Y cells.

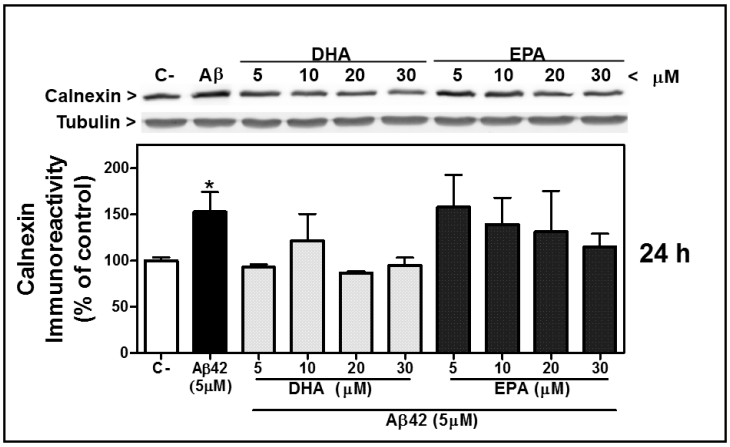

Figure 5.8 Calnexin regulation in differentiated SH-SY5Y cells treated with DHA or EPA, and incubated with Aβ 42 for 24 h. Calnexin protein levels in SH-SY5Y neuron-like cells were determined by immunoblotting. Each bar diagram is showing the mean ± SEM of Calnexin expression after exposure to Aβ42 peptide (5 µM) with or without treatment with DHA or EPA (5 -30 µM) for 24 h compared with untreated controls (C-). Values are expressed as percentage of control, n = 3. The asterisks indicate a significant effect of the treatment as compared with the non treated control (*$p<0.05$).

5.2.4. P-eIF2α Regulation after LP226A1, LP204A1 and LP205A1 Treatments of Differentiated SH-SY5Y Cells

Another important element of ER stress is the eukaryotic translation initiation factor 2α kinase 3 (PERK). Its intrinsic kinase activity is induced by oligomerization, resulting in the phosphorylation of the eukaryotic translation initiation factor 2α (eIF2α), and the suppression of global mRNA translation. Under these conditions, only selected mRNAs are translated, including ATF4 (Lu *et al.*, 2004a), which induces the expression of genes involved in the restoration of ER homeostasis and in autophagy (Lu *et al.*, 2004a; Fujita *et al.*, 2007; Kouroku *et al.*, 2007). Accordingly, compounds that promote a sustained phosphorylation of eIF2α, such as salubrinal (Boyce *et al.*, 2005), may exert cytoprotective effects. However, a prolonged suppression of protein synthesis is incompatible with cell survival, resulting in autophagy (Kim *et al.*, 2008).

Here, SH-SY5Y neuron-like cells treated with LP226A1, LP204A1 and LP205A1 (5 to 30 µM) (Figure 5.9A) were incubated concomitantly with a final concentration of 5 µM Aβ42 peptide (Figure 5.9B). P-eIF2α protein expression was monitored after 7 h or 24 h by carrying out a Western Blot immunoassay. The results in Figure 5.9A indicated a very significant dose-dependent up-regulation of P-eIF2α in SH-SY5Y cells when treated with LP226A1, LP204A1 and LP205A1 for 7 h. By contrast, the results in Figure 5.9B indicated a down-regulation of P-eIF2α in SH-SY5Y cells after incubation with Aβ42 peptide (5 µM) when treated with LP226A1 or LP204A1 for 24 h. P-eIF2α down-regulation was significant at doses of 20 and 30 µM of LP226A1, and 10 to 30 µM of LP204A1. Interestingly, LP205A1 24 h-treatments did not modulate P-eIF2α protein expression. Incubation of SH-SY5Y cells with Aβ42 peptide did not regulate significantly P-eIF2α protein expression (Figure 5.9B).

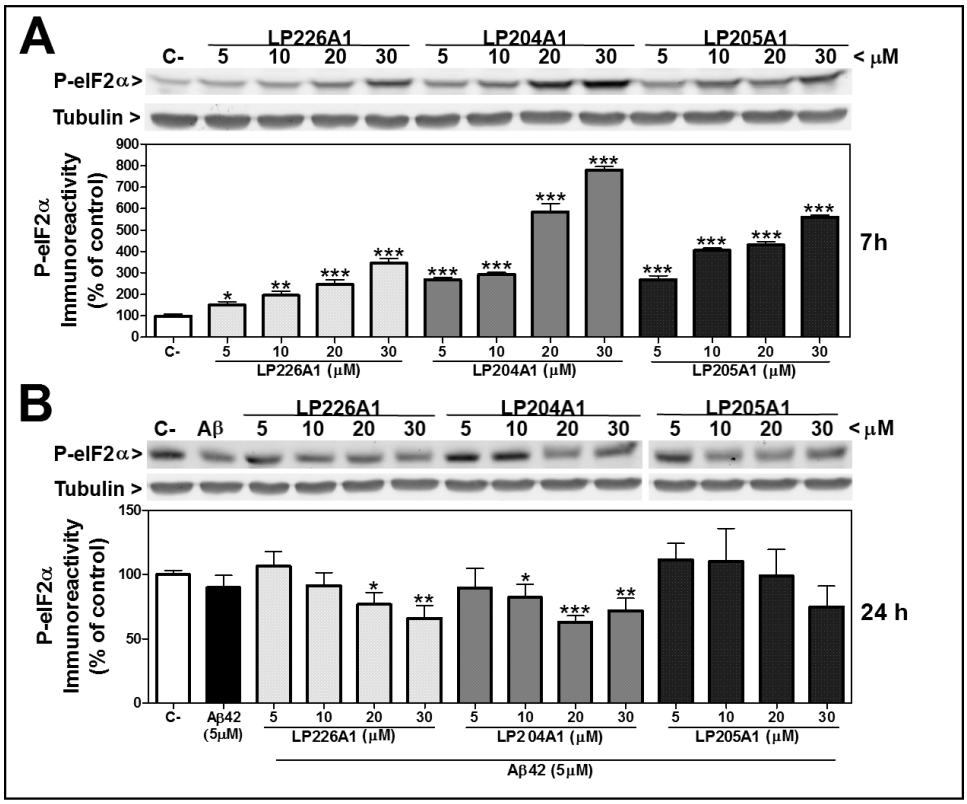

Figure 5.9 P-eIF2α regulation in differentiated SH-SY5Y cells treated with LP226A1, LP204A1, and LP205A1 incubated with or without Aβ 42 for 7 h or 24 h. P-eIF2α protein levels in SH-SY5Y neuron-like cells were determined by immunoblotting. Each bar diagram is showing the mean ± SEM of P-eIF2α expression after treatment with (A) LP226A, LP204A1 or LP205A1 (5-30 μM) for 7 h compared with untreated controls (C-) or (B) after exposure to Aβ42 peptide (5 μM) with or without LP226A, LP204A1 or LP205A1 (5-30 μM) treatment for 24 h compared with untreated controls (C-). Values are expressed as percentage of control, n = 3. The asterisks indicate a significant effect of the treatment as compared with the non treated control (*p<0.05, **p<0.01, ***p<0.001).

Moreover, differentiated SH-SY5Y cells were also treated with DHA or EPA (5 to 30 μM) and incubated with 5 μM of Aβ42 peptide. P-eIF2α expression was monitored after 24 h by carrying out a Western Blot immunoassay (Figure 5.10). The results in Figure 5.10 did not show a significant up-regulation of P-eIF2α in SH-SY5Y cells after incubation with Aβ42 peptide and DHA or EPA treatments. In addition, incubation of SH-SY5Y cells with Aβ42 peptide (5 μM) did not change the P-eIF2α protein expression

The results in this section show an early up-regulation of P-eIF2α protein after 7 h-treatments of SH-SY5Y cells with LP226A1, LP204A1, and LP205A1. These compounds therefore promoted a sustained phosphorylation of eIF2α, which may exert cytoprotective effects. However, prolonged suppression of protein synthesis is incompatible with cell

survival. In agreement with this, 24 h-treatments with LP226A1, LP204A1 and LP205A1 down-regulated the P-eIF2α protein expression.

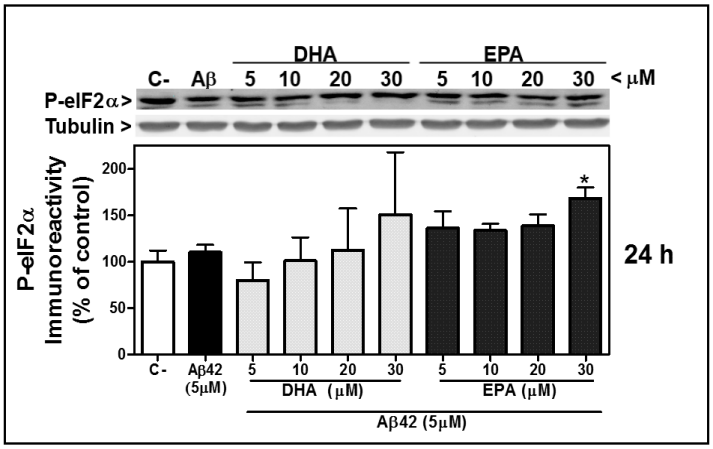

Figure 5.10 P-eIF2α regulation in differentiated SH-SY5Y cells treated with DHA or EPA, and incubated with Aβ 42 for 24 h. P-eIF2α protein levels in SH-SY5Y neuron-like cells were determined by immunoblotting. Each bar diagram is showing the mean ± SEM of P-eIF2α expression after exposure to Aβ42 peptide (5 μM) with or without treatment with DHA or EPA (5 -30 μM) for 24 h compared with untreated controls (C-). Values are expressed as percentage of control, n = 3. The asterisks indicate a significant effect of the treatment as compared with the non treated control (*p<0.05).

5.2.5. IRE1α Up-regulation after LP226A1, LP204A1 and LP205A1 Treatments of Differentiated SH-SY5Y Cells

Three major types of ER resident proteins have been identified as sensors for ER stress: PERK (already mentioned in the previous section), activating transcription factor 6 (ATF6), and inositol-requiring protein-1 (IRE1) (Hosoi and Ozawa, 2012). When these stress-sensor proteins are activated throughout the sensing of unfolded proteins in the ER, this will eventually transmit signals to the nucleus, and increase a subset of specific genes to accommodate such stress (Kaufman, 1999).

Activation of IRE1 induces X-box binding protein 1 (XBP-1) mRNA splicing by cleaving off its intron (Calfon *et al.*, 2002). Spliced XBP-1 then functions as a transcription factor specific for ER stress-related genes (Lee *et al.*, 2003).

One of the proposed mechanisms of AD progression is the accumulation of amyloid β peptide in the cerebral neuritic plaques. Amyloid β activates UPR signaling such as PERK or

XBP-1 splicing induced by IRE1 activation, which in turn is suggested to prevent amyloid β neurotoxicity (Lee do *et al.*, 2010; Casas-Tinto *et al.*, 2011).

In this section, differentiated SH-SY5Y cells treated with LP226A1, LP204A1, and LP205A1 (5 to 30 µM) (Figure 5.11A) were incubated with 5 µM of Aβ42 peptide (Figure 5.11B). IRE1α protein expression was monitored after 7 h or 24 h by carrying out a Western Blot immunoassay. The results in Figure 5.11A did not show an up-regulation of IRE1α in SH-SY5Y cells treated with LP226A1, LP204A1 or LP205A1 for 7 h. In contrast, the results in Figure 5.11B indicated an up-regulation of IRE1α in SH-SY5Y cells after incubation with Aβ42 peptide (5 µM), and 24 h-treatments with LP226A1, LP204A1 and LP205A1. IRE1α up-regulation was very significant at doses of 5 and 10 µM. Interestingly, incubation of SH-SY5Y cells with Aβ42 peptide also up-regulated significantly the IRE1α protein expression (Figure 5.11B).

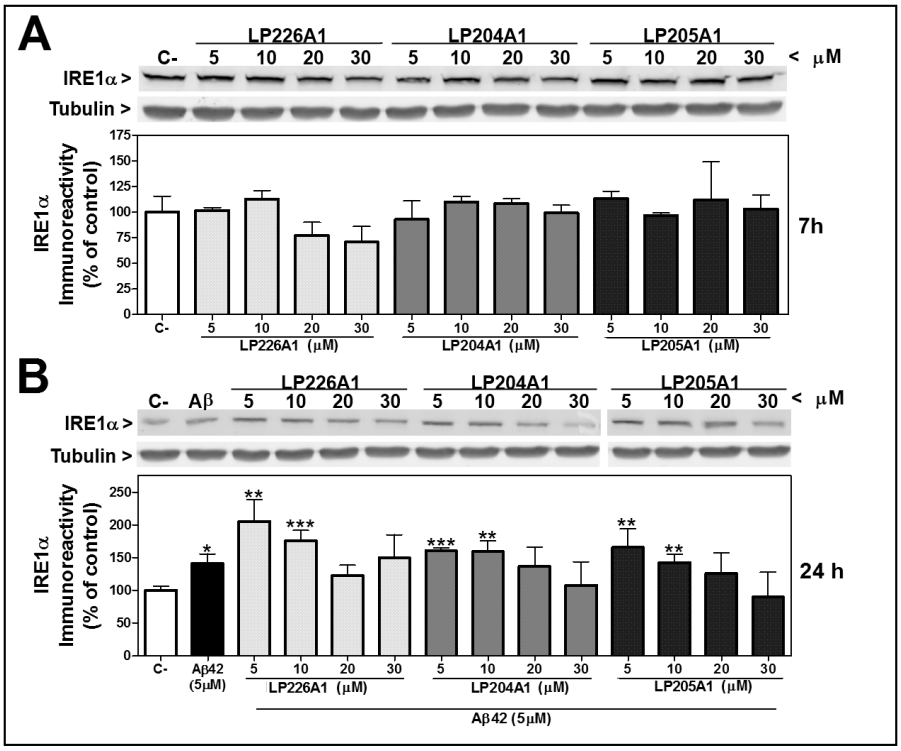

Figure 5.11 IREα regulation in differentiated SH-SY5Y cells treated with LP226A1, LP204A1 and LP205A1 incubated with or without Aβ 42 for 7 h or 24 h. IRE1α protein levels in SH-SY5Y neuron-like cells were determined by immunoblotting. . Each bar diagram is showing the mean ± SEM of IRE1α expression after treatment with (A) LP226A, LP204A1 or LP205A1 (5-30 µM) for 7 h, compared with untreated controls (C-). (B) IRE1α expression after exposure to Aβ42 peptide (5 µM), with or without a 24 h-treatment with LP226A, LP204A1 or LP205A1 (5-30 µM),compared with untreated controls (C-). Values are expressed as percentage of control, n = 3. The asterisks indicate a significant effect of the treatment as compared with the non treated control (*p<0.05, **p<0.01, ***p<0.001).

Furthermore, differentiated SH-SY5Y cells were also treated with DHA or EPA (5 to 30 µM) and incubated concomitantly with a final concentration of 5 µM Aβ42 peptide. IRE1α expression was monitored after 24 h by carrying out a Western Blot immunoassay (Figure 5.12). The results in Figure 5.12 did not show up-regulation of IRE1α in SH-SY5Y cells after incubation with Aβ42 peptide, and DHA or EPA treatments, except with EPA (30 µM) treatment which up-regulated significantly the IRE1α protein expression. Incubation of SH-SY5Y cells with Aβ42 peptide significantly up-regulated the IRE1α protein expression.

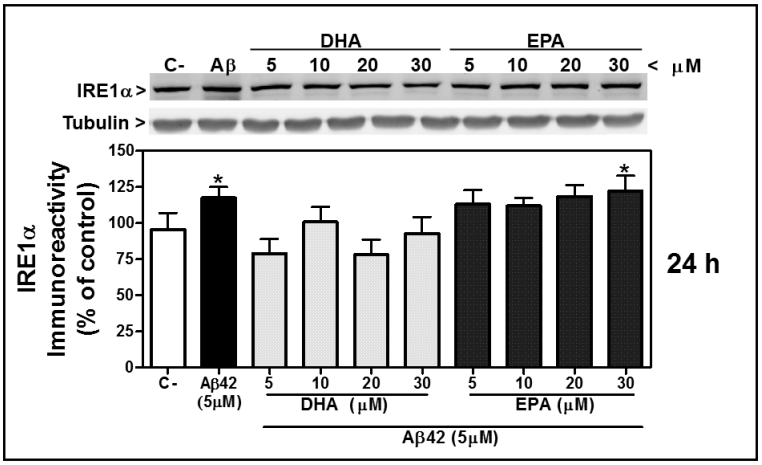

Figure 5.12 IRE1α regulation in differentiated SH-SY5Y cells treated with DHA or EPA, and incubated with Aβ 42 for 24 h. IRE1α protein levels in SH-SY5Y neuron-like cells were determined by immunoblotting. Each bar diagram is showing the mean ± SEM of IRE1α expression after exposure to Aβ42 peptide (5 µM) with or without treatment with DHA or EPA (5 -30 µM) for 24 h compared with untreated controls (C-). Values are expressed as percentage of control, n = 3. The asterisks indicate a significant effect of the treatment as compared with the non treated control (*p<0.05).

The results in this section showed an up-regulation of IRE1α protein after 24 h-treatments of SH-SY5Y cells with LP226A1, LP204A1, and LP205A1. These compounds therefore promoted an activation of IRE1α, which may induce X-box binding protein 1 (XBP-1) mRNA splicing by cleaving off its intron. XBP-1 splicing induced by IRE1α activation has been suggested to prevent amyloid β neurotoxicity. As we have already observed an IRE1α up-regulation in SH-SY5Y cells after treatment, it would be interesting to study XBP-1 splicing in future experiments.

5.2.6. CHOP Up-regulation after LP226A1, LP204A1 and LP205A1 Treatments of Differentiated SH-SY5Y Cells

If the aforementioned pro-survival mechanisms fail to rescue the cell, apoptosis can then occur. It is not clear at which point the switch between pro-survival and pro-apoptotic signaling occurs, nor which mechanisms underline cell death (Doyle *et al.*, 2011).

CHOP, also known as GADD153, is a member of the C/EBP family that heterodimerizes with other members of the C/EBP transcription factor family. This 29 kD factor is expressed at low levels in unstressed cells, and is strongly induced in response to ER stress. It can be induced by all three arms of the UPR (Zinszner *et al.*, 1998). CHOP´s pro-apoptotic effects are linked to down-regulation of BCL-2 and enhanced production of reactive oxygen species (ROS) (McCullough *et al.*, 2001).

Here, differentiated SH-SY5Y cells treated with LP226A1, LP204A1 and LP205A1 (5 to 30 µM) (Figure 5.13A) were incubated concomitantly with a final concentration of 5 µM Aβ42 peptide (Figure 5.13B). CHOP protein expression was monitored after 7 h or 24 h by carrying out a Western Blot immunoassay. The results in Figure 5.13A showed a very significant up-regulation of CHOP in SH-SY5Y cells treated for 7 h with 20 and 30 µM of LP226A1, LP204A1, or LP205A1. Moreover, the results in Figure 5.13B also indicated a very significant up-regulation of CHOP in SH-SY5Y cells after incubation with Aβ42 peptide (5 µM), and 24 h-treatments with LP226A1, LP204A1 or LP205A1. CHOP up-regulation was significant at doses of 20 and 30 µM. Treatments with LP204A1 up-regulated CHOP more strongly than other treatments. A significant up-regulation of CHOP was already observed at a dose of 10 µM of LP204A1. Interestingly, incubation of SH-SY5Y cells with Aβ42 peptide did not up-regulate significantly the CHOP protein expression (Figure 5.13B).

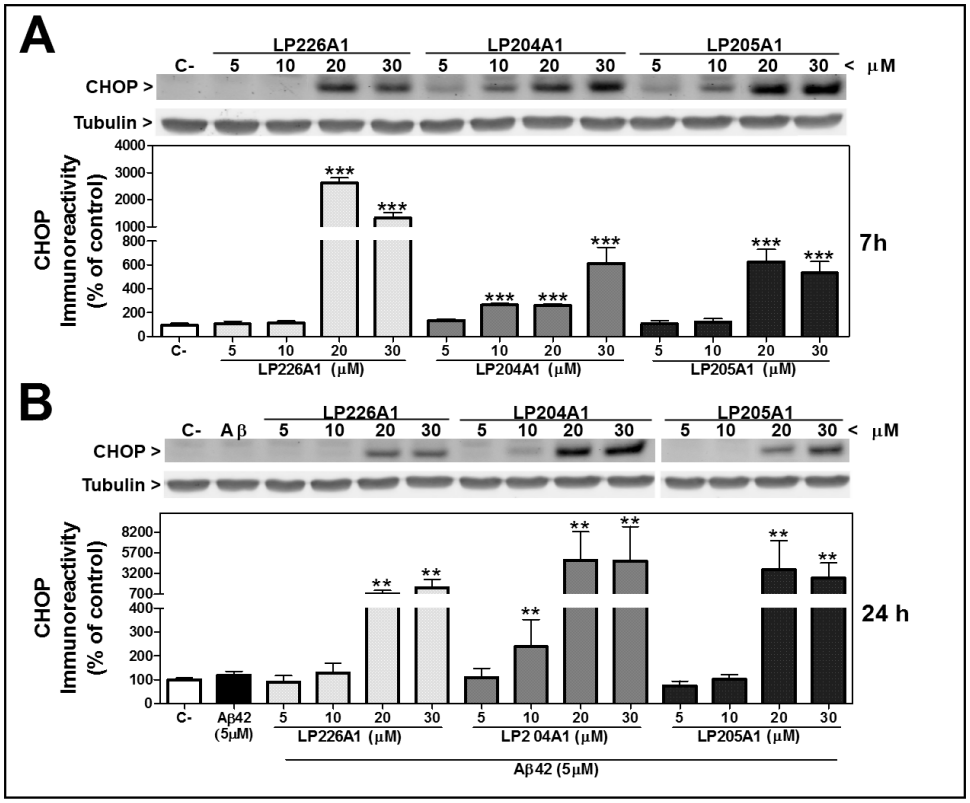

Figure 5.13 CHOP up-regulation in differentiated SH-SY5Y cells treated with LP226A1, LP204A1 or LP205A1 incubated with or without Aβ 42 for 7 h or 24 h. CHOP protein levels in SH-SY5Y neuron-like cells were determined by immunoblotting. Each bar diagram is showing the mean ± SEM of CHOP expression after treatment with (A) LP226A, LP204A1 or LP205A1 (5-30 µM) for 7 h compared with untreated controls (C-) or (B) after exposure to Aβ42 peptide (5 µM) with or without LP226A, LP204A1 or LP205A1 (5-30 µM) treatment for 24 h compared with untreated controls (C-). Values are expressed as percentage of control, n = 3. The asterisks indicate a significant effect of the treatment as compared with the non treated control (*p<0.05, **p<0.01, ***p<0.001).

In addition to this, differentiated SH-SY5Y cells were also treated with DHA or EPA (5 to 30 µM), and incubated with 5 µM of Aβ42 peptide. CHOP expression was monitored after 24 hours by carrying out a Western Blot immunoassay (Figure 5.14). The results in Figure 5.14 did not show a significant up-regulation of CHOP in SH-SY5Y cells after incubation with Aβ42 peptide and DHA or EPA treatments. However, treatment of SH-SY5Y cells with a positive control (LP204A1, 20 µM) up-regulated the CHOP protein expression. Incubation of SH-SY5Y cells with Aβ42 peptide did not up-regulate CHOP protein expression.

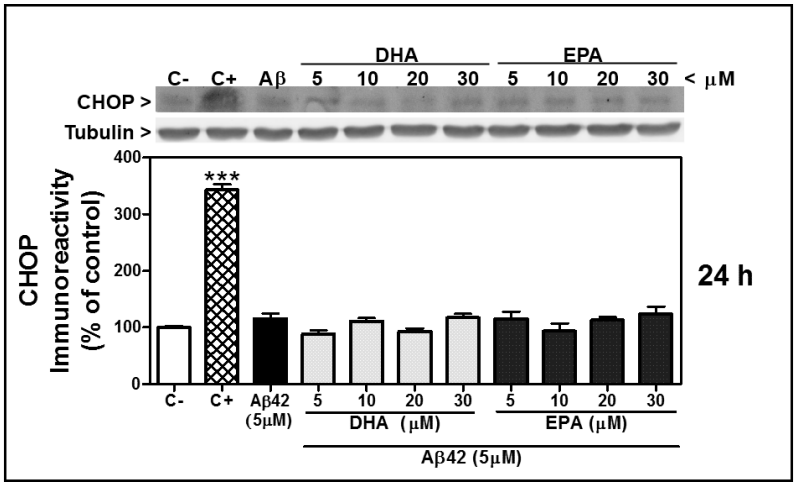

Figure 5.14 CHOP regulation in differentiated SH-SY5Y cells treated with DHA or EPA, and incubated with Aβ 42 for 24 h. CHOP protein levels in SH-SY5Y neuron-like cells were determined by immunoblotting. Each bar diagram is showing the mean ± SEM of CHOP expression after exposure to Aβ42 peptide (5 μM) with or without treatment with DHA or EPA (5-30 μM) for 24 h compared with untreated controls (C-). (C+) is LP204A1 20 μM. Values are expressed as percentage of control, n = 3. The asterisks indicate a significant effect of the treatment as compared with the non-treated control (***$p<0.001$).

The results in this section showed an up-regulation of CHOP protein after treatment of differentiated SH-SY5Y cells with LP226A1, LP204A1 or LP205A1 for 7 h and 24 h at the highest doses: 20 and 30 μM. These compounds, at the highest doses, promoted an activation of CHOP, which may induce apoptosis. These data support our previous results in chapter 4, in relation with the decrease in cell viability of differentiated SH-SY5Y cells after treatments with LP226A1 or LP205A1 at doses of 20 and 30 μM and LP204A1 (10-30 μM). Therefore, high doses of LP226A1, LP204A1 or LP205A1 on differentiated SH-SY5Y neuron-like cells could induce apoptosis throughout CHOP up-regulation.

5.2.7. Beclin-1 Up-regulation after LP226A1, LP204A1 and LP205A1 Treatments of Differentiated SH-SY5Y Cells

Autophagy, similar to ER stress, has both pro-death and pro-survival functions. Accumulating evidence indicates that autophagy may confer neuroprotection by enhancing a clearance of soluble and aggregated misfolded proteins. Conversely, a deregulation of autophagy may lead to neurodegeneration (Nedelsky *et al.*, 2008).

Synthesis of proteins in the ER is monitored by an elaborate quality control mechanism that allows only correctly folded proteins to be transported to their final

destination. Misfolded or unassembled proteins are retained in the ER and subsequently degraded by the Endoplasmic-reticulum-associated protein degradation (ERAD). To remove the aggregates of misfolded proteins that cannot be degraded by the ERAD, the UPR activates autophagy (Ogata *et al.*, 2006). During ER stress-induced autophagy, portions of the ER and aggregates are engulfed in double-membrane structures called autophagosomes and delivered to lysosomes for degradation (Verfaillie *et al.*, 2010).

Different conditions that induce ER stress lead to induction of autophagy (Verfaillie *et al.*, 2010). Both the PERK/eIF2α and IRE1 arms of the UPR have been implicated in the regulation of autophagy (Talloczy *et al.*, 2002; Ding *et al.*, 2007b). The pro-autophagic actions of IRE1 seem to rely on the ability of IRE1 to activate c-Jun N-terminal kinases (JNK). JNK has been shown to regulate autophagy through BCL-2 phosphorylation, which disrupts its interaction with Beclin-1 (Wei *et al.*, 2008). It has also been shown that PERK-eIF2α-dependent ATG12 up-regulation is required for induction of autophagy in response to polyglutamine protein accumulation (Kouroku *et al.*, 2007). PERK-dependent transcription factors ATF4 and CHOP have been proven to induce transcriptional activation of LC3B and ATG5 during hypoxia (Kouroku *et al.*, 2007). However the detailed molecular mechanism behind the activation of autophagy during ER stress has not yet been fully elucidated.

Among the initial steps of vesicle nucleation of the autophagic process is the activation of mammalian Vps34 to generate phosphatidylinositol-3-phosphate (PtdIns3P). Vps34 activation depends on the formation of a multi-protein complex in which beclin-1, UVRAG and Vps15 (or p150 in humans) participate (Part 2 Figure 5.1).

Here, SH-SY5Y neuron-like cells treated with LP226A1, LP204A1 or LP205A1 (5 to 30 µM) (Figure 5.15A) were also incubated with 5 µM Aβ42 peptide (Figure 5.15B). Beclin-1 protein expression was monitored after 7 h or 24 h by carrying out a Western Blot immunoassay. The results in Figure 5.15A showed a significant up-regulation of Beclin-1 in SH-SY5Y cells treated for 7 h with LP226A1, LP204A1 and LP205A1. In contrast, the results in Figure 5.15B did not indicate an up-regulation of Beclin-1 in SH-SY5Y cells after incubation with Aβ42 peptide (5 µM) and 24 h-treatments with LP226A1, LP204A1 and LP205A1 with the exception of 5 and 10 µM LP226A1 treatments which significantly up-regulated Beclin-1. In addition, LP205A1 (20 and 30 µM) 24 h-treatments significantly down-regulated Beclin-1 expression.

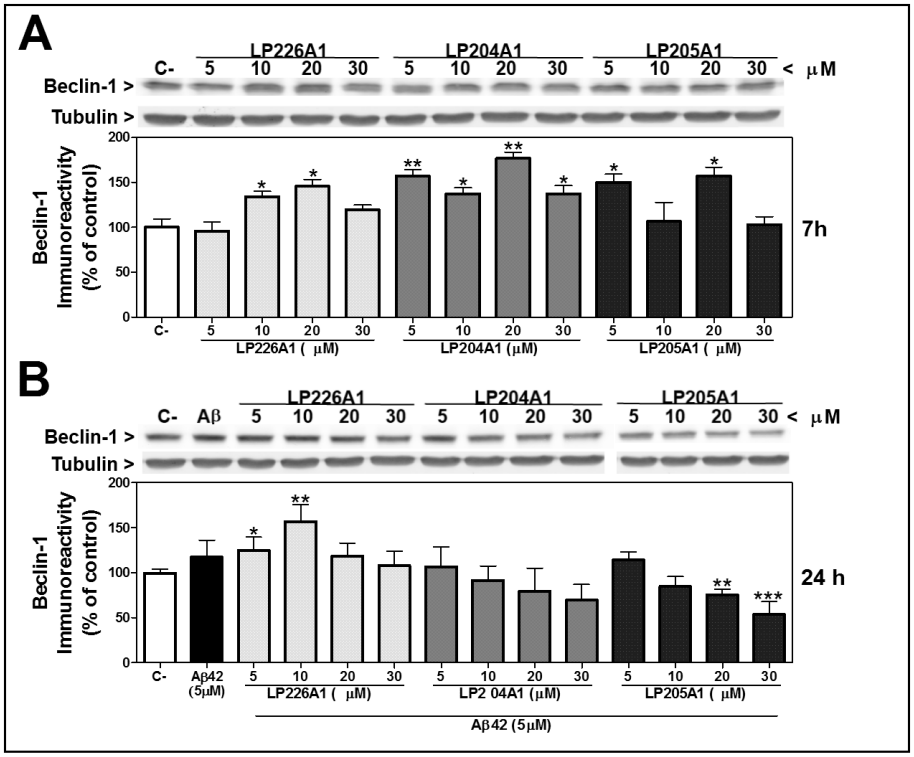

Figure 5.15 Beclin-1 up-regulation in differentiated SH-SY5Y cells treated with LP226A1, LP204A1 or LP205A1, incubated with or without Aβ 42 for 7 h or 24 h. Beclin-1 protein levels in SH-SY5Y neuron-like cells were determined by immunoblotting. Each bar diagram is showing the mean ± SEM of Beclin-1 expression after treatment with (A) LP226A, LP204A1 or LP205A1 (5-30 μM) for 7 h compared with untreated controls (C-). (B) Beclin-1 expression after exposure to Aβ42 peptide (5 μM) with or without LP226A, LP204A1 or LP205A1 (5-30 μM) treatment for 24 h compared with untreated controls (C-). Values are expressed as percentage of control, n = 3. The asterisks indicate a significant effect of the treatment as compared with the non treated control (*p<0.05, **p<0.01, ***p<0.001).

Beclin-1 is an early player of the autophagy process which participates in the vesicle nucleation (Maiuri *et al.*, 2007). LP226A1, LP204A1 and LP205A1 treatments of differentiated SH-SY5Y cells up-regulated Beclin-1 expression at short time points (7 h).

Moreover, differentiated SH-SY5Y cells were also treated with DHA or EPA (5 to 30 µM), and incubated with a final concentration of 5 µM Aβ42 peptide. Beclin-1 expression was monitored after 24 h by carrying out a Western Blot immunoassay (Figure 5.16). The results in Figure 5.17 showed a significant down-regulation of Beclin-1 in SH-SY5Y cells after incubation with Aβ42 peptide and DHA or EPA treatment. In addition, incubation of SH-SY5Y cells with Aβ42 peptide did not up-regulate Beclin-1 protein expression.

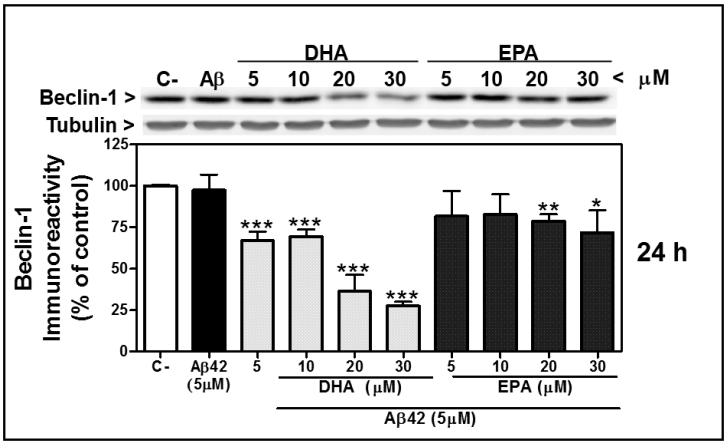

Figure 5.16 Beclin-1 regulation in differentiated SH-SY5Y cells treated with DHA or EPA, and incubated with Aβ 42 for 24 h. Beclin-1 protein levels in SH-SY5Y neuron-like cells were determined by immunoblotting. Each bar diagram is showing the mean ± SEM of Beclin-1 expression after exposure to Aβ42 peptide (5 µM) with or without treatment with DHA or EPA (5-30 µM) for 24 h compared with untreated controls (C-). Values are expressed as percentage of control, n = 3. The asterisks indicate a significant effect of the treatment as compared with the non treated control (*p<0.05, **p<0.01, ***p<0.001).

5.2.8. ATG5, ATG12 and ATG7 Up-regulation after LP226A1, LP204A1 and LP205A1 Treatments of Differentiated SH-SY5Y Cells

The elongation of phagophores requires two ubiquitin-like conjugating systems (see part 3, figure 5.1):

1) ATG12-ATG5-ATG16L system: ATG12 is conjugated into ATG5 via ATG7 (E1-like enzyme) and ATG10 (E2-like enzyme). Then, a conjugated ATG12-ATG5 complex

associates with ATG16L (Mizushima *et al.*, 1998a; Mizushima *et al.*, 1999; Tanida *et al.*, 2001; Mizushima *et al.*, 2003). The ATG12-ATG5-ATG16L complex is localized in the outer membrane of elongating autophagosomes but itdissociates before the completion of autophagosome formation.

2) Phosphatidylethanolamine (PE)-LC3 system: As with the other system, microtubule-associated protein 1 light chain 3 (MAP1-LC3, simply LC3), is conjugated to PE. A cytosolic form of LC3, LC3-I, is generated by cleavage of pro LC by ATG4, and further processed by ATG7. ATG3 is then conjugated to PE (LC3-II) (Tanida *et al.*, 2002a). LC3-II specifically associates with autophagosome membranes. Therefore, the number of autophagosomes correlates with the level of LC3-II. (Nakatogawa *et al.*, 2007; Weidberg *et al.*, 2011).

After completion of autophagosome formation, autophagosomes can be fused with endosomes or lysosomes resulting in the formation of amphisomes or autolysosomes, respectively (Gordon and Seglen, 1988; Stromhaug *et al.*, 1998).

In this section, differentiated SH-SY5Y cells treated with LP226A1, LP204A1 and LP205A1 (5 to 30 µM) (Figure 5.17A) were also incubated with 5 µM Aβ42 peptide (Figure 5.17B). ATG5 protein expression was monitored after 7 h or 24 h by carrying out a Western Blot immunoassay. The results in Figure 5.19A showed a significant up-regulation of ATG5 in SH-SY5Y cells treated with LP226A1, LP204A1 and LP205A1 at all doses and for 7 h. In contrast, the results in Figure 5.17B only indicated a significant up-regulation of ATG5 in SH-SY5Y cells after incubation with Aβ42 peptide (5 µM), and 24 h-treatments with the lower doses of LP226A1, LP204A1, and LP205A1. 24 h-treatments with 5-10 µM of LP226A1 and 5-10 µM of LP204A1 or LP205A1 significantly up-regulated the ATG5 protein expression.

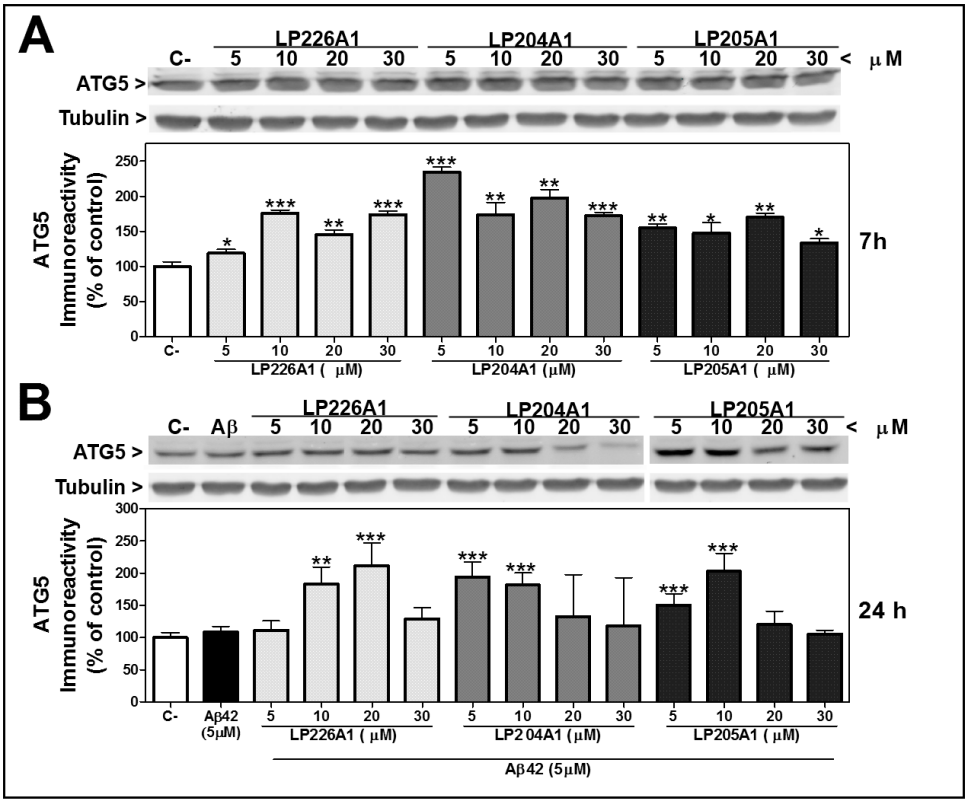

Figure 5.17 ATG5 up-regulation in differentiated SH-SY5Y cells treated with LP226A1, LP204A1 and LP205A1, incubated with or without Aβ 42 for 7 h or 24 h. ATG5 protein levels in SH-SY5Y neuron-like cells determined by immunoblotting. Each bar diagram is showing the mean ± SEM of ATG5 expression after treatment with (A) LP226A, LP204A1, or LP205A1 (5-30 μM) for 7 h compared with untreated controls (C-). (B) ATG5 expression after exposure to Aβ42 peptide (5 μM) with or without 24 h-treatments with LP226A, LP204A1 or LP205A1 (5-30 μM), compared with untreated controls (C-). Values are expressed as percentage of control, n = 3. The asterisks indicate a significant effect of the treatment as compared with the non-treated control (*p<0.05, **p<0.01, ***p<0.001).

Moreover, SH-SY5Y neuron-like cells were treated with DHA or EPA (5 to 30 µM) and incubated concomitantly with a final concentration of 5 µM Aβ42 peptide. ATG5 expression was monitored after 24 h by carrying out a Western Blot immunoassay (Figure 5.18). The results in Figure 5.18 showed a significant down-regulation of ATG5 in SH-SY5Y cells after incubation with Aβ42 peptide, and DHA 30 µM treatments. In addition, an incubation of SH-SY5Y cells with Aβ42 peptide and EPA treatments did not up-regulate the ATG5 protein expression.

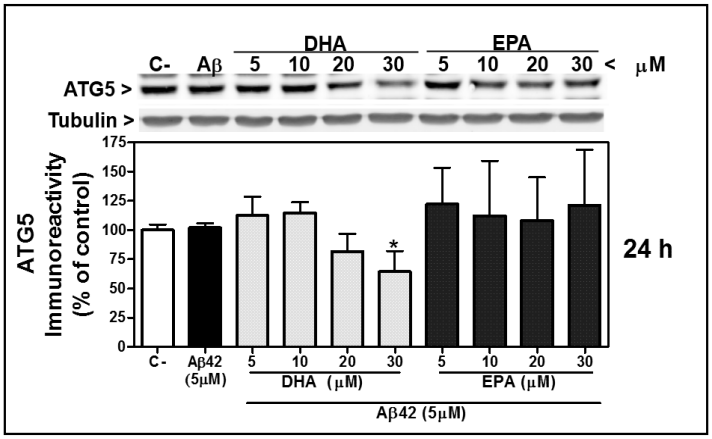

Figure 5.18 ATG5 regulation in differentiated SH-SY5Y cells treated with DHA or EPA, and incubated with Aβ 42 for 24 h. ATG5 protein levels in SH-SY5Y neuron-like cells determined by immunoblotting. Each bar diagram is showing the mean ± SEM of ATG5 expression after exposure to Aβ42 peptide (5 µM) with or without treatment with DHA or EPA (5-30 µM) for 24 h compared with untreated controls (C-). Values are expressed as percentage of control, n = 3. The asterisks indicate a significant effect of the treatment as compared with the non-treated control (*$p<0.05$).

Furthermore, differentiated SH-SY5Y cells treated with LP226A1, LP204A1 or LP205A1 (5 to 30 µM) (Figure 5.19A) were incubated with 5 µM Aβ42 peptide (Figure 5.19B). ATG12 protein expression was monitored after 7 h or 24 h by carrying out a Western Blot immunoassay. The results in Figure 5.19A showed a very significant up-regulation of ATG12 in SH-SY5Y cells treated with LP226A1, LP204A1, or LP205A1 for 7 hours. The results in Figure 5.19B showed that 24 h-treatments with 10-20 µM LP226A1, 10 µM LP204A1, and 5-10 µM LP205A1 up-regulated significantly the ATG12 protein expression in SH-SY5Y cells. In contrast, an incubation of SH-SY5Y cells with Aβ42 peptide (5 µM) did not indicate an up-regulation of ATG12.

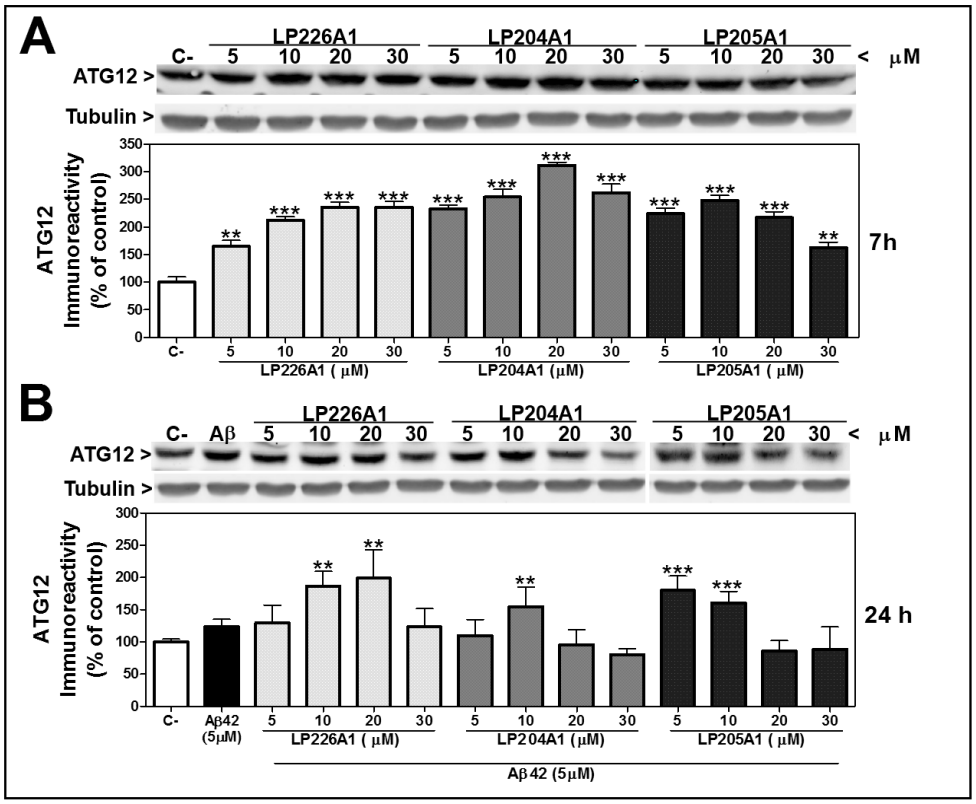

Figure 5.19 ATG12 up-regulation in differentiated SH-SY5Y cells treated with LP226A1, LP204A1 or LP205A1 incubated with or without Aβ 42 for 7 h or 24 h. ATG12 protein levels in SH-SY5Y neuron-like cells were determined by immunoblotting. Each bar diagram is showing the mean ± SEM of ATG12 expression after treatment with (A) LP226A, LP204A1 and LP205A1 (5-30 μM) for 7 h compared with untreated controls (C-). (B) ATG12 expression after exposure to Aβ42 peptide (5 μM) with or without 24 h-treatments with LP226A, LP204A1, or LP205A1 (5-30 μM), compared with untreated controls (C-). Values are expressed as percentage of control, n = 3. The asterisks indicate a significant effect of the treatment as compared with the non treated control (**p<0.01, ***p<0.001).

Differentiated SH-SY5Y cells were also treated with DHA or EPA (5 to 30 μM) and incubated concomitantly with 5 μM Aβ42 peptide. ATG12 expression was monitored after 24 h by carrying out a Western Blot immunoassay (Figure 5.20). The results in Figure 5.20 showed a significant down-regulation of ATG12 in SH-SY5Y cells after incubation with Aβ42 peptide and DHA (20 and 30 μM) treatments. In addition, incubation of SH-SY5Y cells with Aβ42 peptide and EPA treatments did not up-regulate the ATG12 protein expression.

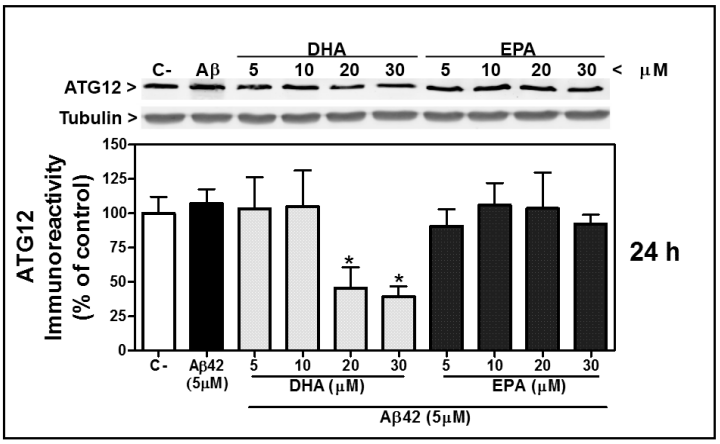

Figure 5.20 ATG12 regulation in differentiated SH-SY5Y cells treated with DHA or EPA, and incubated with Aβ 42 for 24 h. ATG12 protein levels in SH-SY5Y neuron-like cells were determined by immunoblotting. Each bar diagram is showing the mean ± SEM of ATG12 expression after exposure to Aβ42 peptide (5 μM) with or without treatment with DHA or EPA (5-30 μM) for 24 h compared with untreated controls (C-). Values are expressed as percentage of control, n = 3. The asterisks indicate a significant effect of the treatment as compared with the non treated control (*p<0.05).

SH-SY5Y neuron-like cells treated with LP226A1, LP204A1 or LP205A1 (5 to 30 μM) (Figure 5.21A) were incubated concomitantly with 5 μM Aβ42 peptide (Figure 5.21B). ATG7 protein expression was monitored after 7 h or 24 h by carrying out a Western Blot immunoassay. The results in Figure 5.21A showed a very significant up-regulation of ATG7 in SH-SY5Y cells treated with LP226A1, LP204A1 and LP205A1 for 7 h. The results in Figure 5.21B showed that 24 h-treatments with LP204A1 and LP205A1 (10 μM) significantly up-regulated ATG7. In addition, 24 h-treatments with LP226A1 (10-30 μM) significantly down-regulated the ATG7 protein expression. An incubation of SH-SY5Y cells with Aβ42 peptide (5 μM) did not show an up-regulation of ATG7.

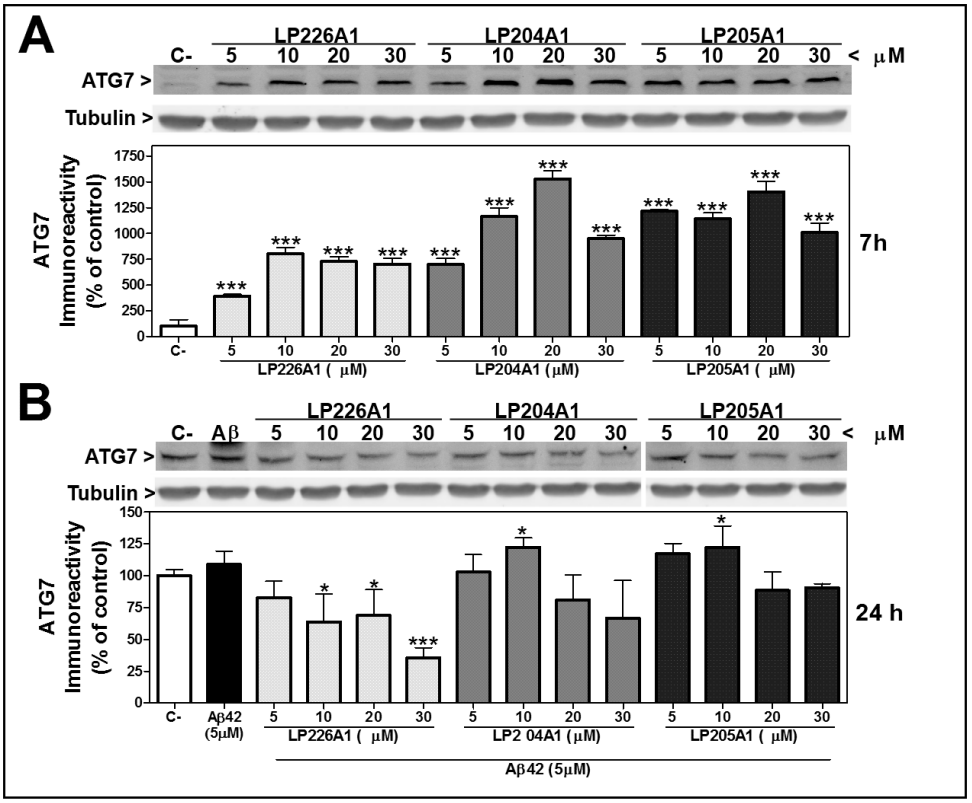

Figure 5.21 ATG7 regulation in differentiated SH-SY5Y cells treated with LP226A1, LP204A1 or LP205A1 incubated with or without Aβ 42 for 7 h or 24 h. ATG7 protein levels in SH-SY5Y neuron-like cells were determined by immunoblotting. Each bar diagram is showing the mean ± SEM of ATG7 expression after treatment with (A) LP226A, LP204A1 and LP205A1 (5-30 µM) for 7 h compared with untreated controls (C-) or (B) after exposure to Aβ42 peptide (5 µM) with or without LP226A, LP204A1 and LP205A1 (5-30 µM) treatment for 24 h compared with untreated controls (C-). Values are expressed as percentage of control, n = 3. The asterisks indicate a significant effect of the treatment as compared with the non-treated control (*p<0.05, **p<0.01, ***p<0.001).

Finally, differentiated SH-SY5Y neuron-like cells were also treated with DHA or EPA (5 to 30 µM), and incubated with 5 µM Aβ42 peptide. ATG12 expression was monitored after 24 h by carrying out a Western Blot immunoassay (Figure 5.22). The results in Figure 5.22 show a significant down-regulation of ATG7 in SH-SY5Y cells after incubation with Aβ42 peptide and DHA (20 and 30 µM) treatments. In addition, an incubation of SH-SY5Y cells with Aβ42 peptide and EPA treatments did not regulate ATG7 protein expression.

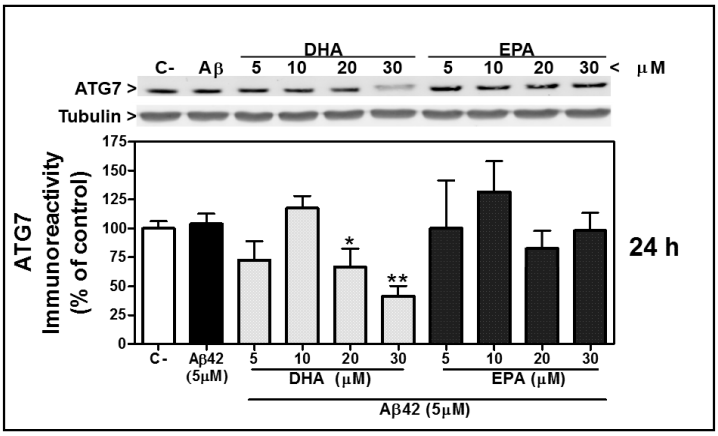

Figure 5.22 AT7down-regulation in differentiated SH-SY5Y cells treated with DHA or EPA, and incubated with Aβ 42 for 24 h. ATG7 protein levels in SH-SY5Y neuron-like cells were determined by immunoblotting. Each bar diagram is showing the mean ± SEM of ATG7 expression after exposure to Aβ42 peptide (5 μM) with or without treatment with DHA or EPA (5-30 μM) for 24 h compared with untreated controls (C-). Values are expressed as percentage of control, n = 3. The asterisks indicate a significant effect of the treatment as compared with the non treated control (*p<0.05, **p<0.01).

5.2.9. ATG3 and LC3BII Up-regulation after LP226A1, LP204A1 and LP205A1 Treatments of Differentiated SH-SY5Y Cells

In order to study the second ubiquitin-like conjugating system (PE-LC3 system), implicated in the elongation of the phagophores, we evaluated ATG3 and LC3BII protein expression in our neuron-like cell model treated with hydroxy derivates.

ATG3, together with ATG7, is in charge of the processing of LC3BI, which is conjugated to PE to generate LC3BII. In order to study ATG3, differentiated SH-SY5Y cells treated with LP226A1, LP204A1 or LP205A1 (5 to 30 μM) (Figure 5.23A) were incubated concomitantly with 5 μM Aβ42 peptide (Figure 5.23B). ATG3 protein expression was monitored after 7 h or 24 h by carrying out a Western Blot immunoassay. The results in Figure 5.23A show a very significant up-regulation of ATG3 in SH-SY5Y cells treated with LP226A1, LP204A1, and LP205A1 for 7 h. The results in Figure 5.23B show a significant up-regulation of ATG3 in SH-SY5Y cells treated with LP226A1 (5 and 10 μM) and LP205A1 (10 μM) for 24 h. However, 24 hour-treatments with LP204A1 (20 μM) of SH-SY5Y cells significantly down-regulated the ATG3 protein expression. An incubation with Aβ42 peptide (5 μM) for 24 h did not modulate ATG3 protein expression in differentiated SH-SY5Y cells.

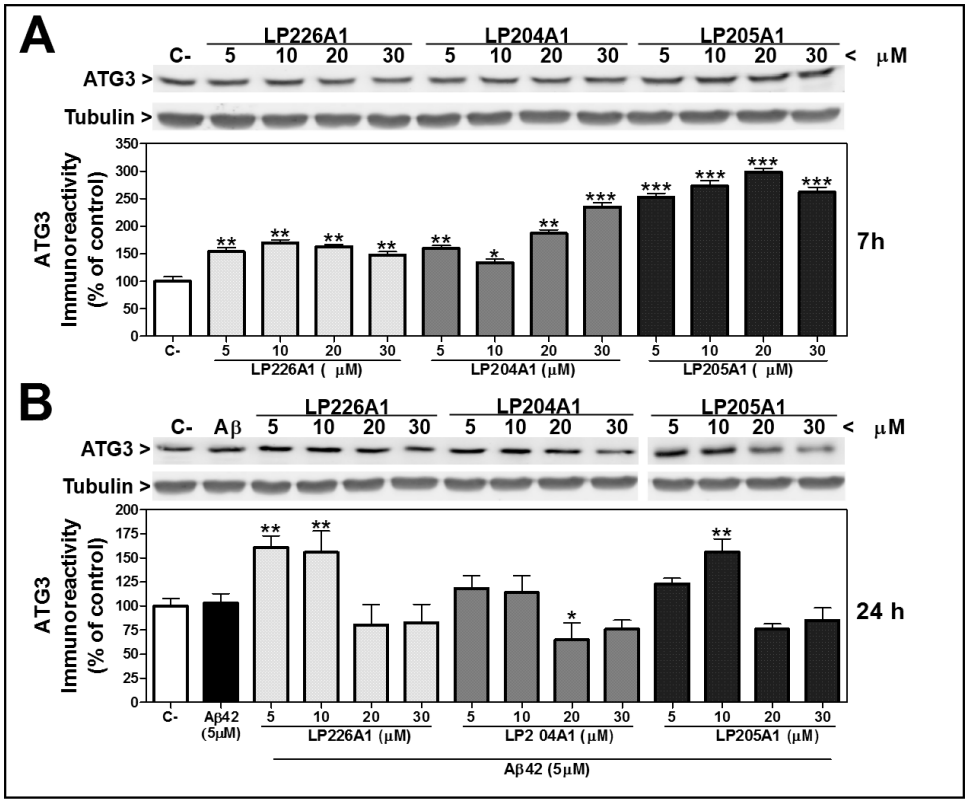

Figure 5.23 ATG3 regulation in differentiated SH-SY5Y cells treated with LP226A1, LP204A1 or LP205A1 incubated with or without Aβ 42 for 7 h or 24 h. ATG3 protein levels in SH-SY5Y neuron-like cells were determined by immunoblotting. Each bar diagram is showing the mean ± SEM of ATG3 expression after treatment with (A) LP226A, LP204A1 and LP205A1 (5-30 µM) for 7 h compared with untreated controls (C-). (B) ATG3 expression after exposure to Aβ42 peptide (5 µM) with or without LP226A, LP204A1, and a LP205A1 (5-30 µM) 24 h-treatment, compared with untreated controls (C-). Values are expressed as percentage of control, n = 3. The asterisks indicate a significant effect of the treatment as compared with the non treated control (*p<0.05, **p<0.01, ***p<0.001).

In addition, differentiated SH-SY5Y cells were also treated with DHA or EPA (5 to 30 µM) and incubated concomitantly with a final concentration of 5 µM Aβ42 peptide. ATG3 expression was monitored after 24 h by carrying out a Western Blot immunoassay (Figure 5.24). The results in Figure 5.24 showed a significant down-regulation of ATG3 in SH-SY5Y cells after incubation with Aβ42 peptide and DHA (20 and 30 µM) treatments. An incubation of SH-SY5Y cells with Aβ42 peptide and EPA treatments did not regulate ATG3 protein expression.

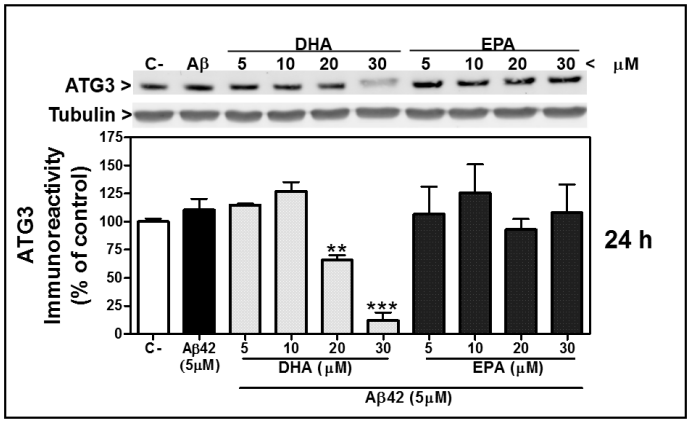

Figure 5.24 AT3 down-regulation in differentiated SH-SY5Y cells treated with DHA or EPA, and incubated with Aβ 42 for 24 h. ATG3 protein levels in SH-SY5Y neuron-like cells were determined by immunoblotting. Each bar diagram is showing the mean ± SEM of ATG3 expression after exposure to Aβ42 peptide (5 μM) with or without treatment with DHA or EPA (5-30 μM) for 24 h compared with untreated controls (C-). Values are expressed as percentage of control, n = 3. The asterisks indicate a significant effect of the treatment as compared with the non treated control (**p<0.01, ***p<0.001).

LC3BII specifically associates with autophagosome membranes and therefore the protein expression of LC3BII directly correlates with the number of autophagosomes. For this reason, SH-SY5Y differentiated cells treated with LP226A1, LP204A1 or LP205A1 (5 to 30 μM) (Figure 5.25A) were also incubated with 5 μM Aβ42 peptide (Figure 5.25B). LC3BII protein expression was monitored after 7 h or 24 h by carrying out a Western Blot immunoassay. The results in Figure 5.25A show a very significant up-regulation of LC3BII in SH-SY5Y cells treated with LP226A1, LP204A1 and LP205A1 for 7 h. The results in Figure 5.25B also show a very significant up-regulation of LC3BII in SH-SY5Y cells after incubation with Aβ42 peptide (5 μM), and treatments with LP226A1, LP204A1 or LP205A1 for 24 h. In addition, a Aβ42 peptide 24 h-incubation significantly up-regulated LC3BII protein expression.

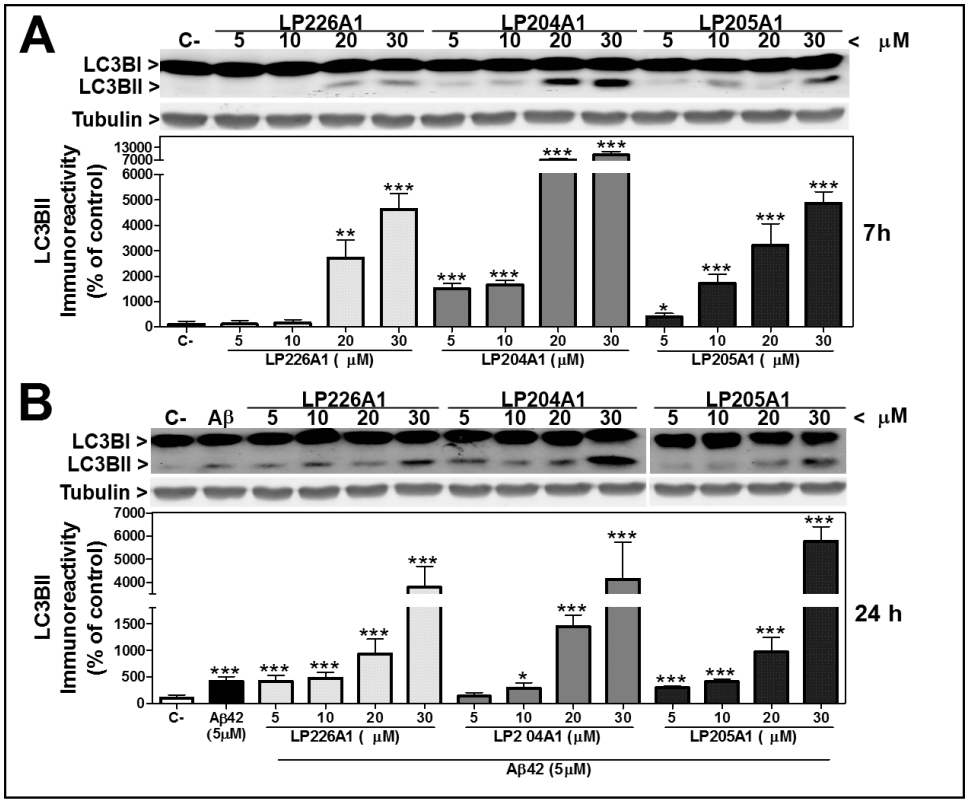

Figure 5.25 LC3BII regulation in SH-SY5Y differentiated cells treated with LP226A1, LP204A1 or LP205A1 incubated with or without Aβ 42 for 7 h or 24 h. LC3BII protein levels in SH-SY5Y neuron-like cells determined by immunoblotting. Each bar diagram is showing the mean ± SEM of LC3BII expression after treatment with (A) LP226A, LP204A1, and LP205A1 (5-30 µM) for 7 h compared to untreated controls (C-). (B) LC3BII expression after exposure to Aβ42 peptide (5 µM) with or without LP226A, LP204A1 and LP205A1 (5-30 µM) treatment for 24 h, compared to untreated controls (C-). Values are expressed as percentage of control, n = 3. The asterisks indicate a significant effect of the treatment as compared with the non-treated control (*p<0.05, **p<0.01, ***p<0.001).

Finally, SH-SY5Y neuron-like cells were treated with DHA or EPA (5 to 30 µM), and incubated concomitantly with a final concentration of 5 µM Aβ42 peptide. LC3BII expression was monitored after 24 h by carrying out a Western Blot immunoassay (Figure 5.26). The results in Figure 5.26 show a significant up-regulation of LC3BII in SH-SY5Y cells after incubation with Aβ42 peptide and DHA (10-30 µM) treatments. However, an incubation of SH-SY5Y cells with Aβ42 peptide and EPA treatments did not up-regulate LC3BII protein expression.

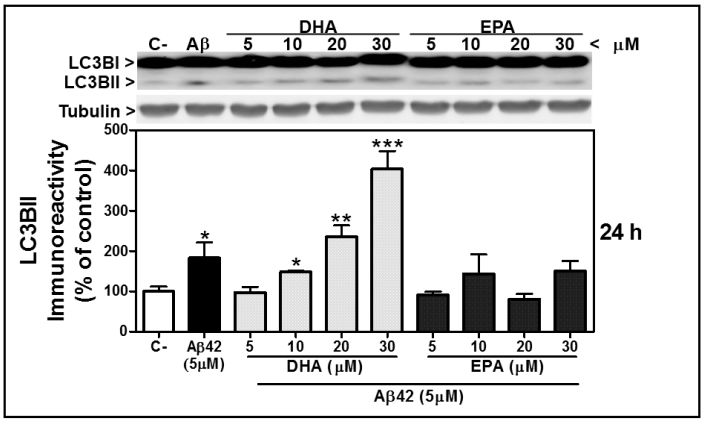

Figure 5.26 LC3BII down-regulation in differentiated SH-SY5Y cells treated with DHA or EPA, and incubated with Aβ 42 for 24 h. LC3BII protein levels in SH-SY5Y neuron-like cells were determined by immunoblotting. Each bar diagram is showing the mean ± SEM of LC3BII expression after exposure to Aβ42 peptide (5 μM) with or without treatment with DHA or EPA (5-30 μM) for 24 h compared with untreated controls (C-). Values are expressed as percentage of control, n = 3. The asterisks indicate a significant effect of the treatment as compared with the non treated control (*p<0.05, **p<0.01, ***p<0.001).

5.1.5 Discussion

As we previously discussed in chapter 4 (Figure 4.7) the cell viability studies allowed us to divide in two groups the treatment doses with LP226A1 and LP205A1: therapeutic doses (5-10 μM) and toxic doses (20-30 μM). LP204A1 treatment doses were also divided in these two groups but with a slightly different distribution: therapeutic doses (5 μM) and toxic doses (10-30 μM). In this chapter, we present the results corresponding to all doses of treatment in order to build a full picture of the molecular signaling in the cell. However, we paid special attention to the results obtained after treatments at therapeutic doses (5-10 μM).

For the sake of clarity, we present in table 5.1 (ER stress proteins) and table 5.2 (autophagy proteins) a concise overview of the main findings reported in this chapter.

The results of the present study have revealed that the three hydroxy derivates: LP226A1, LP204A1, and LP205A1, significantly up-regulated molecular chaperones (BiP and PDI) by allowing productive folding to occur more efficiently (Table 5.1).

Previous studies have shown that the ER chaperone BiP may bind to and facilitate correct folding of nascent APP (Yang *et al.*, 1998). In fact, the increased sensitivity of neurons to ER stress is attributed to the decreased levels of BiP mRNA (Doyle *et al.*, 2011). Our results demonstrate a very significant BiP up-regulation on SH-SY5Y cells treated with LP226A1, LP204A1, and LP205A1 (with or without Aβ42 peptide) (Figure 5.3; Table 5.1),

which is consistent with the cytoprotective effects observed in the previous chapter (Figure 4.13)

PDI, a chaperone that is believed to accelerate the folding of disulfide-bonded proteins, was also significantly up-regulated by the hydroxy derivates LP226A1 and LP205A1 after 7 h treatments on SH-SY5Y neron-like cells (Figure 5.5; Table 5.1). LP204A1 treatments, however, up-regulated PDI after 24 h. PDI prevents the neurotoxicity associated with ER stress and misfolding (Uehara *et al.*, 2006).

Calnexin (CNX) is a molecular chaperone that assists glycoprotein folding and participates in ER quality control. Treatments of differentiated SH-SY5Y cells with the hydroxy derivates did not modulate calnexin protein expression at therapeutic doses (Figure5.7; Table 5.1). Ranging from subtle to essential phenotypes, mixed results have been obtained when CNX genes were disrupted (Leach and Williams, 2000). Much of the complexity can be attributed to the redundant nature of the ER chaperone, wherein the synthesis of BiP or PDI is up-regulated as a compensatory response to impairments in the Calnexin/Calreticulin system (Leach and Williams, 2000).

Similar results were observed after treatments with DHA and EPA. BiP and PDI protein expression were up-regulated while calnexin protein expression was not modulated by these molecules (Figures 5.4; 5.6 and 5.8; Table 5.1).

In conclusion we can say that LP226A1, LP205A1, and LP204A1 treatments (with or without Aβ42 peptide) significantly up-regulated BiP and PDI molecular chaperone protein expression by allowing productive folding to occur more efficiently. As we mentioned above, BiP may bind to and facilitate correct folding of nascent APP (Yang *et al.*, 1998) which would alleviate the cell from Aβ42 peptide production. However once Aβ42 peptide is already formed, chaperones would not be able to eliminate it and other mechanisms such as autophagy should be activated in order to do so. Thus, chaperone activation is positive in order to reduce incorrect folding of nascent APP and Aβ42 peptide production in the context of AD.

Table 5.1 Summary of ER stress markers induced by the hydroxy derivates (LP226A1, LP205A1 and LP204A1) and the original lipids (DHA and EPA) at 10 µM.

	LP226A1		DHA	LP205A1		EPA	LP204A1	
Proteins	7 h	24 h*	24 h*	7 h	24 h*	24 h*	7 h	24 h*
BiP	↑	↑↑↑	↑	↑↑↑	↑↑	↑	↑↑↑	↑↑
PDI	↑	−	↑↑	↑↑	−	↑↑	−	↑↑↑
Calnexin	−	−	−	−	↓	−	−	−
P-eIF2α	↑↑	↓	−	↑↑↑	−	−	↑↑↑	↓
IRE1α	−	↑↑↑	−	−	↑↑	−	−	↑↑
CHOP	−	−	−	−	−	−	↑↑↑	↑↑

Level of induction of ER stress proteins (BiP, PDI, Calnexin, P-eIF2α, IRE1α and CHOP) after treatment of differentiated SH-SY5Y cells with 10 µM of LP226A1, DHA, LP205A1, EPA, and LP204A1. *Cells were incubated concomitantly with Aβ42 peptide. Meaning of the symbols: − no modulation;.↑ significant up-regulation; ↑↑ very significant up-regulation; ↑↑↑ very very significant up-regulation; ↓ significant down-regulation.

Furthermore, P-eIF2α (a protein that corresponds to the PERK axe of the UPR pathway) was first significantly up-regulated in the differentiated SH-SY5Y cells after a 7 h-treatments (Figure 5.9A; Table 5.1), and lately down-regulated after 24 h-treatments with LP226A1, LP204A1, and LP205A1 (+Aβ42 peptide) (Figure 5.9B; Table 5.1). P-eIF2α mediates the suppression of global mRNA translation, and, under these conditions, only selected mRNAs are translated. This includes ATF4 (Lu *et al.*, 2004a) which induces the expression of genes involved in the restoration of ER homeostasis and in autophagy (Lu *et al.*, 2004a; Fujita *et al.*, 2007; Kouroku *et al.*, 2007). Accordingly, compounds that promote a sustained phosphorylation of eIF2α, such as salubrinal (Boyce *et al.*, 2005), may exert cytoprotective effects. However, prolonged suppression of protein synthesis is incompatible with cell survival (Kim *et al.*, 2008). In this context, our results showed an initial up-regulation of P-eIF2α, followed by a down-regulation of the protein, suggesting a protective activation of P-eIF2α in the context of the restoration of ER homeostasis.

IRE1α (second axe of the UPR pathway) was very significantly up-regulated in the differentiated SH-SY5Y cells by the hydroxy derivates (+Aβ42 peptide) at therapeutic doses (5 and 10µM) after a 24 h-treatment (Figure 5.11; Table 5.1). IRE1α transmitted the signals to the nucleus, and increased a subset of specific genes to accommodate the stress.

Meanwhile, CHOP, a pro-apoptotic factor strongly induced in response to ER stress, was significantly up-regulated but only after treatments with toxic doses (20 and 30 µM) of the molecules (LP226A1, LP204A1 and LP205A1) (Figure 5.13). These results suggest a cytoprotective effect of the unfolded protein response (UPR) at early time points and at lower doses of the hydroxy derivates treatments (therapeutic doses) (Table 5.1). The

cytoprotective effect of the unfolded protein response is followed by a cell death induction by the toxic doses (20 to 30 µM) of the molecules. These results are consistent with the cell viability results obtained in the previous chapter (Section 4.2.5).

In contrast, treatments with DHA and EPA did not modulate P-eIF2α, IRE1α and CHOP protein expression (Figures 5.10; 5.12 and 5.14; Table 5.1).

The results in this chapter prove that only the protective arm of the unfolded protein response was activated at therapeutic doses. This means an early activation of P-eIF2α followed by a subsequent inactivation of this protein and an up-regulation of IRE1α. All these were accompanied by an up-regulation of two chaperones (BiP and PDI). CHOP which belongs to the cytocidal arm of the unfolded protein response, was not activated at the therapeutic doses.

Table 5.2 Summary of autophagy markers induced by the hydroxy derivates (LP226A1, LP205A1 and LP204A1) and the original lipids (DHA and EPA) at 10 µM.

	LP226A1		DHA	LP205A1		EPA	LP204A1	
Proteins	**7 h**	**24 h***	**24 h***	**7 h**	**24 h***	**24 h***	**7 h**	**24 h***
Beclin-1	↑	↑↑	↓↓	−	−	−	↑	−
ATG5	↑↑↑	↑↑	−	↑	↑↑↑	−	↑↑	↑↑↑
ATG12	↑↑↑	↑↑	−	↑↑↑	↑↑↑	−	↑↑↑	↑↑
ATG7	↑↑↑	↓	−	↑↑↑	↑↑↑	−	↑↑↑	↑↑↑
ATG3	↑↑	↑↑	−	↑↑↑	↑↑	−	↑	−
LC3BII	−	↑↑↑	↑	↑↑↑	↑↑↑	−	↑↑↑	↑

Level of induction of ER stress proteins (Beclin, ATG5, ATG12, ATG7, ATG3 and LC3BII) after treatment of differentiated SH-SY5Y cells with 10 µM of LP226A1, DHA, LP205A1, EPA and LP204A1. *Cells were incubated concomitantly with Aβ42 peptide. Meaning of the symbols: − no modulation;.↑ significant up-regulation; ↑↑ very significant up-regulation; ↑↑↑ very very significant up-regulation; ↓↓ very significant down-regulation.

Autophagy, similar to ER stress has both pro-death and pro-survival functions. Accumulating evidence indicates that autophagy may confer neuroprotection by enhancing clearance of soluble and aggregated misfolded proteins. Conversely, a deregulation of autophagy may lead to neurodegeneration (Nedelsky *et al.*, 2008).

Different conditions that induce ER stress lead to an induction of autophagy (Verfaillie *et al.*, 2010). Both the PERK/eIF2α and IRE1 arms of the UPR have been implicated in the regulation of autophagy (Talloczy *et al.*, 2002; Ding *et al.*, 2007b).

In this context, several molecules implicated in the autophagy process have been up-regulated in SH-SY5Y neuron-like cells treated with LP226A1, LP204A1, and LP205A1. Beclin-1, one of the proteins responsible of the vesicle nucleation (the earliest step of autophagy), was up-regulated after a 7 h-treatments with LP226A1, and LP204A1 (Figure. 5.15; Table 5.2). We could not observe a modulation of Beclin-1 after treatment with LP205A1 (10µM) but it was up-regulated at 5µM. Since the remaining autophagy proteins studied were up-regulated by LP205A1 (10µM) we believe that Beclin-1 was up-regulated earlier than after a 7 h-treatment with LP205A1at this dose.

Two ubiquin-like conjugation systems are part of the vesicle elongation process. One pathway involves the covalent conjugation of ATG12 to ATG5 with the help of ATG7 and ATG10. The second pathway involves the conjugation of PE to LC3BI by the sequential action of ATG4, ATG7, and ATG3. Lipid conjugation leads to the conversion of the soluble form (LC3BI) to the autophagic-vesicle-associated form (LC3BII).

As seen in this chapter, ATG5, ATG12, ATG7, and ATG3 proteins (responsible for the vesicle elongation) were already very significantly up-regulated already after 7 h-treatments with LP226A1, LP204A1, and LP205A1 (with or without Aβ42 peptide). The up-regulation of ATG7 and ATG3 permitted the conjugation of PE to LC3BI, leading to the formation of the autophagic-vesicle-associated form (LC3BII). LC3BII, which is used as a marker of autophagy, was very significantly up-regulated after treatments of SH-SY5Y neuron-like cells with LP226A1, LP204A1 and LP205A1.

Autophagy induced by the treatments with the hydroxy derivates could be conferring neuroprotection to SH-SY5Y neuron-like cells by enhancing the elimination of soluble and aggregated misfolded proteins.

In summary, the results in this chapter revealed an additional aspect of LP226A1, LP205A1, and LP204A1 molecular mechanism of action in neuron-like SH-SY5Y cells in the context of Alzheimer´s disease. This action mechanism involves the neuroprotective activation of the protective arm of the unfolded protein response as well as an autophagy induction at therapeutic doses.

6. General Discussion

6.1. 2OHOA and Glioma

Lipid alterations are often associated with the etiology of important human diseases, such as atherosclerosis, infectious diseases, Alzheimer's disease and cancer. In cancer, although different types of tumors do not share identical features, a number of lipid changes have been described.

The plasma membrane contains thousands of different lipids that form various types of membrane microdomains which can be differentially and specifically regulated by drugs targeting the lipid bilayer. Thus, membrane-lipid therapy aims at the specific regulation of certain membrane-lipid structures to treat cancer and other human pathologies (Escribá, 2006). In this context, very low levels of SM were found in human glioma (1321N1, SF767, and U118) cells when compared with normal (MRC-5) cells, a characteristic common to all the cancer cell lines we have studied to date (leukemia, lung cancer) (Barceló-Coblijn *et al.*, 2011). In the glioma cells studied, 2OHOA treatments induced a restoration of SM to levels similar to those observed in non-tumor cells (Barceló-Coblijn *et al.*, 2011).

2OHOA induced a recovery of SM levels, associated with potent effects against glioma. This fact suggests that remodeling of the membrane structure and composition would be upstream to the oncogenic action of Ras in cancer cells. Furthermore, this anticancer effect was, up to now, associated with a bimodal mechanism of action up to now. On the one hand, the presence of 2OHOA in membranes and the increase in DAG would induce PKC translocation to membranes followed by CDKI overexpression and pRb hypophosphorylation (Martínez *et al.*, 2005a; Lladó *et al.*, 2009; Terés *et al.*, 2012). On the other hand, Ras translocation to the cytosol would cause MAPK and Akt inactivation. These two pathways have consistently been seen to be involved in the loss of differentiation, increased proliferation, and survival of cancer cells.

Although some of the mechanisms of action induced by 2OHOA have been elucidated, the way this molecule exerts its anticancer action without killing non-cancer cells is not fully understood, neither how a common pathway through 2OHOA exerts its activity against human glioma cells. To address this point we have studied the unfolded protein response which has pro-death and pro-survival arms (Verfaillie *et al.*, 2010), and autophagy cell death induced by the UPR (Ogata *et al.*, 2006; Kouroku *et al.*, 2007). The two possible arms of the UPR could explain the specificity of 2OHOA against glioma cells. In fact, the results of this study indicate that 2OHOA treatments activate the pro-death arm of the unfolded protein response in the three glioma cell lines we studied (1321N1, SF767 and U118), while activating the pro-survival arm in MRC-5 non-cancer cells. It has been proven that 2OHOA interacts with cellular membranes, and endoplasmatic reticulum membrane is among them. For this reason, 2OHOA probably interacts with the ER membrane activating the unfolded protein response. Moreover, lipid alterations can cause ER stress and induce the unfolded protein response in the cell (Basseri and Austin, 2012). The cellular homeostasis is already altered in cancer cells while it is not affected in non-cancer cells (Moenner *et al.*, 2007). For this reason, we believe that 2OHOA (at therapeutic doses) interacts with the ER membrane causing lipid alterations, which induce ER stress that activates the unfolded protein response (pro death arm) in glioma cells. As glioma cells already have an unbalanced cellular homeostasis (Johnson *et al.*, 2011), they are not able to recover from ERstress induced by 2OHOA treatments. The unfolded protein response finally induces autophagy cell death (and apoptosis in some cases). MRC-5 cells (non-cancerous) activate the unfolded protein response (pro-survival). But as their cellular homeostasis is balanced, they can recover from this stress induced by 2OHOA treatments (at therapeutic doses).

Autophagy, similar to ER stress, has both pro-death and pro-survival functions. Different conditions that induce ER stress lead to the induction of autophagy (Verfaillie *et al.*, 2010). The results of this study demonstrate that 2OHOA induces autophagy cell death in the three glioma cells investigated. The autophagic-vesicle-associated form II (LC3BII), which is used as a marker of autophagy, was very significantly up-regulated after treatment with 2OHOA as well as several ATG proteins. In addition, there was an increase of lysosomes and autophagosomes observed by fluorescence and electron microscopy. Autophagy, on the contrary, was not induced in the non-cancer cells studied.

In the study of (Barceló-Coblijn *et al.*, 2011), we showed that cancer cells have very low membrane sphingomyelin and high phosphatidylethanolamine levels. In glioma and other types of cancer cells but not in normal cells, 2OHOA induced changes in these lipids to reach values found in healthy tissues. The present study sheds light on the signaling events that follow the activation of this molecular switch. Here, we demonstrate the selective induction of several key effectors of ER stress/UPR cell death (P-eIF2α, IRE1α, XBP1s, ATF4 and CHOP) by 2OHOA in three human glioma cells. Moreover, we provide cellular and molecular evidence that 2OHOA induces autophagy in these cells. This may constitute a

novel therapeutic strategy to combat glioma when cells are reluctant to enter apoptosis. As a matter of fact, we have demonstrated that 2OHOA has greater efficacy than temozolomide, the reference drug for the treatment of glioma, in subcutaneous and orthotopic xenograft models of human glioma in nude mice (Terés *et al.*, 2012). In conclusion, the design of new lipid molecules such as 2OHOA that can modulate ER stress/UPR, constitutes a promising and novel approach to treat gliomas and other neoplasias.

6.2. LP226A1, LP204A1, and LP205A1 and Alzheimer´s Disease

In the context of the membrane lipid therapy (see section 1.3.3) new molecules were designed in our group for the treatment of AD. We have developed a series of synthetic carbon alpha hydroxylated derivatives [2-hydroxyarachidonic acid (LP204A1), 2-hydroxyeicosapentaenoic acid (LP205A1) and 2-hydroxydocosahexanoic acid (LP226A1)] from its lipid precursors [arachidonic acid (ARA), eicosapentaenoic acid (EPA), docosahexaenoic acid (DHA)].

We have obtained promising results related to memory improvement in 5XFAD transgenic mice treated with LP226A1 (Fiol M.A., manuscript in preparation). Chronic treatment with LP226A1 recovered memory impairment in the 5XFAD mice model of AD with a concomitant increase of the hippocampal neurogenesis. This suggests that memory recovery can be modulated by the rising of adult neurogenesis to normal levels (Fiol M.A., manuscript in preparation).

Although preliminary results in Alzheimer transgenic mice had revealed a restoration of memory deficits, studies with human neuronal cells had not been done to date, nor a molecular study on the effects of these compounds to reveal their action mechanism.

In this thesis, we have studied the expression of several AD-related proteins on SH-SY5Y human neuroblastoma cells differentiated into neuron-like cells and treated with the three hydroxy derivates, LP226A1 (2OH-DHA), LP204A1 (2OH-ARA), and LP205A1 (2OH-EPA). The proteins studied here are α-, β- and γ-secretases, hyperphosphorilated tau, GSK3β, and P-GSK3β. We have observed down-regulation of β- and γ-secretases, hyperphosphorilated tau and an inhibition of GSK3β after treatment. These results suggest that these hydroxy derivates may slow down AD progression by reducing the accumulation of amyloid β-peptide and NFTs.

In this context, we evaluated the cell viability of differentiated SH-SY5Y cells after treatment. This allowed us to divide the treatment doses with LP226A1 and LP205A1 into two groups: therapeutic doses (5-10 μM) and toxic doses (20-30 μM). Treatments with

LP204A1 could also be divided into two groups but a bit differently: therapeutic doses (5 μM) and toxic doses (10-30 μM).

Furthermore, we showed PS-1 (γ-secretase) (Figure 4.9) and BACE1 (β-secretase) (Figure 4.10) down-regulation upon LP226A1, LP205A1, and LP204A1 treatments of SH-SY5Y human neuron-like cells. Also, BACE1 protein activity was down-regulated in 5XFAD transgenic mice after treatment with LP226A1. On the contrary, ADAM10 expression was not modulated by the drugs in SH-SY5Y human neuron-like cells.

Incubation of SH-SY5Y human neuron-like cells with Aβ42 peptide reduced cell viability. Interestingly, treatments with LP226A1 or LP205A1 (5 and 10 μM), after Aβ42 incubation, rescued differentiated SH-SY5Y cells from cell death (Figure 4.12). A similar result was obtained by (Zhao *et al.*, 2011) with DHA-derived neuroprotectin D1 treatment. Moreover, treatment with LP226A1, LP205A1 and LP204A1 (with or without Aβ42) showed a down-regulation of PS-1 (Figure 4.13) and BACE1 (Figure 4.14). In addition, hyperphosphorilated tau (AT8) expression was up-regulated after incubation with Aβ42 (Figure 4.16) compared to non-treated cells. This is in agreement with previous data that demonstrating that Aβ activated GSK-3β, and induced tau hyperphosphorylation in hipocampal neurons (Takashima, 2012). Our data also demonstrated that LP226A1, LP205A1 and LP204A1 (+ Aβ42) treatments down-regulated hyperphosphorilated tau (AT8) up to similar levels of non-treated cells (Figure 4.16). Therefore, the hydroxy derivates inhibited tau hyperphosphorilation induced by Aβ42. Moreover, we also observed GSK-3β inhibition throughout Serine 9 phosphorilation (P-GSK-3β) after treatments of differentiated SH-SY5Y cells with LP226A1, LP205A1 and LP204A1 (+ Aβ42) (Figure 4.17). Again evidence shows that inhibitors of GSK-3β may be potential therapeutic agents for this disease (Takashima, 2012).

Our main findings indicate that PS-1 (γ-secretase) and BACE1 (β-secretase) protein expression is down-regulated by LP226A1, LP205A1, and LP204A1 treatments in differentiated and non-differentiated SH-SY5Y cells. On the contrary, ADAM10 (α-secretase) protein expression is not modulated by the drugs. Treatments with LP226A1 or LP205A1 (5 and 10 μM), after Aβ42 (5 μM) incubation, rescue differentiated SH-SY5Y cells from cell death. Moreover, Aβ42 incubation induces tau hyperphosphorilation in differentiated SH-SY5Y cells, which is reverted after treatments with LP226A1, LP205A1 and LP204A1. Furthermore, GSK-3β is inhibited throughout Serine 9 phosphorilation (P-GSK-3β), impairing tau hyperphosphorilation after treatments of differentiated SH-SY5Y cells with LP226A1, LP205A1 and LP204A1 (+ Aβ42).

Although the working mechanisms of these hydroxy derivate drugs are not yet fully understood, we show clear indications that they modulate the main molecular players of AD, that is the expression of key secretases, P-tau and P-GSK-3β, and offer a promising potential to treat AD.

Moreover, we have deepened our understanding into the molecular mechanisms involved in neuronal recovery by paying special attention to UPR and autophagy pathways as they could be involved in the removal of NFTs and amyloid β-peptide in senile plaques. AD is characterized by an accumulation of unfolded or misfolded proteins in the brain and several reports indicate the activation of UPR in AD brains (Hoozemans *et al.*, 2005; Unterberger *et al.*, 2006; Hoozemans *et al.*, 2009), suggesting a possible link between AD and UPR.

Our results demonstrate UPR activation in the differentiated SH-SY5Y cells treated with LP226A1, LP205A1, and LP204A1. The hydroxy derivate treatments only induce the prosurvival arms of the UPR (at therapeutic doses). In addition, the treatments of SH-SY5Y cells with the molecules also activated an autophagy response.

LP226A1, LP205A1, and LP204A1 treatments (with or without Aβ42 peptide) significantly up-regulate BiP and PDI molecular chaperone protein expression allowing productive folding to occur more efficiently. BiP may bind to and facilitate the correct folding of nascent APP (Yang *et al.*, 1998), which would alleviate the cell from Aβ42 peptide production. Chaperone activation is necessary to reduce incorrect folding of nascent APP and Aβ42 peptide production in the context of Alzheimer´s disease. Only the protective arm of the unfolded protein response is activated at therapeutic doses of the hydroxy derivates. This means an early activation of P-eIF2α followed by a subsequent inactivation of this protein and an up-regulation of IRE1α. All these are accompanied by an up-regulation of the two chaperones, BiP and PDI. CHOP, which belongs to the cytocidal arm of the unfolded protein response, is not activated at therapeutic doses.

Autophagy, similar to ER stress, has both pro-death and pro-survival functions. Accumulating evidence indicates that autophagy may confer neuroprotection by enhancing clearance of soluble and aggregated misfolded proteins. Conversely, a deregulation of autophagy may lead to neurodegeneration (Nedelsky *et al.*, 2008). Different conditions that induce ER stress lead to an induction of autophagy (Verfaillie *et al.*, 2010).

In this context, several molecules implicated in the autophagy process are up-regulated in SH-SY5Y neuron-like cells treated with LP226A1, LP204A1, and LP205A1. Beclin-1, one of the proteins responsible for the vesicle nucleation (the earliest step of autophagy), is up-regulated after 7 h-treatments with LP226A1, LP205A1, and LP204A1 (Figure. 5.15; Table 5.2). ATG5, ATG12, ATG7, and ATG3 proteins, responsible for the vesicle elongation, are very significantly up-regulated already after 7 h-treatments with LP226A1, LP204A1, and LP205A1 (with or without Aβ42 peptide). The up-regulation of ATG7 and ATG3 permits the conjugation of PE to LC3BI, leading to the formation of the autophagic-vesicle-associated form (LC3BII). LC3BII, which is used as a marker of autophagy, is very significantly up-regulated too after treatments of SH-SY5Y neuron-like cells with LP226A1, LP204A1, and LP205A1. We believe that autophagy induced by

treatments with these hydroxy derivates could confer neuroprotection to SH-SY5Y neuron-like cells by enhancing the elimination of soluble and aggregated misfolded proteins.

For this reason, UPR and autophagy could be an action mechanism by which LP226A1, LP205A1, and LP204A1 exert their activities. We consider that this study may be helpful for future research focused on studying the regulation of the unfolded protein response and autophagy in drug therapy against Alzheimer´s Disease.

7. Concluding Remarks

This chapter concludes the thesis. A summary of the main findings is presented here.

1. 2OHOA showed a common molecular and cellular action mechanism in the three glioma (1321N1, SF767 and U118) cell lines studied in this PhD thesis. It selectively induced several key effectors of ER stress/UPR and autophagy.
    a. 2OHOA reduced cell viability and blocked cell cycle progression in G_2/M phase of several glioma (1321N1, SF767, and U118) cells but not of MRC-5 non-cancer cells.
    b. 2OHOA induced the pro-death arm of the unfolded protein response (CHOP, IRE1α, P-eIF2α-mantained in time-, and ATF4) in several glioma cells (1321N1, SF767, and U118) but not in MRC-5 non-cancer cells;
    c. 2OHOA induced autophagy cell death (ATG7, ATG5, LC3BII, lysosomes and autophagosomes formation) in several glioma (1321N1, SF767, and U118) cells, including those that are reluctant to activate apoptosis (as SF767), but not in MRC-5 non-cancer cells;

2. LP226A1 (2OHDHA) and LP205A1 (2OHEPA), after Aβ42 incubation, rescued differentiated SH-SY5Y cells from cell death.
    a. LP226A1 (2OHDHA), LP205A1 (2OHEPA), and LP204A1 (2OHARA) down-regulated PS-1 (γ-secretase) and BACE1 (β-secretase) in differentiated SH-SY5Y cells;
    b. LP226A1 (2OHDHA), LP205A1 (2OHEPA), and LP204A1 (2OHARA) did not modulate ADAM10 (α-secretase) in differentiated SH-SY5Y cells;
    c. Aβ42 incubation induced tau hyperphosphorilation in SH-SY5Y differentiated cells, and was reverted after treatments with LP226A1 (2OHDHA), LP205A1 (2OHEPA), and LP204A1 (2OHARA);

d. GSK-3β was inhibited throughout Serine 9 phosphorilation (P-GSK-3β), after treatments of differentiated SH-SY5Y cells with LP226A1 (2OHDHA), LP205A1 (2OHEPA), and LP204A1 (2OHARA) (+ Aβ42);

3. LP226A1 (2OHDHA), LP205A1 (2OHEPA), and LP204A1 (2OHARA) induced the pro-survival arm of the unfolded protein response and autophagy in differentiated SH-SY5Y cells.
   a. LP226A1 (2OHDHA), LP205A1 (2OHEPA), and LP204A1 (2OHARA) up-regulated several UPR markers (such as BiP, PDI, P-eIF2α and IRE1α) at therapeutic doses;
   b. LP226A1 (2OHDHA), LP205A1 (2OHEPA), and LP204A1 (2OHARA) up-regulated several autophagy markers (such as Beclin, ATG5, ATG12, ATG3, ATG7 and LC3BII) at therapeutic doses.

4. These regulatory effects were most likely associated to the molecular and cellular mechanism of action of these compounds. Thus,
   a. 2OHOA ⟶ ER stress (UPR) + Autophagy ⟶ Glioma treatment
   b. 2OHDHA ⟶ ER stress (UPR) + Autophagy ⟶ AD treatment
   c. 2OHEPA ⟶ ER stress (UPR) + Autophagy ⟶ AD treatment
   d. 2OHARA ⟶ ER stress (UPR) + Autophagy ⟶ AD treatment

8. Experimental Procedures

8.1 Lipids

Minerval (2-hydroxy-oleic acid) was kindly provided by *Lipopharma Therapeutics* (Palma de Mallorca, Spain). Its purity (99.7%) was confirmed by HPLC and gas chromatography as described previously (Lladó *et al.*, 2009). Palmitic acid and Arachidonic acid - sodium salt were purchased from *Sigma Chemicals Co* (Madrid, Spain). LP226A1 (2-hydroxy docosahexaenoic acid - sodium salt), LP204A1 (2-hydroxy-arachidónic acid - sodium salt) and LP205A1 (2-hydroxy-eicosapentaenoic acid - sodium salt) were synthesized by *Medalchemy*, SL (Alicante Spain). Docosahexaenoic acid (Free Fatty Acid) and Eicosapentaenoic acid (Free Fatty Acid) were purchased from *Equateq* (London, UK).

8.2 Cell Culture

The cell lines used in this work (Table 8.1) were obtained from the European Collection of Cell Cultures (*ECCAC*) through *Sigma Aldrich Co* (St Louis, MO, USA). The human glioma SF767 cell line was acquired from the *Brain Tumor Research Center Tissue Bank* (San Francisco, CA, USA).

Cells were maintained at 37°C in a fully-humidified atmosphere of 5% CO2 in air. Monolayer cultures were maintained in exponential growth using the medium indicated in Table 8.1. They contained 10% fetal bovine serum (*Sigma Aldrich Co*, St Louis, MO, USA), 100 units/ml penicillin, 100 µg/ml streptomycin (*PAA Laboratories GmbH*, Austria), and when necessary 1% of non-essential amino acids (NEAA) and 2mM L-glutamine (*Sigma Aldrich Co*, St Louis, MO, USA). Monitoring and observation of morphological changes were performed using an optical inverted microscope Leica DMIL (100 x or 400 x, *Leica*

Microsystems, Wetzlar, Germany). Pictures of cells were taken using a digital camera Coolpix 4500 (*Nikon Corp.*, Tokyo, Japan) coupled to an inverted microscope.

Table 8.1. Cell lines

Cell line	Origin	Culture medium
MRC-5	Human fetal lung fibroblast-like cells	DMEM*§
1321N1	Human astrocytoma	DMEM
U118	Human glioma	DMEM
SF-767	Human glioma	DMEM
SH-SY5Y	Human neuroblastoma	DMEM / Hams F12*

Medium was supplemented with * Non Essential Amino Acids (NEAA, 1%) and/or § L-glutamine (2 mM).

8.3 SH-SY5Y Neuroblastoma Cell Differentiation

The human neuroblastoma cell line SH-SY5Y was maintained in a mixture 1:1 of Ham's F12 and Dulbeco Modified Eagle Medium (DMEM), and supplemented with 10% FBS, 2 mM of L-glutamine, 100 units/ml penicillin, 100 μg/ml streptomycin and 1% of NEAA. Cell medium was replaced every three days, and the cells were sub-cultured once they reached a 90% confluence.

To induce differentiation into neuronal cells, the cells were plated at a density of 2.5 x 10^4 cells / cm^2 in 6 well dishes previously coated with 0.1 mg /ml of Poly-L-Lysine (*Sigma Aldrich Co*, St Louis, MO, USA). 24 hours later, the medium was replaced by fresh medium containing 10 % FBS and retinoic acid (RA, 10 μM) (*Sigma Aldrich Co*, St Louis, MO, USA). Then the cells were incubated in the dark for 5 days. After this, the medium was replaced again by fresh medium without FBS, and supplemented with 50 ng / ml of human brain-derived neurotrophic factor (hBDNF) (*Alomone Labs*, Jerusalem, Israel). The cells were then incubated for 6 days up to complete differentiation.

There are a number of critical points to achieve optimal differentiation of SH-SY5Y cells. First, some care is necessary in the routine culture of the cells, passaging the cells before they reach confluence as well as avoiding excessive dilution (1:3 or 1:4 at best). Second, SH-SY5Y cells of the lowest possible passage number should be used. If the cells switch to a fibroblastlike phenotype after several passages, they should be discarded, and a new frozen vial should be thawed. Finally, counting the cells (and not relying on eye

estimation) before plating is crucial to attain the optimal density required for neuronal differentiation (as indicated above).

8.4 Treatments

The drugs and molecules for the treatments were prepared as indicated in Table 8.2 depending on the experiment. DMSO was always present at a final concentration below 0.1%.

Table 8.2. Molecules dilutions and times of treatment.

Cell line	Drug	Vehicle	Concentration (µM)	Time
1321N1 / U118 / SF767 / MRC-5	2OHOA	FBS	50-1000	12h, 24h,48h and 72h
1321N1 / U118 / SF767 / MRC-5	Palmitate	DMSO	50-1000	12h, 24h,48h and 72h
SH-SY5Y	LP226A1	DMSO	5,10,20,30 / 10-600*	7h, 24h,48h and 72h
SH-SY5Y	LP204A1	DMSO	5,10,20,30 / 10-600*	7h, 24h,48h and 72h
SH-SY5Y	LP205A1	DMSO	5,10,20,30 / 10-600*	7h, 24h,48h and 72h
SH-SY5Y	DHA	DMSO	5,10,20,30 / 10-600*	7h, 24h,48h and 72h
SH-SY5Y	ARA	DMSO	5,10,20,30 / 10-600*	7h, 24h,48h and 72h
SH-SY5Y	EPA	DMSO	5,10,20,30 / 10-600*	7h, 24h,48h and 72h

* SH-SY5Y cells were treated from 5 to 30 µM when they were differentiated and from 10 to 100 µM when they were no differentiated.

For all experiments, 1321N1, U118, SF-767, and MRC-5 cells were plated at densities of 1 x 10^4 cells/cm^2 and 3 x 10^4 cells/cm^2, respectively, and in 10 cm^2 plates containing 8 ml of culture medium (5% FBS).

For all experiments, SH-SY5Y were plated at densities of 2.5 x 10^4 cells / cm^2 in 6-well plates containing 2 ml of culture medium (10% FBS). After an overnight incubation, the cells were treated as indicated above.

8.5 Aβ-42 Peptide Preparation

Beta-Amyloid (1-42) peptide (purity: >95%) with the following amino acid sequence: H-Asp-Ala-Glu-Phe-Arg-His-Asp-Ser-Gly-Tyr-Glu-Val-His-His-Gln-Lys-Leu-Val-Phe-Phe-Ala-Glu-Asp-Val-Gly-Ser-Asn-Lys-Gly-Ala-Ile-Ile-Gly-Leu-Met-Val-Gly-Gly-Val-Val-Ile-Ala-OH (*Bio Basic Canada Inc*, Markham, Ontario, Canada), was resuspended in 1 % NH4OH, at a concentration of 1 mg/mL. It was then sonicated for 30 seconds. And, finally, it was resuspended in 10 x buffer stock (PBS) and water to bring it to 1x buffer.

8.6 Cell Proliferation MTT Assay

Cell proliferation was determined using the MTT (methylthiazolyl diphenyl tetrazolium bromide) method (Mosmann, 1983). 1321N1, U118, SF767, and MRC-5 cells were plated in 96-well plates at densities of 3 x 10^3 cells/well and 6 x 10^3 cells/well, respectively, and with 150 µl culture medium (5% FBS) per well. After an overnight incubation to allow cell attachment, the cells were treated with 50-1000 µM of 2OHOA or palmitate for 24, 48 or 72 hours.

SH-SY5Y non-differentiated and differentiated cells were plated in 24-well plates and in 6-well plates, respectively, at a density of 2.5 x 10^4 cells / cm^2 with culture medium. After overnight incubation to allow cell attachment, the non differentiated cells were treated with 10-600 µM of LP226A1, LP204A1, LP205A1, DHA, ARA or EPA for 24 h, 48 h or 72 h; and the differentiated cells with 5-30 µM of LP226A1, LP204A1, LP205A1, DHA, ARA or EPA or with 1.2-20 µM of Aβ-42 peptide for 24h.

MTT (0.5 mg/ml in PBS; *Sigma-Aldrich Co*, St Louis, MO, USA) reagent was then added for 2 h. The mitochondrial dehydrogenases of viable cells reduced the tetrazolium salt yielding water insoluble colored formazan crystals. Then, the medium was removed and these formazan crystals were solubilized by adding one volume of DMSO to the cells for 5 min. After gently shaking an absorbance at 590 nm was measured spectrophotometrically using a Micro Plate Reader. The absorbance was also measured at 650 nm as a background measurement and subtracted from the 590 nm value.

8.7 Cell Viability: Trypan Blue Exclussion Method

Cell viability was determined using the Trypan blue staining method (Bowling *et al.*, 1997). 1321N1, U118, SF767, and MRC-5 cells were plated in 6-well plates at densities of 2

x 10^4 cells/cm^2 (1.86 x 10^5 cells/well) for MRC-5 cells; 6 x 10^4 cells/cm^2 (6 x 10^5 cells/well) for 1321N1cells, and 3 x 10^4 cells/cm^2 (3 x 10^5 cells/well) for SF-767 and U118 cells. Cells were cultured with 2 ml culture medium (5% FBS) per well. They were plated at 50 % confluence. After an overnight incubation to allow cell attachment, the cells were treated with 50-1000 μM of 2OHOA or palmitate for 24 h, 48 h or 72 h. After 72 h confluence was reached.

Trypan blue staining was done as previously described (Bowling *et al.*, 1997). Briefly, 10 μl of sample (cell suspension) was mixed with 10 μl of trypan blue (*Invitrogen*, Eugene, Oregon, USA), and pipetted into Countess® chamber slide (*Invitrogen*, Eugene, Oregon, USA) that was inserted in the Countess® Automated Cell Counter (*Invitrogen*, Carlsbad, CA, USA).

8.8 Protein Extraction

Cells were washed twice with PBS and harvested with a rubber policeman in 300 μl of protein extraction buffer (10 mM Tris-HCl [pH 7.4] containing 50 mM NaCl, 2 mM $MgCl_2$, 2 mM EDTA, 1% SDS, 5 mM iodoacetamide, 1 mM PMSF, 1mM cantaridin and 1mM sodium orthovanadate) (*Sigma Aldrich Co*, St Louis, MO, USA). Cell suspensions were twice subjected to ultrasonication for 10 s at 20% amplitude, using a Braun Labsonic U sonicator (*Braun*, Melsungen, Germany). 30 μl aliquots were removed for protein quantification. The remaining suspension (about 270 μl) was mixed with 30 μl of 10X electrophoresis loading buffer (120 mM Tris-HCl [pH 6.8], containing 4% SDS, 50% glycerol, 0.1% bromophenol blue, 10% mercaptoethanol), and boiled for 5 min.

The nuclear and cytoplasmic fractioning was done using the *Nuclear extraction kit* (*Active Motif*, UK), and according to the manufacturer's instructions.

8.9 Protein Quantification

Protein concentration was measured using the bicinchoninic acid assay, and according to the manufacturer's instructions (*Pierce Biotechnologies, Thermo Fisher Scientific*, Rockford, IL, USA). Briefly, this assay was based on the reduction of Cu^{+2} to Cu^{+1} by proteins in an alkaline medium, followed by a colorimetric detection of the cuprous cation using bicinchoninic acid. Absorbance was then measured at 560 nm (Smith *et al.*, 1985).

Alternatively, the *RC DC* protein assay was used (*Bio-Rad*, Barcelona, Spain). It is a colorimetric assay for determining the protein concentration in the presence of both reducing agents and detergents. This assay is based on a modification of the Lowry protocol, which

involves the reduction of the Folin phenol reagent, and where the absorbance is measured at 750 nm (Lowry *et al.*, 1951).

In both cases, the protein concentration was calculated by interpolating absorbance values into a standard curve with known amount of bovine serum albumin (*BSA; Pierce, part of Thermo Fisher Scientific*, Rockford, USA).

8.10 Electrophoresis (SDS/PAGE) and Immunobloting

Proteins (30 µg) were fractionated on 8 to 10 % polyacrylamide gels (SDS-PAGE: 15-well and 1.5 mm thick), and transferred to nitrocellulose membranes (*Whatman, Schleicher and Schuell*, Maldstone, England). The nitrocellulose membranes were then blocked for 1 h at room temperature in Tris-buffered saline (TBS 1X), and containing 5% non-fat dry milk and 0.1% Tween 20 (blocking solution). The membranes were incubated overnight at 4ºC with one of the primary anti-human antibodies indicated in Table 8.3, and diluted in TBS containing 0.5% bovine serum albumin and 0.1% Tween 20. After removing the primary antibody, the membranes were washed three times for 10 min with 1X TBS and 0.1% Tween 20 and incubated for 1 h at room temperature in a fresh blocking solution with a horseradish peroxidase-linked goat anti-mouse IgG antibody (1:2,000; *Amersham Pharmacia*) or a horseradish peroxidase-linked goat anti-rabbit IgG antibody (1:2,000; *Cell Signaling Technology Inc*., Beverly, MA, USA). Immunoreactivity was detected using the Enhanced Chemiluminescence Western Blot Detection system and by exposure to ECL hyperfilm (both, *Amersham Pharmacia Biotech Inc*, Piscataway, NJ, USA). The films were scanned at a resolution of 600 dpi for quantification using the Foto Look 32 software (Agfa Gevaert, Leverkusen, Germany). The proteins were also detected using fluorescent-labeled secondary antibody, and the membrane was incubated for 1 h at room temperature in a fresh blocking solution with IRDye 800CW donkey anti-mouse IgG antibody or IRDye 800CW donkey anti-rabbit IgG antibody (1:5,000; *LI-COR, Inc*., Lincoln, NE, USA), and protected from light. After washing with TBS containing 0.1% Tween 20, immunoreactivity was detected using a near-infrared fluorescence spectroscopy (*Odyssey Infrared Imaging System, LI-COR, Inc*., Lincoln, NE, USA). The images were analyzed with TotalLab v2005 (*Nonlinear Dynamics*, All Saints, UK) to obtain the integrated optical density (IOD) of each band. The α-tubulin content of each sample was determined by the same procedure, and the concentration of a given protein was normalized to the α-tubulin content of the same sample.

Table 8.3. Primary antibodies for western blot.

Antibody	Isotype	Manufacturer	Dilution
IRE1α	Rabbit IgG	Cell Signaling	1:1000
CHOP	Mouse IgG2a	Cell Signaling	1:1000
P-eIF2α	Rabbit IgG	Cell Signaling	1:1000
BiP	Rabbit IgG	Cell Signaling	1:1000
Calnexin	Rabbit IgG	Cell Signaling	1:1000
PDI	Rabbit IgG	Cell Signaling	1:1000
Beclin-1	Rabbit IgG	Cell Signaling	1:1000
LC3B	Rabbit IgG	Cell Signaling	1:1000
ATG12	Rabbit IgG	Cell Signaling	1:1000
ATG5	Rabbit IgG	Cell Signaling	1:1000
ATG7	Rabbit IgG	Cell Signaling	1:1000
ATG3	Rabbit IgG	Cell Signaling	1:1000
Presenilin 1	Rabbit IgG	Cell Signaling	1:1000
BACE1	Mouse IgG1	Santa Cruz	1:200
ADAM10	Rabbit IgG	Abcam	1:1000
GSK3	Mouse IgG1	Millipore	1:1000
P-GSk3β (Ser9)	Rabbit IgG	Cell Signaling	1:1000
PHF-Tau (AT8)	Mouse IgG1k	Thermo Scientific	1:1000
Nestin	Mouse IgG1	Abcam	1:1000
Cyclin D3	Mouse IgG1	BD Biosciences	1:1000
Cyclin B	Mouse IgG1	BD Biosciences	1:1000
Cdk1/Cdc2	Rabbit IgG	Cell Signaling	1:1000
Cdk4	Mouse IgG1	Cell Signaling	1:1000
Cdk6	Mouse IgG1	Cell Signaling	1:1000
DHFR	Mouse IgG	Abcam	1:250
Caspase 8	Mouse IgG1	Cell Signaling	1:1000
PARP	Rabbit IgG	Santa Cruz	1:2000
α-tubulin	Mouse IgG1	Sigma	1:10000

8.11 Cell DNA Content

In order to determine cell growth and the cycle phase of the cells, the cellular DNA content was determined by staining cells with propidium iodide (*Sigma-Aldrich Co*, St Louis, MO, USA), followed by single-cell fluorescence flow cytometry. 1321N1 and MRC-5 cells

were seeded in 6-well plates containing 2 ml of culture medium per well at densities of 1 x 10^4 cells/cm^2 and 3 x 10^4 cells/cm^2, respectively. They were incubated for 72 h in the presence or absence of 2OHOA or palmitate (150 μM). SH-SY5Y differentiated and non differentiated cells were plated at a density of 2.5 x 10^4 cells / cm^2 in 6-well plates containing 2 ml of culture medium, and were incubated for 24 h. The cells were then washed twice with phosphate-buffered saline (PBS; 137 mM NaCl, 2.7 mM potassium chloride, 12 mM dibasic sodium phosphate, 1.38 mM monobasic potassium phosphate [pH 7.4]), harvested with trypsin-EDTA in FACS tubes of 5ml and centrifuged 5 min at 200 G. The cellular pellet was washed again with PBS, and centrifuged for 5 min at 200 x G. The cells were fixed in 1 ml cold 70% ethanol (added dropwise) and vortexed. They were subsequently incubated at 4ºC for 1 h, centrifuged for 5 min at 1260 x G, and washed with 1ml of sodium citrate 38 mM pH 7.4 by gently shaking. Then, the cells were centrifuged again for 5 min at 1260 x G. The supernatant was removed, and the pellet was resuspended in a buffer containing sodium citrate 38 mM pH 7.4, propidium iodide (50μg/ml) and RNase A (5μg/ml) (*Sigma-Aldrich Co*, St Louis, MO, USA) and incubated 20 min at 37ºC. Single-cell propidium iodide fluorescence (25,000 events) was measured on a Coulter Epics XL flow cytometer using EXPO 32 flow cytometry software (*Beckman Coulter, Inc.* Washington DC, USA) with the gates set to differentiate between G_0/G_1, S and G_2/M phases. The data was then analyzed using WinMDI 2.9 (*Verity Software House*, Topsham, ME, USA).

8.12 Quantitative Reverse Transcription-Polymerase Chain Reaction (qRT-PCR).

1321N1 and MRC-5 cells were seeded in 6-well plates containing 2 ml of culture medium per well at densities of 1 x 10^4 cells/cm^2 and 3 x 10^4 cells/cm^2, respectively. After incubating overnight, the cells were treated with 2OHOA or palmitate (150 μM) for 24 or 48 h and the regulatory effects of 2OHOA on Chop, Ire1α, Atf4, Atf6 and sXbp1 mRNA expression was assessed by Real-time quantitative PCR (RT-qPCR). SH-SY5Y cells were plated at a density of 2.5 x 10^4 cells / cm^2 in 6-well plates containing 2 ml of culture medium. After differentiation, they were incubated for 24 h with 10 and 20 μM of LP226A1, LP204A1, LP205A1, DHA, ARA or EPA, with or without 5 μM of Aβ-42 peptide. The regulatory effects of these drugs on Psen1, Bace1, Adam10, Chop, Ire1α, Atf4, Atf6, and sXbp1 mRNA expression were assessed by Real-time quantitative PCR (RT-qPCR).

Total RNA was extracted from the cells using the RNeasy Mini kit in combination with the RNase-free DNase kit (*Qiagen*, Hilden, Germany) and according to the manufacturer's instructions. Total amount and purity of RNA was determined using Nanodrop 1000 spectrophotometer (*Thermofisher Scientific*, Walthman, MA, USA), by

optical density at 260 and 280 nm. Product quality was assessed by electrophoresis on 1% agarose gel and ethidium bromide staining.

Reverse transcription of RNA was carried out in a thermal cycler Eppendorf Master Cycler Gradient, using the Transcriptor First Strand cDNA Synthesis Kit (*Roche Diagnostics* Indianapolis, IN, USA) and according to the manufacturer's instructions. Briefly, 1 µg of RNA was mixed with oligonucleotides (random hexamers and Poly-A hexamer, 1 µl from stock 500 µg/ml) and incubated at 65°C for 10 min. Then, it was immediately transferred to ice. In addition, a reaction mix was added containing first-strand buffer (4 µl from 5x stock), dNTP mix (2.5 µl, 10 nM), protector RNase inhibitor (0.5 µl, 40 units/µl), and the transcriptor reverse transcriptase (0.5 µl, 20 units/µl). The reaction tubes were subsequently incubated at 25°C for 10 min, followed by 55°C for 30 min, and finally 85°C for 5 min. The cDNA samples obtained were stored at -20°C before use. For PCR amplification, the primers were designed with a Primer 3 (v 0.4.0) Program (http://frodo.wi.mit.edu) based on the gene sequences obtained from *Ensembl* (http://www.ensembl.org). To differentiate between cDNA and genomic DNA, primers were designed at distinct sites of the exon-exon boundaries (Table 8.4). Finally, a nucleotide Blast (http://blast.ncbi.nlm.nih.gov/Blast.cgi) was performed to discard unspecific boundaries.

Quantitative real-time PCR amplifications were carried out in 96-well plates in a StepOne Plus thermal cycler (*Applied Biosystems*, Foster City, CA, USA) using the SYBR Premix Ex Taq 2× (*Perfect Real Time*, *Takara*, Shiga, Japón). The reaction also contained an internal probe ROX 1 and 0.1 µM of each primer. An initial denaturation step at 95°C for 30 s preceded thermal cycling. DNA amplification and fluorescence quantification were determined over 35 cycles with a denaturation step at 95°C for 5 s, followed by an annealing/extension step at 60°C for 34 s. Fluorescence detection and quantification were carried out after each DNA extension step. The data were analyzed using the StepOne software (v2.0). As it is not modulated by the treatment in 1321N1 cells, the expression of β-actin was determined endogenous control. Gapdh was used as endogenous control for the MRC-5 cell line as its expression is also not modulated by the treatment.

The ratio between the expression of the genes of interest and that of β-actin (for 1321N1) or Gapdh (for MRC-5), whose expression is not modulated by the treatment, was determined by means of the equation described by (Pfaffl, 2001):

$$ddCt = E_x(Ctc\text{-}Ctx)/\ E_{end}\ (Ctc\text{-}Ctx)$$

Where E_x is the efficiency of the gene of interest and E_{end} is the efficiency of the endogenous gene. This value was used to calculate the relative expression in treated cells with respect to untreated cells (control = 1). The efficiency of the reaction was estimated via an increase in absolute fluorescence according to (Pfaffl *et al.*, 2002).

$$\text{Efficiency (E)} = 10^{(-1/m)}$$

(m) = slope of the graph formed by Ct values of mRNA vs the logarithm (log) of its concentration (ng/µl).

Results were expressed as ddCt values that were used to calculate the relative expression in treated cells with respect to untreated (control) cells. The PCR products were further characterized by melting curve analysis and agarose gel electrophoresis.

Table 8.4. Primers used in this study.

Gene	Orientation	Sequence (5'-3')
Xbp1(spliced)	Forward	CCG CAG CAG GTG CAG G
	Reverse	GAG TCA ATA CCG CCA GAA
Chop	Forward	GCC AAA ATC AGA GCT GGA
	Reverse	ACA GTG TCC CGA AGG AGA
Ire1α	Forward	TGT ACC ATT GAG GGA GAG
	Reverse	GAG ACC CTG CGC TAT CTG
Atf4	Forward	TTC CTG AGC AGC GAG GTG
	Reverse	TCC AAT CTG TCC CGG AGA
Atf6	Forward	TGA CAA AGC CCT GAT GGT
	Reverse	TGT TCC AGA GCA CCC TGA
β-actin	Forward	GCG GGA AAT CGT GCG TGA
	Reverse	CTA CCT CAA CTT CCA TCA
Gapdh	Forward	CAA TGA CCC CTT CAT TGA
	Reverse	TTG ATT TTG GAG GGA TCT

8.13 Fluorescence labeling of Lysosomes with Lysosensor

1321N1 and MRC-5 cells were seeded in 4-well (1.7 cm^2) Chambered Coverglass (*Lab-Tek™ II, Thermo Fisher Scientific Inc.,* Roskilde, Dinamarca) containing 750 µl of culture medium (5% FBS) per well at densities of 1 x 10^4 cells/cm^2 and 3 x 10^4 cells/cm^2, respectively. After incubating overnight to allow cell attachment, cells were treated with 2OHOA or palmitate (150 µM) for 48 h. SH-SY5Y cells were plated at a density of 2.5 x 10^4 cells/cm^2 in 2-well (4.2 cm^2) in a Chambered Coverglass (*Lab-Tek™ II, Thermo Fisher Scientific Inc.*, Roskilde, Dinamarca) containing 2 ml of culture medium. After differentiation, they were incubated for 24 h with 5 or 10 µM of LP226A1, LP204A1, LP205A1, DHA, ARA or EPA, with or without 5 µM of Aβ-42 peptide. After treatment, the cells were incubated for 1 h with *LysoSensor Green* DND-189 pH Indicator (2 µM, pH 4.5 - 6: *Invitrogen* molecular probes™, Paisley, UK). During the last 5 minutes of this incubation, Hoechst (trihydrochloride trihydrate) stain (40 µg/ml, *Invitrogen* Molecular probes™, Paisley, UK) was added to each well. The cells were examined on a *Nikon Eclipse* TE2000-S

Fluorescence microscope (40X) and the photomicrographs of the acidic vesicles were analyzed using Image J 1.38x software (*Wayne Rasthatband, National Institutes of Health*; rsb.info.nih.gov). The *LysoSensor*™ dyes were acidotroic probes that seemed to accumulate in acidic organelles, such as lysosomes, as a result of protonation.

8.14 Electron Microscopy

1321N1 and MRC-5 cells were seeded at densities of 1 x 10^4 cells / cm^2 and 3 x 10^4 cells / cm^2 respectively in a *Lab-Tek* chamber slide™ of 4 wells (*Nalge Nunc International*, Naperville, IL, USA), and in the presence or absence of the corresponding treatment as indicated above. After washing twice with 0.1 M phosphate buffer (PB; NaH_2PO_4 20 mM, Na_2HPO_4 80 mM, pH 7.4) for 5 min, cells were fixed in 3.5% glutaraldehyde for 1 h at 37°C. After washing four times with 0.1 M PB for 10 minutes, cells were postfixed in 2% OsO_4 for 1 h at room temperature, and protected from light. Then, cells were washed three times with distilled H_2O for 5 min, and, sequentially washed with ethanol 30°, then ethanol 50°, and ethanol 70°, each time for 5 min. Afterwards, cells were stained in 2% uranyl acetate (in ethanol 70°) in the dark for 2 h at 4°C, and again sequentially dehydrated in ethanol 70° (2 × 5 min), ethanol 96° (2 × 5 min), ethanol 100° (2 × 7 min and 1 × 10 min). Finally, cells were infiltrated overnight in Araldite (in ethanol 100°; *Durcupan, Fluka, Buchs SG*, Switzerland). Following polymerization at 70°C during 3 days, embedded cultures were detached from the chamber slide and glued to Araldite blocks. Serial semi-thin (1.5 μm) sections were cut with an Ultracut UC-6 (*Leica*, Heidelberg, Germany), mounted onto slides, and stained with 1% toluidine blue. Selected semi-thin sections were glued (Super Glue, *Loctite*) to araldite blocks and detached from the glass slide by repeated freezing (in liquid nitrogen) and thawing. Ultrathin (0.06 – 0.09 μm) sections were prepared with the Ultracut and stained with lead citrate. Finally, photomicrographs were obtained under a transmission electron microscope (*FEI Tecnai G2 Spirit Biotwin*) using a digital camera (*Morada, Soft Imaging System, Olympus*, Japan).

8.15 Lipid Extraction

Cellular lipids were extracted directly from the frozen monolayer of cells using a modified *n*-hexane/2-propanol (3:2, by volume) extraction method (Hara and Radin, 1978). After washing cells with phosphate-buffered saline (PBS; 137 mM NaCl, 2.7 mM KCl, 12 mM Na_2HPO_4, 1.38 mM KH_2PO_4, pH 7.4), lipids were extracted by the addition of 2.2 ml of 2-propanol. The frozen cells were removed from the plate by scraping with a Teflon cell scraper. 2-propanol was added to 6 ml of hexane. The cell dish was rinsed with 2.2 ml of 2-

propanol, which was then combined with the hexane containing the first wash (Murphy *et al.*, 1997; Murphy *et al.*, 2000). In order to pellet the denatured protein and other cellular debris, cell extracts were centrifuged at 1,000 *g* for 5 min at room temperature. The lipid-containing organic phase was decanted and stored under a N_2 (g) atmosphere at -80ºC until analysis. The residual protein pellet was dried under a N_2 (g) atmosphere, and stored at -20ºC for protein analysis.

8.16 Thin Layer Chromatography

Individual phospholipids classes and neutral lipids were separated by thin layer chromatography (TLC) or HPTLC. Advancement in TLC is called high-performance TLC (HPTLC) (Sherma, 2000). HPTLC utilizes gel grades that are finer, allowing plates to be thinner and smaller. This provides faster separation times with better separation efficiency. HPTLC has an improved resolution and lowered detection limits (Peterson and Cummings, 2006). Whatman silica gel-60 plates (20 × 20 cm, 250 Am, *GE Healthcare*, England) or (10 × 10 cm, *Merck*, Darmstadt, Germany) were heat-activated at 110°C for 1 h, and samples were streaked onto the plates. On the 10 × 10 Silica gel 60 HPTLC plates, lipids were spotted using a Camag Linomat III auto-TLC spotter (*Camag Scientific Inc*., Wilmington, NC, USA). Phospholipids were separated using chloroform/methanol/acetic acid/water (55:37.5:3:2 by vol); (Jolly *et al.*, 1997), which separates all major glycerophospholipids. Neutral lipids were separated in petroleum ether/diethyl ether/acetic acid (75:25:1.3 by vol); (Marcheselli *et al.*, 1988). Lipids were identified using commercially available standards (*Larodan*, Sweden). In some cases, plates were air-dried after development, sprayed with 8% (w/v) H_3PO_4 containing 10% (w/v) $CuSO_4$, and charred at 180°C for 10 min (Gellermann *et al.*, 2005). Then, lipids were quantified by photodensitometry.

8.17 Nuclei Extraction

Nuclei of control and treated cells or tissues were isolated using the Nuclear Extract Kit (*Active Motive*, Belgium) following the manufacturer's instructions.

8.18 β-Secretase Activity Assay

Control and treated cells were collected and processed using the Protocol for Beta Secretase Activity Assay Kit (Fluorometric) (*Abcam*, UK). After incubation with the β-secretase substrate, samples were read in a fluorescence plate reader.

8.19 Statistics

Statistical analysis was done using GraphPad Prism 4.01 (*GraphPad Software Inc*., San Diego, CA, USA). Unless indicated, data were expressed as mean ± SEM, from at least three independent experiments (*n*). The statistical significance of the mean difference was determined by Student's *t* test. The asterisks indicate a significant effect of the treatment as compared with the control: $*P < 0.05$; $**P < 0.01$; $***P < 0.001$.

9. Publications

Publications related to the thesis

- **Marcilla-Etxenike, A**., Maria Martín, M. L., Noguera-Salvà., Garcia-Verdugo, J. M., Soriano-Navarro, M., Dey, I., Escribá, P. V. and Busquets, X. (2012) 2-Hydroxyoleic Acid Induces ER Stress and Autophagy in Various Human Glioma Cell Lines. *Plos One.* Submitted.

- Terés, S., Lladó, V., Higuera, M., Barceló-Coblijn, G., Martín, M. L., Noguera-Salvà, M. A., **Marcilla-Etxenike, A**., Garcia-Verdugo, J. M., Soriano-Navarro, M., Saus, C., Gomez-Pinedo, U., Busquets, X. and Escribá, P. V. (2012) Normalization of sphingomyelin levels by 2-hydroxyoleic acid induces autophagic cell death of SF767 cancer cells. *Autophagy 8*, 19569-19574.

- Terés, S., Lladó, V., Higuera, M., Barceló-Coblijn, G., Martín, M. L., Noguera-Salvà, M. A., **Marcilla-Etxenike, A**., Garcia-Verdugo, J. M., Soriano-Navarro, M., Saus, C., Gomez-Pinedo, U., Busquets, X. and Escribá, P. V. (2012) 2-Hydroxyoleate, a nontoxic membrane binding anticancer drug, induces glioma cell differentiation and autophagy. *Proc Natl Acad Sci U S A 109*, 8489-94.

- Barceló-Coblijn, G., Martín, M. L., de Almeida, R. F., Noguera-Salvà, M. A., **Marcilla-Etxenike, A**., Guardiola-Serrano, F., Luth, A., Kleuser, B., Halver, J. E. and Escribá, P. V. (2011) Sphingomyelin and sphingomyelin synthase (SMS) in the malignant transformation of glioma cells and in 2-hydroxyoleic acid therapy. *Proc Natl Acad Sci U S A 108*, 19569-74.

Patents

- Escribá PV, Busquets X, Terés S, Barceló-Coblijn G, Barceló J, Lladó V, **Marcilla-Etxenike A**, Martin ML, Higuera M, Álvarez R, López DH. Use of 2-hydroxy-poliunsaturated fatty acids as drugs. P200900725. 09/03/2009.

Conference Presentations

- 2011. The 3rd European Molecular Biology Organization (EMBO). Meeting held in Vienna, Austria. Poster presentation: *Selective induction of autophagy throughout ER stress in glioma cells treated with 2-Hydroxyoleic acid.*

- 2011. Gordon Research Conference: Stress Proteins in Growth, Development & Disease, held in Lucca (Barga), Italy. Poster presentation: *Selective induction of Unfolded Protein Response and autophagy in 1321N1 astrocytoma cells treated with 2-Hydroxyoleic acid.*

- 2010. 51st International Conference on the Bioscience of Lipids (ICBL), held in Bilbao, Pais Vasco, Spain. Poster Presentation: *Minerval induces ER stress, G2/M phase arrest and autophagy in astrocitoma 1321N1 cells but not in MRC-5 fibroblast cells.*

- 2010. 35th Federation of European Biochemical Societies (FEBS) Congress on molecules of life, held in Göteborg, Sweden. Poster presentation: *Minerval induces ER stress and apoptosis in astrocitoma 1321N1 cells but not in MRC-5 fibroblast cells.*

10. References

Aguzzi, A. and O'Connor, T. (2010) Protein aggregation diseases: pathogenicity and therapeutic perspectives. *Nat Rev Drug Discov 9*, 237-48.

Alzheimer, A. (1907) About a peculiar disease of the cerebral cortex (in german). *Centralblatt für Nervenhellkunde Psychiatrie 30*, 177-179.

Allinson, T. M., Parkin, E. T., Turner, A. J. and Hooper, N. M. (2003) ADAMs family members as amyloid precursor protein alpha-secretases. *J Neurosci Res 74*, 342-52.

Asai, M., Hattori, C., Szabo, B., Sasagawa, N., Maruyama, K., Tanuma, S. and Ishiura, S. (2003) Putative function of ADAM9, ADAM10, and ADAM17 as APP alpha-secretase. *Biochem Biophys Res Commun 301*, 231-5.

Axe, E. L., Walker, S. A., Manifava, M., Chandra, P., Roderick, H. L., Habermann, A., Griffiths, G. and Ktistakis, N. T. (2008) Autophagosome formation from membrane compartments enriched in phosphatidylinositol 3-phosphate and dynamically connected to the endoplasmic reticulum. *J Cell Biol 182*, 685-701.

Baba, M., Nakajo, S., Tu, P. H., Tomita, T., Nakaya, K., Lee, V. M., Trojanowski, J. Q. and Iwatsubo, T. (1998) Aggregation of alpha-synuclein in Lewy bodies of sporadic Parkinson's disease and dementia with Lewy bodies. *Am J Pathol 152*, 879-84.

Baehrecke, E. H. (2005) Autophagy: dual roles in life and death? *Nat Rev Mol Cell Biol 6*, 505-10.

Bailey, J. A., Maloney, B., Ge, Y. W. and Lahiri, D. K. (2011) Functional activity of the novel Alzheimer's amyloid beta-peptide interacting domain (AbetaID) in the APP and BACE1 promoter sequences and implications in activating apoptotic genes and in amyloidogenesis. *Gene 488*, 13-22.

Barceló-Coblijn, G., Martín, M. L., de Almeida, R. F., Noguera-Salvà, M. A., Marcilla-Etxenike, A., Guardiola-Serrano, F., Luth, A., Kleuser, B., Halver, J. E. and Escribá, P. V. (2011) Sphingomyelin and sphingomyelin synthase (SMS) in the malignant transformation of glioma cells and in 2-hydroxyoleic acid therapy. *Proc Natl Acad Sci U S A 108*, 19569-74.

Barceló, F., Prades, J., Funari, S. S., Frau, J., Alemany, R. and Escribá, P. V. (2004) The hypotensive drug 2-hydroxyoleic acid modifies the structural properties of model membranes. *Mol Membr Biol 21*, 261-8.

Barten, D. M. and Albright, C. F. (2008) Therapeutic strategies for Alzheimer's disease. *Mol Neurobiol 37*, 171-86.

Basseri, S. and Austin, R. C. (2012) Endoplasmic reticulum stress and lipid metabolism: mechanisms and therapeutic potential. *Biochem Res Int 2012*, 841362.

Baumann, O. and Walz, B. (2001) Endoplasmic reticulum of animal cells and its organization into structural and functional domains. *Int Rev Cytol 205*, 149-214.

Bazan, N. G. and Scott, B. L. (1990) Dietary omega-3 fatty acids and accumulation of docosahexaenoic acid in rod photoreceptor cells of the retina and at synapses. *Ups J Med Sci Suppl 48*, 97-107.

Berchtold, N. C. and Cotman, C. W. (1998) Evolution in the conceptualization of dementia and Alzheimer's disease: Greco-Roman period to the 1960s. *Neurobiol Aging 19*, 173-89.

Bergmans, B. A. and De Strooper, B. (2010) gamma-secretases: from cell biology to therapeutic strategies. *Lancet Neurol 9*, 215-26.

Bernales, S., Papa, F. R. and Walter, P. (2006) Intracellular signaling by the unfolded protein response. *Annu Rev Cell Dev Biol 22*, 487-508.

Bertolotti, A., Zhang, Y., Hendershot, L. M., Harding, H. P. and Ron, D. (2000) Dynamic interaction of BiP and ER stress transducers in the unfolded-protein response. *Nat Cell Biol 2*, 326-32.

Bertram, J. S. (2000) The molecular biology of cancer. *Mol Aspects Med 21*, 167-223.

Bertram, L., Lill, C. M. and Tanzi, R. E. (2010) The genetics of Alzheimer disease: back to the future. *Neuron 68*, 270-81.

Biedler, J. L., Roffler-Tarlov, S., Schachner, M. and Freedman, L. S. (1978) Multiple neurotransmitter synthesis by human neuroblastoma cell lines and clones. *Cancer Res 38*, 3751-7.

Bilmen, J. G., Khan, S. Z., Javed, M. H. and Michelangeli, F. (2001) Inhibition of the SERCA Ca2+ pumps by curcumin. Curcumin putatively stabilizes the interaction between the nucleotide-binding and phosphorylation domains in the absence of ATP. *Eur J Biochem 268*, 6318-27.

Bishop, J. M. (1996) The discovery of proto-oncogenes. *FASEB J 10*, 362-4.

Black, R. A., Rauch, C. T., Kozlosky, C. J., Peschon, J. J., Slack, J. L., Wolfson, M. F., Castner, B. J., Stocking, K. L., Reddy, P., Srinivasan, S., Nelson, N., Boiani, N., Schooley, K. A., Gerhart, M., Davis, R., Fitzner, J. N., Johnson, R. S., Paxton, R. J., March, C. J. and Cerretti, D. P. (1997) A metalloproteinase disintegrin that releases tumour-necrosis factor-alpha from cells. *Nature 385*, 729-33.

Blennow, K., de Leon, M. J. and Zetterberg, H. (2006) Alzheimer's disease. *Lancet 368*, 387-403.

Blurton-Jones, M. and Laferla, F. M. (2006) Pathways by which Abeta facilitates tau pathology. *Curr Alzheimer Res 3*, 437-48.

Boland, B., Kumar, A., Lee, S., Platt, F. M., Wegiel, J., Yu, W. H. and Nixon, R. A. (2008) Autophagy induction and autophagosome clearance in neurons: relationship to autophagic pathology in Alzheimer's disease. *J Neurosci 28*, 6926-37.

Boot-Handford, R. P. and Briggs, M. D. (2010) The unfolded protein response and its relevance to connective tissue diseases. *Cell Tissue Res 339*, 197-211.

Bowling, S. A., Clarke, J. D., Liu, Y., Klessig, D. F. and Dong, X. (1997) The cpr5 mutant of Arabidopsis expresses both NPR1-dependent and NPR1-independent resistance. *Plant Cell 9*, 1573-84.

Boyce, M., Bryant, K. F., Jousse, C., Long, K., Harding, H. P., Scheuner, D., Kaufman, R. J., Ma, D., Coen, D. M., Ron, D. and Yuan, J. (2005) A selective inhibitor of eIF2alpha dephosphorylation protects cells from ER stress. *Science 307*, 935-9.

Braakman, I. and Bulleid, N. J. (2011) Protein folding and modification in the mammalian endoplasmic reticulum. *Annu Rev Biochem 80*, 71-99.

Brandt, R., Leger, J. and Lee, G. (1995) Interaction of tau with the neural plasma membrane mediated by tau's amino-terminal projection domain. *J Cell Biol 131*, 1327-40.

Brookmeyer, R., Johnson, E., Ziegler-Graham, K. and Arrighi, H. M. (2007) Forecasting the global burden of Alzheimer's disease. *Alzheimers Dement 3*, 186-91.

Cai, H., Wang, Y., McCarthy, D., Wen, H., Borchelt, D. R., Price, D. L. and Wong, P. C. (2001) BACE1 is the major beta-secretase for generation of Abeta peptides by neurons. *Nat Neurosci 4*, 233-4.

Calfon, M., Zeng, H., Urano, F., Till, J. H., Hubbard, S. R., Harding, H. P., Clark, S. G. and Ron, D. (2002) IRE1 couples endoplasmic reticulum load to secretory capacity by processing the XBP-1 mRNA. *Nature 415*, 92-6.

Casas-Tinto, S., Zhang, Y., Sanchez-Garcia, J., Gomez-Velazquez, M., Rincon-Limas, D. E. and Fernandez-Funez, P. (2011) The ER stress factor XBP1s prevents amyloid-beta neurotoxicity. *Hum Mol Genet 20*, 2144-60.

Cisse, M., Braun, U., Leitges, M., Fisher, A., Pages, G., Checler, F. and Vincent, B. (2011) ERK1-independent alpha-secretase cut of beta-amyloid precursor protein via M1 muscarinic receptors and PKCalpha/epsilon. *Mol Cell Neurosci 47*, 223-32.

Claeysen, S., Cochet, M., Donneger, R., Dumuis, A., Bockaert, J. and Giannoni, P. (2012) Alzheimer culprits: Cellular crossroads and interplay. *Cell Signal*.

Connor, J. H., Weiser, D. C., Li, S., Hallenbeck, J. M. and Shenolikar, S. (2001) Growth arrest and DNA damage-inducible protein GADD34 assembles a novel signaling complex containing protein phosphatase 1 and inhibitor 1. *Mol Cell Biol 21*, 6841-50.

Cordomi, A., Prades, J., Frau, J., Vogler, O., Funari, S. S., Perez, J. J., Escriba, P. V. and Barcelo, F. (2010) Interactions of fatty acids with phosphatidylethanolamine membranes: X-ray diffraction and molecular dynamics studies. *J Lipid Res 51*, 1113-24.

Corner, J. and Bailey, C. (2001) *Cancer nursing : care in context*, Blackwell Science, Osney Mead, Oxford ; Malden, MA.

Cribb, A. E., Peyrou, M., Muruganandan, S. and Schneider, L. (2005) The endoplasmic reticulum in xenobiotic toxicity. *Drug Metab Rev 37*, 405-42.

Chan, E. Y., Kir, S. and Tooze, S. A. (2007) siRNA screening of the kinome identifies ULK1 as a multidomain modulator of autophagy. *J Biol Chem 282*, 25464-74.

Chen, S., Rehman, S. K., Zhang, W., Wen, A., Yao, L. and Zhang, J. (2010) Autophagy is a therapeutic target in anticancer drug resistance. *Biochim Biophys Acta 1806*, 220-9.

Dalby, K. N., Tekedereli, I., Lopez-Berestein, G. and Ozpolat, B. (2010) Targeting the prodeath and prosurvival functions of autophagy as novel therapeutic strategies in cancer. *Autophagy 6*, 322-9.

Das, A., Banik, N. L. and Ray, S. K. (2010) Flavonoids activated caspases for apoptosis in human glioblastoma T98G and U87MG cells but not in human normal astrocytes. *Cancer 116*, 164-76.

Davies, M. P., Barraclough, D. L., Stewart, C., Joyce, K. A., Eccles, R. M., Barraclough, R., Rudland, P. S. and Sibson, D. R. (2008) Expression and splicing of the unfolded protein response gene XBP-1 are significantly associated with clinical outcome of endocrine-treated breast cancer. *Int J Cancer 123*, 85-8.

De Strooper, B., Saftig, P., Craessaerts, K., Vanderstichele, H., Guhde, G., Annaert, W., Von Figura, K. and Van Leuven, F. (1998) Deficiency of presenilin-1 inhibits the normal cleavage of amyloid precursor protein. *Nature 391*, 387-90.

De Strooper, B., Annaert, W., Cupers, P., Saftig, P., Craessaerts, K., Mumm, J. S., Schroeter, E. H., Schrijvers, V., Wolfe, M. S., Ray, W. J., Goate, A. and Kopan, R. (1999) A presenilin-1-dependent gamma-secretase-like protease mediates release of Notch intracellular domain. *Nature 398*, 518-22.

De Strooper, B. and Konig, G. (1999) Alzheimer's disease. A firm base for drug development. *Nature 402*, 471-2.

Debnath, J., Baehrecke, E. H. and Kroemer, G. (2005) Does autophagy contribute to cell death? *Autophagy 1*, 66-74.

Ding, W. X., Ni, H. M., Gao, W., Hou, Y. F., Melan, M. A., Chen, X., Stolz, D. B., Shao, Z. M. and Yin, X. M. (2007a) Differential effects of endoplasmic reticulum stress-induced autophagy on cell survival. *J Biol Chem 282*, 4702-10.

Ding, W. X., Ni, H. M., Gao, W., Yoshimori, T., Stolz, D. B., Ron, D. and Yin, X. M. (2007b) Linking of autophagy to ubiquitin-proteasome system is important for the regulation of endoplasmic reticulum stress and cell viability. *Am J Pathol 171*, 513-24.

Donmez, G., Wang, D., Cohen, D. E. and Guarente, L. (2010) SIRT1 suppresses beta-amyloid production by activating the alpha-secretase gene ADAM10. *Cell 142*, 320-32.

Doyle, K. M., Kennedy, D., Gorman, A. M., Gupta, S., Healy, S. J. and Samali, A. (2011) Unfolded proteins and endoplasmic reticulum stress in neurodegenerative disorders. *J Cell Mol Med 15*, 2025-39.

Egger, L., Schneider, J., Rheme, C., Tapernoux, M., Hacki, J. and Borner, C. (2003) Serine proteases mediate apoptosis-like cell death and phagocytosis under caspase-inhibiting conditions. *Cell Death Differ 10*, 1188-203.

Ehehalt, R., Keller, P., Haass, C., Thiele, C. and Simons, K. (2003) Amyloidogenic processing of the Alzheimer beta-amyloid precursor protein depends on lipid rafts. *J Cell Biol 160*, 113-23.

Encinas, M., Iglesias, M., Liu, Y., Wang, H., Muhaisen, A., Cena, V., Gallego, C. and Comella, J. X. (2000) Sequential treatment of SH-SY5Y cells with retinoic acid and brain-derived neurotrophic factor

gives rise to fully differentiated, neurotrophic factor-dependent, human neuron-like cells. *J Neurochem 75*, 991-1003.

Escribá, P. V., Sastre, M. and Garcia-Sevilla, J. A. (1995) Disruption of cellular signaling pathways by daunomycin through destabilization of nonlamellar membrane structures. *Proc Natl Acad Sci U S A 92*, 7595-9.

Escribá, P. V., Ozaita, A., Ribas, C., Miralles, A., Fodor, E., Farkas, T. and Garcia-Sevilla, J. A. (1997) Role of lipid polymorphism in G protein-membrane interactions: nonlamellar-prone phospholipids and peripheral protein binding to membranes. *Proc Natl Acad Sci U S A 94*, 11375-80.

Escribá, P. V. (2006) Membrane-lipid therapy: a new approach in molecular medicine. *Trends Mol Med 12*, 34-43.

Escribá, P. V., Gonzalez-Ros, J. M., Goni, F. M., Kinnunen, P. K., Vigh, L., Sanchez-Magraner, L., Fernandez, A. M., Busquets, X., Horvath, I. and Barcelo-Coblijn, G. (2008) Membranes: a meeting point for lipids, proteins and therapies. *J Cell Mol Med 12*, 829-75.

Fagone, P. and Jackowski, S. (2009) Membrane phospholipid synthesis and endoplasmic reticulum function. *J Lipid Res 50 Suppl*, S311-6.

Fahrenholz, F., Gilbert, S., Kojro, E., Lammich, S. and Postina, R. (2000) Alpha-secretase activity of the disintegrin metalloprotease ADAM 10. Influences of domain structure. *Ann N Y Acad Sci 920*, 215-22.

Farzan, M., Schnitzler, C. E., Vasilieva, N., Leung, D. and Choe, H. (2000) BACE2, a beta -secretase homolog, cleaves at the beta site and within the amyloid-beta region of the amyloid-beta precursor protein. *Proc Natl Acad Sci U S A 97*, 9712-7.

Ferreiro, E., Resende, R., Costa, R., Oliveira, C. R. and Pereira, C. M. (2006) An endoplasmic-reticulum-specific apoptotic pathway is involved in prion and amyloid-beta peptides neurotoxicity. *Neurobiol Dis 23*, 669-78.

Fimia, G. M., Stoykova, A., Romagnoli, A., Giunta, L., Di Bartolomeo, S., Nardacci, R., Corazzari, M., Fuoco, C., Ucar, A., Schwartz, P., Gruss, P., Piacentini, M., Chowdhury, K. and Cecconi, F. (2007) Ambra1 regulates autophagy and development of the nervous system. *Nature 447*, 1121-5.

Frand, A. R., Cuozzo, J. W. and Kaiser, C. A. (2000) Pathways for protein disulphide bond formation. *Trends Cell Biol 10*, 203-10.

Freund-Levi, Y., Eriksdotter-Jonhagen, M., Cederholm, T., Basun, H., Faxen-Irving, G., Garlind, A., Vedin, I., Vessby, B., Wahlund, L. O. and Palmblad, J. (2006) Omega-3 fatty acid treatment in 174 patients with mild to moderate Alzheimer disease: OmegAD study: a randomized double-blind trial. *Arch Neurol 63*, 1402-8.

Fujisawa, H., Reis, R. M., Nakamura, M., Colella, S., Yonekawa, Y., Kleihues, P. and Ohgaki, H. (2000) Loss of heterozygosity on chromosome 10 is more extensive in primary (de novo) than in secondary glioblastomas. *Lab Invest 80*, 65-72.

Fujita, E., Kouroku, Y., Isoai, A., Kumagai, H., Misutani, A., Matsuda, C., Hayashi, Y. K. and Momoi, T. (2007) Two endoplasmic reticulum-associated degradation (ERAD) systems for the novel variant of the mutant dysferlin: ubiquitin/proteasome ERAD(I) and autophagy/lysosome ERAD(II). *Hum Mol Genet 16*, 618-29.

Fujita, N., Itoh, T., Omori, H., Fukuda, M., Noda, T. and Yoshimori, T. (2008) The Atg16L complex specifies the site of LC3 lipidation for membrane biogenesis in autophagy. *Mol Biol Cell 19*, 2092-100.

Fukumori, A., Okochi, M., Tagami, S., Jiang, J., Itoh, N., Nakayama, T., Yanagida, K., Ishizuka-Katsura, Y., Morihara, T., Kamino, K., Tanaka, T., Kudo, T., Tanii, H., Ikuta, A., Haass, C. and Takeda, M. (2006) Presenilin-dependent gamma-secretase on plasma membrane and endosomes is functionally distinct. *Biochemistry 45*, 4907-14.

Fulga, T. A., Elson-Schwab, I., Khurana, V., Steinhilb, M. L., Spires, T. L., Hyman, B. T. and Feany, M. B. (2007) Abnormal bundling and accumulation of F-actin mediates tau-induced neuronal degeneration in vivo. *Nat Cell Biol 9*, 139-48.

Furnari, F. B., Fenton, T., Bachoo, R. M., Mukasa, A., Stommel, J. M., Stegh, A., Hahn, W. C., Ligon, K. L., Louis, D. N., Brennan, C., Chin, L., DePinho, R. A. and Cavenee, W. K. (2007) Malignant astrocytic glioma: genetics, biology, and paths to treatment. *Genes Dev 21*, 2683-710.

Furuya, N., Yu, J., Byfield, M., Pattingre, S. and Levine, B. (2005) The evolutionarily conserved domain of Beclin 1 is required for Vps34 binding, autophagy and tumor suppressor function. *Autophagy 1*, 46-52.

Gellermann, G. P., Appel, T. R., Tannert, A., Radestock, A., Hortschansky, P., Schroeckh, V., Leisner, C., Lutkepohl, T., Shtrasburg, S., Rocken, C., Pras, M., Linke, R. P., Diekmann, S. and Fandrich, M. (2005) Raft lipids as common components of human extracellular amyloid fibrils. *Proc Natl Acad Sci U S A 102*, 6297-302.

Gilany, K., Van Elzen, R., Mous, K., Coen, E., Van Dongen, W., Vandamme, S., Gevaert, K., Timmerman, E., Vandekerckhove, J., Dewilde, S., Van Ostade, X. and Moens, L. (2008) The proteome of the human neuroblastoma cell line SH-SY5Y: an enlarged proteome. *Biochim Biophys Acta 1784*, 983-5.

Gills, J. J., Lopiccolo, J. and Dennis, P. A. (2008) Nelfinavir, a new anti-cancer drug with pleiotropic effects and many paths to autophagy. *Autophagy 4*, 107-9.

Glenner, G. G. and Wong, C. W. (1984) Alzheimer's disease and Down's syndrome: sharing of a unique cerebrovascular amyloid fibril protein. *Biochem Biophys Res Commun 122*, 1131-5.

Goate, A., Chartier-Harlin, M. C., Mullan, M., Brown, J., Crawford, F., Fidani, L., Giuffra, L., Haynes, A., Irving, N., James, L. and et al. (1991) Segregation of a missense mutation in the amyloid precursor protein gene with familial Alzheimer's disease. *Nature 349*, 704-6.

Goedert, M., Jakes, R. and Vanmechelen, E. (1995) Monoclonal antibody AT8 recognises tau protein phosphorylated at both serine 202 and threonine 205. *Neurosci Lett 189*, 167-9.

Gomez-Isla, T., Hollister, R., West, H., Mui, S., Growdon, J. H., Petersen, R. C., Parisi, J. E. and Hyman, B. T. (1997) Neuronal loss correlates with but exceeds neurofibrillary tangles in Alzheimer's disease. *Ann Neurol 41*, 17-24.

Gordon, P. B. and Seglen, P. O. (1988) Prelysosomal convergence of autophagic and endocytic pathways. *Biochem Biophys Res Commun 151*, 40-7.

Gorlach, A., Klappa, P. and Kietzmann, T. (2006) The endoplasmic reticulum: folding, calcium homeostasis, signaling, and redox control. *Antioxid Redox Signal 8*, 1391-418.

Gorman, A. M. (2008) Neuronal cell death in neurodegenerative diseases: recurring themes around protein handling. *J Cell Mol Med 12*, 2263-80.

Green, K. N., Martinez-Coria, H., Khashwji, H., Hall, E. B., Yurko-Mauro, K. A., Ellis, L. and LaFerla, F. M. (2007) Dietary docosahexaenoic acid and docosapentaenoic acid ameliorate amyloid-beta and tau pathology via a mechanism involving presenilin 1 levels. *J Neurosci 27*, 4385-95.

Grundke-Iqbal, I., Iqbal, K., George, L., Tung, Y. C., Kim, K. S. and Wisniewski, H. M. (1989) Amyloid protein and neurofibrillary tangles coexist in the same neuron in Alzheimer disease. *Proc Natl Acad Sci U S A 86*, 2853-7.

Gura, T. (2008) Hope in Alzheimer's fight emerges from unexpected places. *Nat Med 14*, 894.

Haass, C., Schlossmacher, M. G., Hung, A. Y., Vigo-Pelfrey, C., Mellon, A., Ostaszewski, B. L., Lieberburg, I., Koo, E. H., Schenk, D., Teplow, D. B. and et al. (1992) Amyloid beta-peptide is produced by cultured cells during normal metabolism. *Nature 359*, 322-5.

Han, C., Nam, M. K., Park, H. J., Seong, Y. M., Kang, S. and Rhim, H. (2008a) Tunicamycin-induced ER stress upregulates the expression of mitochondrial HtrA2 and promotes apoptosis through the cytosolic release of HtrA2. *J Microbiol Biotechnol 18*, 1197-202.

Han, D., Upton, J. P., Hagen, A., Callahan, J., Oakes, S. A. and Papa, F. R. (2008b) A kinase inhibitor activates the IRE1alpha RNase to confer cytoprotection against ER stress. *Biochem Biophys Res Commun 365*, 777-83.

Hanada, T., Noda, N. N., Satomi, Y., Ichimura, Y., Fujioka, Y., Takao, T., Inagaki, F. and Ohsumi, Y. (2007) The Atg12-Atg5 conjugate has a novel E3-like activity for protein lipidation in autophagy. *J Biol Chem 282*, 37298-302.

Hanahan, D. and Weinberg, R. A. (2000) The hallmarks of cancer. *Cell 100*, 57-70.

Hanahan, D. and Weinberg, R. A. (2011) Hallmarks of cancer: the next generation. *Cell 144*, 646-74.

Hansen, K., Wagner, B., Hamel, W., Schweizer, M., Haag, F., Westphal, M. and Lamszus, K. (2007) Autophagic cell death induced by TrkA receptor activation in human glioblastoma cells. *J Neurochem 103*, 259-75.

Hara, A. and Radin, N. S. (1978) Lipid extraction of tissues with a low-toxicity solvent. *Anal Biochem 90*, 420-6.

Harding, H. P., Zhang, Y. and Ron, D. (1999) Protein translation and folding are coupled by an endoplasmic-reticulum-resident kinase. *Nature 397*, 271-4.

Harding, H. P., Novoa, I., Zhang, Y., Zeng, H., Wek, R., Schapira, M. and Ron, D. (2000) Regulated translation initiation controls stress-induced gene expression in mammalian cells. *Mol Cell 6*, 1099-108.

Harding, H. P., Zhang, Y., Zeng, H., Novoa, I., Lu, P. D., Calfon, M., Sadri, N., Yun, C., Popko, B., Paules, R., Stojdl, D. F., Bell, J. C., Hettmann, T., Leiden, J. M. and Ron, D. (2003) An integrated stress response regulates amino acid metabolism and resistance to oxidative stress. *Mol Cell 11*, 619-33.

Hardy, J. and Selkoe, D. J. (2002) The amyloid hypothesis of Alzheimer's disease: progress and problems on the road to therapeutics. *Science 297*, 353-6.

Harvey, R. J., Skelton-Robinson, M. and Rossor, M. N. (2003) The prevalence and causes of dementia in people under the age of 65 years. *J Neurol Neurosurg Psychiatry 74*, 1206-9.

Hayashi-Nishino, M., Fujita, N., Noda, T., Yamaguchi, A., Yoshimori, T. and Yamamoto, A. (2009) A subdomain of the endoplasmic reticulum forms a cradle for autophagosome formation. *Nat Cell Biol 11*, 1433-7.

Haze, K., Yoshida, H., Yanagi, H., Yura, T. and Mori, K. (1999) Mammalian transcription factor ATF6 is synthesized as a transmembrane protein and activated by proteolysis in response to endoplasmic reticulum stress. *Mol Biol Cell 10*, 3787-99.

Hegi, M. E., Diserens, A. C., Gorlia, T., Hamou, M. F., de Tribolet, N., Weller, M., Kros, J. M., Hainfellner, J. A., Mason, W., Mariani, L., Bromberg, J. E., Hau, P., Mirimanoff, R. O., Cairncross, J. G., Janzer, R. C. and Stupp, R. (2005) MGMT gene silencing and benefit from temozolomide in glioblastoma. *N Engl J Med 352*, 997-1003.

Hemelaar, J., Lelyveld, V. S., Kessler, B. M. and Ploegh, H. L. (2003) A single protease, Apg4B, is specific for the autophagy-related ubiquitin-like proteins GATE-16, MAP1-LC3, GABARAP, and Apg8L. *J Biol Chem 278*, 51841-50.

Herreman, A., Serneels, L., Annaert, W., Collen, D., Schoonjans, L. and De Strooper, B. (2000) Total inactivation of gamma-secretase activity in presenilin-deficient embryonic stem cells. *Nat Cell Biol 2*, 461-2.

Hollien, J. and Weissman, J. S. (2006) Decay of endoplasmic reticulum-localized mRNAs during the unfolded protein response. *Science 313*, 104-7.

Hoozemans, J. J., Veerhuis, R., Van Haastert, E. S., Rozemuller, J. M., Baas, F., Eikelenboom, P. and Scheper, W. (2005) The unfolded protein response is activated in Alzheimer's disease. *Acta Neuropathol 110*, 165-72.

Hoozemans, J. J., van Haastert, E. S., Nijholt, D. A., Rozemuller, A. J., Eikelenboom, P. and Scheper, W. (2009) The unfolded protein response is activated in pretangle neurons in Alzheimer's disease hippocampus. *Am J Pathol 174*, 1241-51.

Hosoi, T. and Ozawa, K. (2012) Molecular approaches to the treatment, prophylaxis, and diagnosis of Alzheimer's disease: endoplasmic reticulum stress and immunological stress in pathogenesis of Alzheimer's disease. *J Pharmacol Sci 118*, 319-24.

http://toulousestreet.wordpress.com/2012/02/.

http://www.cancer.org accessed July 26.

http://www.mssm.edu/research/labs/yue-laboratory.

http://www.pantheon.org/articles/j/janus.html.

Hu, B. R., Martone, M. E., Jones, Y. Z. and Liu, C. L. (2000) Protein aggregation after transient cerebral ischemia. *J Neurosci 20*, 3191-9.

Hung, A. Y., Haass, C., Nitsch, R. M., Qiu, W. Q., Citron, M., Wurtman, R. J., Growdon, J. H. and Selkoe, D. J. (1993) Activation of protein kinase C inhibits cellular production of the amyloid beta-protein. *J Biol Chem 268*, 22959-62.

Ichimura, K., Ohgaki, H., Kleihues, P. and Collins, V. P. (2004) Molecular pathogenesis of astrocytic tumours. *J Neurooncol 70*, 137-60.

Imaizumi, K., Miyoshi, K., Katayama, T., Yoneda, T., Taniguchi, M., Kudo, T. and Tohyama, M. (2001) The unfolded protein response and Alzheimer's disease. *Biochim Biophys Acta 1536*, 85-96.

Imbimbo, B. P., Del Giudice, E., Colavito, D., D'Arrigo, A., Dalle Carbonare, M., Villetti, G., Facchinetti, F., Volta, R., Pietrini, V., Baroc, M. F., Serneels, L., De Strooper, B. and Leon, A. (2007) 1-(3',4'-Dichloro-2-fluoro[1,1'-biphenyl]-4-yl)-cyclopropanecarboxylic acid (CHF5074), a novel gamma-secretase modulator, reduces brain beta-amyloid pathology in a transgenic mouse model of Alzheimer's disease without causing peripheral toxicity. *J Pharmacol Exp Ther 323*, 822-30.

Ishibashi, K., Tomiyama, T., Nishitsuji, K., Hara, M. and Mori, H. (2006) Absence of synaptophysin near cortical neurons containing oligomer Abeta in Alzheimer's disease brain. *J Neurosci Res 84*, 632-6.

Ishiguro, K., Ihara, Y., Uchida, T. and Imahori, K. (1988) A novel tubulin-dependent protein kinase forming a paired helical filament epitope on tau. *J Biochem 104*, 319-21.

Ishiguro, K., Shiratsuchi, A., Sato, S., Omori, A., Arioka, M., Kobayashi, S., Uchida, T. and Imahori, K. (1993) Glycogen synthase kinase 3 beta is identical to tau protein kinase I generating several epitopes of paired helical filaments. *FEBS Lett 325*, 167-72.

Itakura, E., Kishi, C., Inoue, K. and Mizushima, N. (2008) Beclin 1 forms two distinct phosphatidylinositol 3-kinase complexes with mammalian Atg14 and UVRAG. *Mol Biol Cell 19*, 5360-72.

Jakobsen, C. H., Storvold, G. L., Bremseth, H., Follestad, T., Sand, K., Mack, M., Olsen, K. S., Lundemo, A. G., Iversen, J. G., Krokan, H. E. and Schonberg, S. A. (2008) DHA induces ER stress and growth arrest in human colon cancer cells: associations with cholesterol and calcium homeostasis. *J Lipid Res 49*, 2089-100.

Jamsa, A., Hasslund, K., Cowburn, R. F., Backstrom, A. and Vasange, M. (2004) The retinoic acid and brain-derived neurotrophic factor differentiated SH-SY5Y cell line as a model for Alzheimer's disease-like tau phosphorylation. *Biochem Biophys Res Commun 319*, 993-1000.

Jarrett, J. T., Berger, E. P. and Lansbury, P. T., Jr. (1993) The carboxy terminus of the beta amyloid protein is critical for the seeding of amyloid formation: implications for the pathogenesis of Alzheimer's disease. *Biochemistry 32*, 4693-7.

Jia, W., Loria, R. M., Park, M. A., Yacoub, A., Dent, P. and Graf, M. R. (2010) The neuro-steroid, 5-androstene 3beta,17alpha diol; induces endoplasmic reticulum stress and autophagy through PERK/eIF2alpha signaling in malignant glioma cells and transformed fibroblasts. *Int J Biochem Cell Biol 42*, 2019-29.

Johnson, A. J., Hsu, A. L., Lin, H. P., Song, X. and Chen, C. S. (2002) The cyclo-oxygenase-2 inhibitor celecoxib perturbs intracellular calcium by inhibiting endoplasmic reticulum Ca2+-ATPases: a plausible link with its anti-tumour effect and cardiovascular risks. *Biochem J 366*, 831-7.

Johnson, G. G., White, M. C. and Grimaldi, M. (2011) Stressed to death: targeting endoplasmic reticulum stress response induced apoptosis in gliomas. *Curr Pharm Des 17*, 284-92.

Jolly, C. A., Hubbell, T., Behnke, W. D. and Schroeder, F. (1997) Fatty acid binding protein: stimulation of microsomal phosphatidic acid formation. *Arch Biochem Biophys 341*, 112-21.

Jorissen, E., Prox, J., Bernreuther, C., Weber, S., Schwanbeck, R., Serneels, L., Snellinx, A., Craessaerts, K., Thathiah, A., Tesseur, I., Bartsch, U., Weskamp, G., Blobel, C. P., Glatzel, M., De

Strooper, B. and Saftig, P. (2010) The disintegrin/metalloproteinase ADAM10 is essential for the establishment of the brain cortex. *J Neurosci 30*, 4833-44.

Karaskov, E., Scott, C., Zhang, L., Teodoro, T., Ravazzola, M. and Volchuk, A. (2006) Chronic palmitate but not oleate exposure induces endoplasmic reticulum stress, which may contribute to INS-1 pancreatic beta-cell apoptosis. *Endocrinology 147*, 3398-407.

Kardosh, A., Golden, E. B., Pyrko, P., Uddin, J., Hofman, F. M., Chen, T. C., Louie, S. G., Petasis, N. A. and Schonthal, A. H. (2008) Aggravated endoplasmic reticulum stress as a basis for enhanced glioblastoma cell killing by bortezomib in combination with celecoxib or its non-coxib analogue, 2,5-dimethyl-celecoxib. *Cancer Res 68*, 843-51.

Karran, E., Mercken, M. and De Strooper, B. (2011) The amyloid cascade hypothesis for Alzheimer's disease: an appraisal for the development of therapeutics. *Nat Rev Drug Discov 10*, 698-712.

Katayama, T., Imaizumi, K., Sato, N., Miyoshi, K., Kudo, T., Hitomi, J., Morihara, T., Yoneda, T., Gomi, F., Mori, Y., Nakano, Y., Takeda, J., Tsuda, T., Itoyama, Y., Murayama, O., Takashima, A., St George-Hyslop, P., Takeda, M. and Tohyama, M. (1999) Presenilin-1 mutations downregulate the signalling pathway of the unfolded-protein response. *Nat Cell Biol 1*, 479-85.

Katayama, T., Imaizumi, K., Honda, A., Yoneda, T., Kudo, T., Takeda, M., Mori, K., Rozmahel, R., Fraser, P., George-Hyslop, P. S. and Tohyama, M. (2001) Disturbed activation of endoplasmic reticulum stress transducers by familial Alzheimer's disease-linked presenilin-1 mutations. *J Biol Chem 276*, 43446-54.

Kaufman, R. J. (1999) Stress signaling from the lumen of the endoplasmic reticulum: coordination of gene transcriptional and translational controls. *Genes Dev 13*, 1211-33.

Kaufman, R. J. (2002) Orchestrating the unfolded protein response in health and disease. *J Clin Invest 110*, 1389-98.

Kihara, A., Kabeya, Y., Ohsumi, Y. and Yoshimori, T. (2001) Beclin-phosphatidylinositol 3-kinase complex functions at the trans-Golgi network. *EMBO Rep 2*, 330-5.

Kim, I., Xu, W. and Reed, J. C. (2008) Cell death and endoplasmic reticulum stress: disease relevance and therapeutic opportunities. *Nat Rev Drug Discov 7*, 1013-30.

Kimura, T., Yamashita, S., Fukuda, T., Park, J. M., Murayama, M., Mizoroki, T., Yoshiike, Y., Sahara, N. and Takashima, A. (2007) Hyperphosphorylated tau in parahippocampal cortex impairs place learning in aged mice expressing wild-type human tau. *EMBO J 26*, 5143-52.

Kimura, T., Fukuda, T., Sahara, N., Yamashita, S., Murayama, M., Mizoroki, T., Yoshiike, Y., Lee, B., Sotiropoulos, I., Maeda, S. and Takashima, A. (2010) Aggregation of detergent-insoluble tau is involved in neuronal loss but not in synaptic loss. *J Biol Chem 285*, 38692-9.

Klausner, R. D., Donaldson, J. G. and Lippincott-Schwartz, J. (1992) Brefeldin A: insights into the control of membrane traffic and organelle structure. *J Cell Biol 116*, 1071-80.

Kleihues, P. and Sobin, L. H. (2000) World Health Organization classification of tumors. *Cancer 88*, 2887.

Klionsky, D. J., Abeliovich, H., Agostinis, P., Agrawal, D. K., Aliev, G., Askew, D. S., Baba, M., Baehrecke, E. H., Bahr, B. A., Ballabio, A., Bamber, B. A., Bassham, D. C., Bergamini, E., Bi, X., Biard-Piechaczyk, M., Blum, J. S., Bredesen, D. E., Brodsky, J. L., Brumell, J. H., Brunk, U. T., Bursch, W., Camougrand, N., Cebollero, E., Cecconi, F., Chen, Y., Chin, L. S., Choi, A., Chu, C. T.,

Chung, J., Clarke, P. G., Clark, R. S., Clarke, S. G., Clave, C., Cleveland, J. L., Codogno, P., Colombo, M. I., Coto-Montes, A., Cregg, J. M., Cuervo, A. M., Debnath, J., Demarchi, F., Dennis, P. B., Dennis, P. A., Deretic, V., Devenish, R. J., Di Sano, F., Dice, J. F., Difiglia, M., Dinesh-Kumar, S., Distelhorst, C. W., Djavaheri-Mergny, M., Dorsey, F. C., Droge, W., Dron, M., Dunn, W. A., Jr., Duszenko, M., Eissa, N. T., Elazar, Z., Esclatine, A., Eskelinen, E. L., Fesus, L., Finley, K. D., Fuentes, J. M., Fueyo, J., Fujisaki, K., Galliot, B., Gao, F. B., Gewirtz, D. A., Gibson, S. B., Gohla, A., Goldberg, A. L., Gonzalez, R., Gonzalez-Estevez, C., Gorski, S., Gottlieb, R. A., Haussinger, D., He, Y. W., Heidenreich, K., Hill, J. A., Hoyer-Hansen, M., Hu, X., Huang, W. P., Iwasaki, A., Jaattela, M., Jackson, W. T., Jiang, X., Jin, S., Johansen, T., Jung, J. U., Kadowaki, M., Kang, C., Kelekar, A., Kessel, D. H., Kiel, J. A., Kim, H. P., Kimchi, A., Kinsella, T. J., Kiselyov, K., Kitamoto, K., Knecht, E. et al. (2008) Guidelines for the use and interpretation of assays for monitoring autophagy in higher eukaryotes. *Autophagy 4*, 151-75.

Knops, J., Suomensaari, S., Lee, M., McConlogue, L., Seubert, P. and Sinha, S. (1995) Cell-type and amyloid precursor protein-type specific inhibition of A beta release by bafilomycin A1, a selective inhibitor of vacuolar ATPases. *J Biol Chem 270*, 2419-22.

Kojro, E., Gimpl, G., Lammich, S., Marz, W. and Fahrenholz, F. (2001) Low cholesterol stimulates the nonamyloidogenic pathway by its effect on the alpha -secretase ADAM 10. *Proc Natl Acad Sci U S A 98*, 5815-20.

Kojro, E. and Fahrenholz, F. (2005) The non-amyloidogenic pathway: structure and function of alpha-secretases. *Subcell Biochem 38*, 105-27.

Kojro, E., Fuger, P., Prinzen, C., Kanarek, A. M., Rat, D., Endres, K., Fahrenholz, F. and Postina, R. (2010) Statins and the squalene synthase inhibitor zaragozic acid stimulate the non-amyloidogenic pathway of amyloid-beta protein precursor processing by suppression of cholesterol synthesis. *J Alzheimers Dis 20*, 1215-31.

Komatsu, M., Waguri, S., Chiba, T., Murata, S., Iwata, J., Tanida, I., Ueno, T., Koike, M., Uchiyama, Y., Kominami, E. and Tanaka, K. (2006) Loss of autophagy in the central nervous system causes neurodegeneration in mice. *Nature 441*, 880-4.

Kondo, Y., Kanzawa, T., Sawaya, R. and Kondo, S. (2005) The role of autophagy in cancer development and response to therapy. *Nat Rev Cancer 5*, 726-34.

Koo, E. H., Sisodia, S. S., Archer, D. R., Martin, L. J., Weidemann, A., Beyreuther, K., Fischer, P., Masters, C. L. and Price, D. L. (1990) Precursor of amyloid protein in Alzheimer disease undergoes fast anterograde axonal transport. *Proc Natl Acad Sci U S A 87*, 1561-5.

Kouroku, Y., Fujita, E., Tanida, I., Ueno, T., Isoai, A., Kumagai, H., Ogawa, S., Kaufman, R. J., Kominami, E. and Momoi, T. (2007) ER stress (PERK/eIF2alpha phosphorylation) mediates the polyglutamine-induced LC3 conversion, an essential step for autophagy formation. *Cell Death Differ 14*, 230-9.

Kubicek, G. J., Werner-Wasik, M., Machtay, M., Mallon, G., Myers, T., Ramirez, M., Andrews, D., Curran, W. J., Jr. and Dicker, A. P. (2009) Phase I trial using proteasome inhibitor bortezomib and concurrent temozolomide and radiotherapy for central nervous system malignancies. *Int J Radiat Oncol Biol Phys 74*, 433-9.

Kudo, T., Kanemoto, S., Hara, H., Morimoto, N., Morihara, T., Kimura, R., Tabira, T., Imaizumi, K. and Takeda, M. (2008) A molecular chaperone inducer protects neurons from ER stress. *Cell Death Differ 15*, 364-75.

Kuhn, P. H., Wang, H., Dislich, B., Colombo, A., Zeitschel, U., Ellwart, J. W., Kremmer, E., Rossner, S. and Lichtenthaler, S. F. (2010) ADAM10 is the physiologically relevant, constitutive alpha-secretase of the amyloid precursor protein in primary neurons. *EMBO J 29*, 3020-32.

Kukar, T., Prescott, S., Eriksen, J. L., Holloway, V., Murphy, M. P., Koo, E. H., Golde, T. E. and Nicolle, M. M. (2007) Chronic administration of R-flurbiprofen attenuates learning impairments in transgenic amyloid precursor protein mice. *BMC Neurosci 8*, 54.

LaFerla, F. M., Green, K. N. and Oddo, S. (2007) Intracellular amyloid-beta in Alzheimer's disease. *Nat Rev Neurosci 8*, 499-509.

Lammich, S., Kojro, E., Postina, R., Gilbert, S., Pfeiffer, R., Jasionowski, M., Haass, C. and Fahrenholz, F. (1999) Constitutive and regulated alpha-secretase cleavage of Alzheimer's amyloid precursor protein by a disintegrin metalloprotease. *Proc Natl Acad Sci U S A 96*, 3922-7.

Leach, M. R. and Williams, D. B. (2000) (Bioscience, A. T. L., Ed.), Madame Curie Bioscience Database [Internet]. http://www.ncbi.nlm.nih.gov/books/NBK6095/.

Lee, A. H., Iwakoshi, N. N. and Glimcher, L. H. (2003) XBP-1 regulates a subset of endoplasmic reticulum resident chaperone genes in the unfolded protein response. *Mol Cell Biol 23*, 7448-59.

Lee do, Y., Lee, K. S., Lee, H. J., Kim do, H., Noh, Y. H., Yu, K., Jung, H. Y., Lee, S. H., Lee, J. Y., Youn, Y. C., Jeong, Y., Kim, D. K., Lee, W. B. and Kim, S. S. (2010) Activation of PERK signaling attenuates Abeta-mediated ER stress. *PLoS One 5*, e10489.

Lee, G. (2005) Tau and src family tyrosine kinases. *Biochim Biophys Acta 1739*, 323-30.

Lee, J., Retamal, C., Cuitino, L., Caruano-Yzermans, A., Shin, J. E., van Kerkhof, P., Marzolo, M. P. and Bu, G. (2008) Adaptor protein sorting nexin 17 regulates amyloid precursor protein trafficking and processing in the early endosomes. *J Biol Chem 283*, 11501-8.

Lee, S., Sato, Y. and Nixon, R. A. (2011) Primary lysosomal dysfunction causes cargo-specific deficits of axonal transport leading to Alzheimer-like neuritic dystrophy. *Autophagy 7*, 1562-3.

Leissring, M. A., LaFerla, F. M., Callamaras, N. and Parker, I. (2001) Subcellular mechanisms of presenilin-mediated enhancement of calcium signaling. *Neurobiol Dis 8*, 469-78.

Levine, B. and Klionsky, D. J. (2004) Development by self-digestion: molecular mechanisms and biological functions of autophagy. *Dev Cell 6*, 463-77.

Levine, B. and Kroemer, G. (2008) Autophagy in the pathogenesis of disease. *Cell 132*, 27-42.

Levy-Lahad, E., Wasco, W., Poorkaj, P., Romano, D. M., Oshima, J., Pettingell, W. H., Yu, C. E., Jondro, P. D., Schmidt, S. D., Wang, K. and et al. (1995) Candidate gene for the chromosome 1 familial Alzheimer's disease locus. *Science 269*, 973-7.

Li, D. D., Wang, L. L., Deng, R., Tang, J., Shen, Y., Guo, J. F., Wang, Y., Xia, L. P., Feng, G. K., Liu, Q. Q., Huang, W. L., Zeng, Y. X. and Zhu, X. F. (2009) The pivotal role of c-Jun NH2-terminal kinase-mediated Beclin 1 expression during anticancer agents-induced autophagy in cancer cells. *Oncogene 28*, 886-98.

Liang, C., Feng, P., Ku, B., Dotan, I., Canaani, D., Oh, B. H. and Jung, J. U. (2006) Autophagic and tumour suppressor activity of a novel Beclin1-binding protein UVRAG. *Nat Cell Biol 8*, 688-99.

Lichtenthaler, S. F. (2011) Alpha-secretase in Alzheimer's disease: molecular identity, regulation and therapeutic potential. *J Neurochem 116*, 10-21.

Lin, J. H., Li, H., Yasumura, D., Cohen, H. R., Zhang, C., Panning, B., Shokat, K. M., Lavail, M. M. and Walter, P. (2007) IRE1 signaling affects cell fate during the unfolded protein response. *Science 318*, 944-9.

Lin, J. H., Li, H., Zhang, Y., Ron, D. and Walter, P. (2009) Divergent effects of PERK and IRE1 signaling on cell viability. *PLoS One 4*, e4170.

Lindholm, D., Wootz, H. and Korhonen, L. (2006) ER stress and neurodegenerative diseases. *Cell Death Differ 13*, 385-92.

Lopes, F. M., Schroder, R., da Frota, M. L., Jr., Zanotto-Filho, A., Muller, C. B., Pires, A. S., Meurer, R. T., Colpo, G. D., Gelain, D. P., Kapczinski, F., Moreira, J. C., Fernandes Mda, C. and Klamt, F. (2010) Comparison between proliferative and neuron-like SH-SY5Y cells as an in vitro model for Parkinson disease studies. *Brain Res 1337*, 85-94.

Lopez-Perez, E., Zhang, Y., Frank, S. J., Creemers, J., Seidah, N. and Checler, F. (2001) Constitutive alpha-secretase cleavage of the beta-amyloid precursor protein in the furin-deficient LoVo cell line: involvement of the pro-hormone convertase 7 and the disintegrin metalloprotease ADAM10. *J Neurochem 76*, 1532-9.

Lowry, O. H., Rosebrough, N. J., Farr, A. L. and Randall, R. J. (1951) Protein measurement with the Folin phenol reagent. *J Biol Chem 193*, 265-75.

Lu, P. D., Harding, H. P. and Ron, D. (2004a) Translation reinitiation at alternative open reading frames regulates gene expression in an integrated stress response. *J Cell Biol 167*, 27-33.

Lu, P. D., Jousse, C., Marciniak, S. J., Zhang, Y., Novoa, I., Scheuner, D., Kaufman, R. J., Ron, D. and Harding, H. P. (2004b) Cytoprotection by pre-emptive conditional phosphorylation of translation initiation factor 2. *EMBO J 23*, 169-79.

Luo, J., Solimini, N. L. and Elledge, S. J. (2009) Principles of cancer therapy: oncogene and non-oncogene addiction. *Cell 136*, 823-37.

Lladó, V., Terés, S., Higuera, M., Álvarez, R., Noguera-Salvà, M. A., Halver, J. E., Escribá, P. V. and Busquets, X. (2009) Pivotal role of dihydrofolate reductase knockdown in the anticancer activity of 2-hydroxyoleic acid. *Proc Natl Acad Sci U S A 106*, 13754-8.

Lladó, V., Gutierrez, A., Martínez, J., Casas, J., Terés, S., Higuera, M., Galmes, A., Saus, C., Besalduch, J., Busquets, X. and Escribá, P. V. (2010) Minerval induces apoptosis in Jurkat and other cancer cells. *J Cell Mol Med 14*, 659-70.

Ma, Y., Brewer, J. W., Diehl, J. A. and Hendershot, L. M. (2002) Two distinct stress signaling pathways converge upon the CHOP promoter during the mammalian unfolded protein response. *J Mol Biol 318*, 1351-65.

Ma, Y. and Hendershot, L. M. (2004) ER chaperone functions during normal and stress conditions. *J Chem Neuroanat 28*, 51-65.

Maas, T., Eidenmuller, J. and Brandt, R. (2000) Interaction of tau with the neural membrane cortex is regulated by phosphorylation at sites that are modified in paired helical filaments. *J Biol Chem 275*, 15733-40.

Macdonald, F., Ford, C. H. J. and Casson, A. G. (2004) *Molecular biology of cancer*, 2nd ed., BIOS Scientific Publishers, London ; New York, N.Y.

Maeda, S., Sahara, N., Saito, Y., Murayama, M., Yoshiike, Y., Kim, H., Miyasaka, T., Murayama, S., Ikai, A. and Takashima, A. (2007) Granular tau oligomers as intermediates of tau filaments. *Biochemistry 46*, 3856-61.

Maiuri, M. C., Zalckvar, E., Kimchi, A. and Kroemer, G. (2007) Self-eating and self-killing: crosstalk between autophagy and apoptosis. *Nat Rev Mol Cell Biol 8*, 741-52.

Malhotra, J. D. and Kaufman, R. J. (2007) The endoplasmic reticulum and the unfolded protein response. *Semin Cell Dev Biol 18*, 716-31.

Mandelkow, E. M., Biernat, J., Drewes, G., Steiner, B., Lichtenberg-Kraag, B., Wille, H., Gustke, N. and Mandelkow, E. (1993) Microtubule-associated protein tau, paired helical filaments, and phosphorylation. *Ann N Y Acad Sci 695*, 209-16.

Marcheselli, V. L., Scott, B. L., Reddy, T. S. and Bazan, N. G. (1988) Quantitative analysis of acyl group composition of brain phospholipids, neutral lipids, and free fatty acids, in Neuromethods 7 Lipids and related compounds. *Clifton, NJ.: Humana Press*.

Martinet, W., Agostinis, P., Vanhoecke, B., Dewaele, M. and De Meyer, G. R. (2009) Autophagy in disease: a double-edged sword with therapeutic potential. *Clin Sci (Lond) 116*, 697-712.

Martinez, J., Vogler, O., Casas, J., Barcelo, F., Alemany, R., Prades, J., Nagy, T., Baamonde, C., Kasprzyk, P. G., Teres, S., Saus, C. and Escriba, P. V. (2005) Membrane structure modulation, protein kinase C alpha activation, and anticancer activity of minerval. *Mol Pharmacol 67*, 531-40.

Martínez, J., Gutierrez, A., Casas, J., Lladó, V., Lopez-Bellan, A., Besalduch, J., Dopazo, A. and Escribá, P. V. (2005a) The repression of E2F-1 is critical for the activity of Minerval against cancer. *J Pharmacol Exp Ther 315*, 466-74.

Martínez, J., Vögler, O., Casas, J., Barceló, F., Alemany, R., Prades, J., Nagy, T., Baamonde, C., Kasprzyk, P. G., Terés, S., Saus, C. and Escribá, P. V. (2005b) Membrane structure modulation, protein kinase C alpha activation, and anticancer activity of minerval. *Mol Pharmacol 67*, 531-40.

Masliah, E., Ellisman, M., Carragher, B., Mallory, M., Young, S., Hansen, L., DeTeresa, R. and Terry, R. D. (1992) Three-dimensional analysis of the relationship between synaptic pathology and neuropil threads in Alzheimer disease. *J Neuropathol Exp Neurol 51*, 404-14.

Masters, C. L., Simms, G., Weinman, N. A., Multhaup, G., McDonald, B. L. and Beyreuther, K. (1985) Amyloid plaque core protein in Alzheimer disease and Down syndrome. *Proc Natl Acad Sci U S A 82*, 4245-9.

Mathew, R., Karantza-Wadsworth, V. and White, E. (2007) Role of autophagy in cancer. *Nat Rev Cancer 7*, 961-7.

Mattson, M. P. (2003) Neurobiology: Ballads of a protein quartet. *Nature 422*, 385, 387.

Matus, S., Lisbona, F., Torres, M., Leon, C., Thielen, P. and Hetz, C. (2008) The stress rheostat: an interplay between the unfolded protein response (UPR) and autophagy in neurodegeneration. *Curr Mol Med 8*, 157-72.

Maytin, E. V., Ubeda, M., Lin, J. C. and Habener, J. F. (2001) Stress-inducible transcription factor CHOP/gadd153 induces apoptosis in mammalian cells via p38 kinase-dependent and -independent mechanisms. *Exp Cell Res 267*, 193-204.

McCullough, K. D., Martindale, J. L., Klotz, L. O., Aw, T. Y. and Holbrook, N. J. (2001) Gadd153 sensitizes cells to endoplasmic reticulum stress by down-regulating Bcl2 and perturbing the cellular redox state. *Mol Cell Biol 21*, 1249-59.

Mills, J. and Reiner, P. B. (1999) Mitogen-activated protein kinase is involved in N-methyl-D-aspartate receptor regulation of amyloid precursor protein cleavage. *Neuroscience 94*, 1333-8.

Mizushima, N., Noda, T., Yoshimori, T., Tanaka, Y., Ishii, T., George, M. D., Klionsky, D. J., Ohsumi, M. and Ohsumi, Y. (1998a) A protein conjugation system essential for autophagy. *Nature 395*, 395-8.

Mizushima, N., Sugita, H., Yoshimori, T. and Ohsumi, Y. (1998b) A new protein conjugation system in human. The counterpart of the yeast Apg12p conjugation system essential for autophagy. *J Biol Chem 273*, 33889-92.

Mizushima, N., Noda, T. and Ohsumi, Y. (1999) Apg16p is required for the function of the Apg12p-Apg5p conjugate in the yeast autophagy pathway. *EMBO J 18*, 3888-96.

Mizushima, N., Kuma, A., Kobayashi, Y., Yamamoto, A., Matsubae, M., Takao, T., Natsume, T., Ohsumi, Y. and Yoshimori, T. (2003) Mouse Apg16L, a novel WD-repeat protein, targets to the autophagic isolation membrane with the Apg12-Apg5 conjugate. *J Cell Sci 116*, 1679-88.

Mizushima, N. (2007) Autophagy: process and function. *Genes Dev 21*, 2861-73.

Mizushima, N., Levine, B., Cuervo, A. M. and Klionsky, D. J. (2008) Autophagy fights disease through cellular self-digestion. *Nature 451*, 1069-75.

Moenner, M., Pluquet, O., Bouchecareilh, M. and Chevet, E. (2007) Integrated endoplasmic reticulum stress responses in cancer. *Cancer Res 67*, 10631-4.

Morishima-Kawashima, M., Hasegawa, M., Takio, K., Suzuki, M., Yoshida, H., Watanabe, A., Titani, K. and Ihara, Y. (1995) Hyperphosphorylation of tau in PHF. *Neurobiol Aging 16*, 365-71; discussion 371-80.

Morris, J. A., Dorner, A. J., Edwards, C. A., Hendershot, L. M. and Kaufman, R. J. (1997) Immunoglobulin binding protein (BiP) function is required to protect cells from endoplasmic reticulum stress but is not required for the secretion of selective proteins. *J Biol Chem 272*, 4327-34.

Mosmann, T. (1983) Rapid colorimetric assay for cellular growth and survival: application to proliferation and cytotoxicity assays. *J Immunol Methods 65*, 55-63.

Murphy, E. J., Rosenberger, T. A. and Horrocks, L. A. (1997) Effects of maturation on the phospholipid and phospholipid fatty acid compositions in primary rat cortical astrocyte cell cultures. *Neurochem Res 22*, 1205-13.

Murphy, E. J., Stiles, T. and Schroeder, F. (2000) Sterol carrier protein-2 expression alters phospholipid content and fatty acyl composition in L-cell fibroblasts. *J Lipid Res 41*, 788-96.

Myriad-Genetics. (2008).

Nakatogawa, H., Ichimura, Y. and Ohsumi, Y. (2007) Atg8, a ubiquitin-like protein required for autophagosome formation, mediates membrane tethering and hemifusion. *Cell 130*, 165-78.

Nedelsky, N. B., Todd, P. K. and Taylor, J. P. (2008) Autophagy and the ubiquitin-proteasome system: collaborators in neuroprotection. *Biochim Biophys Acta 1782*, 691-9.

Nemoto, T., Tanida, I., Tanida-Miyake, E., Minematsu-Ikeguchi, N., Yokota, M., Ohsumi, M., Ueno, T. and Kominami, E. (2003) The mouse APG10 homologue, an E2-like enzyme for Apg12p conjugation, facilitates MAP-LC3 modification. *J Biol Chem 278*, 39517-26.

Nishitoh, H., Matsuzawa, A., Tobiume, K., Saegusa, K., Takeda, K., Inoue, K., Hori, S., Kakizuka, A. and Ichijo, H. (2002) ASK1 is essential for endoplasmic reticulum stress-induced neuronal cell death triggered by expanded polyglutamine repeats. *Genes Dev 16*, 1345-55.

Nixon, R. A., Wegiel, J., Kumar, A., Yu, W. H., Peterhoff, C., Cataldo, A. and Cuervo, A. M. (2005) Extensive involvement of autophagy in Alzheimer disease: an immuno-electron microscopy study. *J Neuropathol Exp Neurol 64*, 113-22.

Nixon, R. A. (2007) Autophagy, amyloidogenesis and Alzheimer disease. *J Cell Sci 120*, 4081-91.

Noble, W., Planel, E., Zehr, C., Olm, V., Meyerson, J., Suleman, F., Gaynor, K., Wang, L., LaFrancois, J., Feinstein, B., Burns, M., Krishnamurthy, P., Wen, Y., Bhat, R., Lewis, J., Dickson, D. and Duff, K. (2005) Inhibition of glycogen synthase kinase-3 by lithium correlates with reduced tauopathy and degeneration in vivo. *Proc Natl Acad Sci U S A 102*, 6990-5.

Noiva, R. and Lennarz, W. J. (1992) Protein disulfide isomerase. A multifunctional protein resident in the lumen of the endoplasmic reticulum. *J Biol Chem 267*, 3553-6.

Nordberg, A. (2004) PET imaging of amyloid in Alzheimer's disease. *Lancet Neurol 3*, 519-27.

O'Connor, T., Sadleir, K. R., Maus, E., Velliquette, R. A., Zhao, J., Cole, S. L., Eimer, W. A., Hitt, B., Bembinster, L. A., Lammich, S., Lichtenthaler, S. F., Hebert, S. S., De Strooper, B., Haass, C., Bennett, D. A. and Vassar, R. (2008) Phosphorylation of the translation initiation factor eIF2alpha increases BACE1 levels and promotes amyloidogenesis. *Neuron 60*, 988-1009.

Oakley, H., Cole, S. L., Logan, S., Maus, E., Shao, P., Craft, J., Guillozet-Bongaarts, A., Ohno, M., Disterhoft, J., Van Eldik, L., Berry, R. and Vassar, R. (2006) Intraneuronal beta-amyloid aggregates, neurodegeneration, and neuron loss in transgenic mice with five familial Alzheimer's disease mutations: potential factors in amyloid plaque formation. *J Neurosci 26*, 10129-40.

Ogata, M., Hino, S., Saito, A., Morikawa, K., Kondo, S., Kanemoto, S., Murakami, T., Taniguchi, M., Tanii, I., Yoshinaga, K., Shiosaka, S., Hammarback, J. A., Urano, F. and Imaizumi, K. (2006) Autophagy is activated for cell survival after endoplasmic reticulum stress. *Mol Cell Biol 26*, 9220-31.

Olton, D. S. and Samuelson, R. J. (1976) Remembrance of places passed: Spatial memory in rats. *Journal of Experimental Psychology: Animal Behavior Processes. 2*, 97-116.

Olton, D. S. and Papas, B. C. (1979) Spatial memory and hippocampal function. *Neuropsychologia 17*, 669-82.

Oyadomari, S. and Mori, M. (2004) Roles of CHOP/GADD153 in endoplasmic reticulum stress. *Cell Death Differ 11*, 381-9.

Ozcan, U., Cao, Q., Yilmaz, E., Lee, A. H., Iwakoshi, N. N., Ozdelen, E., Tuncman, G., Gorgun, C., Glimcher, L. H. and Hotamisligil, G. S. (2004) Endoplasmic reticulum stress links obesity, insulin action, and type 2 diabetes. *Science 306*, 457-61.

Parvathy, S., Hussain, I., Karran, E. H., Turner, A. J. and Hooper, N. M. (1999) Cleavage of Alzheimer's amyloid precursor protein by alpha-secretase occurs at the surface of neuronal cells. *Biochemistry 38*, 9728-34.

Pattingre, S., Tassa, A., Qu, X., Garuti, R., Liang, X. H., Mizushima, N., Packer, M., Schneider, M. D. and Levine, B. (2005) Bcl-2 antiapoptotic proteins inhibit Beclin 1-dependent autophagy. *Cell 122*, 927-39.

Peterson, B. L. and Cummings, B. S. (2006) A review of chromatographic methods for the assessment of phospholipids in biological samples. *Biomed Chromatogr 20*, 227-43.

Pfaffl, M. W. (2001) A new mathematical model for relative quantification in real-time RT-PCR. *Nucleic Acids Res 29*, e45.

Pfaffl, M. W., Georgieva, T. M., Georgiev, I. P., Ontsouka, E., Hageleit, M. and Blum, J. W. (2002) Real-time RT-PCR quantification of insulin-like growth factor (IGF)-1, IGF-1 receptor, IGF-2, IGF-2 receptor, insulin receptor, growth hormone receptor, IGF-binding proteins 1, 2 and 3 in the bovine species. *Domest Anim Endocrinol 22*, 91-102.

Pickford, F., Masliah, E., Britschgi, M., Lucin, K., Narasimhan, R., Jaeger, P. A., Small, S., Spencer, B., Rockenstein, E., Levine, B. and Wyss-Coray, T. (2008) The autophagy-related protein beclin 1 shows reduced expression in early Alzheimer disease and regulates amyloid beta accumulation in mice. *J Clin Invest 118*, 2190-9.

Postina, R., Schroeder, A., Dewachter, I., Bohl, J., Schmitt, U., Kojro, E., Prinzen, C., Endres, K., Hiemke, C., Blessing, M., Flamez, P., Dequenne, A., Godaux, E., van Leuven, F. and Fahrenholz, F. (2004) A disintegrin-metalloproteinase prevents amyloid plaque formation and hippocampal defects in an Alzheimer disease mouse model. *J Clin Invest 113*, 1456-64.

Prentice, E., Jerome, W. G., Yoshimori, T., Mizushima, N. and Denison, M. R. (2004) Coronavirus replication complex formation utilizes components of cellular autophagy. *J Biol Chem 279*, 10136-41.

Pyrko, P., Kardosh, A., Liu, Y. T., Soriano, N., Xiong, W., Chow, R. H., Uddin, J., Petasis, N. A., Mircheff, A. K., Farley, R. A., Louie, S. G., Chen, T. C. and Schonthal, A. H. (2007a) Calcium-activated endoplasmic reticulum stress as a major component of tumor cell death induced by 2,5-dimethyl-celecoxib, a non-coxib analogue of celecoxib. *Mol Cancer Ther 6*, 1262-75.

Pyrko, P., Kardosh, A., Wang, W., Xiong, W., Schonthal, A. H. and Chen, T. C. (2007b) HIV-1 protease inhibitors nelfinavir and atazanavir induce malignant glioma death by triggering endoplasmic reticulum stress. *Cancer Res 67*, 10920-8.

Ramsden, M., Kotilinek, L., Forster, C., Paulson, J., McGowan, E., SantaCruz, K., Guimaraes, A., Yue, M., Lewis, J., Carlson, G., Hutton, M. and Ashe, K. H. (2005) Age-dependent neurofibrillary tangle formation, neuron loss, and memory impairment in a mouse model of human tauopathy (P301L). *J Neurosci 25*, 10637-47.

Rao, R. V. and Bredesen, D. E. (2004) Misfolded proteins, endoplasmic reticulum stress and neurodegeneration. *Curr Opin Cell Biol 16*, 653-62.

Ravikumar, B., Sarkar, S., Davies, J. E., Futter, M., Garcia-Arencibia, M., Green-Thompson, Z. W., Jimenez-Sanchez, M., Korolchuk, V. I., Lichtenberg, M., Luo, S., Massey, D. C., Menzies, F. M.,

Moreau, K., Narayanan, U., Renna, M., Siddiqi, F. H., Underwood, B. R., Winslow, A. R. and Rubinsztein, D. C. (2010) Regulation of mammalian autophagy in physiology and pathophysiology. *Physiol Rev 90*, 1383-435.

Reef, S., Zalckvar, E., Shifman, O., Bialik, S., Sabanay, H., Oren, M. and Kimchi, A. (2006) A short mitochondrial form of p19ARF induces autophagy and caspase-independent cell death. *Mol Cell 22*, 463-75.

Reitz, C. (2012) Alzheimer's disease and the amyloid cascade hypothesis: a critical review. *Int J Alzheimers Dis 2012*, 369808.

Rizzuto, R., Duchen, M. R. and Pozzan, T. (2004) Flirting in little space: the ER/mitochondria Ca2+ liaison. *Sci STKE 2004*, re1.

Roberson, E. D., Scearce-Levie, K., Palop, J. J., Yan, F., Cheng, I. H., Wu, T., Gerstein, H., Yu, G. Q. and Mucke, L. (2007) Reducing endogenous tau ameliorates amyloid beta-induced deficits in an Alzheimer's disease mouse model. *Science 316*, 750-4.

Rochet, J. C. (2007) Novel therapeutic strategies for the treatment of protein-misfolding diseases. *Expert Rev Mol Med 9*, 1-34.

Ron, D. and Walter, P. (2007) Signal integration in the endoplasmic reticulum unfolded protein response. *Nat Rev Mol Cell Biol 8*, 519-29.

Rutkowski, D. T., Arnold, S. M., Miller, C. N., Wu, J., Li, J., Gunnison, K. M., Mori, K., Sadighi Akha, A. A., Raden, D. and Kaufman, R. J. (2006) Adaptation to ER stress is mediated by differential stabilities of pro-survival and pro-apoptotic mRNAs and proteins. *PLoS Biol 4*, e374.

Salazar, M., Carracedo, A., Salanueva, I. J., Hernandez-Tiedra, S., Lorente, M., Egia, A., Vazquez, P., Blazquez, C., Torres, S., Garcia, S., Nowak, J., Fimia, G. M., Piacentini, M., Cecconi, F., Pandolfi, P. P., Gonzalez-Feria, L., Iovanna, J. L., Guzman, M., Boya, P. and Velasco, G. (2009) Cannabinoid action induces autophagy-mediated cell death through stimulation of ER stress in human glioma cells. *J Clin Invest 119*, 1359-72.

Salminen, A., Kauppinen, A., Suuronen, T., Kaarniranta, K. and Ojala, J. (2009) ER stress in Alzheimer's disease: a novel neuronal trigger for inflammation and Alzheimer's pathology. *J Neuroinflammation 6*, 41.

Sankaranarayanan, S., Price, E. A., Wu, G., Crouthamel, M. C., Shi, X. P., Tugusheva, K., Tyler, K. X., Kahana, J., Ellis, J., Jin, L., Steele, T., Stachel, S., Coburn, C. and Simon, A. J. (2008) In vivo beta-secretase 1 inhibition leads to brain Abeta lowering and increased alpha-secretase processing of amyloid precursor protein without effect on neuregulin-1. *J Pharmacol Exp Ther 324*, 957-69.

Scheuner, D., Song, B., McEwen, E., Liu, C., Laybutt, R., Gillespie, P., Saunders, T., Bonner-Weir, S. and Kaufman, R. J. (2001) Translational control is required for the unfolded protein response and in vivo glucose homeostasis. *Mol Cell 7*, 1165-76.

Schonthal, A. H. (2009) Endoplasmic reticulum stress and autophagy as targets for cancer therapy. *Cancer Lett 275*, 163-9.

Schroder, M. and Kaufman, R. J. (2005) The mammalian unfolded protein response. *Annu Rev Biochem 74*, 739-89.

Seiffert, D., Bradley, J. D., Rominger, C. M., Rominger, D. H., Yang, F., Meredith, J. E., Jr., Wang, Q., Roach, A. H., Thompson, L. A., Spitz, S. M., Higaki, J. N., Prakash, S. R., Combs, A. P., Copeland, R.

A., Arneric, S. P., Hartig, P. R., Robertson, D. W., Cordell, B., Stern, A. M., Olson, R. E. and Zaczek, R. (2000) Presenilin-1 and -2 are molecular targets for gamma-secretase inhibitors. *J Biol Chem 275*, 34086-91.

Selkoe, D. J. (1986) Altered structural proteins in plaques and tangles: what do they tell us about the biology of Alzheimer's disease? *Neurobiol Aging 7*, 425-32.

Selkoe, D. J. (2001) Alzheimer's disease: genes, proteins, and therapy. *Physiol Rev 81*, 741-66.

Seubert, P., Oltersdorf, T., Lee, M. G., Barbour, R., Blomquist, C., Davis, D. L., Bryant, K., Fritz, L. C., Galasko, D., Thal, L. J. and et al. (1993) Secretion of beta-amyloid precursor protein cleaved at the amino terminus of the beta-amyloid peptide. *Nature 361*, 260-3.

Shen, J., Chen, X., Hendershot, L. and Prywes, R. (2002) ER stress regulation of ATF6 localization by dissociation of BiP/GRP78 binding and unmasking of Golgi localization signals. *Dev Cell 3*, 99-111.

Sherma, J. (2000) Thin-layer chromatography in food and agricultural analysis. *J Chromatogr A 880*, 129-47.

Sherr, C. J. and Roberts, J. M. (1999) CDK inhibitors: positive and negative regulators of G1-phase progression. *Genes Dev 13*, 1501-12.

Sherr, C. J. and McCormick, F. (2002) The RB and p53 pathways in cancer. *Cancer Cell 2*, 103-12.

Sherrington, R., Rogaev, E. I., Liang, Y., Rogaeva, E. A., Levesque, G., Ikeda, M., Chi, H., Lin, C., Li, G., Holman, K., Tsuda, T., Mar, L., Foncin, J. F., Bruni, A. C., Montesi, M. P., Sorbi, S., Rainero, I., Pinessi, L., Nee, L., Chumakov, I., Pollen, D., Brookes, A., Sanseau, P., Polinsky, R. J., Wasco, W., Da Silva, H. A., Haines, J. L., Perkicak-Vance, M. A., Tanzi, R. E., Roses, A. D., Fraser, P. E., Rommens, J. M. and St George-Hyslop, P. H. (1995) Cloning of a gene bearing missense mutations in early-onset familial Alzheimer's disease. *Nature 375*, 754-60.

Shingu, T., Chumbalkar, V. C., Gwak, H. S., Fujiwara, K., Kondo, S., Farrell, N. P. and Bogler, O. (2010) The polynuclear platinum BBR3610 induces G2/M arrest and autophagy early and apoptosis late in glioma cells. *Neuro Oncol 12*, 1269-77.

Shirotani, K., Edbauer, D., Prokop, S., Haass, C. and Steiner, H. (2004) Identification of distinct gamma-secretase complexes with different APH-1 variants. *J Biol Chem 279*, 41340-5.

Sinha, S., Anderson, J. P., Barbour, R., Basi, G. S., Caccavello, R., Davis, D., Doan, M., Dovey, H. F., Frigon, N., Hong, J., Jacobson-Croak, K., Jewett, N., Keim, P., Knops, J., Lieberburg, I., Power, M., Tan, H., Tatsuno, G., Tung, J., Schenk, D., Seubert, P., Suomensaari, S. M., Wang, S., Walker, D., Zhao, J., McConlogue, L. and John, V. (1999) Purification and cloning of amyloid precursor protein beta-secretase from human brain. *Nature 402*, 537-40.

Skovronsky, D. M., Moore, D. B., Milla, M. E., Doms, R. W. and Lee, V. M. (2000) Protein kinase C-dependent alpha-secretase competes with beta-secretase for cleavage of amyloid-beta precursor protein in the trans-golgi network. *J Biol Chem 275*, 2568-75.

Smith, D. H., Chen, X. H., Iwata, A. and Graham, D. I. (2003) Amyloid beta accumulation in axons after traumatic brain injury in humans. *J Neurosurg 98*, 1072-7.

Smith, P. K., Krohn, R. I., Hermanson, G. T., Mallia, A. K., Gartner, F. H., Provenzano, M. D., Fujimoto, E. K., Goeke, N. M., Olson, B. J. and Klenk, D. C. (1985) Measurement of protein using bicinchoninic acid. *Anal Biochem 150*, 76-85.

Soto, C. (2003) Unfolding the role of protein misfolding in neurodegenerative diseases. *Nat Rev Neurosci 4*, 49-60.

Soto, C. and Estrada, L. D. (2008) Protein misfolding and neurodegeneration. *Arch Neurol 65*, 184-9.

Spires, T. L., Orne, J. D., SantaCruz, K., Pitstick, R., Carlson, G. A., Ashe, K. H. and Hyman, B. T. (2006) Region-specific dissociation of neuronal loss and neurofibrillary pathology in a mouse model of tauopathy. *Am J Pathol 168*, 1598-607.

St George-Hyslop, P. H. and Petit, A. (2005) Molecular biology and genetics of Alzheimer's disease. *C R Biol 328*, 119-30.

Stromhaug, P. E., Berg, T. O., Fengsrud, M. and Seglen, P. O. (1998) Purification and characterization of autophagosomes from rat hepatocytes. *Biochem J 335 (Pt 2)*, 217-24.

Sun, Q., Fan, W., Chen, K., Ding, X., Chen, S. and Zhong, Q. (2008) Identification of Barkor as a mammalian autophagy-specific factor for Beclin 1 and class III phosphatidylinositol 3-kinase. *Proc Natl Acad Sci U S A 105*, 19211-6.

Tabira, T., Chui, D. H. and Kuroda, S. (2002) Significance of intracellular Abeta42 accumulation in Alzheimer's disease. *Front Biosci 7*, a44-9.

Takahashi, Y., Coppola, D., Matsushita, N., Cualing, H. D., Sun, M., Sato, Y., Liang, C., Jung, J. U., Cheng, J. Q., Mule, J. J., Pledger, W. J. and Wang, H. G. (2007) Bif-1 interacts with Beclin 1 through UVRAG and regulates autophagy and tumorigenesis. *Nat Cell Biol 9*, 1142-51.

Takashima, A., Noguchi, K., Sato, K., Hoshino, T. and Imahori, K. (1993) Tau protein kinase I is essential for amyloid beta-protein-induced neurotoxicity. *Proc Natl Acad Sci U S A 90*, 7789-93.

Takashima, A. (2008) Hyperphosphorylated tau is a cause of neuronal dysfunction in tauopathy. *J Alzheimers Dis 14*, 371-5.

Takashima, A. (2012) GSK-3beta and memory formation. *Front Mol Neurosci 5*, 47.

Takasugi, N., Tomita, T., Hayashi, I., Tsuruoka, M., Niimura, M., Takahashi, Y., Thinakaran, G. and Iwatsubo, T. (2003) The role of presenilin cofactors in the gamma-secretase complex. *Nature 422*, 438-41.

Talloczy, Z., Jiang, W., Virgin, H. W. t., Leib, D. A., Scheuner, D., Kaufman, R. J., Eskelinen, E. L. and Levine, B. (2002) Regulation of starvation- and virus-induced autophagy by the eIF2alpha kinase signaling pathway. *Proc Natl Acad Sci U S A 99*, 190-5.

Tanida, I., Tanida-Miyake, E., Ueno, T. and Kominami, E. (2001) The human homolog of Saccharomyces cerevisiae Apg7p is a Protein-activating enzyme for multiple substrates including human Apg12p, GATE-16, GABARAP, and MAP-LC3. *J Biol Chem 276*, 1701-6.

Tanida, I., Nishitani, T., Nemoto, T., Ueno, T. and Kominami, E. (2002a) Mammalian Apg12p, but not the Apg12p.Apg5p conjugate, facilitates LC3 processing. *Biochem Biophys Res Commun 296*, 1164-70.

Tanida, I., Tanida-Miyake, E., Komatsu, M., Ueno, T. and Kominami, E. (2002b) Human Apg3p/Aut1p homologue is an authentic E2 enzyme for multiple substrates, GATE-16, GABARAP, and MAP-LC3, and facilitates the conjugation of hApg12p to hApg5p. *J Biol Chem 277*, 13739-44.

Tanida, I., Sou, Y. S., Ezaki, J., Minematsu-Ikeguchi, N., Ueno, T. and Kominami, E. (2004) HsAtg4B/HsApg4B/autophagin-1 cleaves the carboxyl termini of three human Atg8 homologues and delipidates microtubule-associated protein light chain 3- and GABAA receptor-associated protein-phospholipid conjugates. *J Biol Chem 279*, 36268-76.

Tatevossian, R. G., Lawson, A. R., Forshew, T., Hindley, G. F., Ellison, D. W. and Sheer, D. (2010) MAPK pathway activation and the origins of pediatric low-grade astrocytomas. *J Cell Physiol 222*, 509-14.

Teng, D. H., Hu, R., Lin, H., Davis, T., Iliev, D., Frye, C., Swedlund, B., Hansen, K. L., Vinson, V. L., Gumpper, K. L., Ellis, L., El-Naggar, A., Frazier, M., Jasser, S., Langford, L. A., Lee, J., Mills, G. B., Pershouse, M. A., Pollack, R. E., Tornos, C., Troncoso, P., Yung, W. K., Fujii, G., Berson, A., Steck, P. A. and et al. (1997) MMAC1/PTEN mutations in primary tumor specimens and tumor cell lines. *Cancer Res 57*, 5221-5.

Terés, S., Lladó, V., Higuera, M., Barceló-Coblijn, G., Martín, M. L., Noguera-Salvà, M. A., Marcilla-Etxenike, A., Garcia-Verdugo, J. M., Soriano-Navarro, M., Saus, C., Gomez-Pinedo, U., Busquets, X. and Escribá, P. V. (2012) 2-Hydroxyoleate, a nontoxic membrane binding anticancer drug, induces glioma cell differentiation and autophagy. *Proc Natl Acad Sci U S A 109*, 8489-94.

Thastrup, O., Cullen, P. J., Drobak, B. K., Hanley, M. R. and Dawson, A. P. (1990) Thapsigargin, a tumor promoter, discharges intracellular Ca2+ stores by specific inhibition of the endoplasmic reticulum Ca2(+)-ATPase. *Proc Natl Acad Sci U S A 87*, 2466-70.

Tirasophon, W., Lee, K., Callaghan, B., Welihinda, A. and Kaufman, R. J. (2000) The endoribonuclease activity of mammalian IRE1 autoregulates its mRNA and is required for the unfolded protein response. *Genes Dev 14*, 2725-36.

Triton, T. R. and Yee, G. (1982) The anticancer agent adriamycin can be actively cytotoxic without entering cells. *Science 217*, 248-50.

Tully, A. M., Roche, H. M., Doyle, R., Fallon, C., Bruce, I., Lawlor, B., Coakley, D. and Gibney, M. J. (2003) Low serum cholesteryl ester-docosahexaenoic acid levels in Alzheimer's disease: a case-control study. *Br J Nutr 89*, 483-9.

Uehara, T., Nakamura, T., Yao, D., Shi, Z. Q., Gu, Z., Ma, Y., Masliah, E., Nomura, Y. and Lipton, S. A. (2006) S-nitrosylated protein-disulphide isomerase links protein misfolding to neurodegeneration. *Nature 441*, 513-7.

Unterberger, U., Hoftberger, R., Gelpi, E., Flicker, H., Budka, H. and Voigtlander, T. (2006) Endoplasmic reticulum stress features are prominent in Alzheimer disease but not in prion diseases in vivo. *J Neuropathol Exp Neurol 65*, 348-57.

Urano, F., Wang, X., Bertolotti, A., Zhang, Y., Chung, P., Harding, H. P. and Ron, D. (2000) Coupling of stress in the ER to activation of JNK protein kinases by transmembrane protein kinase IRE1. *Science 287*, 664-6.

Vassar, R., Bennett, B. D., Babu-Khan, S., Kahn, S., Mendiaz, E. A., Denis, P., Teplow, D. B., Ross, S., Amarante, P., Loeloff, R., Luo, Y., Fisher, S., Fuller, J., Edenson, S., Lile, J., Jarosinski, M. A., Biere, A. L., Curran, E., Burgess, T., Louis, J. C., Collins, F., Treanor, J., Rogers, G. and Citron, M. (1999) Beta-secretase cleavage of Alzheimer's amyloid precursor protein by the transmembrane aspartic protease BACE. *Science 286*, 735-41.

Vembar, S. S. and Brodsky, J. L. (2008) One step at a time: endoplasmic reticulum-associated degradation. *Nat Rev Mol Cell Biol 9*, 944-57.

Verfaillie, T., Salazar, M., Velasco, G. and Agostinis, P. (2010) Linking ER Stress to Autophagy: Potential Implications for Cancer Therapy. *Int J Cell Biol 2010*, 930509.

Vermeulen, K., Van Bockstaele, D. R. and Berneman, Z. N. (2003) The cell cycle: a review of regulation, deregulation and therapeutic targets in cancer. *Cell Prolif 36*, 131-49.

Vögler, O., Casas, J., Capo, D., Nagy, T., Borchert, G., Martorell, G. and Escribá, P. V. (2004) The Gbetagamma dimer drives the interaction of heterotrimeric Gi proteins with nonlamellar membrane structures. *J Biol Chem 279*, 36540-5.

Volkmann, K., Lucas, J. L., Vuga, D., Wang, X., Brumm, D., Stiles, C., Kriebel, D., Der-Sarkissian, A., Krishnan, K., Schweitzer, C., Liu, Z., Malyankar, U. M., Chiovitti, D., Canny, M., Durocher, D., Sicheri, F. and Patterson, J. B. (2011) Potent and selective inhibitors of the inositol-requiring enzyme 1 endoribonuclease. *J Biol Chem 286*, 12743-55.

Vousden, K. H. and Lu, X. (2002) Live or let die: the cell's response to p53. *Nat Rev Cancer 2*, 594-604.

Wang, G., Yang, Z. Q. and Zhang, K. (2010) Endoplasmic reticulum stress response in cancer: molecular mechanism and therapeutic potential. *Am J Transl Res 2*, 65-74.

Wang, X. Z., Harding, H. P., Zhang, Y., Jolicoeur, E. M., Kuroda, M. and Ron, D. (1998) Cloning of mammalian Ire1 reveals diversity in the ER stress responses. *EMBO J 17*, 5708-17.

Weggen, S., Eriksen, J. L., Das, P., Sagi, S. A., Wang, R., Pietrzik, C. U., Findlay, K. A., Smith, T. E., Murphy, M. P., Bulter, T., Kang, D. E., Marquez-Sterling, N., Golde, T. E. and Koo, E. H. (2001) A subset of NSAIDs lower amyloidogenic Abeta42 independently of cyclooxygenase activity. *Nature 414*, 212-6.

Wei, Y., Pattingre, S., Sinha, S., Bassik, M. and Levine, B. (2008) JNK1-mediated phosphorylation of Bcl-2 regulates starvation-induced autophagy. *Mol Cell 30*, 678-88.

Weidberg, H., Shpilka, T., Shvets, E., Abada, A., Shimron, F. and Elazar, Z. (2011) LC3 and GATE-16 N termini mediate membrane fusion processes required for autophagosome biogenesis. *Dev Cell 20*, 444-54.

Weskamp, G., Kratzschmar, J., Reid, M. S. and Blobel, C. P. (1996) MDC9, a widely expressed cellular disintegrin containing cytoplasmic SH3 ligand domains. *J Cell Biol 132*, 717-26.

Winklhofer, K. F., Tatzelt, J. and Haass, C. (2008) The two faces of protein misfolding: gain- and loss-of-function in neurodegenerative diseases. *EMBO J 27*, 336-49.

Winslow, A. R. and Rubinsztein, D. C. (2008) Autophagy in neurodegeneration and development. *Biochim Biophys Acta 1782*, 723-9.

Wirsching, B. A., Beninger, R. J., Jhamandas, K., Boegman, R. J. and El-Defrawy, S. R. (1984) Differential effects of scopolamine on working and reference memory of rats in the radial maze. *Pharmacol Biochem Behav 20*, 659-62.

Wiseman, R. L., Zhang, Y., Lee, K. P., Harding, H. P., Haynes, C. M., Price, J., Sicheri, F. and Ron, D. (2010) Flavonol activation defines an unanticipated ligand-binding site in the kinase-RNase domain of IRE1. *Mol Cell 38*, 291-304.

Wolfe, M. S., Xia, W., Ostaszewski, B. L., Diehl, T. S., Kimberly, W. T. and Selkoe, D. J. (1999) Two transmembrane aspartates in presenilin-1 required for presenilin endoproteolysis and gamma-secretase activity. *Nature 398*, 513-7.

Wolfe, M. S. (2009) gamma-Secretase in biology and medicine. *Semin Cell Dev Biol 20*, 219-24.

Wong, G. T., Manfra, D., Poulet, F. M., Zhang, Q., Josien, H., Bara, T., Engstrom, L., Pinzon-Ortiz, M., Fine, J. S., Lee, H. J., Zhang, L., Higgins, G. A. and Parker, E. M. (2004) Chronic treatment with the gamma-secretase inhibitor LY-411,575 inhibits beta-amyloid peptide production and alters lymphopoiesis and intestinal cell differentiation. *J Biol Chem 279*, 12876-82.

Wu, J., Rutkowski, D. T., Dubois, M., Swathirajan, J., Saunders, T., Wang, J., Song, B., Yau, G. D. and Kaufman, R. J. (2007) ATF6alpha optimizes long-term endoplasmic reticulum function to protect cells from chronic stress. *Dev Cell 13*, 351-64.

Xu, C., Bailly-Maitre, B. and Reed, J. C. (2005) Endoplasmic reticulum stress: cell life and death decisions. *J Clin Invest 115*, 2656-64.

Yacoub, A., Park, M. A., Gupta, P., Rahmani, M., Zhang, G., Hamed, H., Hanna, D., Sarkar, D., Lebedeva, I. V., Emdad, L., Sauane, M., Vozhilla, N., Spiegel, S., Koumenis, C., Graf, M., Curiel, D. T., Grant, S., Fisher, P. B. and Dent, P. (2008) Caspase-, cathepsin-, and PERK-dependent regulation of MDA-7/IL-24-induced cell killing in primary human glioma cells. *Mol Cancer Ther 7*, 297-313.

Yamamoto, K., Sato, T., Matsui, T., Sato, M., Okada, T., Yoshida, H., Harada, A. and Mori, K. (2007) Transcriptional induction of mammalian ER quality control proteins is mediated by single or combined action of ATF6alpha and XBP1. *Dev Cell 13*, 365-76.

Yan, R., Bienkowski, M. J., Shuck, M. E., Miao, H., Tory, M. C., Pauley, A. M., Brashier, J. R., Stratman, N. C., Mathews, W. R., Buhl, A. E., Carter, D. B., Tomasselli, A. G., Parodi, L. A., Heinrikson, R. L. and Gurney, M. E. (1999) Membrane-anchored aspartyl protease with Alzheimer's disease beta-secretase activity. *Nature 402*, 533-7.

Yang, X., Sheng, W., Sun, G. Y. and Lee, J. C. (2011) Effects of fatty acid unsaturation numbers on membrane fluidity and alpha-secretase-dependent amyloid precursor protein processing. *Neurochem Int 58*, 321-9.

Yang, Y., Turner, R. S. and Gaut, J. R. (1998) The chaperone BiP/GRP78 binds to amyloid precursor protein and decreases Abeta40 and Abeta42 secretion. *J Biol Chem 273*, 25552-5.

Yang, Z., Wang, Y., Fang, J., Chen, F., Liu, J., Wu, J., Song, T., Zeng, F. and Rao, Y. (2010) Downregulation of WIF-1 by hypermethylation in astrocytomas. *Acta Biochim Biophys Sin (Shanghai) 42*, 418-25.

Ye, J., Rawson, R. B., Komuro, R., Chen, X., Dave, U. P., Prywes, R., Brown, M. S. and Goldstein, J. L. (2000) ER stress induces cleavage of membrane-bound ATF6 by the same proteases that process SREBPs. *Mol Cell 6*, 1355-64.

Yla-Anttila, P., Vihinen, H., Jokitalo, E. and Eskelinen, E. L. (2009) 3D tomography reveals connections between the phagophore and endoplasmic reticulum. *Autophagy 5*, 1180-5.

Yoshida, H., Matsui, T., Yamamoto, A., Okada, T. and Mori, K. (2001) XBP1 mRNA is induced by ATF6 and spliced by IRE1 in response to ER stress to produce a highly active transcription factor. *Cell 107*, 881-91.

Yoshida, H., Uemura, A. and Mori, K. (2009) pXBP1(U), a negative regulator of the unfolded protein response activator pXBP1(S), targets ATF6 but not ATF4 in proteasome-mediated degradation. *Cell Struct Funct 34*, 1-10.

Younkin, S. G. (1998) The role of A beta 42 in Alzheimer's disease. *J Physiol Paris 92*, 289-92.

Zhang, K. and Kaufman, R. J. (2008) From endoplasmic-reticulum stress to the inflammatory response. *Nature 454*, 455-62.

Zhao, Y., Calon, F., Julien, C., Winkler, J. W., Petasis, N. A., Lukiw, W. J. and Bazan, N. G. (2011) Docosahexaenoic acid-derived neuroprotectin D1 induces neuronal survival via secretase- and PPARgamma-mediated mechanisms in Alzheimer's disease models. *PLoS One 6*, e15816.

Zinszner, H., Kuroda, M., Wang, X., Batchvarova, N., Lightfoot, R. T., Remotti, H., Stevens, J. L. and Ron, D. (1998) CHOP is implicated in programmed cell death in response to impaired function of the endoplasmic reticulum. *Genes Dev 12*, 982-95.

The most exciting phrase to hear in science, the one that heralds new discoveries, is not 'Eureka!' (I found it!) but 'That's funny ...'-Isaac Asimov